RESTRICTED REPORT 303R

CSIRO
AUSTRALIA

Division of
EXPLORATION GEOSCIENCE

Institute of Minerals, Energy and Construction

ROCK MAGNETISM AND MAGNETIC PETROLOGY APPLIED TO GEOLOGICAL INTERPRETATION OF MAGNETIC SURVEYS

D.A. Clark, D.H. French, M.A. Lackie
and P.W. Schmidt

Notes for Technology Transfer Meetings : AMIRA Project P96C

Brisbane 29 April
Melbourne 6 May
Mount Isa 14 May
Perth 5 and 8 June
Kalgoorlie 4 June

P.O. Box 136
North Ryde
NSW 2113

April 1992

AMIRA
Australian Mineral Industries Research Association Limited

CSIRO
AUSTRALIA

Division of Exploration Geoscience
Institute of Minerals, Energy and Construction
51 Delhi Road, North Ryde. NSW. Postal Address: PO Box 136, North Ryde. NSW 2113
Telephone: (02) 887 8666. Telex: AA25817. Fax: (02) 887 8909

POLICY ON RESTRICTED REPORTS

Restricted Reports issued by this Division deal with projects where CSIRO has been granted privileged access to research material. Initially, circulation of Restricted Reports is strictly controlled, and we treat them as confidential documents at this stage. They should not be quoted publicly, but may be referred to as a "personal communication" from the author(s) if my approval is sought and given beforehand.

The results embodied in a Restricted Report may eventually form part of a more widely circulated CSIRO publication. Agreements with sponsors or companies generally specify that drafts will be first submitted for their approval, to ensure that proprietary information of a confidential nature is not inadvertently included.

After a certain period of time, the confidentiality of particular Restricted Reports will no longer be an important issue. It may then be appropriate for CSIRO to announce the titles of such reports, and to allow inspection and copying by other persons. This procedure would disseminate information about CSIRO research more widely to Industry. However, it will not be applicable to all Restricted Reports. Proprietary interests of various kinds may require an extended period of confidentiality. Premature release of Restricted Reports arising from continuing collaborative projects (especially AMIRA projects) may also be undesirable, and a separate policy exists in such cases.

You are invited to express an opinion about the security status of the enclosed Restricted Report. **Unless I hear to the contrary,** I will assume that in eighteen months time I have your permission to place this Restricted Report on open file, when it will be generally available to interested persons for reading, making notes, or photocopying, as desired.

Graham F. Taylor
Acting Chief

Floreat Park
Location: Underwood Avenue, Floreat Park
Postal Address: CSIRO Private Bag,
PO Wembley WA 6014
Telephone: (09) 387 0200
Fax: (09) 387 8642
Telex: AA92178

Townsville
Location: Davies Laboratory, University Road, Townsville
Postal Address: Private Mail Bag,
PO Aitkenvale QLD 4814
Telephone: (077) 71 9511
Fax: (077) 25 1009

Lindfield
Location: Bradfield Road, Lindfield
Postal Address: PO Box 218
Lindfield NSW 2070
Telephone: (02) 413 7733, 413 7211
Fax: (02) 413 7202
Telex: AA26296

TABLE OF CONTENTS

SECTION 1. BASIC ROCK MAGNETISM

What is Magnetism?

Magnetic fields arise from the movement of electric charges or, equivalently, from electric currents. Magnetic fields are a relativistic effect. An observer at rest with respect to an electric charge observes only an electric field, **E**, of the form shown in Fig. 1(a). Any observer in motion with respect to the first will observe a (different) electric field (Fig. 1(b)), plus a magnetic field **B** (Fig. 1(c)). Flow of electric current along a straight conductor, as in Fig. 1(d), produces a magnetic field of the same form as that due to the moving charge. Just as an electric field is defined in terms of the force exerted on a static electric charge, which is equal to the charge times **E**, magnetic field is defined in terms of the extra force exerted on a unit charge that is moving with velocity **v**, which is **v** x **B**.

When current flows in a loop, the magnetic field has the form shown in Fig.1 (e). The magnetic dipole moment **m** is defined as the product of the current, i, and the area of the loop, a. The term dipole moment is used because the far field of the current loop is identical in form to the electric field arising from an electric dipole, as shown in Fig.1 (f). The fictitious magnetic analogues to point charges are known as magnetic poles.

Magnetised matter produces a magnetic field due to internal subatomic currents. The internal currents arise from two main effects (see Fig.1(g)):

(i) Orbital motion of electrons around nuclei
(ii) Spin of electrons about their own axes

Induced and Remanent Magnetisation

Magnetised matter contains a distribution of microscopic magnetic moments. Magnetisation, **M**, or **J** is defined as the magnetic dipole moment per unit volume of the material. There are two basic types of magnetisation: that which arises in response to an applied field, and that which is permanently present, even in the absence of an applied field.

Induced magnetisation, $\mathbf{M}_I$, is the component of magnetisation produced in response to an applied field. The induced magnetisation varies sympathetically with changes in the applied field and disappears when the field is removed.

Remanent magnetisation, $\mathbf{M}_R$, is the "permanent" magnetisation that remains when the applied field is removed, and is essentially unaffected by weak fields. The total magnetisation is given by:

$$\mathbf{M} = \mathbf{M}_I + \mathbf{M}_R.$$

For sufficiently weak fields, such as the geomagnetic field, the induced magnetisation is proportional to the applied field, to a good approximation. The constant of proportionality is known as the susceptibility, k. Thus, if the applied field is **F**, the induced and total magnetisations are given by:

ELECTRIC AND MAGNETIC FIELDS

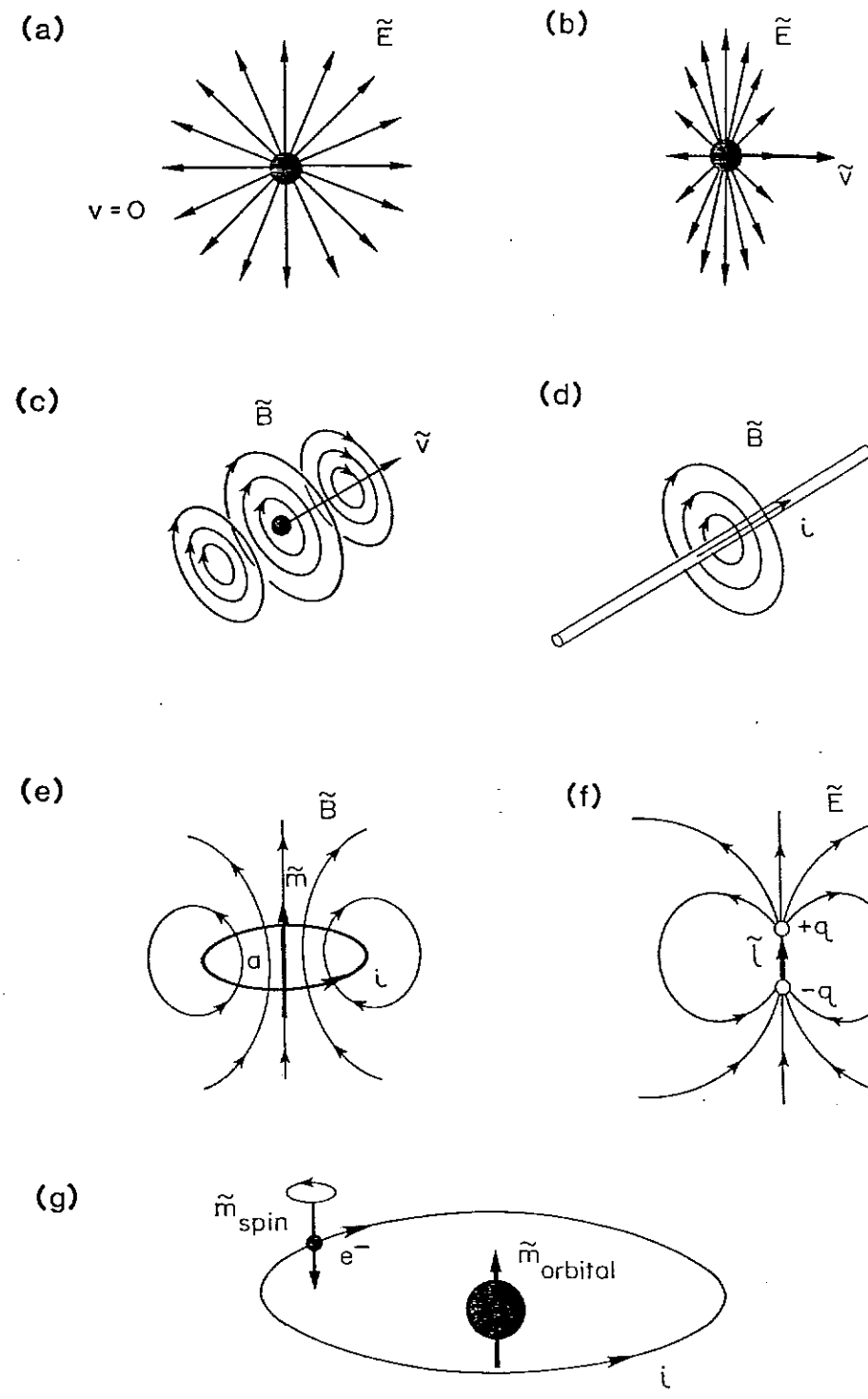

Fig. 1

$$\mathbf{M_I} = k\mathbf{F};\ \mathbf{M} = k\mathbf{F} + \mathbf{M_R}.$$

Two systems of units are used in rock magnetism, the Gaussian (CGS) system and SI. SI is now becoming the standard, although in practice it is much less convenient for magnetic petrophysics and magnetic modelling. Magnetisation is expressed in gauss (G) or microgauss (μG) and the field is expressed in oersteds (Oe) or gammas (1 $\gamma = 10^{-5}$ Oe) in the Gaussian system. Thus susceptibility can be given the units of G/Oe (or, for small susceptibilities, μG/Oe), or else referred to as the "CGS susceptibility". In SI, magnetisation is measured in amps/metre (A/m) or milliamps/metre (mA/m) and field is measured in Teslas (T), for very strong laboratory fields, or in nanoTeslas (nT), equal to 10^{-9} T, when referring to the magnetic flux density, **B**. The magnetic intensity, **H**, is measured in A/m or mA/m, and SI susceptibility is dimensionless. In free space, **B** and **H** differ only by a multiplicative factor, but inside magnetised matter the magnetisation contributes to **B** but not to **H**. The two systems of units are related by:

	Gaussian (CGS) $\mathbf{B} = (\mu_o)(\mathbf{H} + 4\pi\mathbf{M})$		SI $\mathbf{B} = \mu_o(\mathbf{H} + \mathbf{M})$
Flux density (**B**)	1 Gauss	=	10^{-4} Tesla
Field intensity (**H**)	1 Oersted	=	$1000/4\pi$ A/m
Magnetisation (**M**)	1 Gauss	=	1000 A/m
	1 μG	=	1 mA/m
Permeability of free space	$\mu_o = 1$ G/Oe		$\mu_o = 4\pi \times 10^{-7}$ Henry/m
Susceptibility	1 G/Oe	=	$4\pi = 12.56$

For most rocks, the induced magnetisation is essentially parallel to the applied field. In this case the susceptibility is a scalar quantity, i.e. it is characterised simply by its magnitude and has no directional quality. For these rocks the susceptibility is independent of the field direction, i.e. they are magnetically isotropic.

Magnetic field and magnetisation, on the other hand, are vector quantities, which have both magnitude and direction. In some cases, rocks are significantly anisotropic magnetically. Then the susceptibility varies with the field direction and, in general, the magnetisation is not parallel to the applied field, because the magnetisation tends to be deflected away from an axis of relatively low susceptibility, towards an axis of higher susceptibility.

SUSCEPTIBILITY ELLIPSOID : MAGNETIC FABRIC

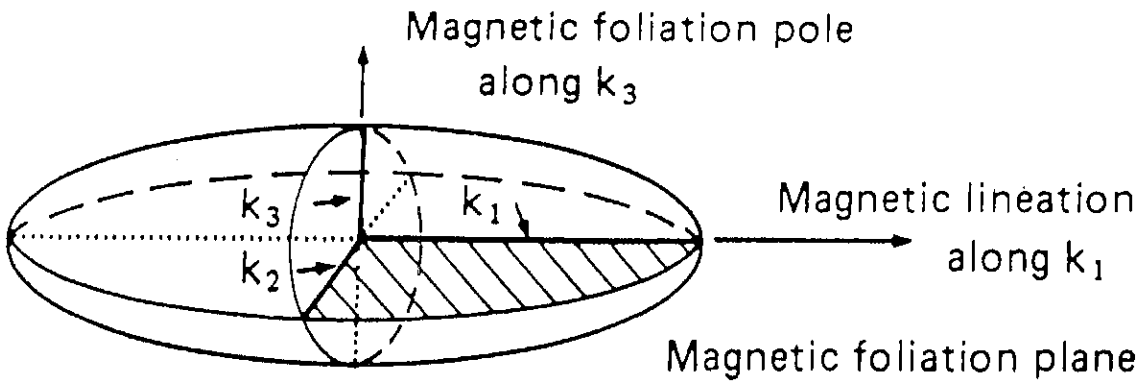

Anisotropy Magnitude $A = k_1/k_3$

Lineation Magnitude $L = k_1/k_2$

Foliation Magnitude $F = k_2/k_3$

Ellipsoid Prolateness $P = L/F$

- $P = 0$ uniaxial oblate ellipsoid (disc)
- $P = \infty$ uniaxial prolate ellipsoid (needle)

Fig. 2

ROCK MAGNETIZATION (J) - LABORATORY MEASUREMENTS

INDUCED MAGNETIZATION
SUSCEPTIBILITY k(in field H)
$J_{IND} = kH$

Transformer Bridge

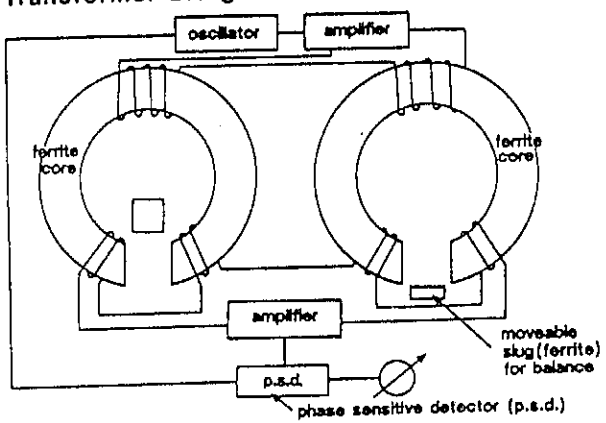

REMANENT MAGNETIZATION
J_{NRM}

Spinner Magnetometer (Fluxgate)

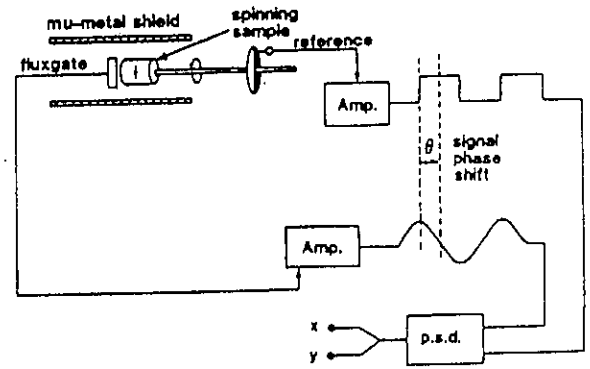

Frequency Shift Meter (Portable)

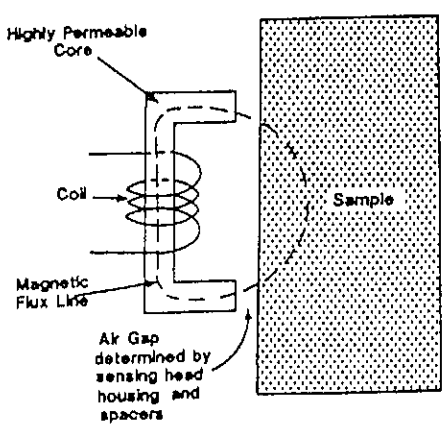

Sample has permeability μ

$\mu = 1 + k$ (SI)

$\mu = 1 + 4\pi k$ (cgs)

oscillator energised coil has inductance L which is inversely proportial to magnetic reluctance $\mathcal{R}$ where $\mathcal{R}$ is proportional to a constant plus μ^{-1}

The oscillator frequency is measured ; freq = $(2\pi\sqrt{LC})^{-1}$ where the capacitance C is an instrumental constant

The instrument correlates the change in susceptibility with the oscillator frequency

Cryogenic Magnetometer (SQUID)

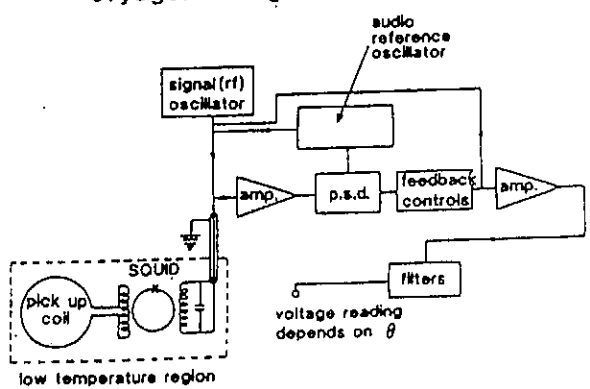

sample to be measured is suspended in pick-up coils of superconducting quantum interference device magnetometer

Fig. 3

Anisotropic susceptibility cannot be described by a scalar quantity, but takes the form of a symmetric second order tensor. As a consequence, for any homogeneous, but anisotropic, rock, three mutually orthogonal axes may be found along which the susceptibility has maximum, minimum and intermediate values. These principal axes define an ellipsoid, known as the susceptibility ellipsoid, which describes the behaviour of the susceptibility and induced magnetisation uniquely and also characterises the magnetic fabric of the rock (see Fig. 2). The magnetic foliation contains the major and intermediate susceptibility axes, and reflects planar structures in the rock, and the magnetic lineation coincides with the major susceptibility axis and reflects linear structures.

The Koenigsberger ratio, or Q value, is a convenient parameter, which expresses the relative importance of remanent and induced magnetisations. It is given by:

$$Q = M_R/M_I = M_R/kF.$$

Thus $Q > 1$, indicates that remanence dominates induced magnetisation, whereas $Q < 1$ implies that induced magnetisation is dominant.

Measurement of Susceptibility and Remanence

Fig.3 shows schematically the principles governing measurement of susceptibility and remanence. Both methods of susceptibility measurement rely on detecting changes in the reluctance of a magnetic circuit when a permeable specimen is introduced into the flux path (analogous to the change in resistance of an electrical circuit). The change in inductance of the transformer core when the specimen is placed in the gap produces an unbalance signal that is dependent on the specimen susceptibility. Placing the hand-held susceptibility meter against the surface of a magnetic sample changes the inductance of the core winding, and hence the resonant frequency of the LC oscillator. The change in frequency is dependent on the susceptibility. Spinner fluxgate magnetometers are sufficiently sensitive to measure the remanence of small rock specimens for all but the most weakly magnetized rocks. The specimen rotates within a magnetic shield and produces a sinusoidal magnetic field at the fluxgate sensor. The amplitude and phase of the fluxgate signal are used to determine the intensity and direction of the remanence component in the plane orthogonal to the spin axis. By repeating the measurement with the specimen reoriented the complete remanence vector is determined. Cryogenic magnetmeters are very sensitive instruments, capable of measuring remanences as low as 10^{-9} G (1 μA/m SI). The specimen is lowered into the measurement region within a superconducting shield and the change in flux passing through SQUID detectors is measured. If three detectors are used the full remanence vector can be determined almost instantaneously.

Distinction between Induced, Viscous and Remanent Magnetization

Fig.4 illustrates the distinction between induced magnetization, viscous remanence and stable remanence. Fig.4(a) shows the changes in magnetization of an initially demagnetized sample in response to an applied field, which is switched on and off as shown in Fig.4(b). Small applied fields, comparable in strength to the geomagnetic field,

produce small, reversible changes in magnetization, i.e. the magnetization vanishes on removal of the field. This induced magnetization is approximately proportional to the strength of the applied field. Thus the susceptibility, which is defined as the induced magnetization divided by the applied field, is approximately independent of the field. If a larger field is applied and then removed an irreversible change in magnetization occurs - an isothermal remanent magnetization J_{IRM} has been imparted to the sample. This magnetization can be regarded as permanent on the experimental time scale. Fig.4(c) illustrates this behaviour in terms of the hysteresis loop, plotting magnetization J versus applied field H. The initial portion of the J-H curve is approximately linear and is traversed reversibly when a small field is applied and removed. When the larger field is applied and instantaneously removed, the sample follows the trajectory abc. At the point b the total magnetization is the sum of the induced magnetization, which by definition is the component that vanishes when the field is removed, and the isothermal remanence, which is an essentially permanent magnetization on the experimental time scale.

If the field is again switched on, the magnetization follows the path cd and returns initially to its former value ($J_{IRM} + J_{IND}$). If the applied field remains on, however, the total magnetization increases gradually with time, from d to e. After an initial period that depends on the grain size distribution, the increase in magnetization is usually found to be approximately proportional to the logarithm of time, over several decades of t. When the field is removed this excess magnetization, which is known as viscous remanent magnetization (VRM), remains and augments the isothermal remanence, but decays at a rate comparable to the acquistion rate. After sufficient time in zero field the VRM has decayed completely and only the stable IRM remains. Thus viscous remanence is a temporary magnetization that is intermediate in character between induced magnetization and more stable forms of remanence. The separation of magnetization into induced, viscous and stable components is not exact, because the distinctions depend on the time scale under consideration. In general the sample may not be initially in a demagnetized state. If the sample carries a stable remanence component initially the magnetization plots in Fig.4(a) and 4(c) are simply shifted upwards.

Ferromagnetism, Paramagnetism and Diamagnetism

Diamagnetic minerals (e.g. calcite and quartz) have very weak, negative susceptibilities and can be regarded as nonmagnetic for geophysical purposes. Paramagnetic minerals (e.g. olivines, pyroxenes and pure ilmenite) have weak positive susceptibilities and do not carry remanence. They are, therefore, often unimportant for magnetic interpretation, although in some geological environments paramagnetic mineralogy is detectable by modern high resolution magnetic surveys. Magnetically ordered phases that possess spontaneous magnetisations can be ferromagnetic *sensu stricto* (e.g. iron) or ferrimagnetic (e.g. magnetite). For simplicity, all these strongly magnetic minerals will be referred to hereafter as ferromagnetic. Ferromagnetic minerals lose their spontaneous magnetisation at a characteristic temperature, the Curie point, which is a function only of composition and which can therefore be used to detect particular ferromagnetic phases. Below its Curie temperature a ferromagnetic mineral has high susceptibility and can carry remanence. Above the Curie temperature the mineral becomes paramagnetic, with low susceptibility and no remanence. Paramagnetic minerals have greater susceptibility at low temperatures, reflecting a $\sim 1/T$ dependence, and may become magnetically ordered, i.e.

ISOTHERMAL AND VISCOUS REMANENCE

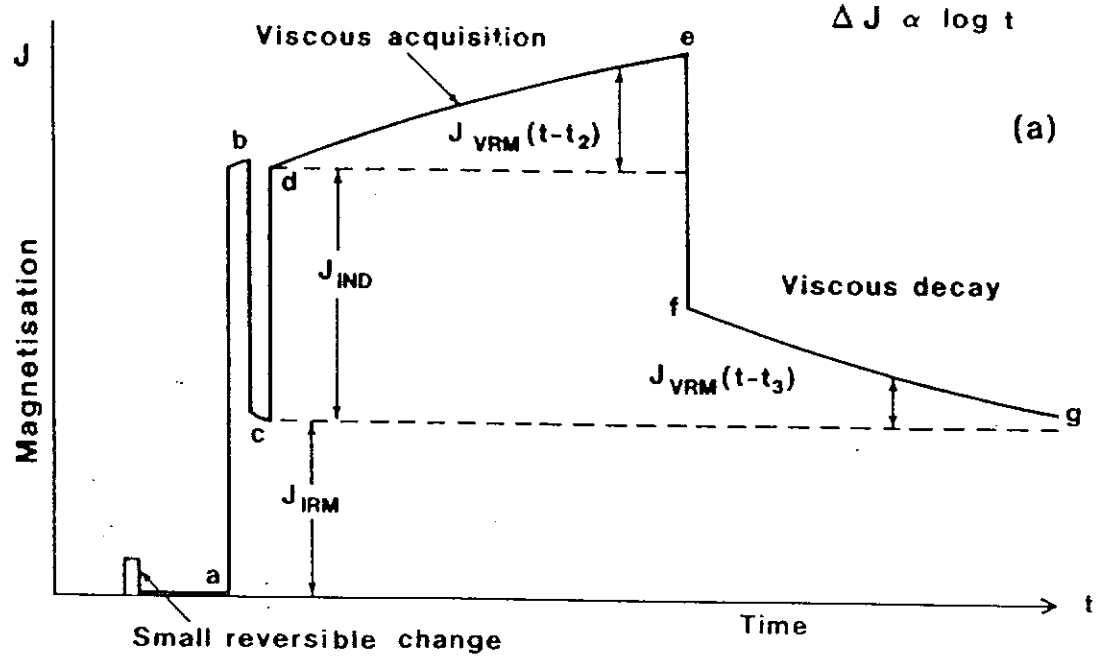

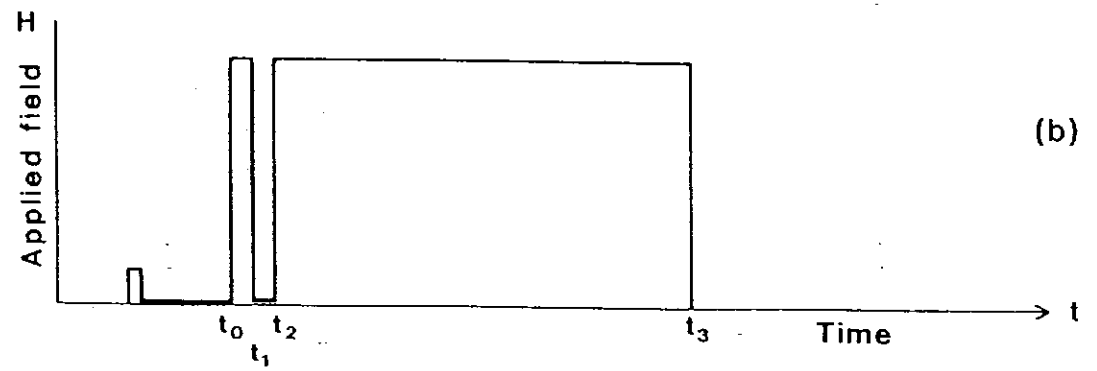

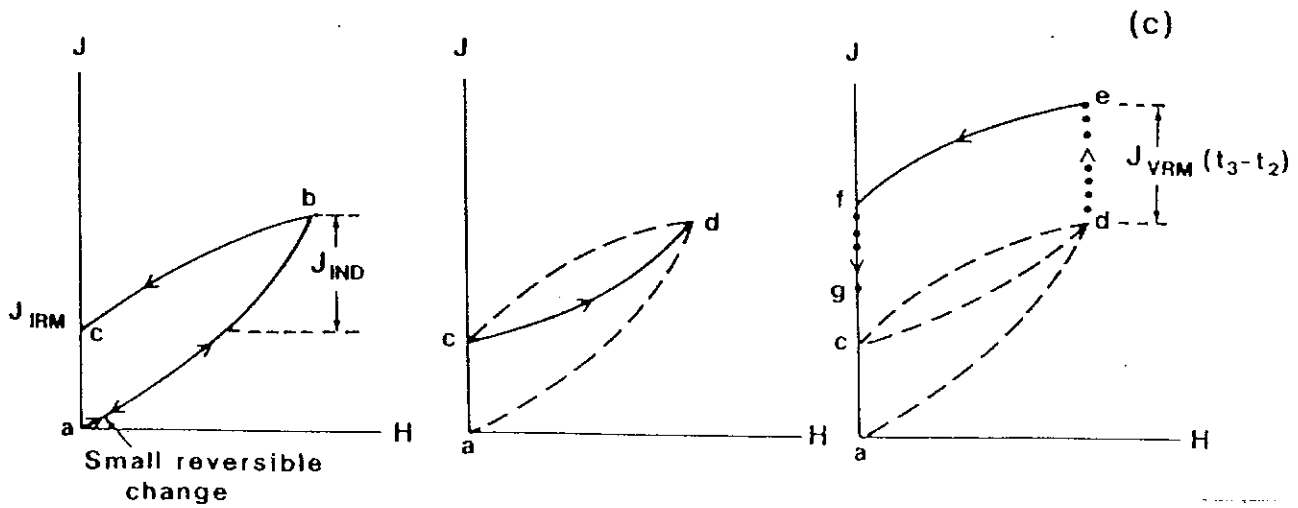

Fig. 4

ferromagnetic or antiferromagnetic, below a transition temperature (the Curie point or the Néel point, respectively) which is composition dependent and can be used to determine the presence of particular paramagnetic minerals.

Fig. 5(a) illustrates the characteristic magnetic hysteresis of ferromagnetic *sensu lato* materials, whereby the magnetisation-field relationship exhibits non-linearity, irreversibility and reflects past magnetic history. Fig. 5(b) shows the arrangement of atomic spin moment in the different classes of magnetic materials.

Domain Structure

The bulk magnetic properties of rocks reflect the modal proportions, compositions and microstructure of the magnetic mineral grains, which are usually present in only minor amounts. Microstructure includes, *inter alia*, grain size and shape, degree of crystallinity and textural relationships and strongly influences the magnetic domain state of the grains. The most important control on domain structure is the effective grain size, which is equivalent to the actual grain size in a homogeneous grain, but is related to lamella size in grains with exsolution lamellae and the size of the ferromagnetic zone in a zoned grain.

Sufficiently small grains are uniformly magnetised, i.e. they have single domain (SD) structure. Ultrafine SD grains (< 0.03 μm for equant magnetite) are sufficiently perturbed by thermal fluctuations that the orientation of the spontaneous magnetisation flips rapidly between two or more easy directions. Such grains cannot retain a stable remanence and their magnetisations tend to relax rapidly towards any applied field, leading to a very high susceptibility. This behaviour is called superparamagnetism, and the grains are termed superparamagnetic (SPM).

The relaxation time for superparamagnetism increases exponentially with grain volume. Thus slightly larger grains have very long relaxation times, even on a geological time scale, and can retain remanent magnetisation indefinitely. These stable SD grains, typically in the micron size range, are important carriers of remanent magnetisation in many rocks. Acicular grain shape, or elongated lamellar shape, favours SD behaviour and extends the maximum size for SD behaviour.

With increasing size it becomes energetically favourable for the grain to subdivide into a number of magnetic domains with differently oriented magnetisations. Figure 6 illustrates the magnetisation distribution in SD and multidomain (MD) grains. These multidomain grains have susceptibilities, controlled by self-demagnetisation, which in the case of strongly magnetic minerals, such as magnetite, are comparable to the susceptibilities of SD grains with similar composition. The remanence of MD grains is more easily demagnetised ("softer") than that carried by SD grains and is of lower specific intensity. The case of magnetite will be considered in some detail, but other magnetic minerals exhibit qualitatively similar behaviour. Magnetite grains larger than ~ 20 μm exhibit true MD behaviour. The coercivity, which is a measure of the ease of demagnetisation, and the remanent intensity decrease steadily with increasing grain size until they level out for grain sizes greater than ~ 100 μm. One measure of coercivity is the median destructive field (MDF) during alternating field demagnetisation (see below).

FERROMAGNETISM

(a) J-H hysteresis loop

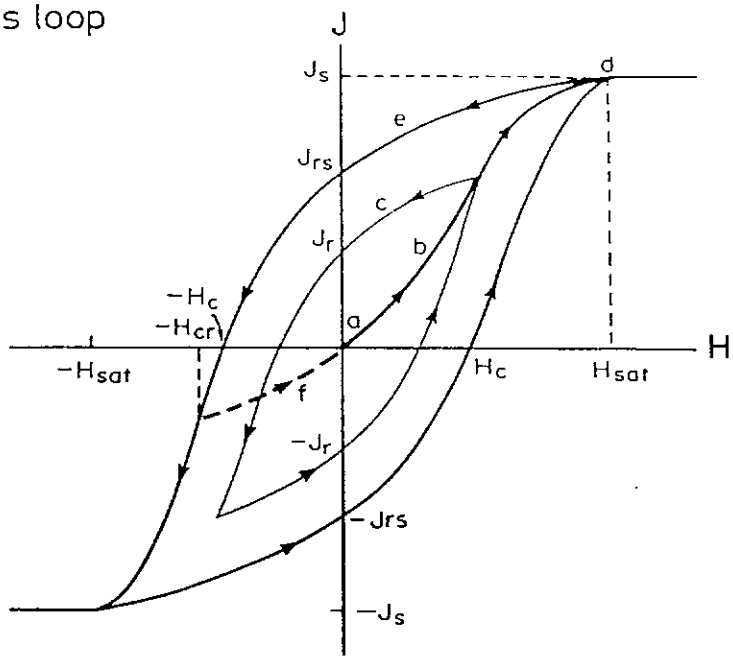

(b) Atomic structure

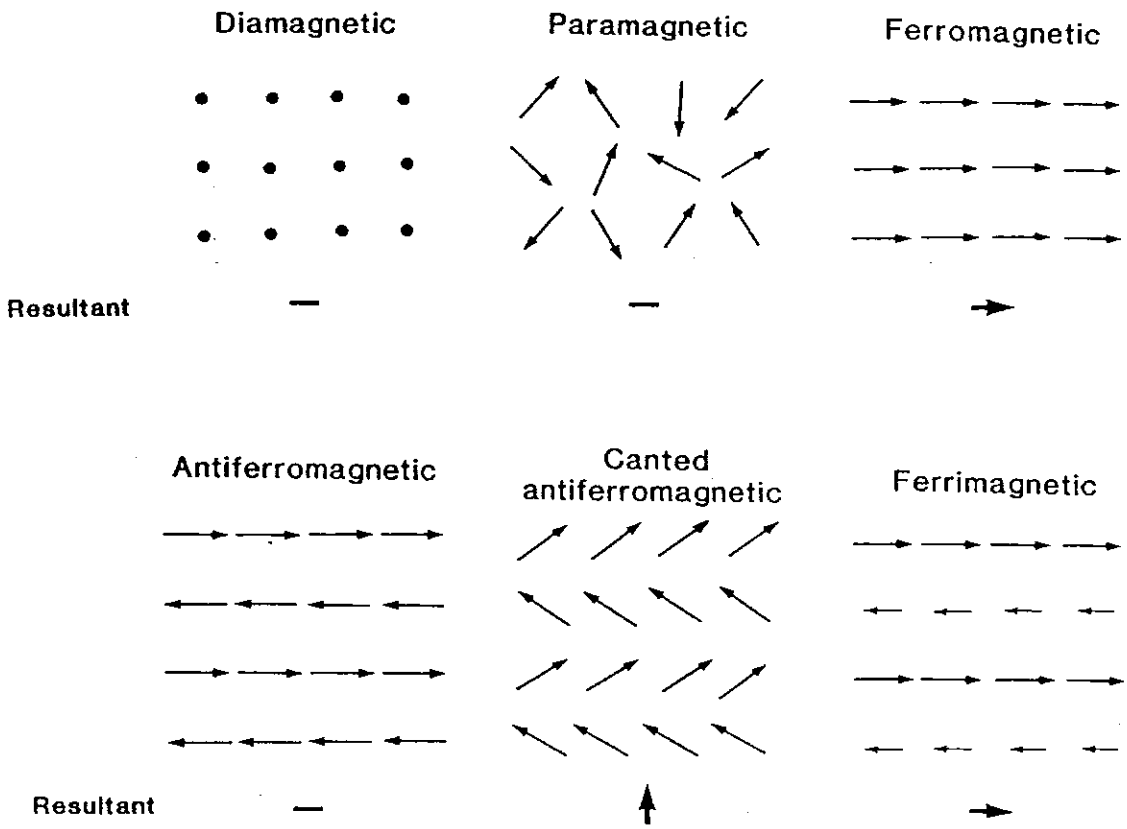

Fig. 5

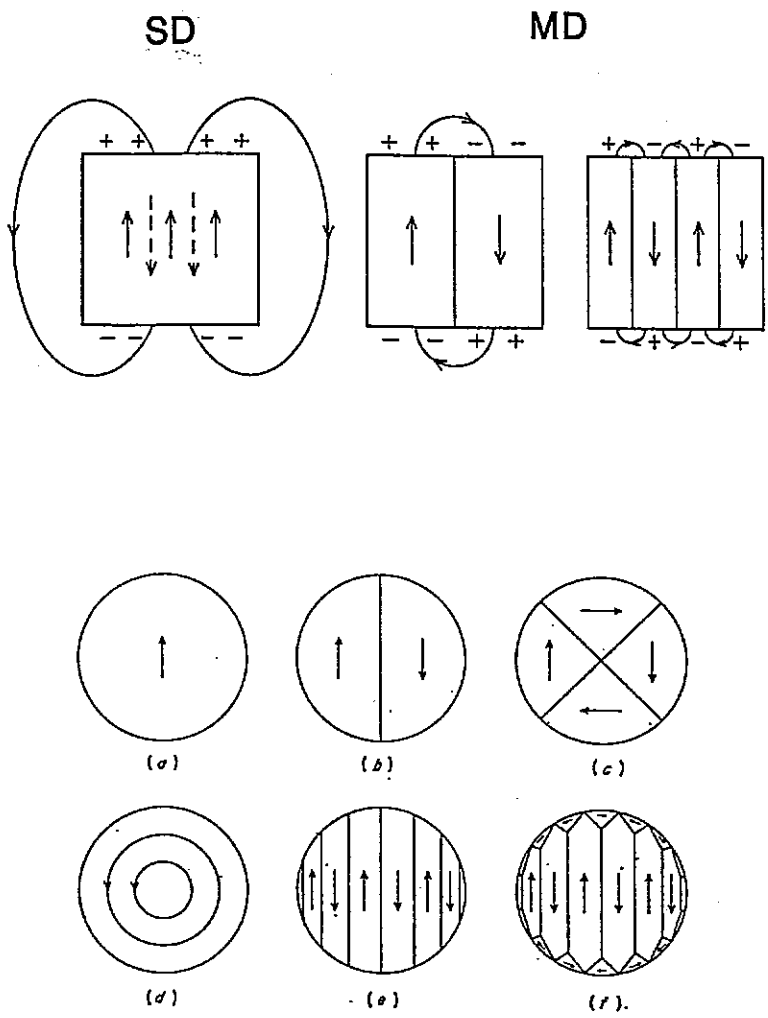

Fig. 6

Grains smaller than ~20 μm have properties intermediate between those of SD and true MD grains and are called pseudosingle domain (PSD). Small PSD grains, a few microns in size, are relatively hard and carry relatively intense remanence. For this reason, small PSD grains are the most important remanence carriers in many rocks, in spite of the fact that they constitute a minor proportion of the magnetic mineral assemblage and even though relatively large MD grains may dominate the susceptibility of the rocks.

The behaviour of some important magnetic properties with increasing grain size (above the SPM threshold size) can be summarised as: remanence, coercivity and Koenigsberger ratio (remanent/induced magnetisation) decrease; susceptibility increases slightly. Typical values of susceptibility, remanent intensity and Koenigsberger ratio of various domain states for a number of magnetic minerals are summarised in Fig. 7 (from Clark, 1983). The theoretical maximum sizes for superparamagnetic and single domain behaviour for equant grains of a number of magnetic minerals are summarised below:

Mineral	**SPM threshold size (μm)**	**Critical SD size (μm)**
Iron	< 0.008	0.023
Magnetite	0.03	0.06
Maghemite	0.02	0.06
Titanomagnetite (60% usp; 40% mt)	0.08	0.40
Hematite	0.03	15.0
Monoclinic pyrrhotite	0.018	1.6

It has become apparent in recent years that magnetic grains frequently occupy metastable domain states of anomalously low domain multiplicity. The above values for the critical SD size assume equilibrium, i.e. that the grain is in the absolute energy minimum state. In fact, grains an order of magnitude larger than the theoretical size can remain in a metastable SD state, because formation of a domain wall requires an energy barrier to be overcome. Thus the effective upper limit for SD behaviour has been extended to ~ 1 μm for magnetite and by a similar factor for other minerals. The threshold sizes are also larger for elongated grains than for equant grains. The domain structure transition sizes for titanomagnetites and other spinel phases with lower spontaneous magnetisations are larger than for magnetite. Thus the single domain/two domain transition, the upper limit of the PSD size range etc. occur at larger grain sizes for spinels with decreasing magnetite contents. Taking metastable behaviour into account, the approximate size ranges and coercivities for SPM, (stable) SD, PSD and MD behaviour for magnetite are listed below:

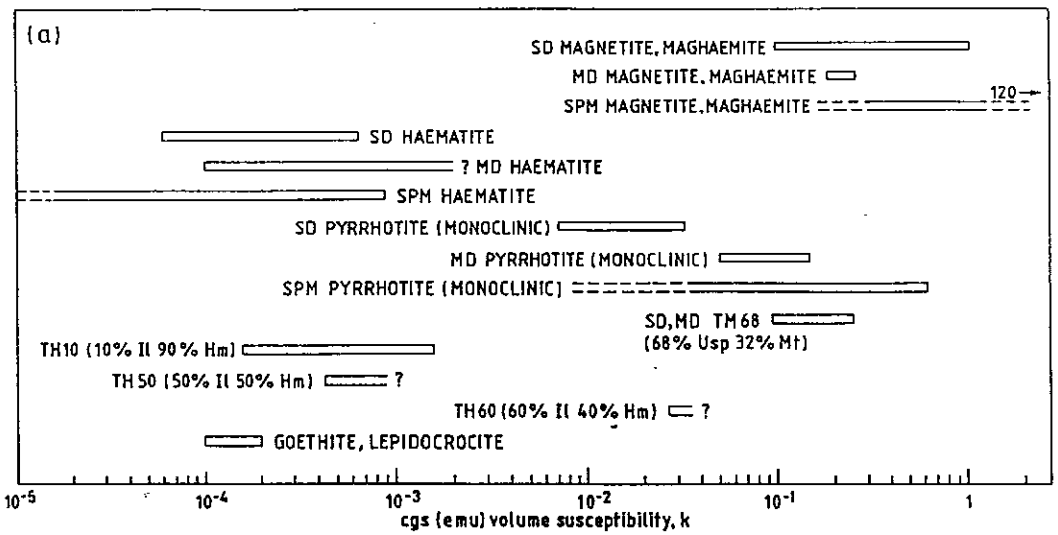
(a)
SD MAGNETITE, MAGHAEMITE
MD MAGNETITE, MAGHAEMITE
SPM MAGNETITE, MAGHAEMITE
120
SD HAEMATITE
? MD HAEMATITE
SPM HAEMATITE
SD PYRRHOTITE (MONOCLINIC)
MD PYRRHOTITE (MONOCLINIC)
SPM PYRRHOTITE (MONOCLINIC)
SD, MD TM 68
(68% Usp 32% Mt)
TH10 (10% Il 90% Hm)
TH 50 (50% Il 50% Hm) ?
TH60 (60% Il 40% Hm) ?
GOETHITE, LEPIDOCROCITE
10⁻⁵
10⁻⁴
10⁻³
10⁻²
10⁻¹
1
cgs (emu) volume susceptibility, k

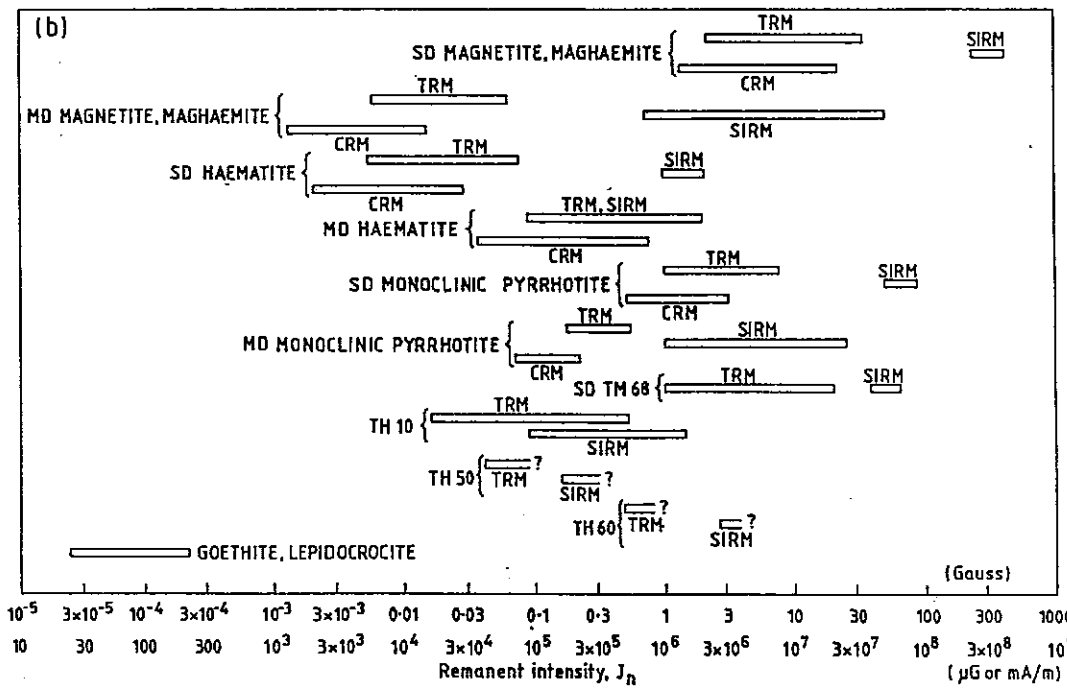
(b)
SD MAGNETITE, MAGHAEMITE
MD MAGNETITE, MAGHAEMITE
SD HAEMATITE
MD HAEMATITE
SD MONOCLINIC PYRRHOTITE
MD MONOCLINIC PYRRHOTITE
SD TM 68
TH 10
TH 50
TH 60
TRM
CRM
SIRM
TRM, SIRM
GOETHITE, LEPIDOCROCITE
(Gauss)
10⁻⁵ 3×10⁻⁵ 10⁻⁴ 3×10⁻⁴ 10⁻³ 3×10⁻³ 0·01 0·03 0·1 0·3 1 3 10 30 100 300 1000
10 30 100 300 10³ 3×10³ 10⁴ 3×10⁴ 10⁵ 3×10⁵ 10⁶ 3×10⁶ 10⁷ 3×10⁷ 10⁸ 3×10⁸ 10⁹
Remanent intensity, Jn
(μG or mA/m)

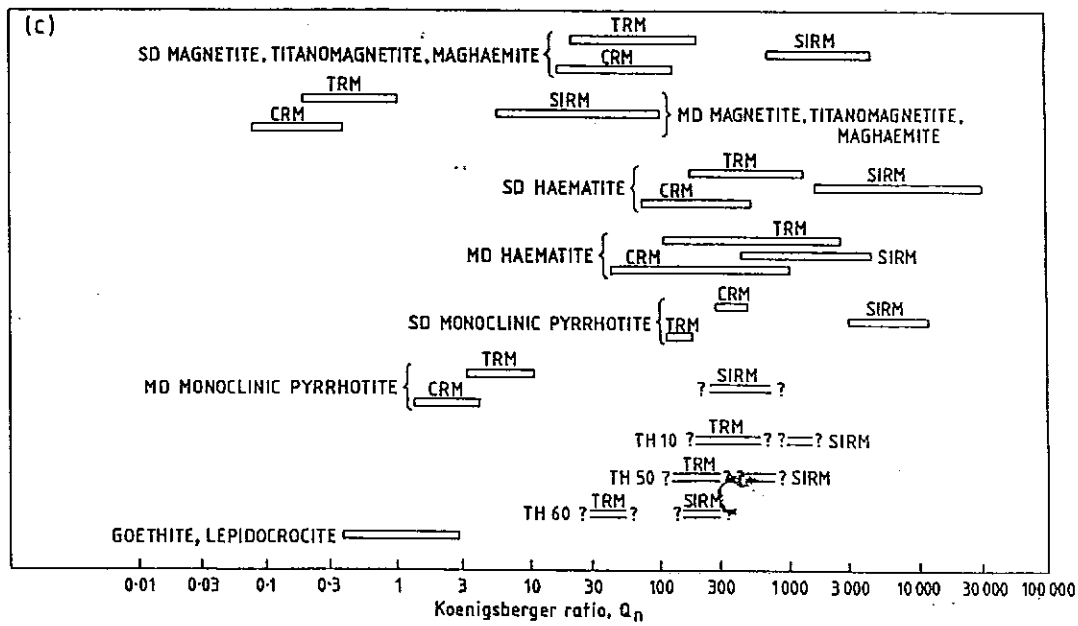
(c)
SD MAGNETITE, TITANOMAGNETITE, MAGHAEMITE
MD MAGNETITE, TITANOMAGNETITE, MAGHAEMITE
SD HAEMATITE
MD HAEMATITE
SD MONOCLINIC PYRRHOTITE
MD MONOCLINIC PYRRHOTITE
TH 10 ? ? ? ? SIRM
TH 50 ? ? ? SIRM
TH 60 ? ? ? SIRM
TRM
CRM
SIRM
GOETHITE, LEPIDOCROCITE
0·01 0·03 0·1 0·3 1 3 10 30 100 300 1000 3 000 10 000 30 000 100 000
Koenigsberger ratio, Qn

Fig. 7

Domain structure	Size (μm)	Coercivity (Oe)
SPM	< 0.05	0
(acicular) SD	0.05-1	> 600
PSD	~1-20	100-600
MD	> 20	< 100

Intrinsic Magnetic Properties of Minerals

The intrinsic magnetic properties, spontaneous magnetisation at room temperature, (J_s) and Curie temperature (T_C), which are dependent only on composition, are given below for a number of minerals, including some end-member spinel phases:

Mineral name	Chemical formula	Magnetic properties
Iron	Fe	$T_C = 770°C$, $J_s = 1710$ G
Awaruite	Ni_3Fe	$T_C = 620°C$, $J_s = 950$ G
Magnetite	Fe_3O_4	$T_C = 580°C$, $J_s = 480$ G
Ulvospinel	Fe_2TiO_4	$T_C = -153°C$, $J_s = 0$
Titanomagnetite (100x mole% usp)	$Fe_{3-x}Ti_xO_4$	$0 \le x \le 0.8$ ferro; $x \ge 0.8$ paramag.
Maghemite	γFe_2O_3	$T_C >> 300°C$*, $J_s = 440$ G
Hematite	αFe_2O_3	$T_C = 670°C$, $J_s = 2$ G
Titanohematite (100x mole% ilm)	$Fe_{2-x}Ti_xO_3$	$0 \le x \le 0.5$ antiferro; $0.5 \le x \le 0.8$ ferro; $0.8 < x < 1$ paramagnetic
Ilmenite	$FeTiO_3$	$T_C = -205°C$, $J_s = 0$
Monoclinic (4C) pyrrhotite	Fe_7S_8	$T_C = 320°C$, $J_s = 90$ G
Magnesioferrite	$MgFe_2O_4$	$T_C \lesssim 420°C$, $J_s \lesssim 220$ G
Chromite	$FeCr_2O_4$	$T_C = -185°C$, $J_s = 0$
Ferrichromite/ Cr-magnetite	$Fe_{3-x}Cr_xO_4$ e.g. Fe_2CrO_4	ferromagnetic for $0 \le x \le 1.2$, $T_C = 200°C$, $J_s = 250$ G
Hercynite	$FeAl_2O_4$	$T_C = -265°C$, $J_s = 0$
Magnesian ulvospinel	Mg_2TiO_4	diamagnetic
Picrochromite	$MgCr_2O_4$	$T_C = -258°C$, $J_s = 0$
Spinel	$MgAl_2O_4$	diamagnetic
Jacobsite/ Mn-magnetite	$Fe_{3-x}Mn_xO_4$ e.g. Fe_2MnO_4	ferromagnetic for $0 \le x \le 2.5$ $T_C = 300°C$, $J_s = 398$G
Trevorite	$NiFe_2O_4$	$T_C = 595°C$, $J_s = 330$ G
Coulsonite	FeV_2O_4	$T_C = -164°C$, $J_s = 0$

The Curie point of maghaemite cannot be observed directly because maghaemite inverts to haematite at temperatures > 300°C, depending on impurities. The Curie temperature of magnetite-bearing spinel minerals varies systematically with magnetite content. To a first approximation, the Curie point of a particular spinel composition can be estimated by linear interpolation between T_C of the constituent end members. Diamagnetic minerals can be assigned a nominal T_C of absolute zero (-273°C) for this purpose. For the titanomagnetite series, a more accurate expression relating Curie temperature to mole fraction of ulvospinel (x) is:

$$Fe_{3-x}Ti_xO_4: T_C\,(°C) = 578 - 580x - 150x^2.$$

The effect on T_C of substitution of Cr, Al and V into magnetite is broadly similar to that of Ti substitution. Substitution of Ni increases the Curie point slightly, as does cation deficiency. Thus cation-deficient magnetites ("kenomagnetite"), representing compositions intermediate between stoichiometric magnetite and maghaemite, can have T_C above 600°C. Magnesioferrite is the only important spinel end member, other than magnetite, that is ferromagnetic at room temperature. The magnetic properties of magnesioferrite depend strongly on the cation distribution, which reflects thermal history. The Curie point of $MgFe_2O_4$ is given by:

$$MgFe_2O_4:\ T_C\,(°C) = 417 - 490f,$$

where f is the fraction of Mg^{2+} ions on tetrahedral sites. Because of the elevated T_C and high spontaneous magnetisation, magnesioferrite-rich spinels and Mg-magnetites are strongly magnetic and can be important contributors to the magnetic properties of rocks in which they occur.

A note of caution concerning the magnetic properties of spinels needs to be sounded. Although a number of three component solid solution series have been studied, in most cases the data are restricted to the edges of the spinel prisms. Large portions of the interiors have not been systematically investigated. Although there is some theoretical basis for predicting the properties of complex spinel compositions, unusual behaviour has been found in special cases and it is conceivable that some kimberlitic spinels may have unexpected behaviour. As an example, solid solutions between ulvospinel and chromite have been investigated by Schmidbauer (1971) and by Banerjee (1972). Schmidbauer's samples were paramagnetic, as expected. Banerjee's samples were analogues of lunar titanchromites and, in contrast to those of Schmidbauer, contained no Fe^{3+}. Some compositions showed unexpected behaviour. For example, a synthetic solid solution containing 15 mole % ulvospinel and 86 mole % chromite, prepared under reducing conditions, has T_C = 150°C and a reversible transition, with a large increase in susceptibility, on cooling through -170°C. The magnetic phase diagram of the titanohematite series is complex and the magnetic properties of the compositions that are ferromagnetic at room temperature are influenced by thermal history. $FeTiO_3$-Fe_2O_3 solid solutions have been thoroughly studied. The Curie temperature decreases approximately linearly with increasing ilmenite content. Compositions with less than 20 mole% haematite are paramagnetic at room temperature. The magnetic properties of picroilmenites (solid solutions between ilmenite, haematite and geikielite, $MgTiO_3$) have not been systematically studied outside the Soviet Union. Most of the data have been

gathered from kimberlitic ilmenite megacrysts, but the Russian literature on this subject is often difficult to interpret, even in translation, and some inconsistencies between different studies are evident.

Pure haematite has a diagnostic magnetic transition (the Morin transition) at -20°C. Below this temperature atomic magnetic moments are aligned with the crystallographic c-axis and haematite is antiferromagnetic. Above the transition the moments lie in the basal plane but are slightly canted out of antiparallelism, giving rise to weak ferromagnetism and an increased susceptibility. The Morin transition can also be exploited for diagnosis of well-crystallised hematite by the effect of low temperature demagnetisation on remanence (see below).

Fig.8(a) shows the compositions of the Fe-Ti oxide minerals that play a major role in rock magnetism. The rhombohedral titanohematites are second in importance only to the titanomagnetites. Titanohematites containing between 50 mole% and 80 mole% ilmenite are strongly magnetic and are efficient carriers of remanence. Compositions closer to ilmenite are paramagnetic at room temperature and hematite-rich compositions are only weakly magnetic. Titanomagnetites with less than ~80 mole% ulvospinel are ferromagnetic at room temperature. Although the spontaneous magnetization and Curie temperature of titanomagnetites decrease steadily with increasing titanium content (Fig.8(b)-(c)), the susceptibility and specific remanent intensity of TRM are not strongly dependent on composition for the ferromagnetic phases. Thus high titanium content in magnetite does not generally produce weaker magnetic properties, contrary to popular opinion. In fact, grain size is a more important factor influencing magnetization of titanomagnetite-bearing rocks (see Fig.8(d)-(e)).

Palaeomagnetic Cleaning Techniques

The natural remanent magnetisation (NRM) of a rock may consist of components, carried by different subpopulations of magnetic minerals, acquired at different times. During initial cooling of an igneous rock, magnetic mineral grains make the transition from paramagnetism to ferromagnetism as they cool through their Curie points. A spontaneous magnetisation appears that is initially in equilibrium with the applied field, but becomes "frozen in" or blocked at a somewhat lower temperature, called the blocking temperature, when the relaxation time of the grain's magnetic moment increases prodigiously. Below the blocking temperature the magnetisation is a stable remanence that is known as thermoremanent magnetisation (TRM). If grain growth of magnetic minerals or creation of new magnetic phases occurs below the Curie temperature, there is a huge increase in relaxation time as the grains become larger than the SPM threshold size. This produces a stable chemical remanent magnetisation (CRM). If CRM is acquired at elevated temperatures, the remanence has both thermal and chemical character and is known as thermochemical remanence.

Other components of remanence may be acquired at later times due to metamorphic overprinting, weathering etc. Each separate component of remanence is acquired parallel to the ambient field at the time of its acquisition. Rock samples may also acquire palaeomagnetic noise components due to exposure to magnetic fields, for instance during mining operations or during or after collection. All these components contribute to the

(a) Iron-titanium oxide minerals

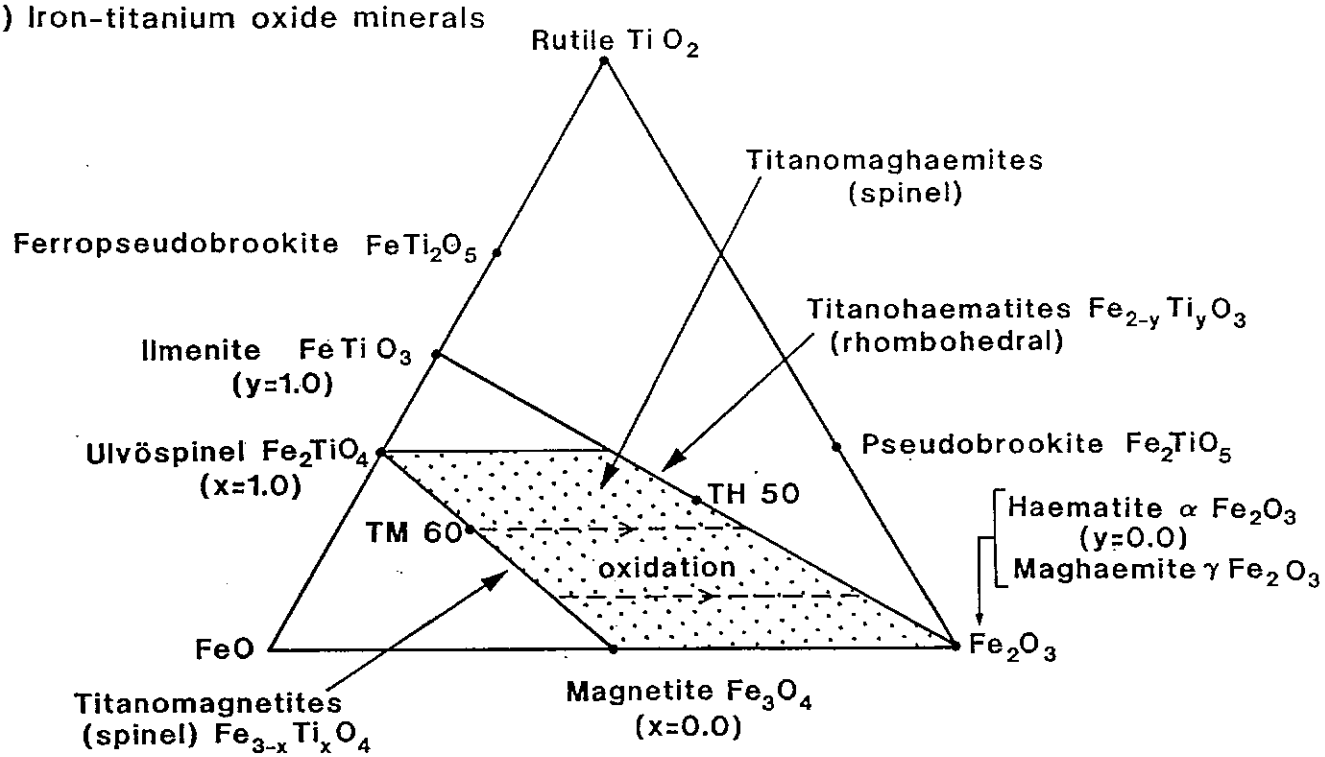

(b) Curie temperature of TMs

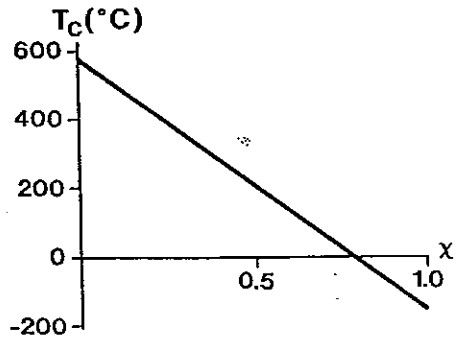

(c) Spontaneous magnetisation of TMs

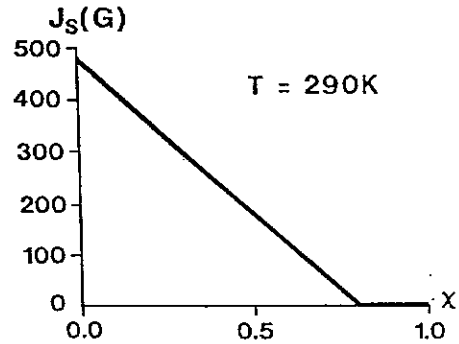

(d) Susceptibility of TMs

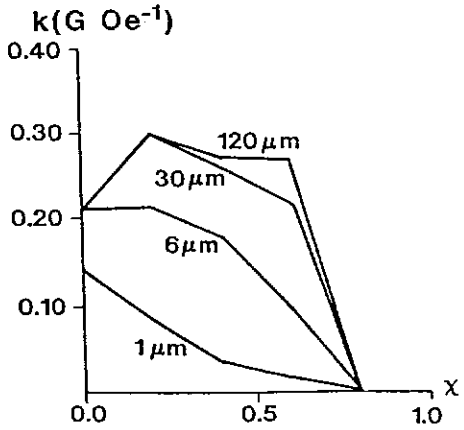

(e) TRM of TMs (H = 1Oe)

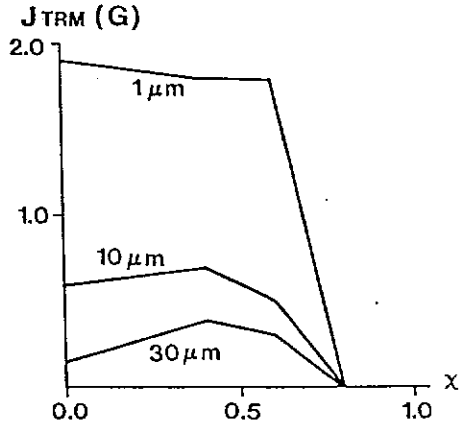

Fig. 8

measured NRM of a rock sample. Figure 9 illustrates a possible scenario for acquisition of a complex multicomponent NRM. Because different remanence components are carried by subpopulations of grains with different characteristics, they can usually be distinguished by their different responses to various demagnetisation techniques.

Alternating field (AF) demagnetisation is similar to degaussing of permanent magnetisation of ships or tape recorder heads. The sample is subjected to an alternating magnetic field that is gradually reduced to zero, thereby randomising the moments of all grains with coercivity less than the initial AF amplitude. This procedure is repeated at successively higher fields, demagnetising successively harder fractions of the magnetic mineral assemblage and isolating the most stable component of remanence. AF demagnetisation is particularly effective at removing isothermal remanent magnetisation (IRM) acquired by exposure to strong magnetic fields, such as those produced by mining equipment or lightning strikes etc.

Thermal demagnetisation involves heating the sample and recooling to room temperature, in zero magnetic field. This randomises the magnetic moments of all grains with blocking temperatures less than the heating temperature. This procedure is repeated at successively higher temperatures, thereby demagnetising successively higher blocking temperature fractions. Thermal demagnetisation is particularly effective at unravelling the thermal history of the rock, for instance by resolving primary TRM from a later metamorphic overprint.

Low temperature demagnetisation involves cooling the sample to very low temperatures (e.g. the boiling point of liquid nitrogen) and rewarming to room temperature, in zero field. This technique exploits low temperature magnetic transitions of particular magnetic minerals, to isolate remanence components carried by different minerals or by different grain size fractions of magnetite, for example. The effect of low temperature demagnetisation can be characterised by the parameter R_K, which is the ratio of the remanence remaining at room temperature, after cooling to -196°C in zero field, to the original remanence.

Palaeomagnetic cleaning techniques have three main applications, which can be termed palaeomagnetic, petrophysical and rock magnetic respectively:

(i) Resolution of remanence components acquired at different times, allowing estimation of palaeofield directions and palaeopole positions at the time of formation, at the time of metamorphism etc.,

(ii) Removal of palaeomagnetic noise components, which are not representative of the bulk in situ properties, allowing characteristic NRMs of the rock to be determined,

(iii) Identification of magnetic minerals by their demagnetisation characteristics. Information on compositions, domain states and grain sizes of the magnetic minerals can be obtained.

The most useful method of depicting demagnetisation of multicomponent remanence is that of orthogonal projections. These are generally termed Zijderveld plots. The basic idea of these plots is illustrated in Fig.10. The end-points of the remanence vectors after successive demagnetisation steps describe a trajectory in 3D space. Over a treatment interval where a single remanence component is removed this trajectory defines a linear segment. Where two or more remanence components are being removed simultaneously, due to their having overlapped stability spectra, the trajectory is curved. After removal of all less stable components, the trajectory of the most stable component is a straight line heading towards the origin, indicating decreasing intensity without change in direction. The stability spectrum corresponding to thermal demagnetisation is the blocking temperature spectrum and for AF demagnetisation it is the coercivity spectrum.

The differences in AF demagnetisation behaviour of acicular SD, small PSD and large MD magnetite is shown in Fig.11. The remanence that is being demagnetised is an artificially imparted saturation IRM (SIRM), produced by placing the samples in a very strong field. The plot shows the remanent intensity, normalised to the initial value before AF treatment, versus AF field. The corresponding coercivity spectra can be obtained from the demagnetisation curves by differentiation, as the coercivity spectrum is the magnitude of the slope of the demagnetisation curve. Thus the coercivity spectrum of the large MD grains peaks at low fields (less than 5 mT), the spectrum for the small PSD grains peaks at ~ 15 mT and that of the SD grains peaks above 40 mT. The Lowrie-Fuller test exploits the differences between AF demagnetisation behaviour of small and large grains. For SD and PSD grains weak field remanence, such as TRM, is more resistant to demagnetisation than strong field remanence, particularly SIRM. For true MD grains the relative stability of weak and strong field remanences is reversed.

Demagnetisation behaviour can be used to detect the presence of other magnetic minerals. For example, haematite is very hard (MDF > 1000 Oe = 100 mT) and does not thermally demagnetise until close to 670°C. Goethite has even greater coercivity than haematite, but breaks down to haematite at ~120°C, and is therefore very easily thermally demagnetised.

Thermomagnetic Analysis of Magnetic Mineralogy

The variation of magnetic properties of magnetic minerals with temperature depends on composition and, in some cases, on domain state and microstructure. This variation can therefore be used for analysis of magnetic minerals. The variation of susceptibility with temperature is particularly useful, because of the rapid change in susceptibility close to T_C, which enables well-defined Curie points to be determined, and because of the sensitivity of susceptibility to domain state and microstructure.

The characteristic susceptibility (k) versus temperature (T) behaviour of different magnetic minerals is shown in Fig.12. The k-T curve for paramagnetic minerals is hyperbolic, reflecting the 1/T dependence of paramagnetic susceptibility. The k-T curve of magnetite with MD structure, including PSD grains as well as true MD, grains is very diagnostic. There is a prominent peak at -155°C, which corresponds to the isotropic point of magnetite. Below this temperature the easy magnetisation directions are along the <100> cubic axes, whereas above it the easy directions lie along <111> body diagonals of

ACQUISITION OF MULTICOMPONENT MAGNETISATION

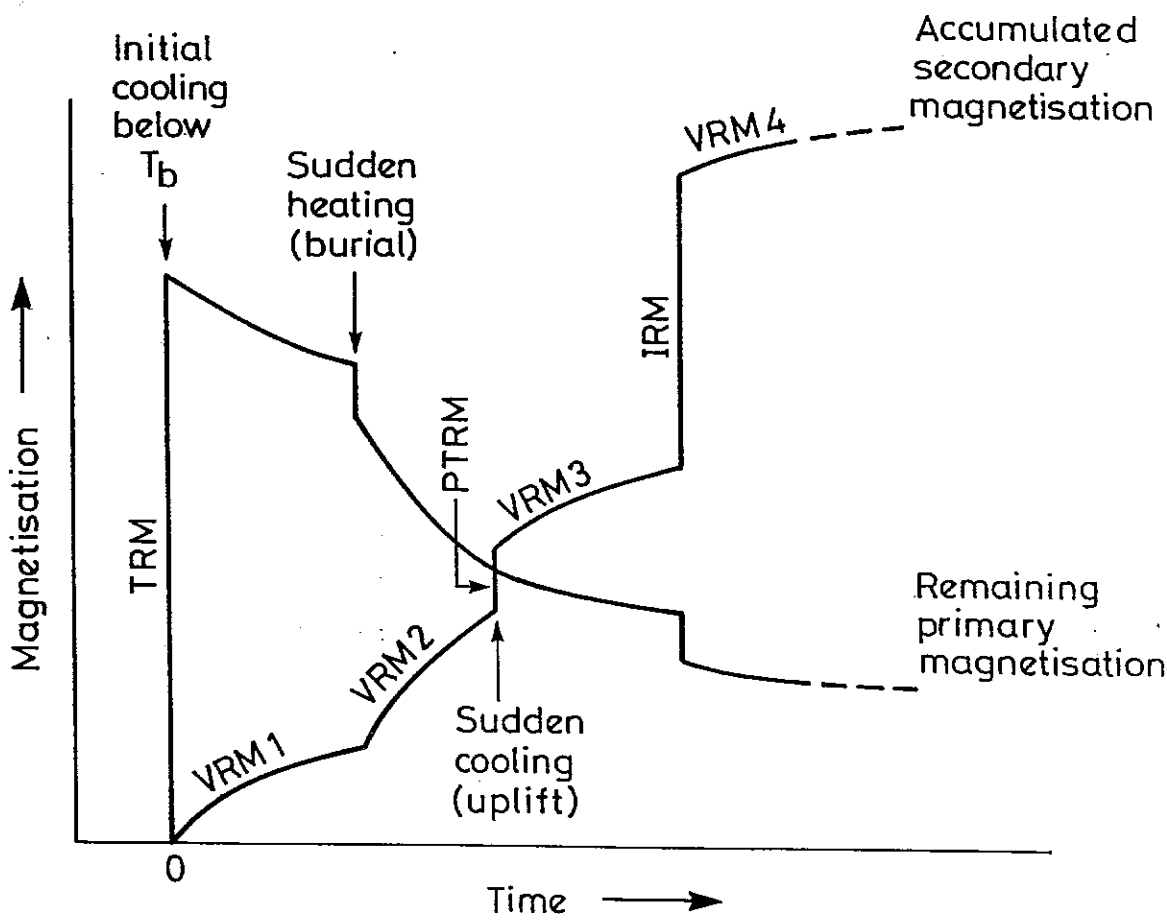

Fig. 9.

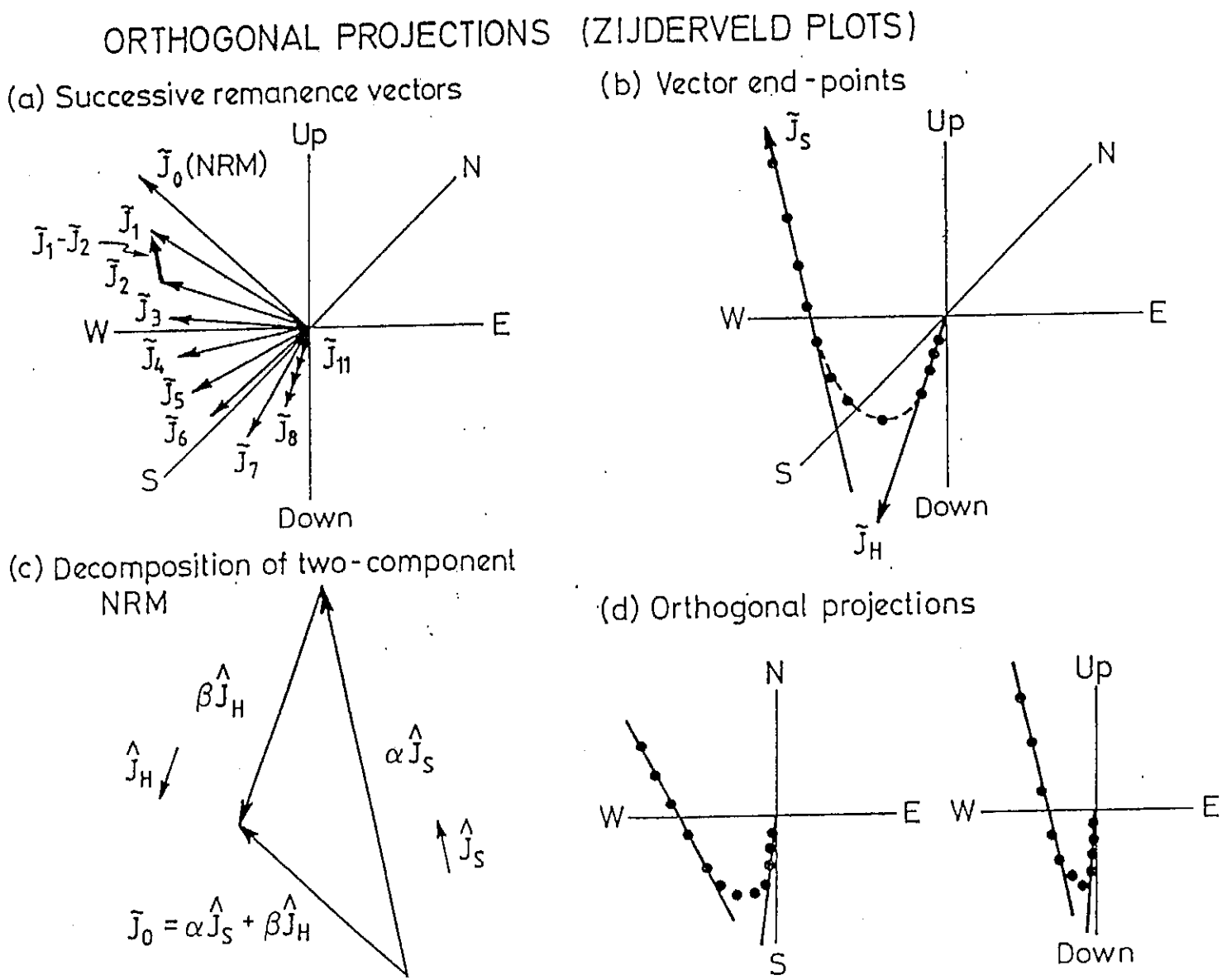
ORTHOGONAL PROJECTIONS (ZIJDERVELD PLOTS)
(a) Successive remanence vectors
Up
N
E
W
S
Down
$\tilde{J}_0$(NRM)
$\tilde{J}_1$
$\tilde{J}_1$-$\tilde{J}_2$
$\tilde{J}_2$
$\tilde{J}_3$
$\tilde{J}_4$
$\tilde{J}_5$
$\tilde{J}_6$
$\tilde{J}_7$
$\tilde{J}_8$
$\tilde{J}_{11}$
(b) Vector end-points
$\tilde{J}_S$
$\tilde{J}_H$
(c) Decomposition of two-component NRM
$\beta\hat{J}_H$
$\alpha\hat{J}_S$
$\hat{J}_H$
$\hat{J}_S$
$\tilde{J}_0 = \alpha\hat{J}_S + \beta\hat{J}_H$
(d) Orthogonal projections

Fig. 10

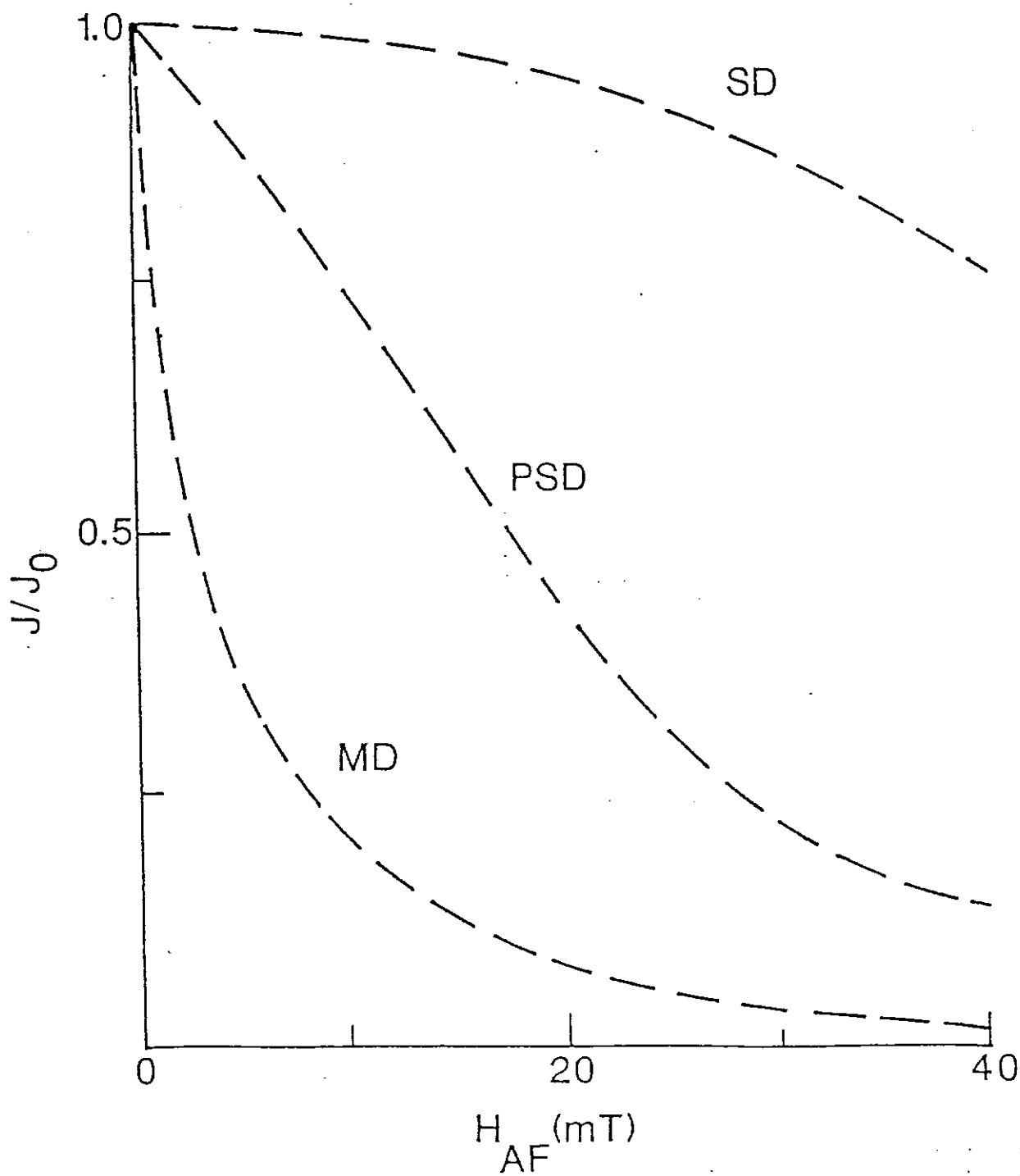

Fig. 11

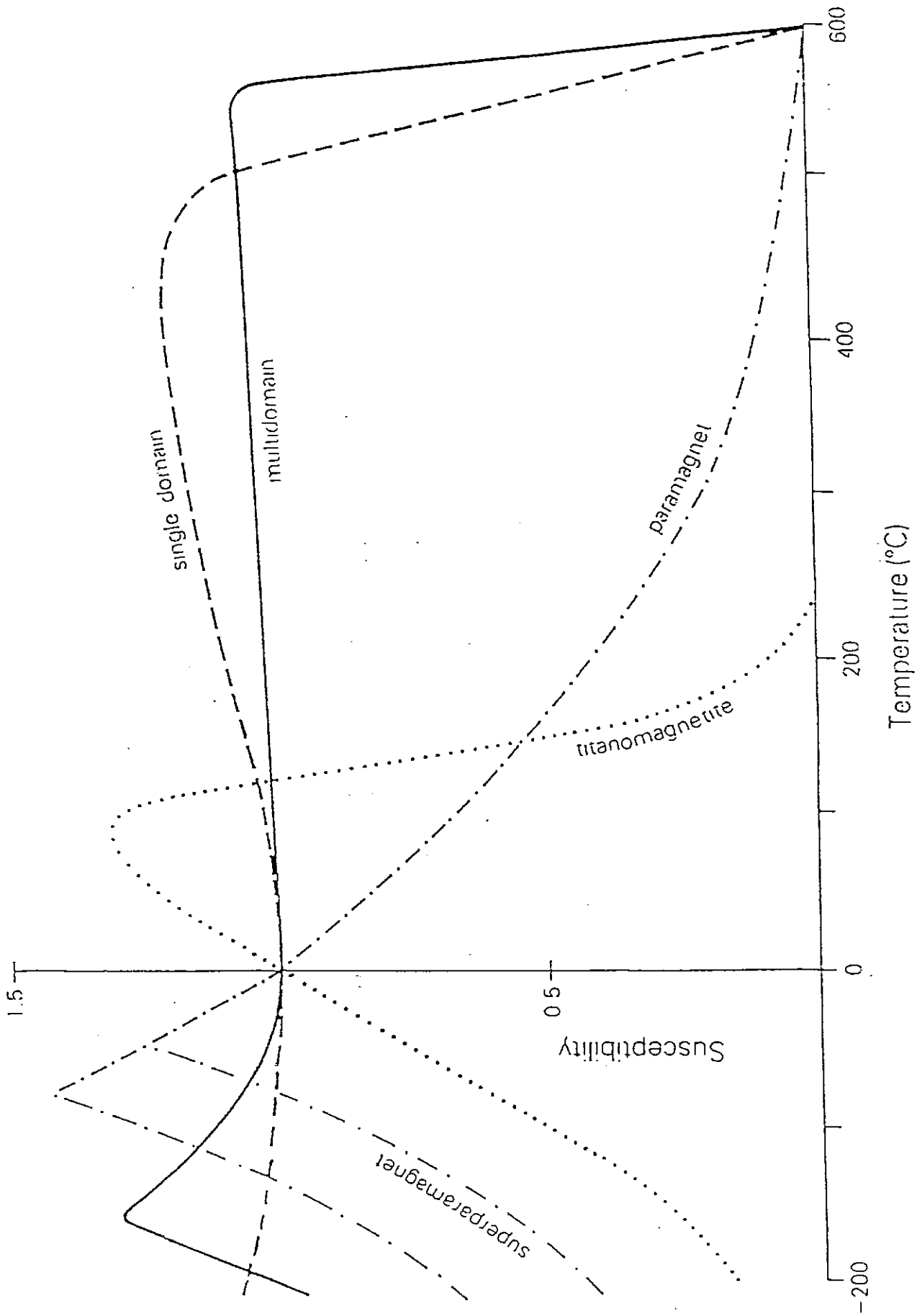
600
400
200
0
−200
Temperature (°C)
1.5
0.5
Susceptibility
single domain
multidomain
paramagnet
titanomagnetite
superparamagnet

Fig. 12

the cubic unit cell. At the isotropic point the magnetisation rotates freely to align with an applied field, giving rise to an increase in susceptibility. The susceptibility of MD grains is limited by self-demagnetisation and the observed susceptibility remains almost constant until just below the Curie temperature, when it plummets to paramagnetic values. The isotropic point is very sensitive to composition and substitution of cations other than iron, or departures from stoichiometry, tend to lower the isotropic point. Titanomagnetites containing more than ~10 mole% ulvospinel have isotropic points below liquid nitrogen temperature. Thus the presence of a well-defined peak at ~-155°C is diagnostic of the presence of nearly pure PSD and/or MD magnetite.

The titanomagnetite for which the k-T curve is shown has a Curie point of ~200°C and contains ~60 mole% ulvospinel. The k-T curve is irreversible on cooling from high temperature (not shown), due to exsolution of more magnetite-rich and magnetite-poor titanomagnetites than the original composition. Thus two Curie points, one above 500°C and the other shifted somewhat lower than the original T_C, would be seen in the cooling curve.

The k-T curve for SD magnetite does not exhibit a peak at the isotropic point because the properties of SD grains are controlled largely by shape anisotropy, rather than by magnetocrystalline anisotropy. The susceptibility is almost constant at low temperatures, but increases as the Curie temperature is approached. This increase in k reflects unblocking of fine grains below T_C.

The susceptibility of grains increases sharply at the unblocking temperature because the relaxation time suddenly decreases, allowing the magnetic moments of the grains to align freely with the applied field. Above the unblocking temperature the superparamagnetic susceptibility of grains of specified volume is proportional to J_s^2/T and is much higher than the room temperature susceptibility, until the Curie temperature is approached (at which point $J_s \rightarrow 0$, so $k \rightarrow 0$). Thus the presence of significant unblocking of remanence well below the Curie temperature indicates that this portion of the remanence is carried by very fine (submicron) single domain grains.

Even smaller grains unblock at much lower temperatures and exhibit superparamagnetism at room temperature. The k-T curve shown for SPM grains is idealised for an assemblage of identical grains. In rocks there is always a distribution of grain sizes and the superposition of unblocking peaks over a wide range of temperatures leads to a steady increase in susceptibility from below room temperature up to the maximum unblocking temperature of the ultrafine SPM + SD assemblage. This behaviour is commonly seen in soil samples, particularly lateritic soils.

As the Curie temperature of a magnetic mineral is approached, there is a rapid decrease in spontaneous magnetisation and an even more rapid decrease in magnetocrystalline anisotropy. As a consequence the remanence of even the most stable grains unblocks, but without an increase in k. In fact, the susceptibility plummets until it attains paramagnetic values at T_C.

Typical k-T curves of a monzonite containing only PSD/MD magnetite and a basalt containing only MD titaniferous magnetite are shown in Fig.13. The thermomagnetic

curve of paramagnetic ilmenite separated from a beach sand deposit is depicted in Fig.14. The irreversibility of the curves for the basalt and the ilmenite extract indicates chemical change has occurred. This illustrates the sensitivity of k-T curves to changes, such as oxidation, exsolution and rehomogenisation, in magnetic minerals during heating.

Thermal demagnetisation of remanence provides another analytical technique. MD grains exhibit a spectrum of unblocking temperatures right up to T_C, whereas the unblocking temperature spectrum of SD grains cuts off below the Curie point. However, given that the grain size range of a particular mineral extends at least to the upper end of the SD range, the maximum unblocking temperature lies just below T_C. Thus Curie points can also be estimated from thermal demagnetisation data. Prominent inflexions in the demagnetisation curve, corresponding to a sharp peak in the blocking temperature spectrum, indicate the approximate Curie temperature of a particular phase. Comparison of the blocking temperature spectra with k-T curves enable phases originally present in samples to be distinguished from phases created during heating. Low temperature demagnetisation also allows magnetic transitions characteristic of magnetite and haematite to be detected. Judicious application of a variety of rock magnetic techniques, including thermomagnetic analysis, allows the relative contributions to susceptibility and remanence of different compositions and grain size ranges to be estimated.

Thermomagnetic curves for a number of iron ore samples with different mineralogies are presented in Fig.15. The detection of MD magnetite, SD magnetite, haematite and maghaemite by thermomagnetic analysis is well illustrated by this collection of k-T curves. A final example is afforded by the k-T curve of a lateritic soil sample (Fig. 16), which illustrates well many of the features discussed above.

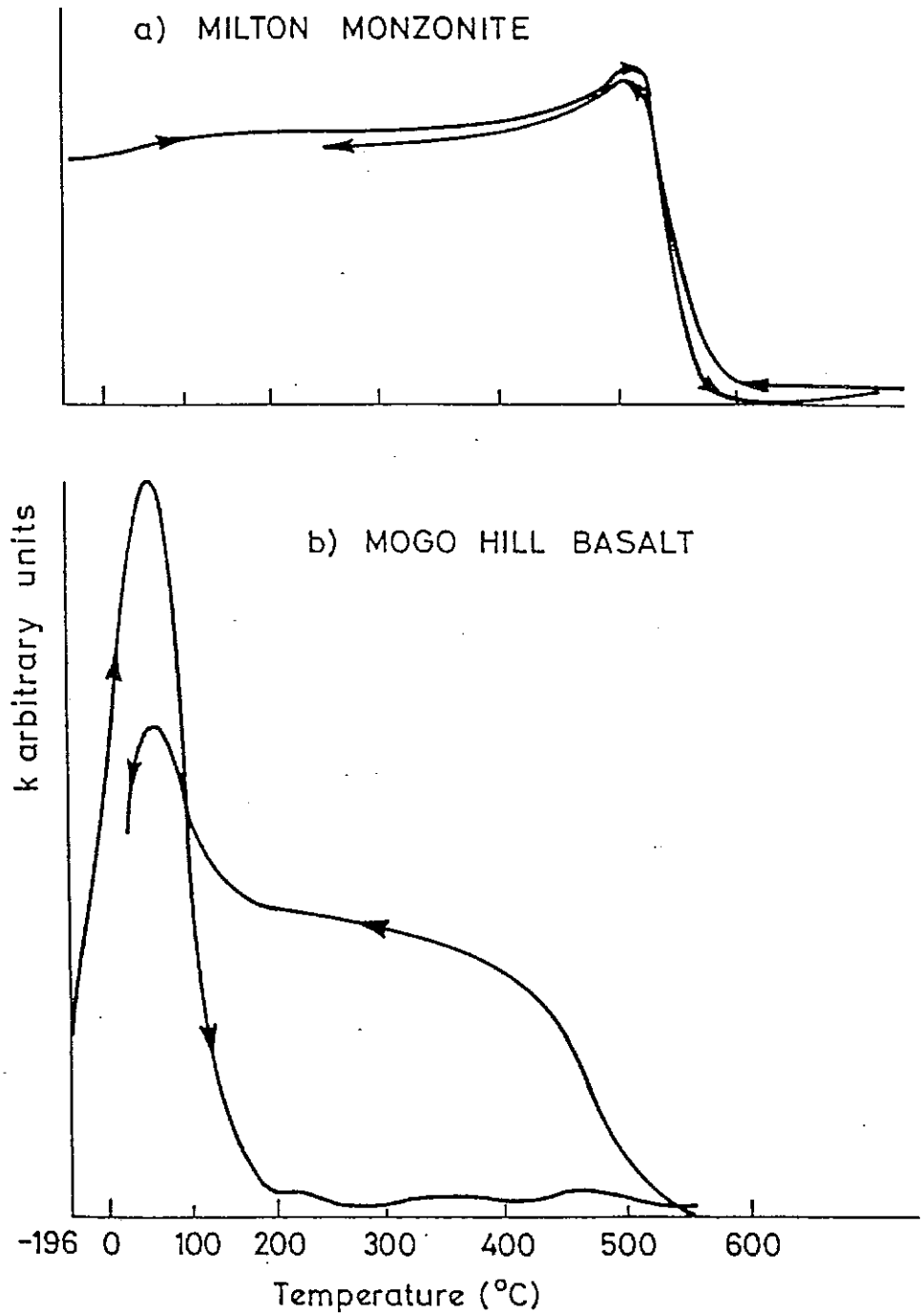
a) MILTON MONZONITE
b) MOGO HILL BASALT
k arbitrary units
-196
0
100
200
300
400
500
600
Temperature (°C)

Fig. 13

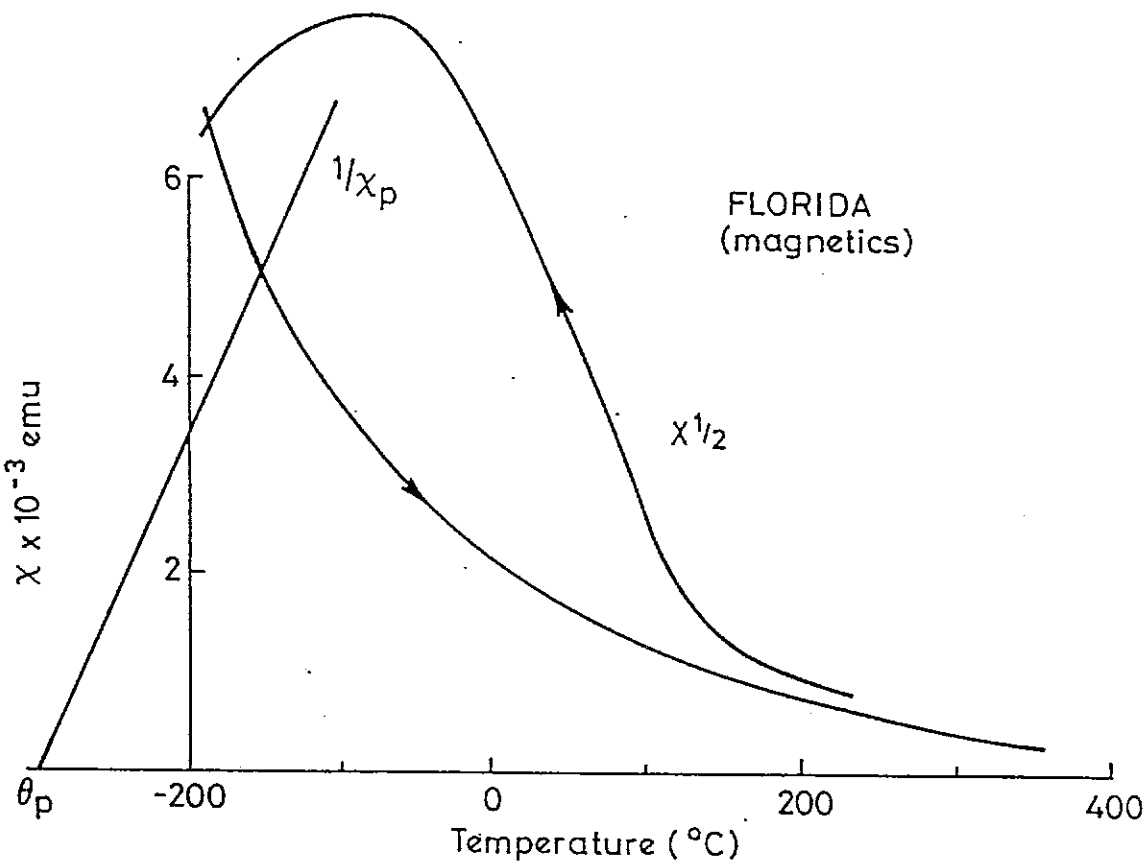
FLORIDA
(magnetics)
$1/\chi_p$
$\chi^{1/2}$
$\chi \times 10^{-3}$ emu
6
4
2
θ_p
-200
0
200
400
Temperature (°C)

Fig. 14

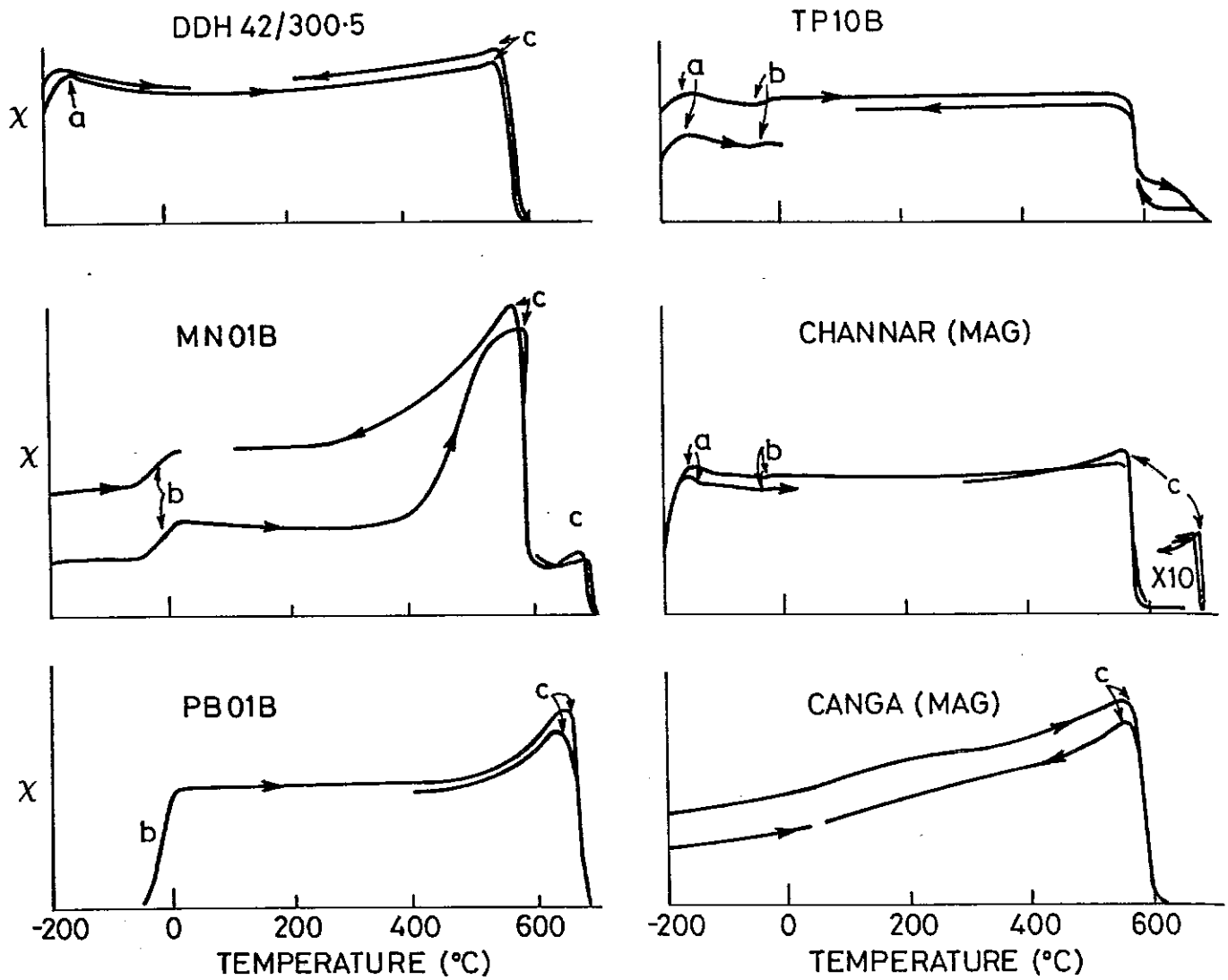
DDH 42/300·5
χ
a
c
TP10B
a
b
MN01B
χ
b
c
c
CHANNAR (MAG)
a
b
c
X10
PB01B
χ
b
c
-200
0
200
400
600
TEMPERATURE (°C)
CANGA (MAG)
c
-200
0
200
400
600
TEMPERATURE (°C)

Fig. 15

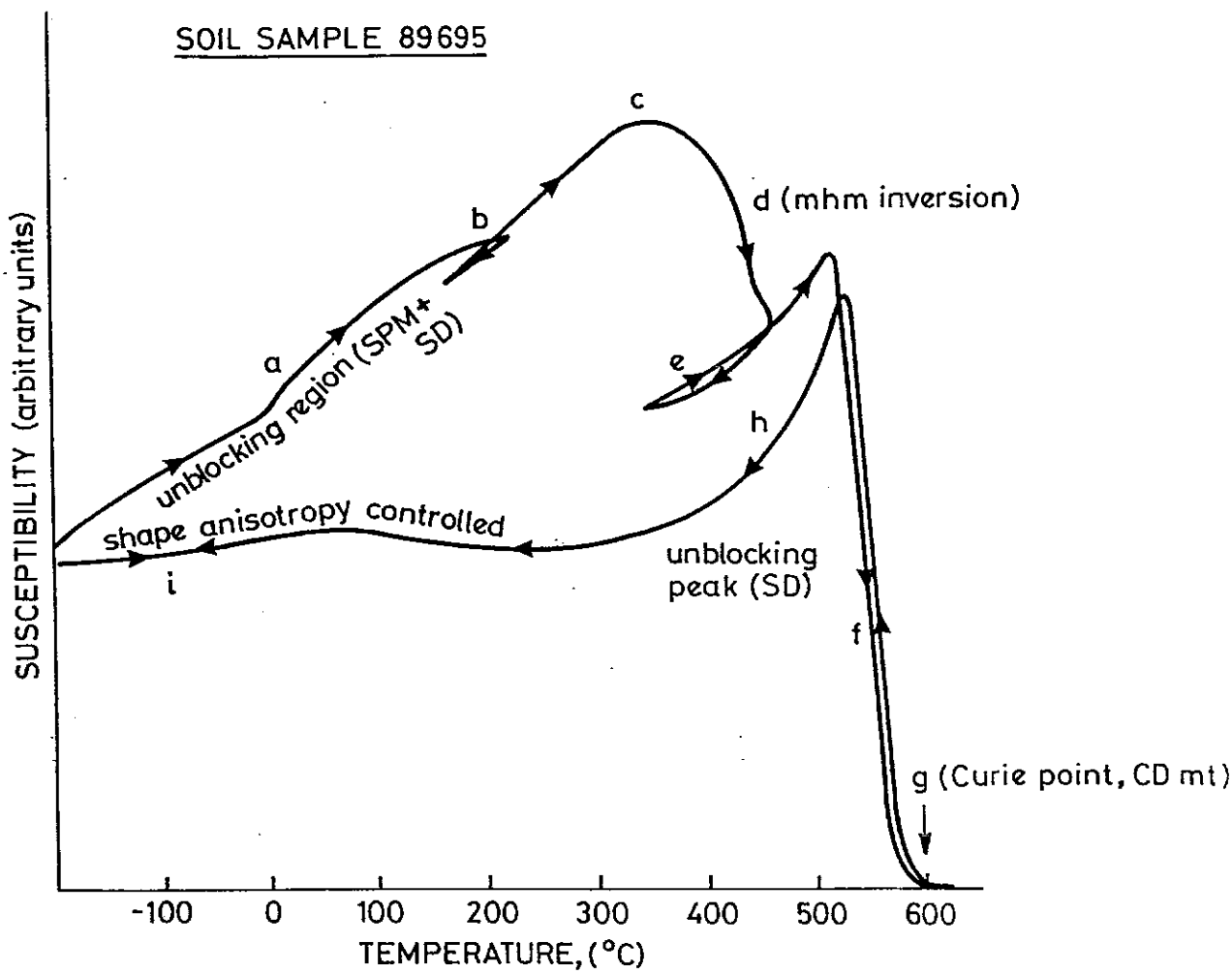
SOIL SAMPLE 89695
SUSCEPTIBILITY (arbitrary units)
TEMPERATURE, (°C)
-100
0
100
200
300
400
500
600
a
b
c
d (mhm inversion)
e
f
g (Curie point, CD mt)
h
i
unblocking region (SPM+ SD)
shape anisotropy controlled
unblocking peak (SD)

Fig. 16

SECTION 2. ASPECTS OF MAGNETIC MODELLING

Geophysical Anomalies

An anomaly can be defined as an irregularity or deviation from the norm. A geophysical anomaly is a deviation of some physical quantity (that is dependent on the physical properties of the Earth) from the "normal" value, corresponding to a smoothed or simplified version of the Earth. This normal value may be derived from an extensive set of measurements by some sort of averaging or calculated theoretically from a model of the internal structure of the Earth.

In exploration we are concerned with extracting information about the subsurface by measuring spatial variations of various quantities. These measurements constitute the geophysical signal, which is the sum of the message, representing the information in the data, and the noise. Normally the survey area is sufficiently small for the curvature of the Earth's surface to be neglected and for the subsurface to be considered, for practical purposes, to have infinite lateral and depth extents.

Consider measurements made over a horizontal plane, parallel to the surface of the Earth, which is assumed, for the moment, to be perfectly flat. If the subsurface were laterally uniform it is clear that there would be no lateral variation in the geophysical message, i.e. no geophysical anomalies. A homogeneous half-space and a stratified Earth consisting of horizontal layers, each of which is homogeneous, are examples of laterally uniform subsurfaces. It follows that geophysical anomalies reflect inhomogeneities in physical properties.

In reality, the surface of the Earth has topographic relief. Even if the subsurface is homogeneous, topographic anomalies will arise from the lateral inhomogeneities associated with the contrast in physical properties between rock and air (or rock and water in the case of marine geophysics). Such anomalies are generally uninteresting from the explorationist's viewpoint and may obscure subtle anomalies which could otherwise elucidate geological structure. It may be necessary, therefore to correct the data for topographic effects or otherwise suppress topographic noise.

Geological noise arises from subsurface heterogeneity (in particular, shallow small-scale features) which is unrelated to the geological features of interest. In areas where the exploration targets lie within fresh bedrock, sharp, irregular anomalies arising from differential weathering, variable thickness of overburden or local compositional variations may degrade the geophysical message. Geological and topographic noise may be significantly greater sources of error than instrumental noise.

Ward and Rogers (1967) point out that the geophysical message due to a discrete subsurface body can be quite generally expressed in the form:

> Anomaly = inducing field factor x size factor x physical property factor x geometric factor.

In the case of gravity and magnetic field components the size factor is simply the volume of the body. By the very nature of geophysical anomalies the physical property factor involves the physical properties of both the body and the surrounding material. For gravity anomalies the inducing field factor is unity and the physical property factor is the density contrast i.e. the difference between the densities of the body and the surrounding material. Similarly, the inducing field factor is unity for magnetic anomalies when the physical property is taken to be magnetisation, in which case the physical property factor is the magnetisation contrast. Alternatively, if the magnetisation is entirely induced, the inducing field factor can be taken as the ambient geomagnetic field. The physical property factor is then a function of the susceptibilities of the body and its surroundings which, for low susceptibilities, reduces to the susceptibility contrast.

Interpretation of geophysical surveys encompasses the tasks of anomaly identification or detection, resolution, enhancement and evaluation. Although an anomaly may in principle be represented by a single data point which deviates significantly from neighbouring points, such a one-point anomaly cannot be distinguished from instrumental noise or a recording error. Thus, in practice, unambiguous identification of an anomaly requires anomalous values to be registered at a minimum of two consecutive data points along a profile, or at approximately collinear points on at least three adjacent profiles.

Anomaly resolution requires density and extent of sampling sufficient to define the form of the anomaly without significant distortion. The adequacy of sampling obviously depends on the smoothness of the anomaly and on its total width, which in turn depends on the depth and lateral extent of the sources. As a guide, the sampling interval should be less than half the depth to the shallowest source and the measurements should extend beyond the edge of a laterally extensive source by about 10 times the depth to the source, or about three times the depth on either side of a compact source.

Provided an anomaly has been adequately sampled, the signal may be processed in order to increase the message-to-noise ratio or to emphasise particular features of which are related to the geological structures of interest. In particular, the signal may be filtered to reduce the effects of geological or instrumental noise, to enhance the response of sources from a particular depth or to separate anomalies due to closely spaced bodies. There is a vast literature devoted to enhancement of potential field data, but further discussion is beyond the scope of this course.

Qualitative Interpretation

When the anomalies have been identified, defined, and possibly enhanced, the most demanding task of interpretation - evaluation - can begin. For the most part, evaluation of the hundreds or thousands of anomalies recorded on a map is necessarily qualitative. Only after the qualitative phase of interpretation is well advanced is it feasible to select a small subset of the anomalies for detailed, quantitative interpretation. The results obtained from quantitative evaluation, supplemented by semi-quantitative rules-of-thumb which can be rapidly applied to many anomalies may then be used to modify the qualitative interpretation, thus completing a feedback loop. The loop may be traversed more than once in order to refine the interpretation, particularly when additional information, such as drill-hole data, come to hand. Although only a few anomalies are

evaluated quantitatively the information obtained is disproportionately valuable because it is essential for targetting of drill holes, as well as improving the qualitative interpretation. In particular, the hypotheses of the qualitative phase of evaluation, whereby magnetic or gravimetric signatures are attributed to particular geological features, can be tested for geological plausibility. If quantitative interpretation reveals that the form of the body (belonging to the hypothesised class) required to match the observed signature is geologically unreasonable or the physical property contrasts are improbably extreme, then the interpretation must be revised. In this way the qualitative interpretation of anomalies in terms of geology can be checked for self-consistency and the geological plausibility can be maximised. The interpretation can never be definitive, however, because construction of a geologically reasonable model which matches the observed signatures does not guarantee that the model is correct.

The treatment of magnetics as a mapping tool in textbooks is generally rather cursory and thin, although Grant and West (1965) and Nettleton (1976) contain useful material. The manual by Breiner (1973) is a useful elementary introductions to applications of magnetic surveys. Perhaps the most useful published discussions are case history papers, which represent a regrettably small proportion of the geophysical literature. Several useful review articles have been published, including Reford and Summer (1964), Steenland (1970), Grant (1972), Zeitz and Bhattacharyya (1975), Reford (1980), LaFehr (1980) and Paterson and Reeves (1985). Readers are also referred to symposium proceedings edited by Emerson and Falvey (1977) and Emerson (1979) and to course notes by Boyd and Richards (1983).

The principal use of aeromagnetic surveys in mineral exploration is as a geological mapping tool. The great advantages of aeromagnetic surveys are the rapid acquisition of data over extensive areas and the relatively low costs. Magnetic features can be used to interpolate between mapped surface exposures in areas of limited outcop and to trace lithological boundaries beneath overburden, water or dense vegetation, even in areas which are otherwise inaccessible. Magnetic maps can also give a rapid qualitative impression of the thickness of non-magnetic cover - usually called the "depth to magntic basement". Shallow magnetic basement is associated with narrow, large amplitude magnetic anomalies and high gradients whereas a deeper interface is recognisable by smoother, more subdued anomalies.

An important element of qualitative interpretation is "pattern recognition", whereby characteristic signatures of various source geometries are identified and tentatively given a geological interpretation. This is a task which is best performed by an experienced interpreter, in spite of human subjectivity, because of the facility of the brain with perception of form. Currently the human beings perform the task of pattern recognition much better than computers, although more slowly. Future developments in the field of artificial intelligence may eventually lead to partly automated qualitative interpretation, but this appears to be a long way off. Dampney (1977) argues for ingenuous methods (based on human perception) in preference to ingenious computer-based methods for semi-quantitative, as well as qualitative, interpretation.

Boyd and Richards (1983) classify characteristic signatures into those produced by:

(i) equidimensional bodies (in plan view),
(ii) simple sheets,
(iii) complex zones,
(iv) dislocations,
(v) superficial layers.

Type (i) bodies may be either more magnetic or less magnetic than the surrounding rocks. Depending on scale and the geological environment they include intrusives, small sedimentary basins and ore bodies and are marked by nearby circular "bulls-eye" anomalies or simple dipolar high-low pairs. Such signatures can also arise from complex structures such as fold closures.

Type (ii) bodies produce a single maximum and minimum normal to strike and exhibit continuity along strike. Such anomalies mostly arise from sheets which are more magnetic than the surrounding rocks, because the effects of thin non-magnetic sheet-like bodies within heterogeneous magnetic rocks are difficult to discern. Simple sheets may correspond to dykes (particularly basic and ultrabasic), iron formations, mineralised veins and magnetic sedimentary or metasedimentary units which may serve as marker beds. Similar anomalies are also associated with lithological contacts.

Type (iii) signatures represent broad complex zones containing several anomaly peaks. These zones may correspond to greenstone belts, thick iron formations, sequences of metasediments and/or metavolcanics, ultramafic intrusions and serpentinites etc.

Type (iv) signatures (dislocations) represent disturbances of the macroscopic magnetic fabric of the area, including attenuation, truncation or offsetting of anomalies. Dislocations marked by observable displacement of magnetic horizons are often, but not always associated with faults. Facies changes, unconformities, shear zones and folds may also produce dislocations.

Superficial layers, corresponding to type (v) signatures, include lavas, sediments or lateritic soils. Shallow magnetic layers produce intense, spiky anomalies which tend to confuse the magnetic pattern arising from deeper sources. On the other hand non-magnetic cover has a blanketing effect, tending to attenuate anomalies arising from the magnetic rocks at depth.

Some authors place great emphasis on magnetic lineaments and their relationship with pervasive, ancient fracture patterns within the crust (e.g. Gay, 1972). In many cases mineralisation appears to occur along lineaments defined by magnetic, gravity and geological features, particularly where they are intersected by other lineaments. Some of these lineaments presumably represent fractures which have acted as conduits for mineralising fluids. According to Gay, magnetic lineaments can be recognised on contour maps as one or more of the following features:

(i) terminations of highs or lows,
(ii) steeping or flattening of gradients,
(iii) linear contour patterns,
(iv) alignments of highs or lows.

Identified lineaments can be classified into sets according to their strike. It is generally found that a few strike directions predominate. Analysis proceeds by determining the sense and magnitude of strike-slip movement and vertical throw, for individual fault-related lineaments, where possible. The spacing and length of lineaments within sets and the areal distribution of the various lineament sets may yield useful geological information. The relative ages of two lineaments, and possibly the corresponding lineament sets, may be determined by careful analysis of truncations of one against another.

A common approach to qualitative interpretation involves subdivision of the study area on the basis of textural characteristics such as linearity, relief, background level, and the shape and width of anomalies. This is referred to as "zoning" by Paterson and Reeves (1985) and "domain mapping" by D'Addario and Tucker (1986). The textural characteristics within each macroscopic magnetic domain are classified as diagnostic if they occupy more than 20 per cent of the area. Non-diagnostic characteristics comprising just under 20 per cent of the area are noted but are not used to define the domain boundaries. The classification scheme must be adapted to the characteristics of the particular area and to the map scale. As an example, the Albany (Western Australia) 1:1,000,000 grey-scaled pixel map (Tucker and D'Addario, 1987) has been subdivided on the basis of the following "textures" (with their geological associations in parentheses):

(i) flat-smooth areas with widths of at least 20 kms (thick, non-magnetic sediments and/or non-magnetic granites),
(ii) narrow, curvilinear anomalies, 1-4 km wide (thin steeply dipping layered magnetic metasediments and metavolcanics),
(iii) granular and uniform, with anomalies 1-2 km wide (extensive granitoids)
(iv) mottled, with anomalies 1-3 km wide (extensive granitoids)
(v) circular/elliptical closed areas, 10-50 km wide (large igneous intrusions)
(vi) linear/cross-cutting features, 0.5-2 km wide (basic dykes, faults and drainage lines)
(vii) wide elongated and/or irregular closed areas, with anomalies 3-20 km wide (greenstone belts).

Domzalski (1966) gives examples of relationships between mineralisation and magnetic lineaments, domain boundaries and marker horizons, with the emphasis on delineating structural controls of mineralisation.

The increasing use of aeromagnetic surveys in exploration, in particular, has stemmed, in part from developments in data presentation and processing which have facilitated qualitative interpretation and made the data more comprehensible to non-specialists. For instance, geologists are making increasing use of image processors for manipulation and evaluation of potential field data. Presentation formats which are commonly used nowadays supplement the traditional contour maps and stacked profiles. They include grey-scale and colour pixel images and pseudotopographic representations illuminated by an artificial sun positioned to highlight particular trends. Qualitative interpretation is also

assisted by processing of the data to emphasise particular features or to simplify the form of the maps.

The Geomagnetic Field

To a first approximation the magnetic field of the Earth corresponds to a geocentric dipole of moment ~8×10^{25} emu aligned nearly parallel to the axis of rotation. The configuration of an axial geocentric dipole field is depicted in Fig. 17(a). The geomagnetic field shows complex variation in both time and space, but can be unambiguously separated into slowly varying components of internal origin and more rapidly varying components originating outside the Earth or arising from eddy currents within the Earth which are induced by external fields.

Field components of internal origin are obtained by averaging the geomagnetic field (nominally over a period of 1 year). The time-averaged field derived in this way has two constituents - the main field, which can be defined as the steady field averaged over areas of about 10^6 km^2, and the local field.

The main field has a relatively simple configuration and varies systematically with latitude: the field strength is ~30,000 nT in equatorial regions where the field lines are sub-horizontal and ~60,000 nT near the poles where the field is steep. The local field is highly irregular with mean amplitude of the order of 100 nT (but attaining much higher values in some areas) and dominant wavelengths ranging from metres to hundreds of kilometres.

The main field arises from the geomagnetic dynamo associated with convection in the liquid and conductive metallic outer core of the Earth. The local field is due to the inhomogeneously magnetised crust above the Curie point geotherm. In some areas the upper mantle may possibly contribute to longer wavelength components of the local field. The contributions of the solid inner core and the lower mantle to the geomagnetic field are completely negligible.

The external fields arise from the ionosphere and magnetosphere and vary over periods ranging from seconds to days with corresponding amplitudes of a few gammas to a few hundred gammas. In addition, field changes of comparable period and about half the intensity of each of these external field constituents (pulsations, diurnal variation and storm fields) are associated with induced currents in the electrically conducting crust, upper mantle and oceans. These rapidly varying geomagnetic field components constitute a major source of noise in magnetic surveys, which seek to define the contribution due to geology by isolating the local field component.

At any point on the Earth's surface the elements of the geomagnetic field F are defined with respect to Cartesian axes true north, true east and vertically down or in polar coordinates (refer to Fig. 17(b)) and are conventionally written X,Y,Z,D,I,H and F, where:

THE GEOMAGNETIC FIELD

(a)

$\tan I = 2 \tan \lambda$

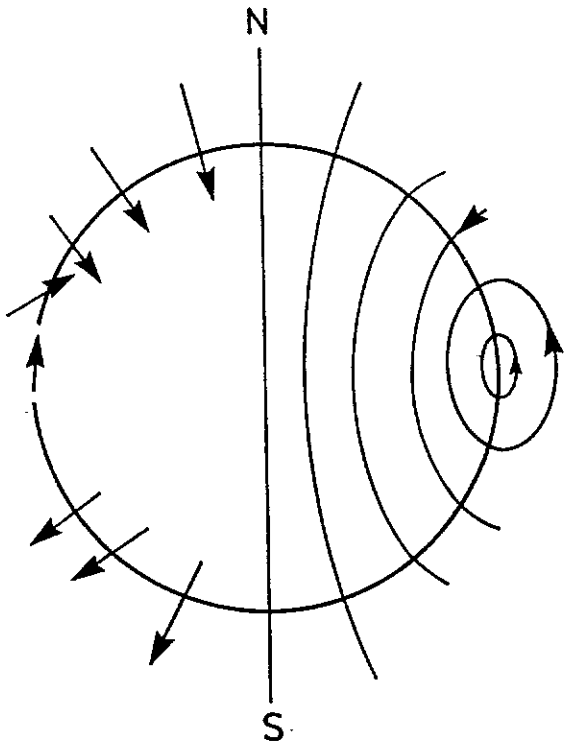

(b)

$X = F \cos D \cos I$

$Y = F \sin D \cos I$

$Z = F \sin I$

$F^2 = X^2 + Y^2 + Z^2 = H^2 + Z^2$

$\tan D = Y/X$

$\tan I = Z/H$

$\sin I = Z/F$

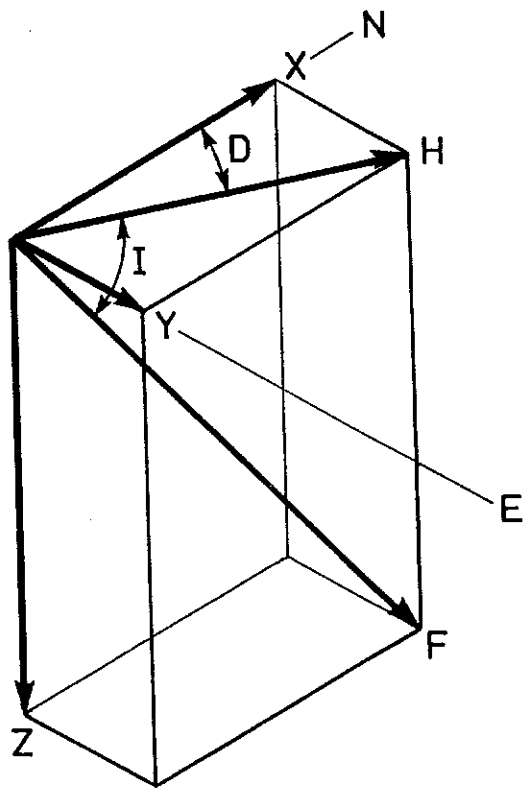

Fig. 17

X,Y,Z are the Cartesian components of **F**

D = declination is the angle from true north to the horizontal component of **F**, defined positive clockwise,

I = inclination is the angle from the horizontal plane to **F**, measured positive downwards

H = horizontal intensity is the magnitude of the horizontal component of **F**

F = total intensity, the magnitude of **F**.

The field of an axial geocentric dipole at latitude λ is D=0, $I=\tan^{-1}(2\tan\lambda)$.

From simple trigonometry the elements are related by the following expressions:

$H = F\cos I, \quad Z = F\sin I$

$X = H\cos D = F\cos D\cos I, \quad Y = H\sin D = F\sin D\cos I$

$\tan D = Y/X, \quad \tan I = Z/H, \quad \sin I = Z/F$

$H = \sqrt{(X^2 + Y^2)} \quad F = \sqrt{(H^2 + Z^2)} = \sqrt{(X^2 + Y^2 + Z^2)}$

At any point all the elements of the field change measurably over periods of several years. This is due to a slow, smoothly varying change in the main field known as secular variation. The most prominent feature of secular variation is a westward drift of non-dipole components of the main field (i.e. departures of the main field from the field produced by a geocentric dipole) at a rate of about 0.2° per year. The dominant periods for secular variation are of the order of 10^3-10^4 years.

Throughout geological time the geomagnetic field has frequently reversed its polarity. Following such a field reversal the declination changes by approximately 180° and the sign of the inclination is reversed. The average interval between field reversals is typically about 10^6 years.

At present the main field is better represented by a geocentric dipole inclined 11½° to the axis of rotation than by an axial dipole. The antipodal points where the axis of the inclined dipole cut the surface of the Earth are the geomagnetic poles. Note that the geomagnetic poles are not analogous to the "poles" of a long thin magnet, the external field of which bears little resemblance to the geomagnetic field. The magnetic poles or dip poles are points where the (short term) time-averaged field is vertical.

If the main field were exactly represented by the inclined dipole field, contours of H, Z and F would be circles centred on the dipole axis. Departures from this pattern represent the non-dipole field which arises from sources more complex than a geocentric dipole.

At any point the orientation of a geocentric dipole which would produce the observed D and I can be calculated. Each of the corresponding poles is called a virtual geomagnetic pole (VGP). Because of the non-dipole field, present day VGPs do not coincide with the geomagnetic poles, but form a tight cluster about them. The position of VGP changes slowly because of secular variation, but if the VGPs obtained from historical records, archaeomagnetism and palaeomagnetism are averaged over the last few thousand years the mean pole position is found to coincide with the rotation axis. This observation is the basis of the axial geocentric dipole hypothesis or model which states that the geomagnetic field averaged over "sufficient" time to eliminate effects of secular variation corresponds

to the field of an axial dipole at the Earth's centre. It is estimated that 10^4-10^5 years is sufficient to average secular variation completely (Merrill and McElhinny, 1983, p.82). Palaeomagnetic sampling is designed to represent palaeofield directions recorded by rocks over time spans of this order, or greater. The pole position calculated either from the average of the palaeofield directions or from the average of the corresponding VGPs is called a palaeomagnetic pole and, as a consequence of the axial geocentric dipole hypothesis, is considered to represent the ancient geographic pole position with respect to the sampling site. From consistency of the results obtained and from independent evidence there is good reason to believe that the axial geocentric dipole hyopthesis is valid, to a first approximation, for at least the last 600 million years (Merrill and McElhinny, 1983, chapter 6). There is evidence that the geomagnetic dynamo has been operating for at least 3.6×10^9 years.

If the age of remanence acquisition can be assumed for a rock unit, the corresponding direction of the remanence can be inferred from the palaeomagnetic pole position with the corresponding age, as shown in Fig.18. In practice, this possibility is likely to occur only for the following cases:

(i) igneous rocks that post-date all other major geological events in the area and for which the assocaiated anomalies are inconsistent with magnetisation subparallel to the present field. These rocks can be assumed to carry a primary TRM parallel to the palaeofield direction at the time of emplacement.

(ii) rocks which have been subjected to regionally pervasive and thorough overprinting, usually a thermal event, of known age and show evidence in the associated anomalies that substantial remanence oblique to the present field is present. These rocks can be assumed to carry a secondary remanence with direction corresponding to the palaeofield direction at the time of the overprinting event.

Formulae for the inversion of palaeomagnetic poles to palaeofield directions are given by Clark (1983). The polarity of the calculated palaeofield direction is ambiguous, but the polarity of the remanence should be evident from the form of the anomaly. To some extent the polarity can be deduced from the age of the remanence, because the relative frequency of normal and reversed polarities has varied through geological time, as shown for the Phanerozoic in Fig.19(a). There has also been a trend to increasing obliquity of the palaeofield direction from the present field direction with increasing age, as shown in Fig.19(b).

Types of Magnetic Anomaly

Magnetometers belong to one of two categories:

(i) those that measure particular components of the magnetic field vector (e.g. fluxgates), and
(ii) those that measure the scalar magnitude of the magnetic field, the so-called total field, (e.g. proton precession and optical pumping magnetometers).

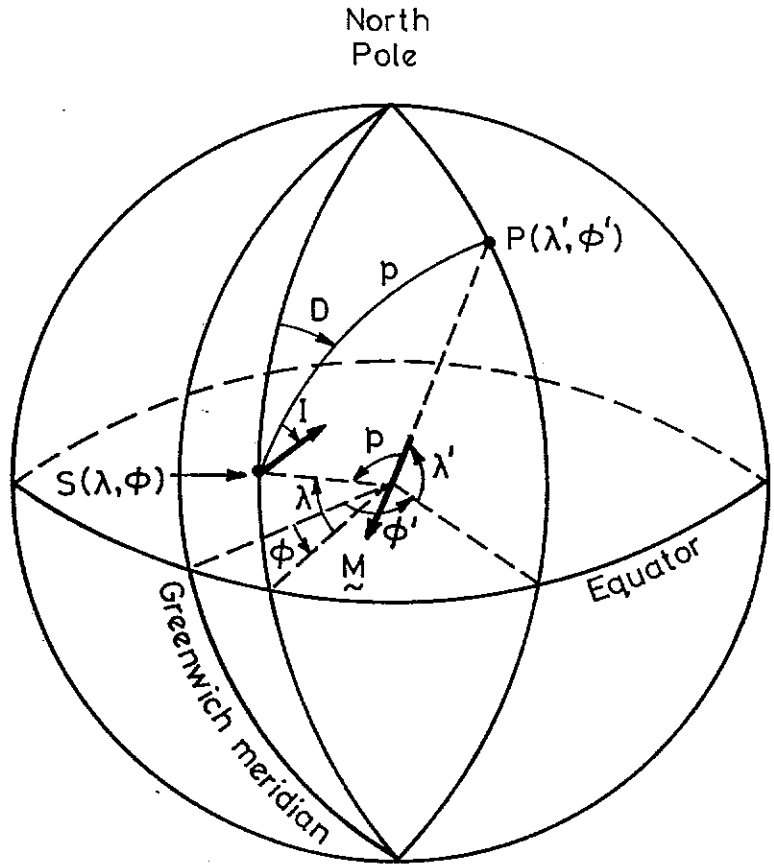

$\underset{\sim}{M}$ = ancient axial geocentric dipole

tan I = 2 cot p

Fig. 18

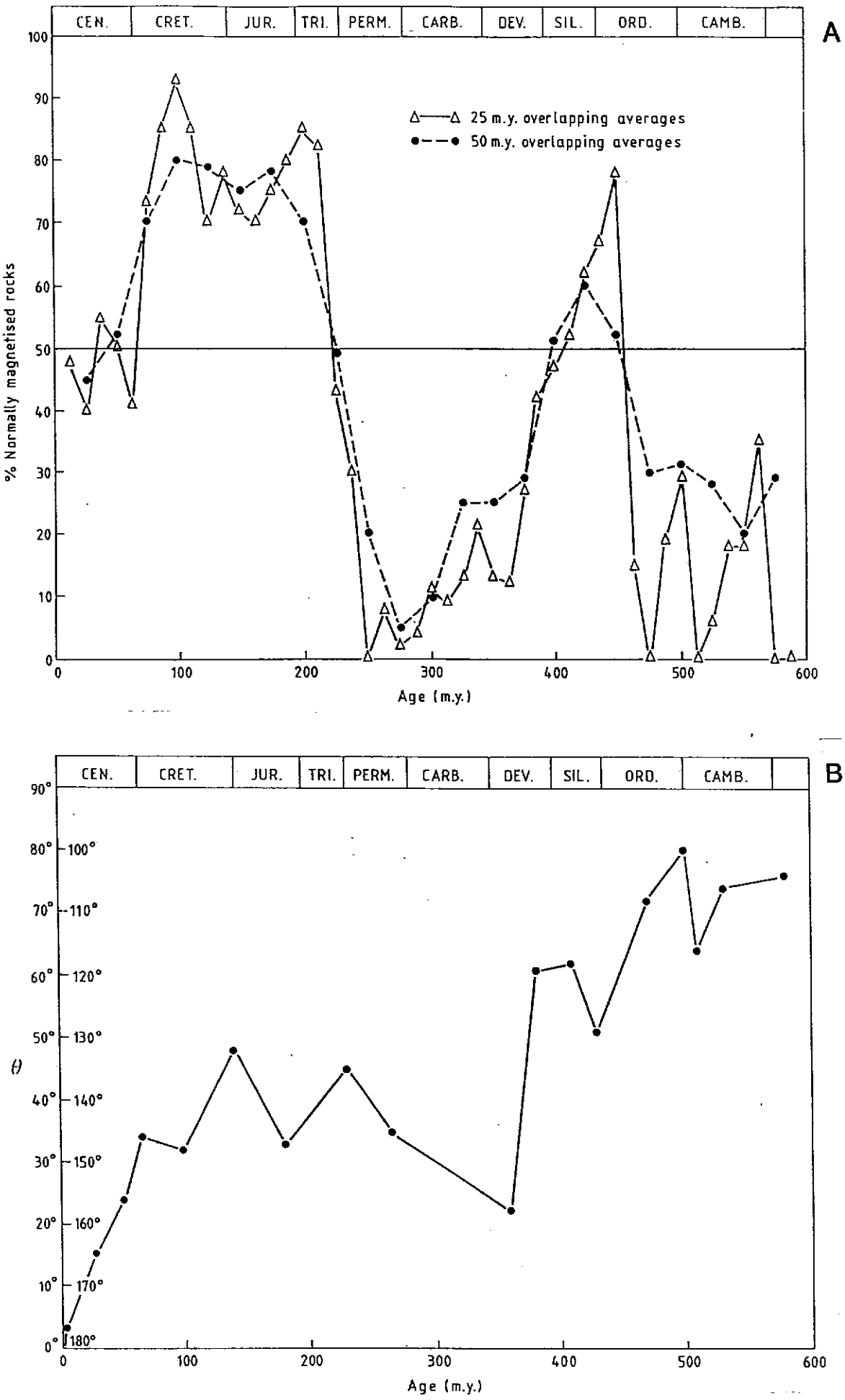
A
CEN.
CRET.
JUR.
TRI.
PERM.
CARB.
DEV.
SIL.
ORD.
CAMB.
25 m.y. overlapping averages
50 m.y. overlapping averages
% Normally magnetised rocks
Age (m.y.)
B
θ
Age (m.y.)

Fig. 19

Figure 20 shows the relationship between the regional and anomalous field vectors, their scalar intensities and their components. Because modern surveys are almost invariably carried out using total field magnetometers, magnetic interpretation emphasises total field anomalies, i.e. deviations in the magnitude of the local field from the regional geomagnetic field intensity.

Because local anomalous fields are generally small compared to the geomagnetic field, the direction of the local field is usually almost constant. For historical reasons, the unfortunate assumption has been adopted in modelling programs that the local field direction is constant and therefore that the total field anomalies correspond to the projection of the anomalous field vector $\Delta\mathbf{B}$ onto the regional (unperturbed) geomagnetic field direction. We denote this type of total field anomaly by ΔB_T, whereas the measured total field anomaly is written ΔB_m. The assumption is good when the anomalous field is small, but can be the source of substantial errors when the anomalous field is large, as indicated in Fig.21. The maximum relative error in assuming that $\Delta B_T = \Delta B_m$ is $(\Delta B/F)^2/2$.

When the anomaly is small, a picture of the form of the anomaly due to various simple sources can be visualised by drawing field lines arising from the source and projecting these onto to the regional geomagnetic field direction, as shown in Fig.22. This procedure illustrates the way that magnetic anomalies depend not only on the source geometry and magnetisation, but also the regional field direction, and explains the common paired high-low form of many magnetic anomalies.

To eliminate possible errors, modelling software should be modified to calculate ΔB_m rather than ΔB_T, so that calculated anomalies are directly comparable with the measured anomalies. Details are given in Clark and Schmidt (1986).

Non-uniqueness in Magnetic Interpretation

Magnetic anomalies have the fundamental property of scale invariance. Thus for a compact source, the anomaly width increases proportional to increasing depth, with no change in anomaly amplitude if the source dimension/depth ratio remains unchanged. If we consider a source of constant size, on the other hand, the anomaly amplitude decreases with increasing source depth. Figure 23 illustrates these points. Since there is a direct relationship between anomaly width and source depth, we can deduce the source depth from the anomaly width, provided the source geometry is stipulated.

In general, inverting anomaly width to source depth is not unique, unless there is additional information about the source. It is a well known property of potential fields that different source distributions can give rise to identical effects. The best-known example of this is the equivalence of the gravitational field of a homogeneous sphere to that of a particle of the same mass at the centre of the sphere. The magnetic analogue is a uniformly magnetised sphere, which produces an external field identical to that of a point dipole. Thus concentric spheres can be regarded as equivalent bodies from the point of view of potential field modelling. This is a special case of a less well-known set of equivalent bodies, confocal ellipsoids. If the magnetisation of the source is known, however, the ambiguity in the size of the spherical source is determined. This illustrates a

SCHEMATIC RELATIONSHIP BETWEEN MEASURED, TRUE AND CALCULATED TOTAL MAGNETIC INTENSITY ANOMALIES

Southern hemisphere fields depicted with negative inclination

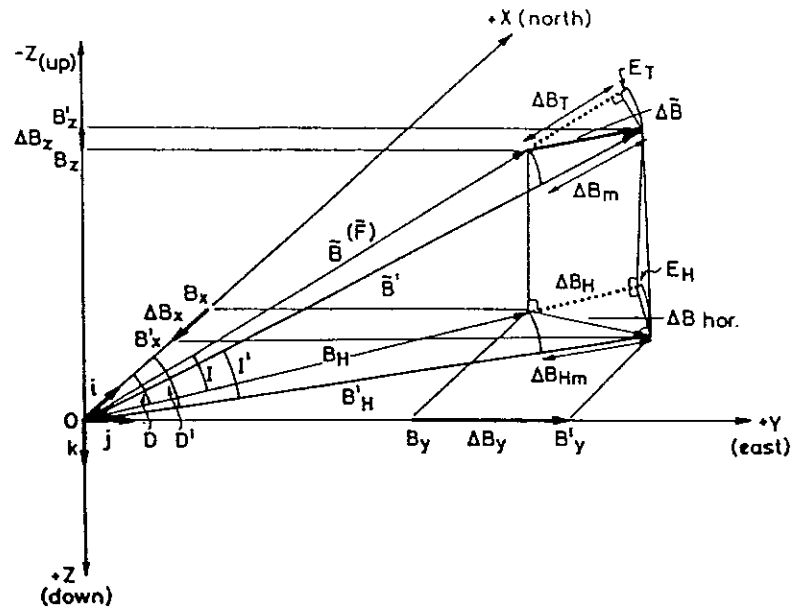

$\Delta B_T = \Delta B_H \cos I + \Delta B_z \sin I$ (computed total field anomaly)

$\Delta B_m = |\tilde{B}'| - |\tilde{B}|$ (measured total field anomaly)

$\Delta E_T = \Delta B_m - \Delta B_T = (|\Delta\tilde{B}|^2 - \Delta B_m^2)/2|\tilde{B}|$, $|\Delta\tilde{B}| \neq \Delta B_T \neq \Delta B_m$

θ (= D) is the angle between the +X axis and the horizontal projection of the field vector (ℓ,m,n)

$\tilde{I}$, $\tilde{J}$, $\tilde{K}$ unit vectors parallel to X, Y, Z axes respectively

ℓ, m, n direction cosines. For $\tilde{B}(F)$: $\ell = B_x/|\tilde{B}|$, $m = B_y/|\tilde{B}|$, $n = B_z/|\tilde{B}|$

$\ell\tilde{I} + m\tilde{J} + n\tilde{K}$ unit vector in direction (ℓ,m,n)

$\Delta\tilde{B}$ local magnetic anomaly vector, perturbing $\tilde{B}$

$\tilde{B}(\tilde{F})$ regional or "normal" magnetic field vector of Earth (constant over limited region)

$\tilde{B}'$ resultant (local) field = $\tilde{B} + \Delta\tilde{B}$; with declination D', inclination I'

ΔB_T component of $\Delta\tilde{B}$ along normal field $\tilde{B}$. This is the theoretical computed anomaly. Usually $\Delta B_T \tilde{\simeq} \Delta B_m$

ΔB_m measured residual total field anomaly (scalar measurement of variation in magnitude of resultant field)

E_T departure of computed anomaly (ΔB_T) from measured anomaly (ΔB_m). Usually small

ΔB_{hor} horizontal projection of $\Delta\tilde{B}$ = true horizontal component of anomalous field

B_H component of $\tilde{B}(\tilde{F})$ along regional magnetic meridian

B_H' component of $\tilde{B}'$ along local anomalous magnetic meridian

ΔB_H computed horizontal field anomaly = component of $\Delta\tilde{B}$ along regional magnetic meridian

ΔB_{H_m} measured horizontal field anomaly $\Delta B_{H_m} = B_H' - B_H \neq \Delta B_{hor} \neq \Delta B_H$

$E_H = (\Delta B_H^2 - \Delta B_{H_m}^2)/2B_H = B_H'[1-\cos(D'-D)]$. Departure of computed from measured horizontal anomaly

ΔB_x true horizontal anomaly component along X axis = $B_x' - B_x$

ΔB_y true horizontal anomaly component along Y axis = $B_y' - B_y$

$\Delta B_{hor} = (\Delta B_x^2 + \Delta B_y^2)^{\frac{1}{2}}$

ΔB_z true vertical intensity anomaly, measured anomaly = vertical component.

Fig. 20

ADDITION OF MAGNETIZATION VECTORS

$\tilde{J}$: [J,D,I]

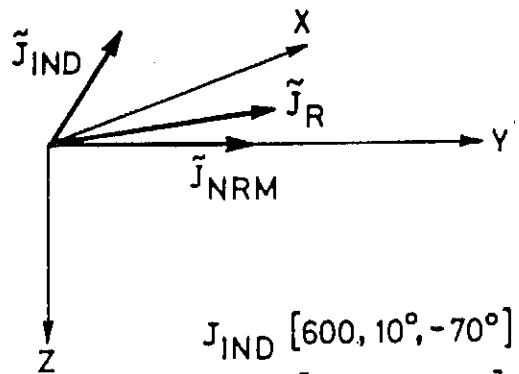

J_{IND} [600, 10°, -70°]

J_{NRM} [1000, 90°, 0°]

J_R [1196, 79°, -28°]

ANOMALOUS ΔB COMPONENTS IN VARIOUS DIRECTIONS

(l,m,n : direction cosines)

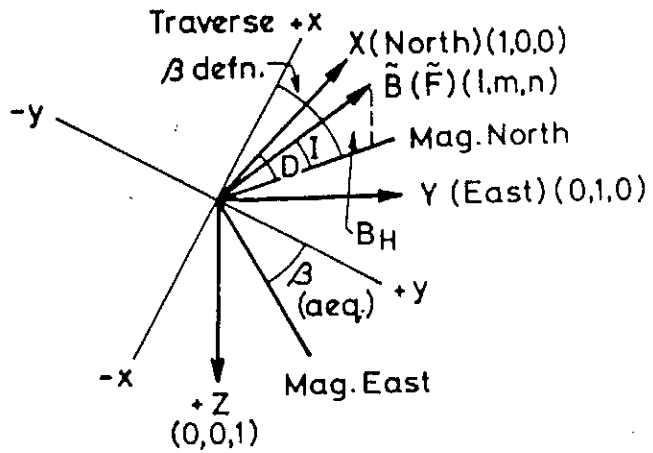

ERROR ARISING FROM ΔB_T APPROXIMATING ΔB_m

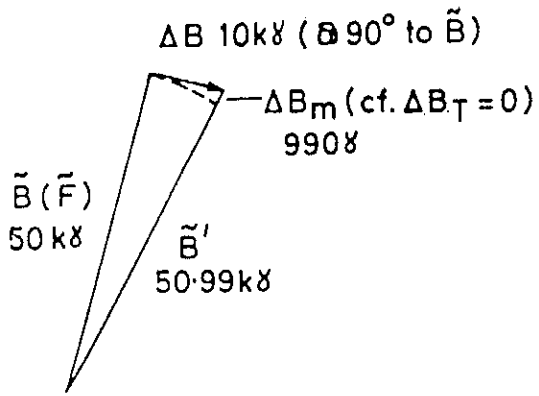

MAXIMUM DIFFERENCE BETWEEN ΔB_T AND ΔB_m WHEN $\Delta B_m = 0$

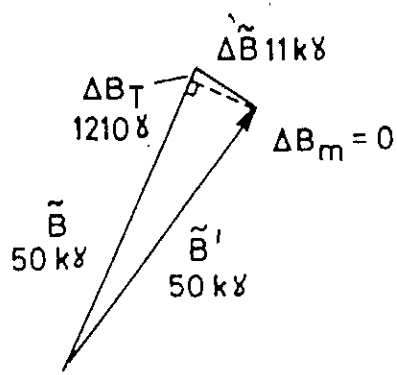

Fig. 21

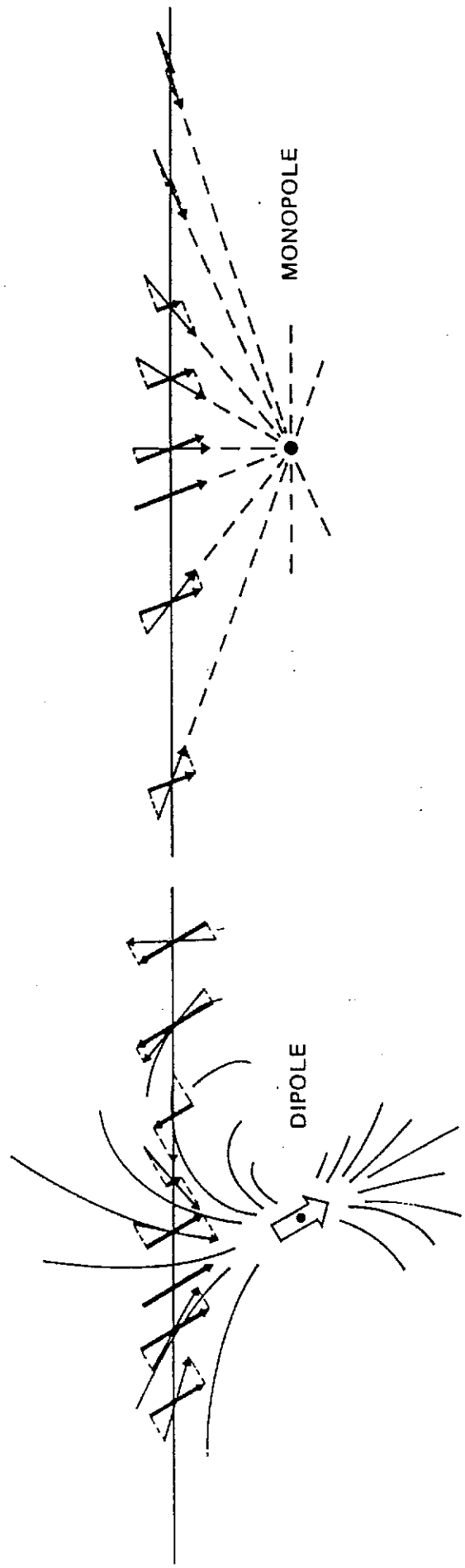

Fig. 22

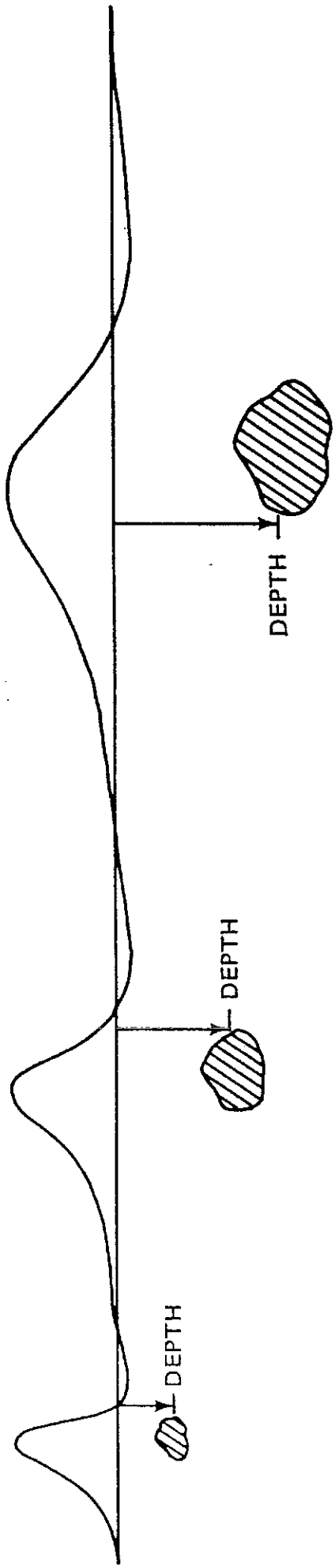

Fig. 23

general point, that additional information can overcome the inherent non-uniqueness of magnetic modelling.

Yet another important case concerns the equivalence between a deep compact source and a shallower, broader source, which gives rise to an anomaly identical in width and amplitude. It is this sort of non-equivalence that can cause the greatest problems with source depth determination.

Another geologically important type of non-uniqueness concerns the interpreted dip of tabular bodies for which the magnetisation direction is unknown. Figure 24 shows that 2D dipping sheet-like bodies produce an anomaly of a form that depends only on the angle between the plane of the sheet and the projected magnetisation vector. Thus, if the observed anomaly is consistent with a vertically dipping sheet that is magnetised parallel to the geomagnetic field, it could also arise from a north-dipping sheet with vertical magnetisation, or from a south-dipping sheet with N horizontal magnetisation, as well as an infinite number of other combinations. Thus if substantial remanence is present, assumption of magnetisation by induction could seriously mislead interpretation of the dip, with the possibility of drilling down-dip. On the other hand, if information about remanence is available, the dip can be interpreted uniquely for this source geometry.

Resolution of the problem of non-uniqueness can be achieved in various ways, including geological constraints, drilling information, magnetic property measurements on exposures or drill core, and other geophysical techniques. Although it might be argued that magnetic property measurements on drill core are too late to assist drill targetting, Fig.25 demonstrates the utility of such measurements for testing of magnetic anomalies. The original drilling target is an interpreted compact magnetic orebody, which was not intersected. However, a magnetic horizon containing disseminated magnetite or pyrrhotite, which obviously contributes to the observed anomaly, was intersected. The important implication for exploration is that the unmineralised magnetic horizon may fully account for the anomaly, thereby eliminating the need for further drilling to test the anomaly. On the other hand, if the intersected horizon does not account for all of the anomaly, the residual effect can be modelled and, if a potential orebody is indicated, further drilling would be justified.

Magnetic property measurements on the intersected horizon are very useful for this stage of prospect evaluation. It is commonly found, for instance, that the susceptibility of the magnetic horizon is insufficient to produce all of the anomaly, but when remanence is taken into account, the anomaly is fully explained and further drilling is unnecessary. An example where the opposite conclusion can be drawn is shown in Fig. 26. In this case the intersected magnetite-rich sulphidic schists cannot account for all of the observed anomaly, and a deeper, unintersected source is indicated.

Another possible approach to the problem of non-uniqueness is to determine *in situ* magnetic properties, prior to any drilling. This can be achieved in principle by use of geomagnetic (temporal) variations to separate the contributions to the anomaly from the induced and remanent magnetisation of the source. The principle of this method is illustrated in Fig.27.

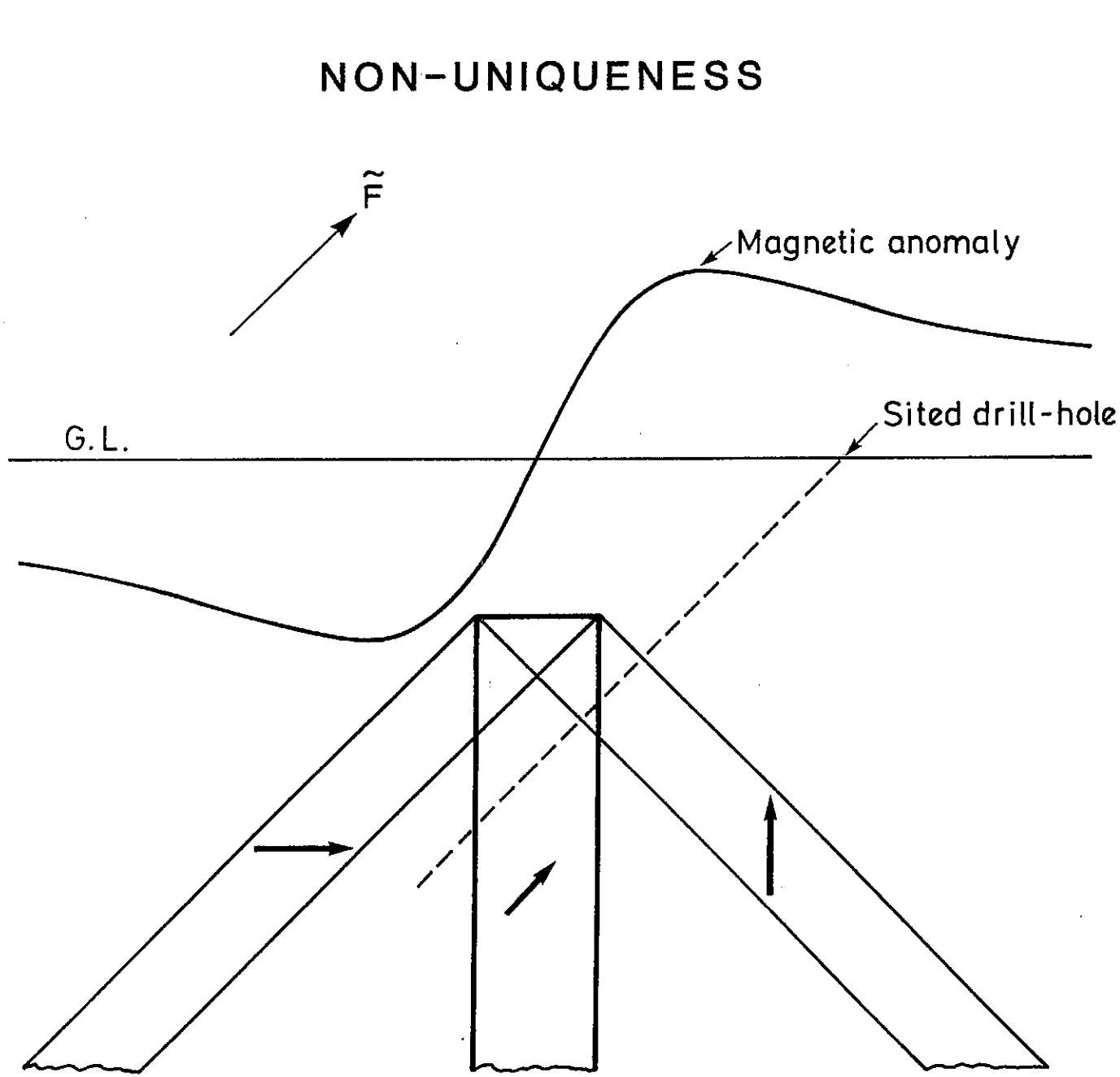

Fig. 24

TESTING MAGNETIC ANOMALIES

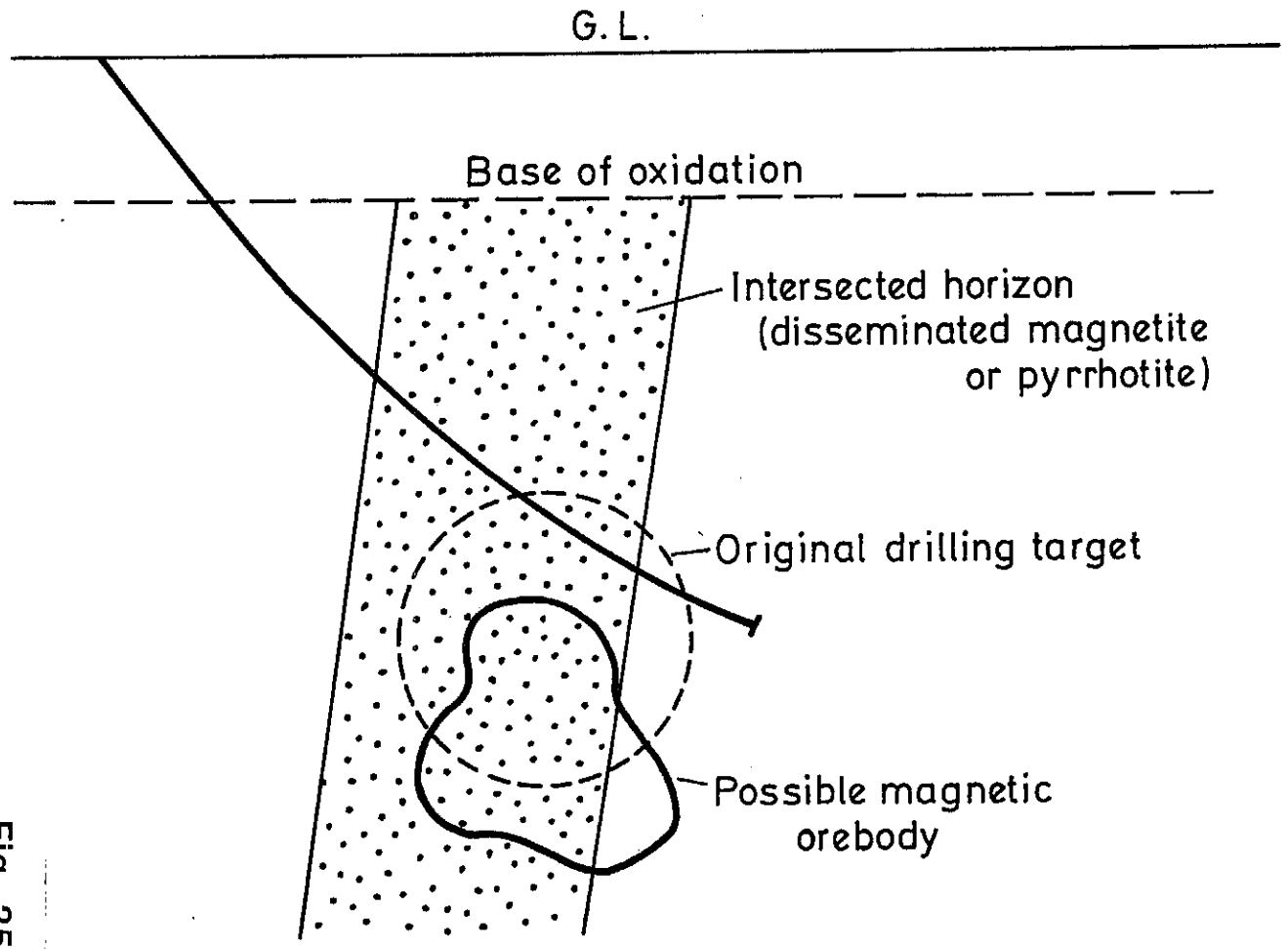

Fig. 25

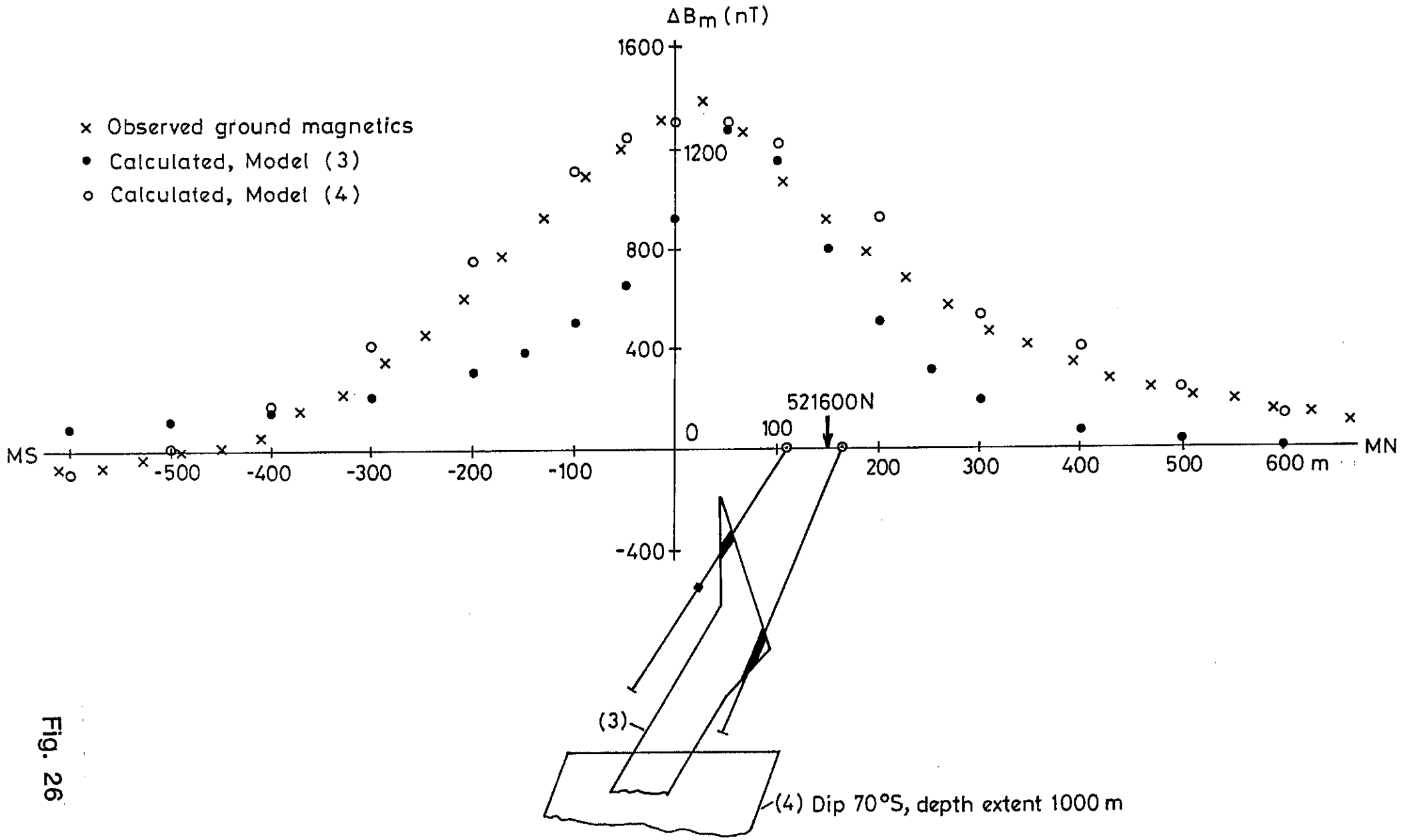

Fig. 26

ATTEMPTS TO EXPLAIN THE ANOMALY

IN SITU DETERMINATION OF Q

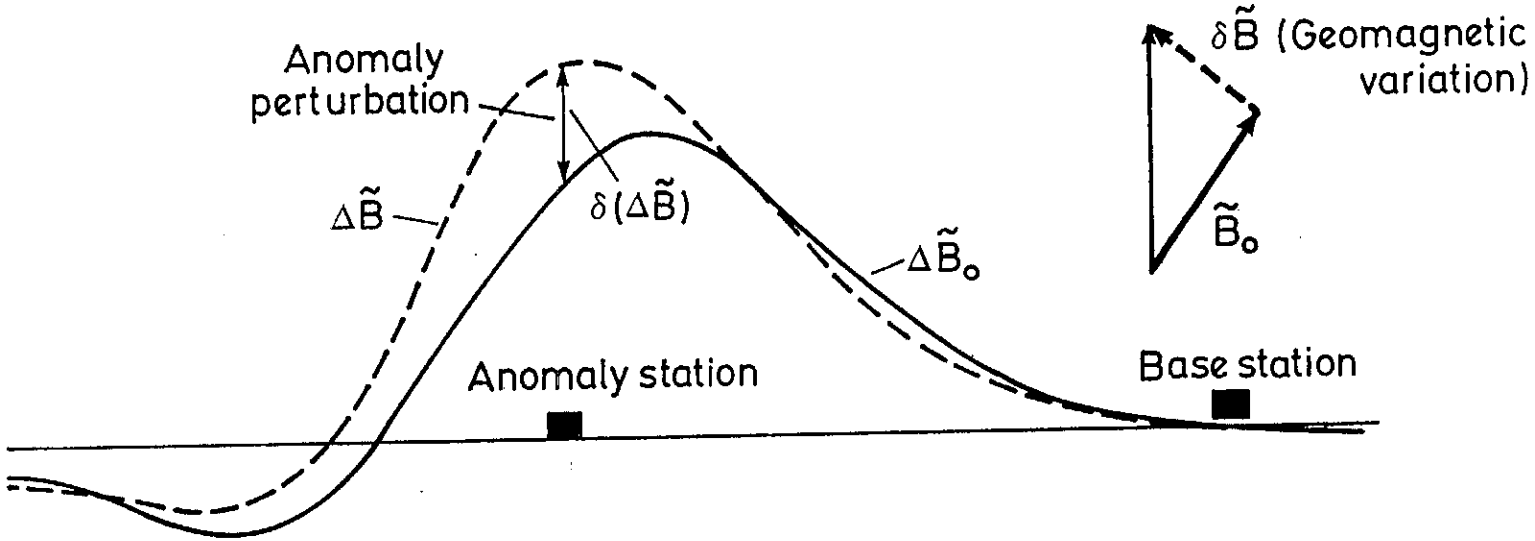

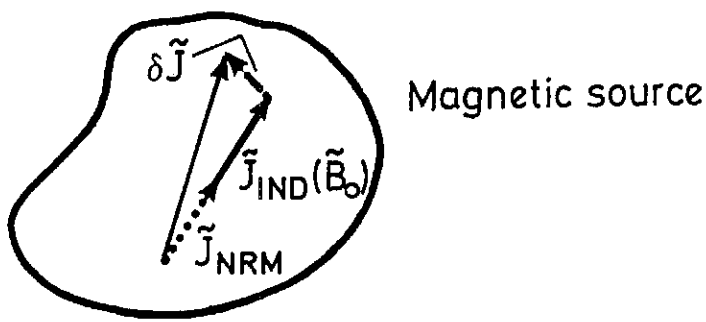

Fig. 27

An Anomaly dominated by Remanence - Peculiar Knob Prospect

The Peculiar Knob prospect in South Australia corresponded to a huge local magnetic anomaly (+35,000 nT), coincident with a 5 milligal gravity high. Drilling intersected three horizons of massive hematite with high susceptibility (typically ~0.02 G/Oe). However the susceptibilities are too low to account for the very intense anomaly. The NRM intensities of the samples were very high and the Q values were very variable, but usually greater than unity and sometimes very large. NRMs fell into two categories: hard monocomponent remanence directed steeply upwards, and multicomponent remanence, composed of easily demagnetised palaeomagnetic noise and a hard stable remanence with similar direction to the monocomponent NRMs. Fig.28(a) shows the effects of AF cleaning of NRMs for several samples. Fig.28(b) shows the k-T curve for the massive hematite, which indicates that the susceptibility is dominated by magnetite and maghemite, although weakly magnetic hematite is volumetrically dominant. The intense and stable remanence is attributable to the microstructure, consisting of fine intergrowths of magnetite and maghemite within hematite, which have PSD character. When remanence is included in the modelling, the anomaly is satisfactorily explained by a consistent model for the magnetic and gravitational sources (see Fig.29).

Paramagnetism and Magnetisation Contrast - Magnetic Ridge

The magnetic ridge anomaly, in the Cobar area, is a prominent local magnetic high, elongated along the trend of a linear high. The anomaly is associated with pyrrhotite-bearing metasediments of the CSA Siltstone. The measured susceptibilities of the sediments are much too low to account for the anomaly, but the Koenigsberger ratios of the samples are high and palaeomagnetic cleaning reveals that the NRMs are multicomponent, consisting of a consistent normal polarity low temperature, soft component overprinting a higher temperature, harder component of dual polarity. Estimation of the average total magnetisation of the magnetic zone, which contains slightly elevated levels of pyrrhotite, however, leads to a predicted anomaly that is about 30% too high, as shown in Fig.30(a). This discrepancy is attributable to the background pyrrhotite content of the enclosing metasediments, which implies that the magnetisation *contrast* is lower than the bulk magnetisation of the magnetic zone (Clark, 1988). This is an illustration of the general principle that magnetisation contrast is the important physical parameter in magnetic interpretation, rather than absolute magnetisation. Detailed analysis of the magnetic properties and the associated anomaly (Fig.30(b)), showed that reliable calculation of the magnetisation contrast required allowance for the background level of paramagnetic susceptibility (~ 50 μG/Oe or 630 x 10-6 SI) of the metasediments. This is an example of the ability of modern magnetic surveys to detect paramagnetism in certain environments.

Magnetic Signatures of BIFs - Anisotropy and Remanence

Figure 31(a) shows the classic dip dependence of anomaly form associated with a dipping sheet model, magnetised parallel to the geomagnetic field. This is applicable to magnetically isotropic bodies, magnetised by induction, or with the magnetisation augmented by VRM, or possibly stable remanence that happens to be parallel to the present field. Figure 31(b), by contrast, shows the very different behaviour of a highly

A

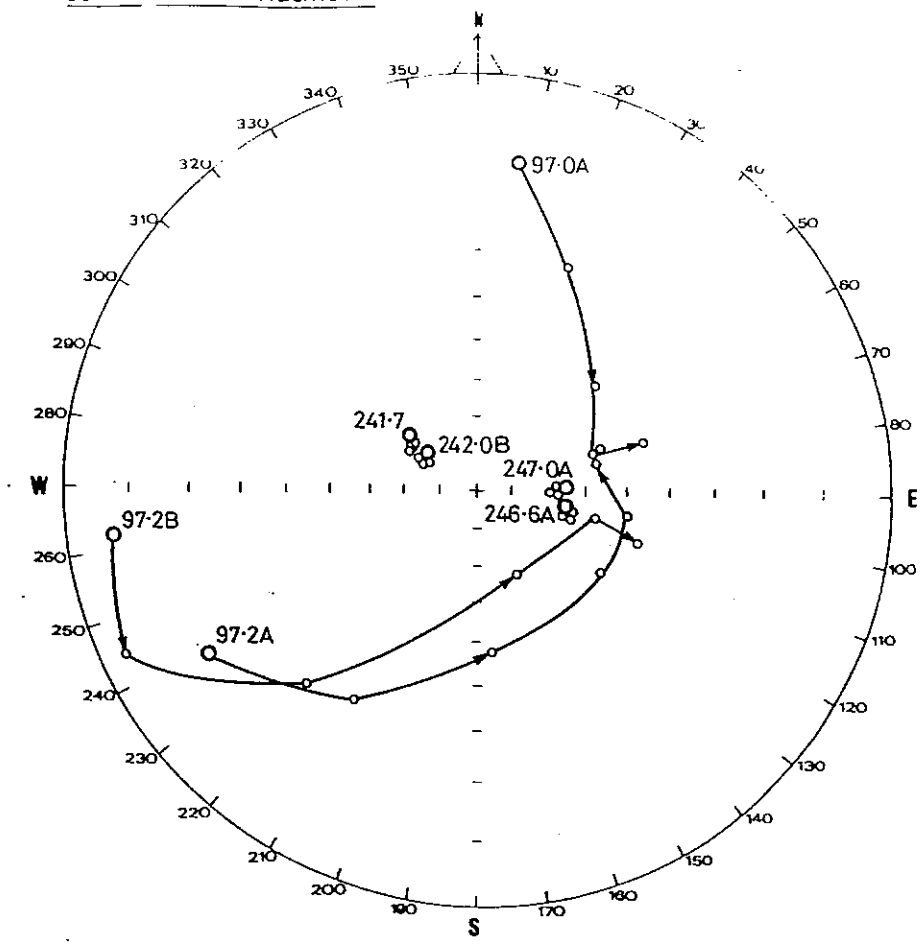

FIG.2b STEREOGRAPHIC PROJECTIONS OF MAGNETIC DIRECTIONS FOR SAMPLES FROM PECULIAR KNOB PROSPECT

B

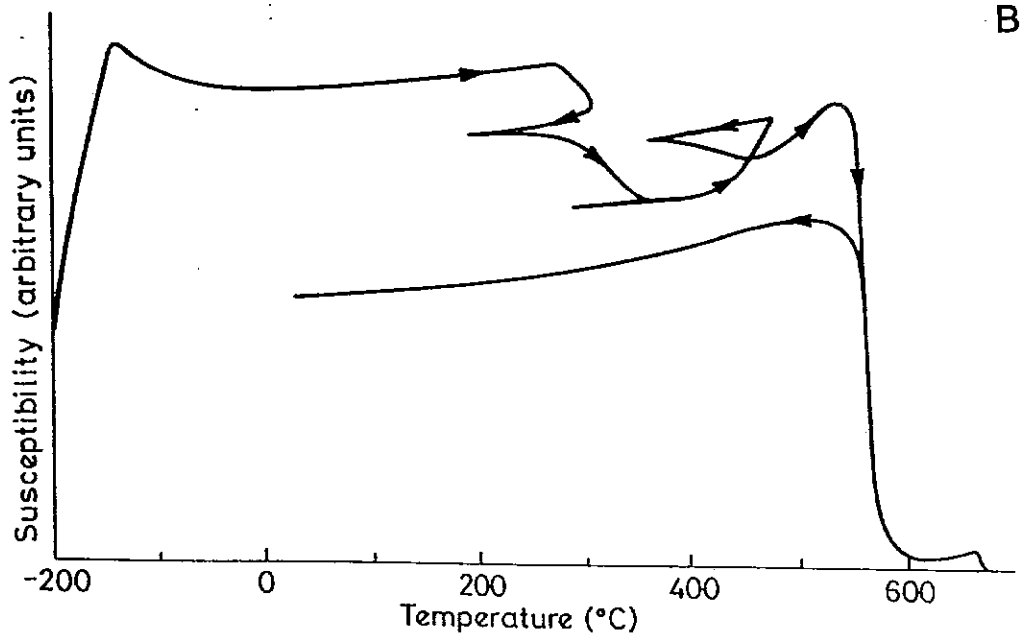

FIG.1 SUSCEPTIBILITY VERSUS TEMPERATURE CURVE FOR PECULIAR KNOB PROSPECT

Fig. 28

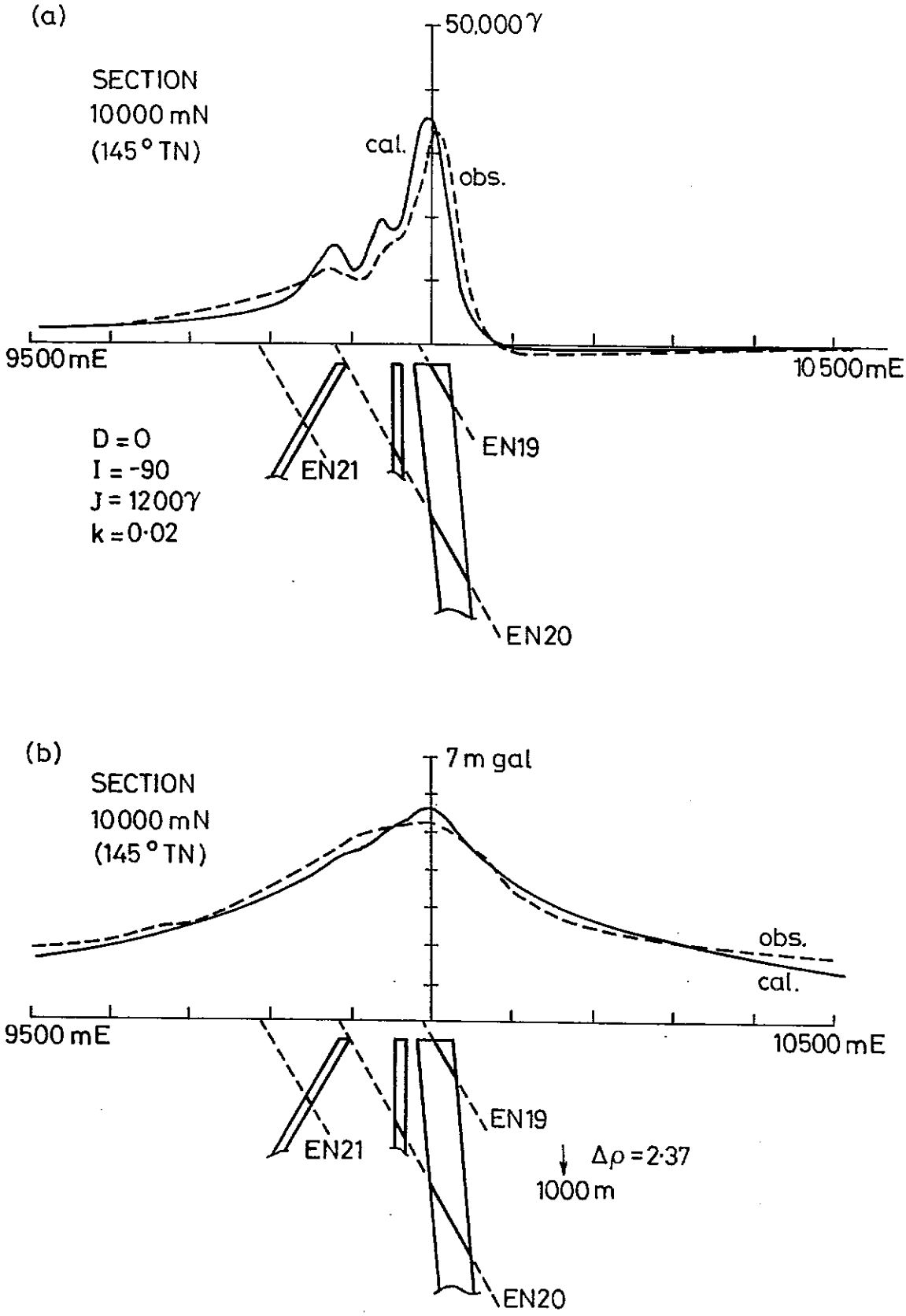

MODELS FOR PECULIAR KNOB PROSPECT (a) MAGNETIC AND (b) GRAVITY

Fig. 29

MAGNETIC RIDGE – THEORETICAL AND MEASURED ANOMALIES

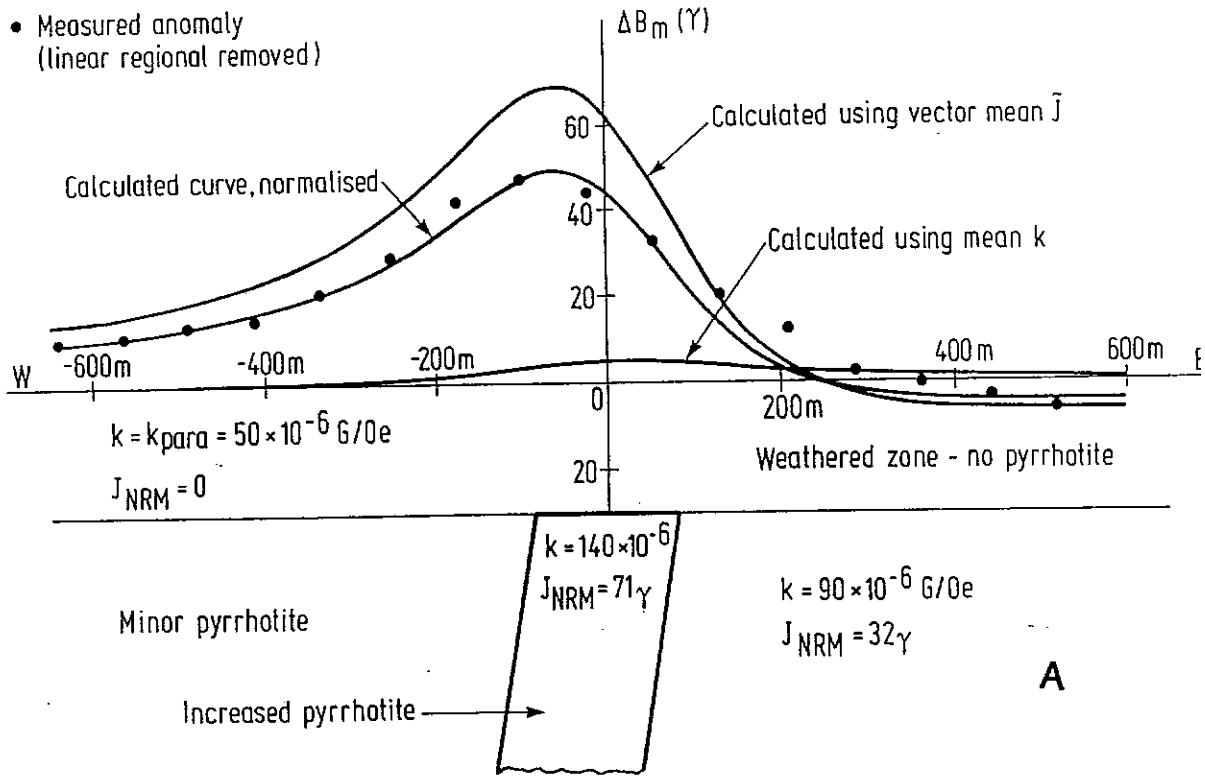

MAGNETIC RIDGE MODEL

$$\left.\begin{aligned} k &= k_{para} + k_{ferro} \\ Q &= \frac{J_{NRM}}{k_{ferro} F} \end{aligned}\right\} \quad J_{NRM} = (k - k_{para})\, QF \quad \text{(SINGLE COMPONENT)}$$

LINEAR REGRESSION OF J_{NRM} ON k (ZONE 2)

			SN + HN	SN + HR
SLOPE	⇒	Q	29	5
INTERCEPT	⇒	k_{para}	46×10^{-6}	56×10^{-6}

$\therefore k_{para} = 50 \times 10^{-6}$ G/Oe

$Q_{soft} = 17$

$Q_{hard} = 12$

B

MAGNETISATION CONTRAST

$$\left.\begin{aligned} &\text{ZONE 1 : } k = 90 \times 10^{-6} \Rightarrow J_{NRM} = 71 \times \frac{90-50}{140-50} \\ &\text{ZONE 2 : } k = 140 \times 10^{-6} \quad J_{NRM} = 71\gamma \end{aligned}\right\} \quad \begin{aligned} \Delta k &= 50 \times 10^{-6} \text{ G/Oe} \\ \Delta J_{NRM} &= 39\gamma \end{aligned}$$

Fig. 30

anisotropic body, with very high magnetic foliation, magnetised by induction. When the anisotropy is extreme, the anomaly shape is actually independent of dip, with the caveat that the sign of the anomaly actually reverses for shallow northerly dips, for which the normal to the sheet becomes steeper than the geomagnetic field. Although this represents a hypothetical extreme case, the principle is qualitatively applicable to banded iron formations, which generally have high anisotropy (A = 2-4, typically).

Remanent magnetisation may have any direction, in principle, and if the Koenigsberger ratio is comparable to, or greater than, unity, the anomaly form can be greatly affected. Fig.32 shows the dip dependence of the anomaly for a dipping sheet, for the case of magnetisation dominated by post-folding remanence, which is vertical irrespective of the degree of tectonic rotation of the sheet. The opposite extreme, when the magnetisation is dominated by pre-folding remanence, which rotates with the sheet during tilting is exemplified by Fig.24. The behaviour of pre- folding remanence during generation of a fold is shown in Fig.33(a). Figure 33(b) shows the magnetic signature of a synclinal magnetic unit with magnetisation dominated by pre- folding remanence.

The major difference between anomalies associated with pre- and post-folding remanence is evident from the signatures of a thin anticlinal bed shown in Fig.34. If the total magnetisation is dominated by post-folding remanence, or by isotropic induction, the signature is almost indistinguishable from that of a single sheet in the axial plane. This is another example of non- uniqueness of magnetic signatures. On the other hand, if the magnetisation is predominantly pre-folding remanence, the signature is much weaker and very different in form.

Therefore, when interpreting structure from magnetic anomalies over remanently magnetised units, the age of remanence relative to folding is of crucial importance, and is best characterised by palaeomagnetic studies in the area. The anomalies associated with Hamersley BIF units have been shown to be influenced by remanence (Q~1) and remanence acquisition has been found to vary from pre-folding in the lowest grade areas, to post-folding in higher grade areas (e.g. Tom Price area). Clark and Schmidt (1986) have shown that quantitative modelling of structure in the Turner Syncline requires an understanding of both anisotropy and post-folding remanence (see Fig.35).

Effects of Self-demagnetisation - Tennant Creek and Trough Tank

The effective magnetisation of bodies with very high susceptibilities is strongly influenced by self-demagnetisation. This occurs when the anomalous internal field produced by the body is comparable to the ambient field, thus greatly modifying the induced magnetisation. The induced magnetisation is reduced with respect to that calculated from multiplying the intrinsic susceptibiltity by the ambient field, and the direction of magnetisation is deflected away from the plane of flattened bodies, or towards the long axis of an elongated body. This affects the interpreted dip or plunge of these bodies. Ellipsoidal models have been developed to cope with this problem, and have particular application to drill targetting for discrete highly magnetic targets, such as those in Tennant Creek (Farrar, 1979; Clark *et al*, 1987). The ellipsoidal geometry is convenient because demagnetising fields are uniform and the effect of self-demagnetisation can be calculated analytically.

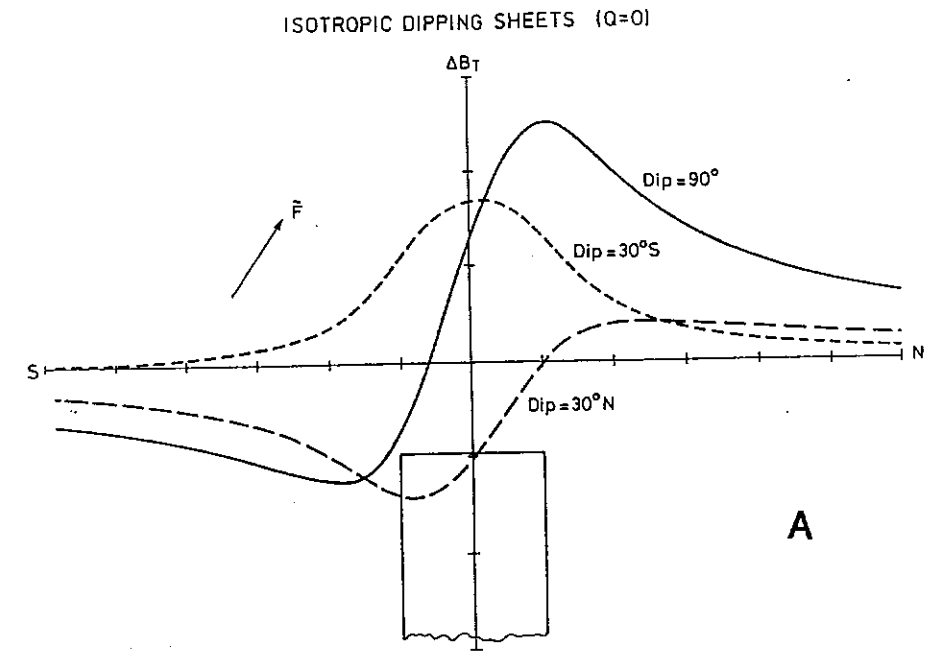
ISOTROPIC DIPPING SHEETS (Q=0)
ΔBT
F̃
Dip=90°
Dip=30°S
Dip=30°N
S
N
A

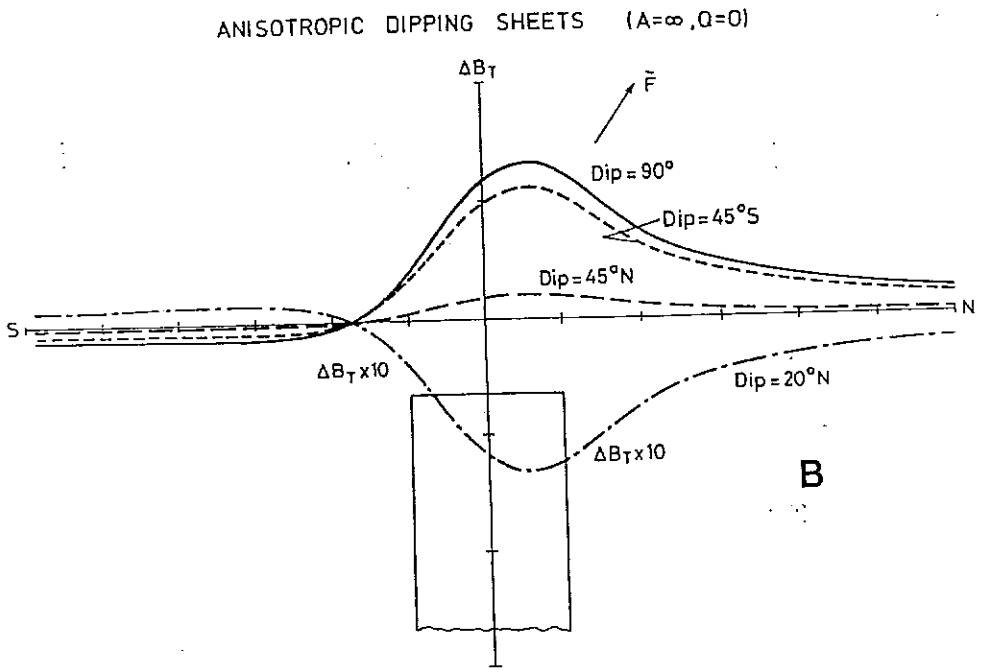
ANISOTROPIC DIPPING SHEETS (A=∞, Q=0)
ΔBT
F̃
Dip=90°
Dip=45°S
Dip=45°N
Dip=20°N
ΔBT x10
ΔBT x10
S
N
B

Fig. 31

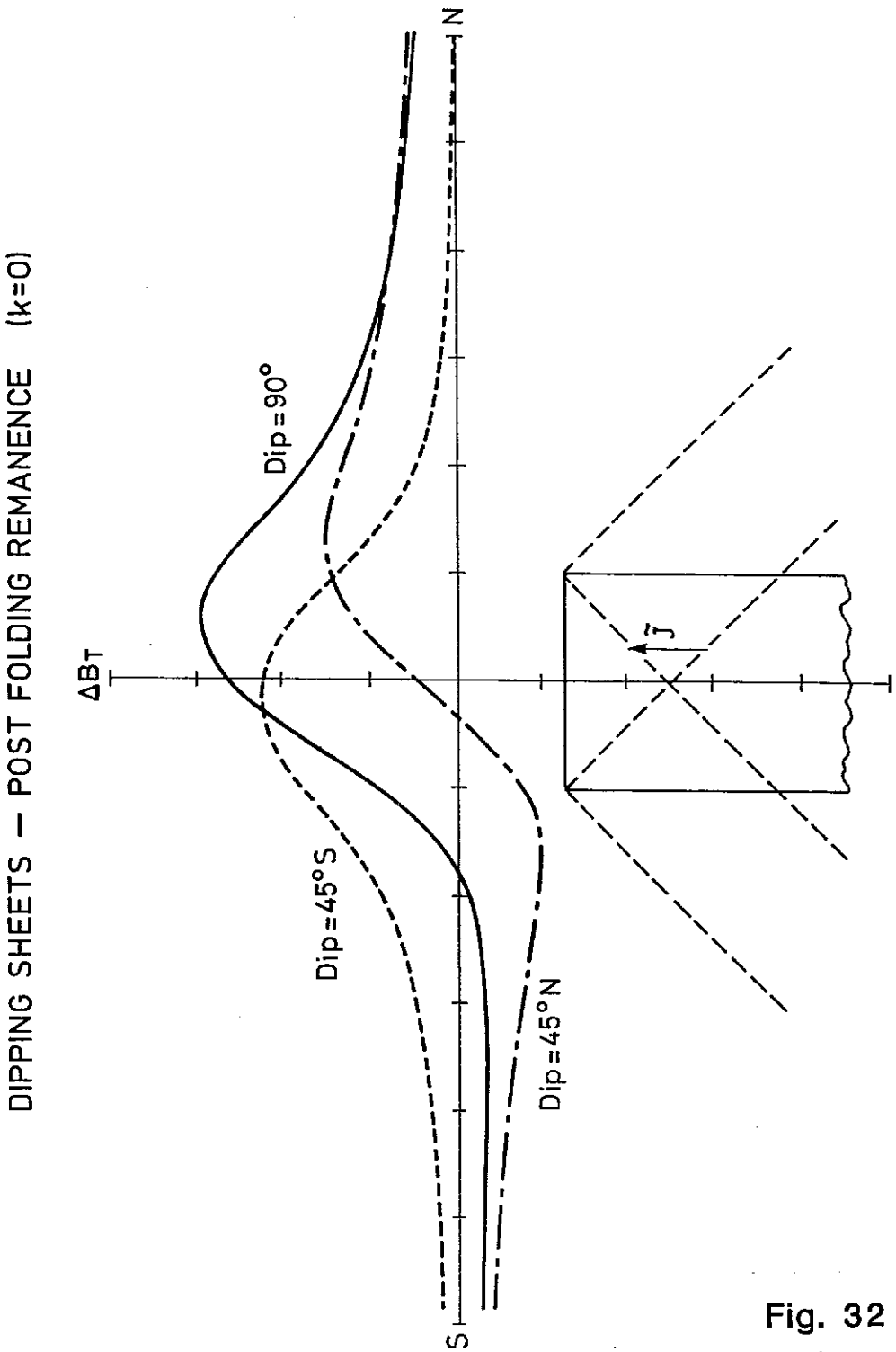
DIPPING SHEETS — POST FOLDING REMANENCE (k=0)
ΔBT
N
S
Dip=90°
Dip=45°S
Dip=45°N
J

Fig. 32

EFFECT OF TECTONIC TILTING ON REMANENCE DIRECTIONS

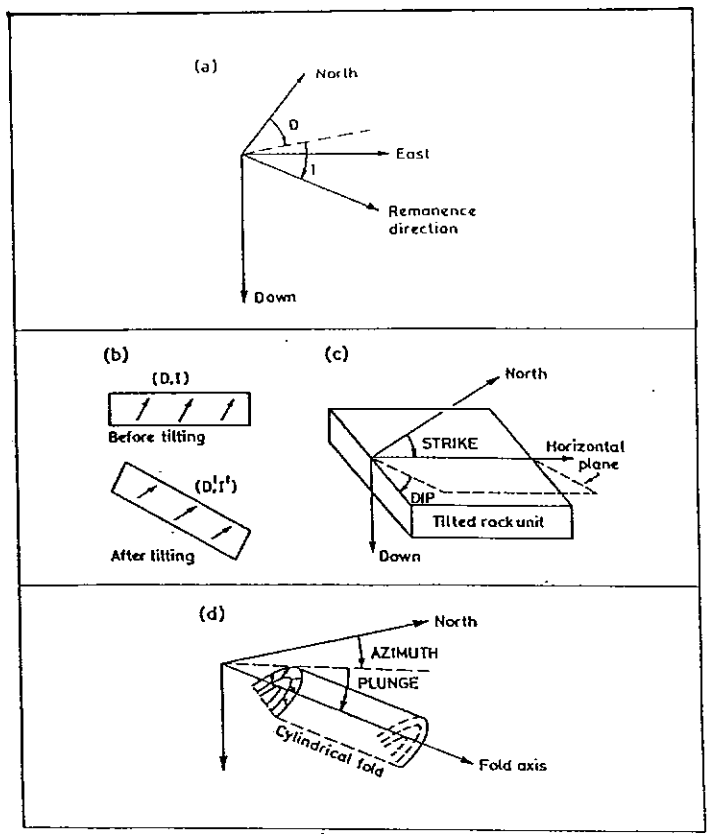

A

SYNCLINE WITH PRE-FOLDING REMANENCE (k=0)

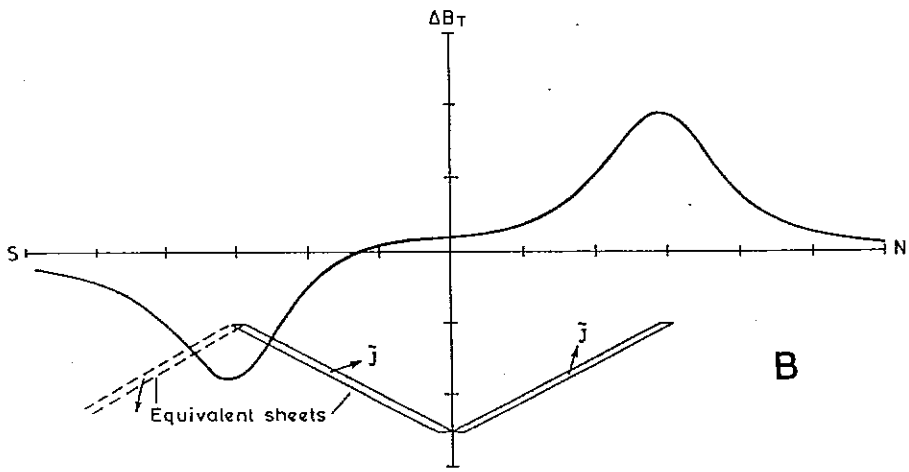

B

Fig. 33

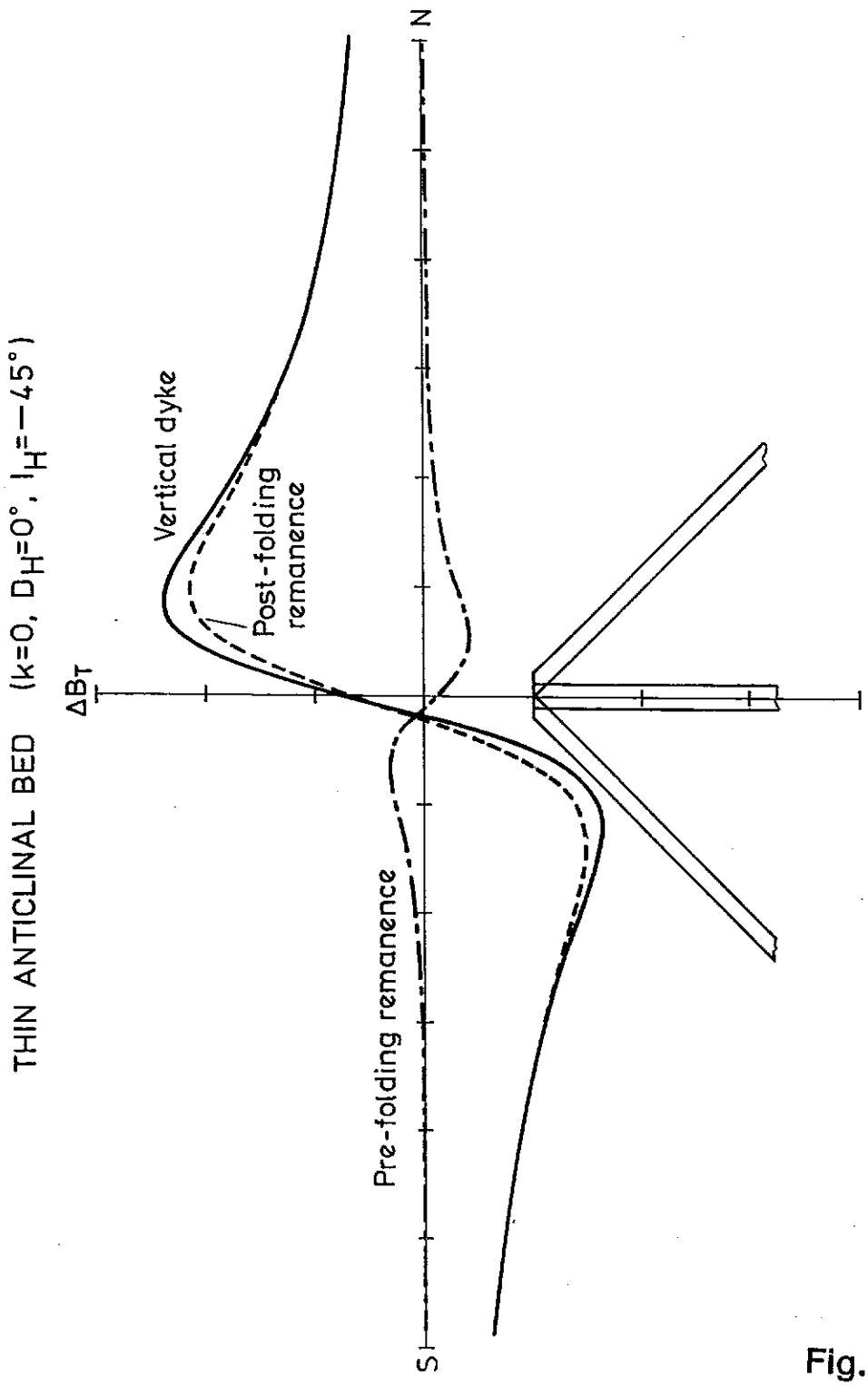
THIN ANTICLINAL BED (k=0, D_H=0°, I_H=−45°)
ΔBT
Vertical dyke
Post-folding remanence
Pre-folding remanence
N
S

Fig. 34

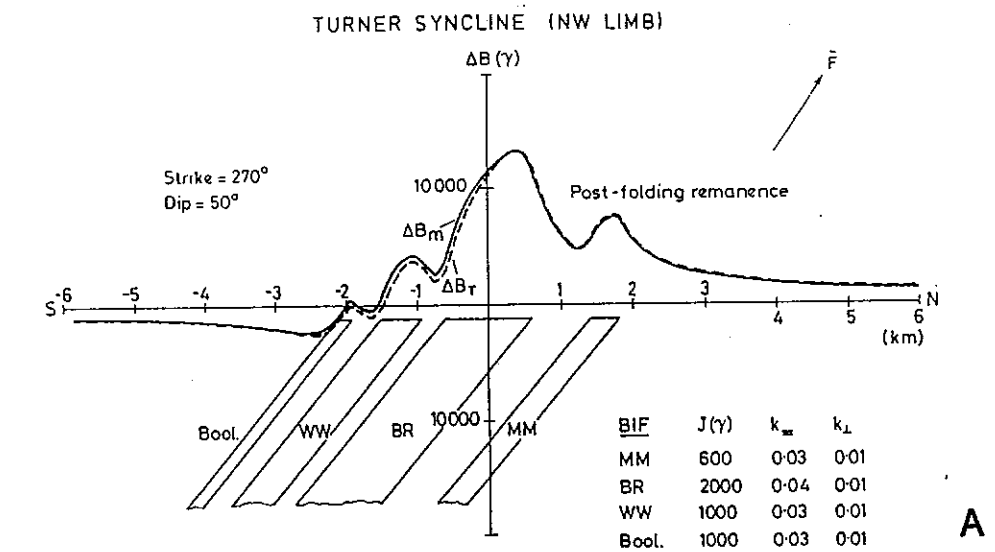
TURNER SYNCLINE (NW LIMB)
ΔB (γ)
F̃
Strike = 270°
Dip = 50°
10 000
Post-folding remanence
ΔBm
ΔBT
S
N
-6 -5 -4 -3 -2 -1 1 2 3 4 5 6
(km)
Bool.
WW
BR
10000
MM
BIF J(γ) k∥ k⊥
MM 600 0·03 0·01
BR 2000 0·04 0·01
WW 1000 0·03 0·01
Bool. 1000 0·03 0·01

A

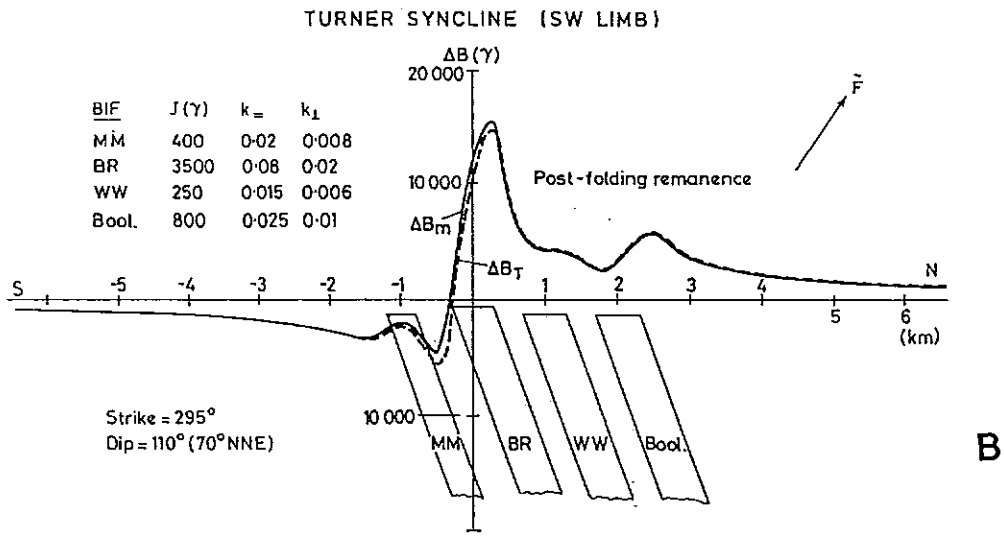
TURNER SYNCLINE (SW LIMB)
ΔB (γ)
20 000
F̃
BIF J(γ) k∥ k⊥
MM 400 0·02 0·008
BR 3500 0·08 0·02
WW 250 0·015 0·006
Bool. 800 0·025 0·01
10 000
Post-folding remanence
ΔBm
ΔBT
S
N
-6 -5 -4 -3 -2 -1 1 2 3 4 5 6
(km)
Strike = 295°
Dip = 110° (70°NNE)
10 000
MM
BR
WW
Bool.

B

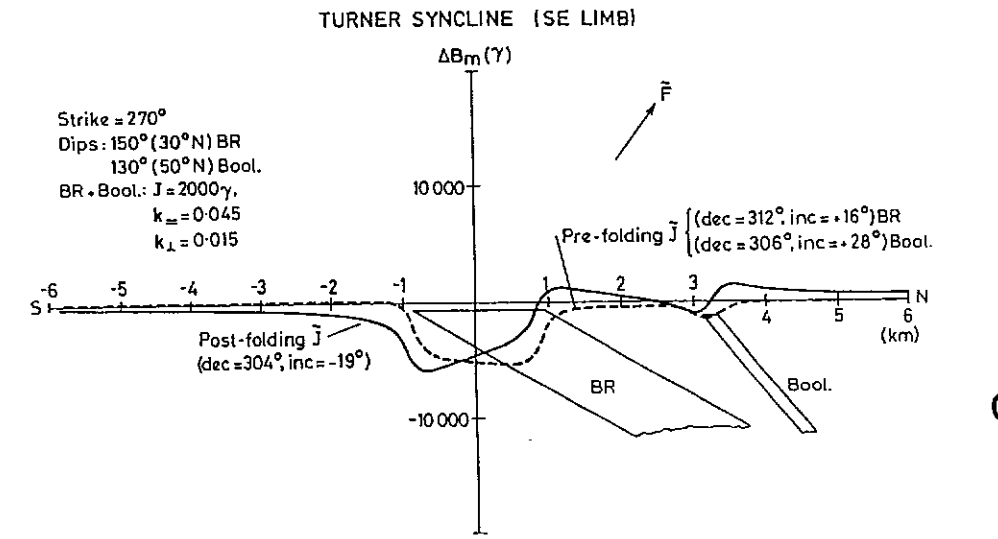
TURNER SYNCLINE (SE LIMB)
ΔBm (γ)
F̃
Strike = 270°
Dips: 150° (30°N) BR
130° (50°N) Bool.
BR + Bool.: J = 2000γ,
k∥ = 0·045
k⊥ = 0·015
10 000
Pre-folding J̃ (dec = 312°, inc = +16°) BR
(dec = 306°, inc = +28°) Bool.
S
N
-6 -5 -4 -3 -2 -1 1 2 3 4 5 6
(km)
Post-folding J̃
(dec = 304°, inc = -19°)
BR
Bool.
-10 000

C

Fig. 35

Fig.36 shows a magnetic model for the Warrego orebody, near Tennant Creek (from Clark and Tonkin, 1987). The magnetic signature of this body is strongly affected by self-demagnetisation, which swings the anomaly axis from N-S into the plunge plane and changes the relative amplitudes of the high and associated low. The observed anomaly is well explained by the measured susceptibilities and remanence vectors.

The Trough Tank Prospect (now the Osborne Prospect), in the eastern Mount Isa Inlier, is another example of the effects of self-demagnetisation and of perturbation of the local geomagnetic field by an intense local anomaly. Failure to recognise these factors led to the initial drilling going down dip. Fig.37 shows the discrepancy between the apparent and true dips. Figure 38 illustrates another complication for interpretation of intense anomalies, namely that ΔB_m anomalies due to composite sources do not obey the principle of superposition, unlike component anomalies along fixed directions. Figure 39 shows the effect on anomaly shape of self-demagnetisation, anisotropy and perturbation of the local field for the source of the Trough Tank anomaly. For a different dip, the effects can be even larger (see Fig.40).

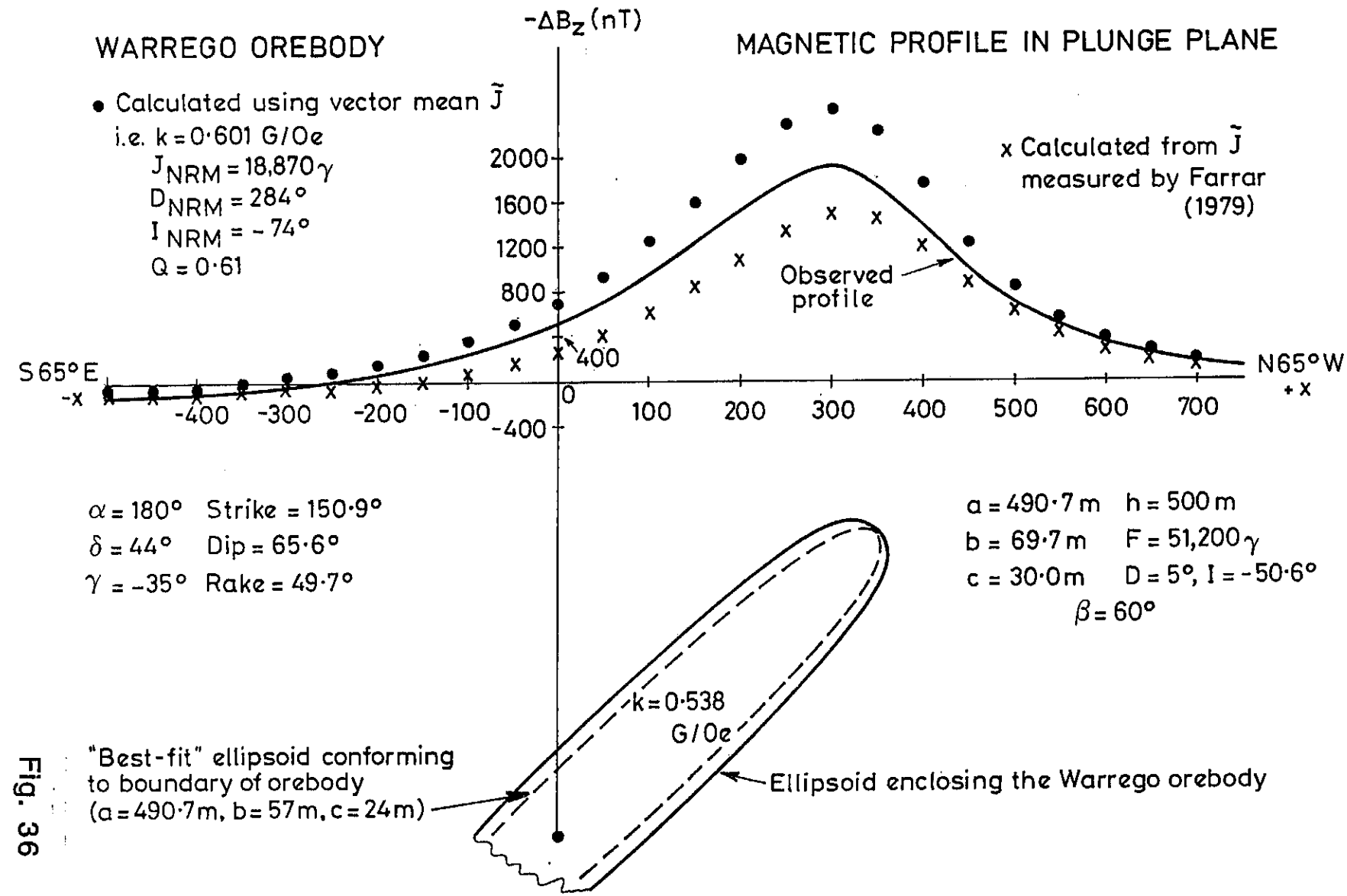
WARREGO OREBODY
MAGNETIC PROFILE IN PLUNGE PLANE
-ΔBz (nT)
• Calculated using vector mean J̃
i.e. k = 0·601 G/Oe
JNRM = 18,870γ
DNRM = 284°
INRM = -74°
Q = 0·61
x Calculated from J̃ measured by Farrar (1979)
Observed profile
2000
1600
1200
800
400
0
-400
-400
-300
-200
-100
100
200
300
400
500
600
700
S65°E
-x
N65°W
+x
α = 180° Strike = 150·9°
δ = 44° Dip = 65·6°
γ = -35° Rake = 49·7°
a = 490·7 m h = 500 m
b = 69·7 m F = 51,200γ
c = 30·0 m D = 5°, I = -50·6°
β = 60°
k = 0·538 G/Oe
"Best-fit" ellipsoid conforming to boundary of orebody (a = 490·7m, b = 57m, c = 24m)
Ellipsoid enclosing the Warrego orebody

Fig. 36

ANOMALOUS APPARENT DIP OF TROUGH TANK BIF

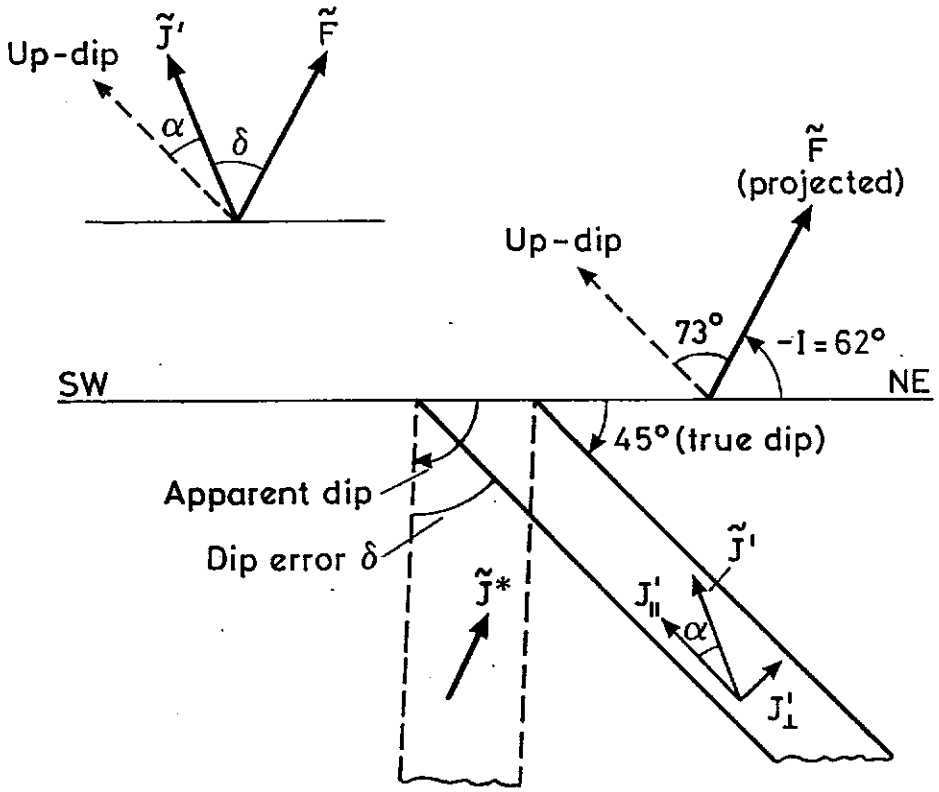

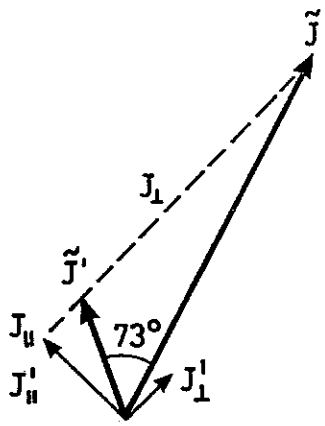

Without self-demagnetisation:

$J_{II} = kF \cos 73°$

$J_{\perp} = kF \sin 73°$

With self-demagnetisation:

$J'_{II} = J_{II} \qquad (N_{II} = 0)$

$J'_{\perp} = \dfrac{J_{\perp}}{1+4\pi k} \qquad (N_{\perp} = 4)$

$$\therefore \tan\alpha = \frac{J'_{\perp}}{J'_{II}} = \frac{\tan 73°}{1+4\pi k}$$

Fig. 37

OBSERVED AND PREDICTED TOTAL FIELD ANOMALIES, TROUGH TANK (LINE 1770N, KEEL GRID)

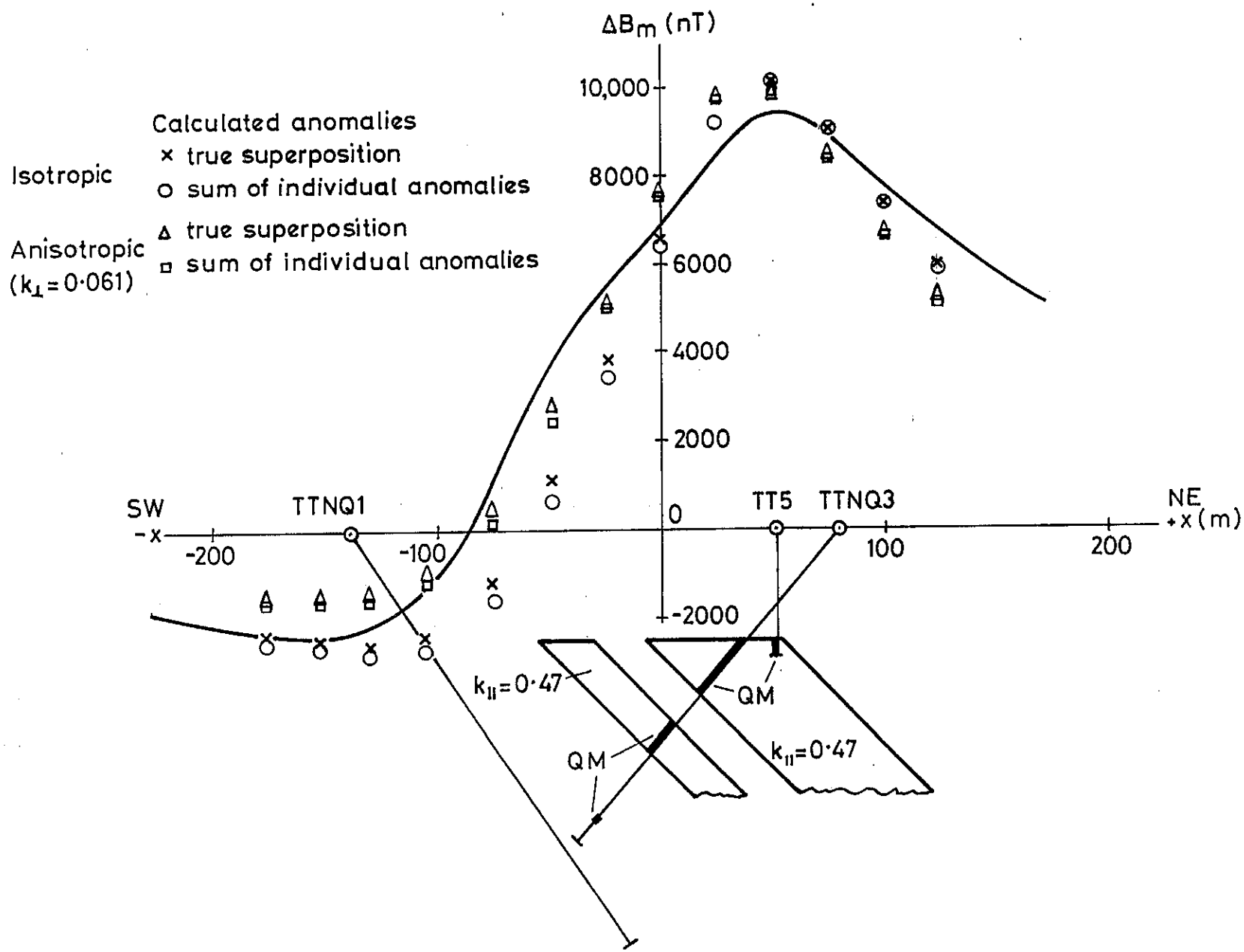

Fig. 38

EFFECTS OF SELF—DEMAGNETISATION AND ANISOTROPY ON ANOMALY SHAPE

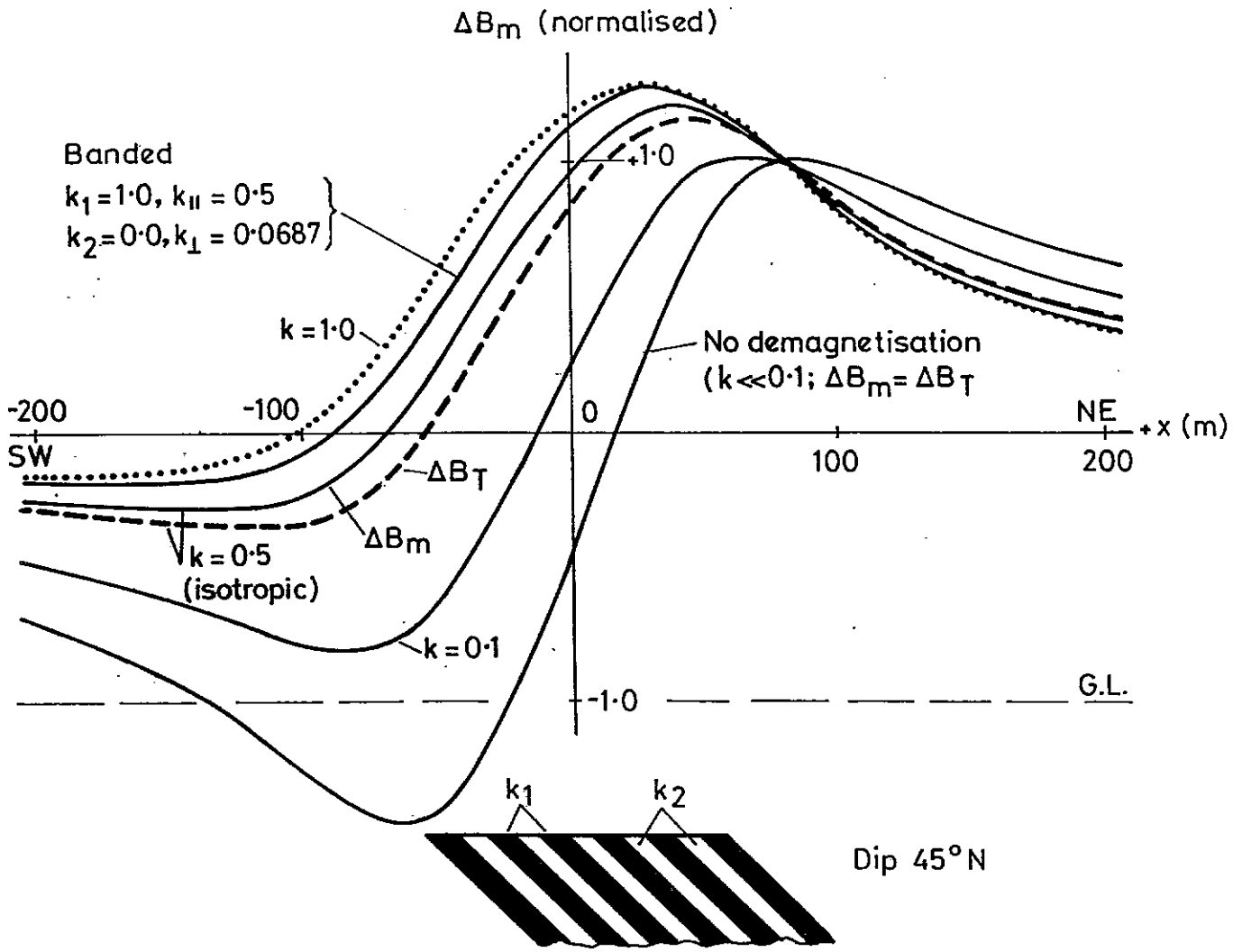

Fig. 39

DIP DEPENDENCE OF ΔB_m AND ΔB_T ANOMALIES

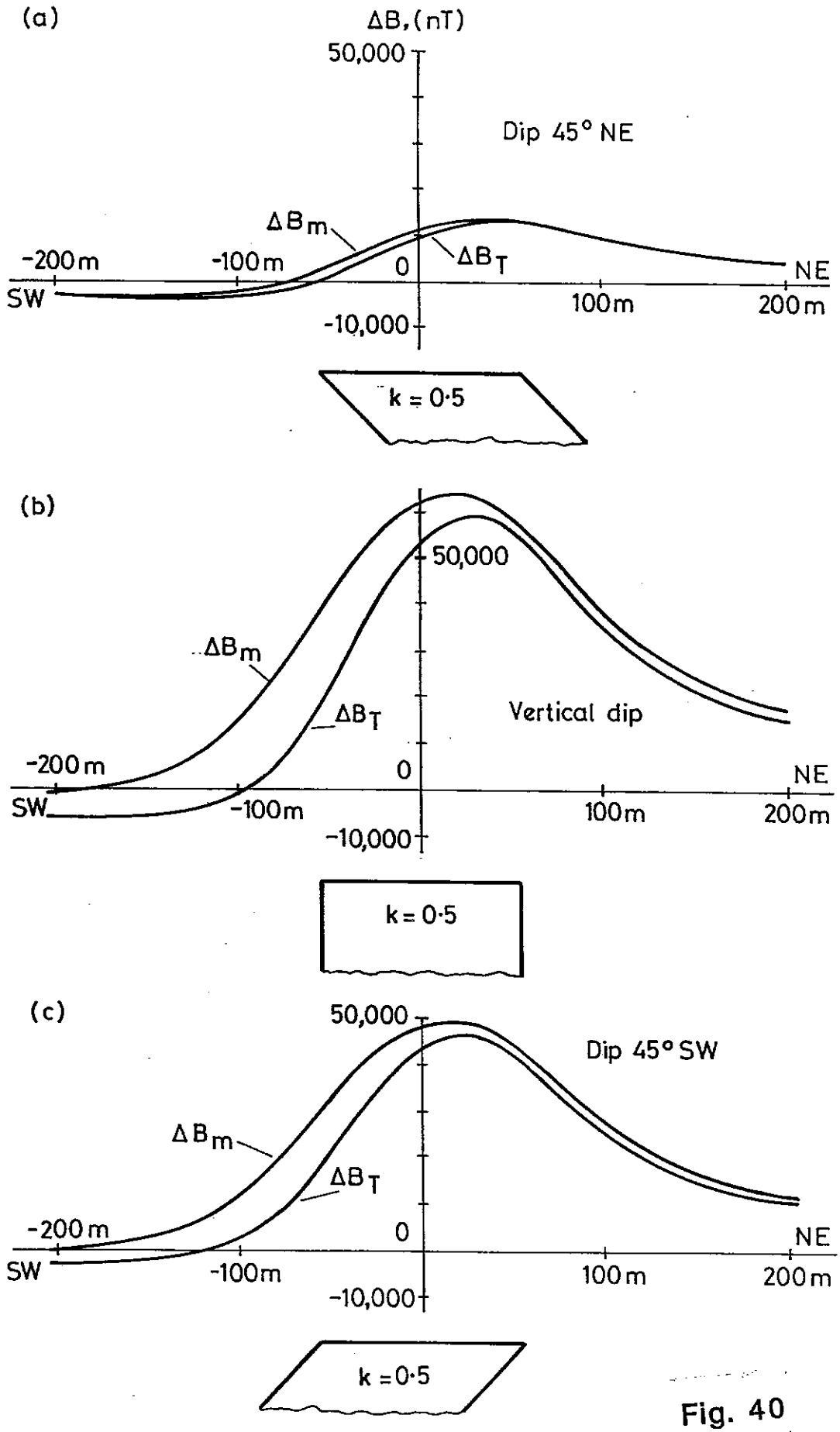

Fig. 40

SECTION 3. MAGNETIC PETROLOGY

What is Magnetic Petrology?

Magnetic petrology is the integrated application of rock magnetic and conventional petrologic techniques to identify and characterise the magnetic minerals present in rocks. This information elucidates the factors, such as bulk composition, magmatic differentiation and emplacement conditions, that produce, alter and destroy magnetic minerals and thereby influence the bulk magnetic properties of the rocks and their associated magnetic anomalies.

Overview of Magnetic Properties of Rocks

The data of Figs. 41-42 are based on magnetic property measurements at the CSIRO Division of Exploration Geoscience over the last 12 years and published studies and compilations. The systematic collection of petrophysical data by the Geological Surveys of Scandinavian countries, in particular, has greatly expanded the size and scope of the information available. It is evident from Fig. 41 that each rock type exhibits a wide range of susceptibilities and that susceptibility values are not generally diagnostic of lithology. Classical rock names are in fact much too broad to be useful for classification of magnetic properties. This is because the susceptibility of most rocks reflects the abundance of accessory minerals, particularly magnetite (*sensu lato*), which are ignored in petrological classification. At a more refined level, however, there is significant geological information in basic magnetic properties, especially if the statistical characteristics of large collections are considered and if the measurements are supplemented by rock magnetic experiments to characterise the compositions and microstructures of the magnetic minerals. The magnetic minerals in a metaigneous rock, for example are sensitive to its geological history, including the bulk composition and petrogenetic affinities of the magma, the degree of differentiation, conditions of emplacement, degree and type of hydrothermal alteration and conditions of metamorphism (temperature, pressure, fugacities of oxygen, water, sulphur, CO_2 etc.). Differences in magnetic properties can therefore reflect subtle variations in some or all of these influences. More detailed clasification schemes, based on the most important of these factors, may therefore allow more meaningful interpretation of magnetic surveys in terms of geology. In some cases observed differences in magnetic anomaly patterns within single mapped units have indicated hitherto unsuspected heterogeneity, which has then been confirmed by remapping.

The variations in magnetic properties for given lithologies are generally greater between geological provinces than within them, although large variations are also possible over smaller areas, even down to the outcrop scale. A notable feature of Fig. 41 is that the susceptibilities of a number of rock types have distinctly bimodal distributions. In the case of granitoids, this reflects the existence of two distinct categories, that have only recently been recognised: the magnetite-series and ilmenite-series granitoids of Ishihara (1977). Magnetite-series granitoids are relatively oxidised and correspond broadly to the I-type granitoids of Chappell and White (1974), whereas ilmenite-series granitoids are more reduced and are usually S-type. The new classifications, which have important petrogenetic and metallogenic implications, have led to the concept of mapping granitoid

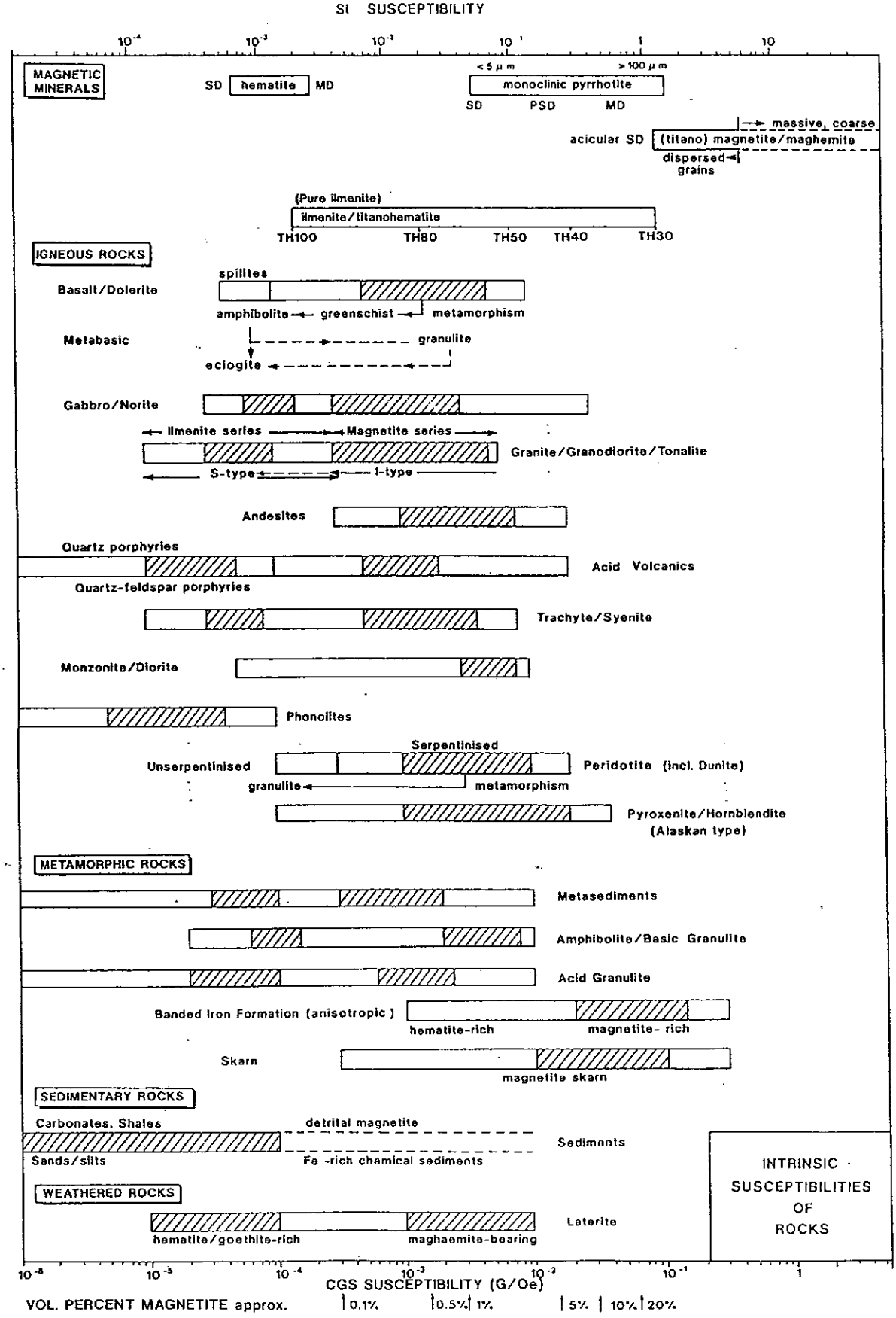
SI SUSCEPTIBILITY
10⁻⁴
10⁻³
10⁻²
10⁻¹
1
10
MAGNETIC MINERALS
SD
hematite
MD
< 5 μm
> 100 μm
monoclinic pyrrhotite
SD
PSD
MD
massive, coarse
acicular SD
(titano) magnetite/maghemite
dispersed grains
(Pure ilmenite)
ilmenite/titanohematite
TH100
TH80
TH50
TH40
TH30
IGNEOUS ROCKS
spilites
Basalt/Dolerite
amphibolite
greenschist
metamorphism
Metabasic
granulite
eclogite
Gabbro/Norite
Ilmenite series
Magnetite series
Granite/Granodiorite/Tonalite
S-type
I-type
Andesites
Quartz porphyries
Acid Volcanics
Quartz-feldspar porphyries
Trachyte/Syenite
Monzonite/Diorite
Phonolites
Serpentinised
Unserpentinised
Peridotite (incl. Dunite)
granulite
metamorphism
Pyroxenite/Hornblendite (Alaskan type)
METAMORPHIC ROCKS
Metasediments
Amphibolite/Basic Granulite
Acid Granulite
Banded Iron Formation (anisotropic)
hematite-rich
magnetite- rich
Skarn
magnetite skarn
SEDIMENTARY ROCKS
Carbonates, Shales
detrital magnetite
Sediments
Sands/silts
Fe -rich chemical sediments
WEATHERED ROCKS
Laterite
hematite/goethite-rich
maghaemite-bearing
INTRINSIC SUSCEPTIBILITIES OF ROCKS
10⁻⁶
10⁻⁵
10⁻⁴
10⁻³
10⁻²
10⁻¹
1
CGS SUSCEPTIBILITY (G/Oe)
VOL. PERCENT MAGNETITE approx.
0.1%
0.5%
1%
5%
10%
20%

FIG. 41

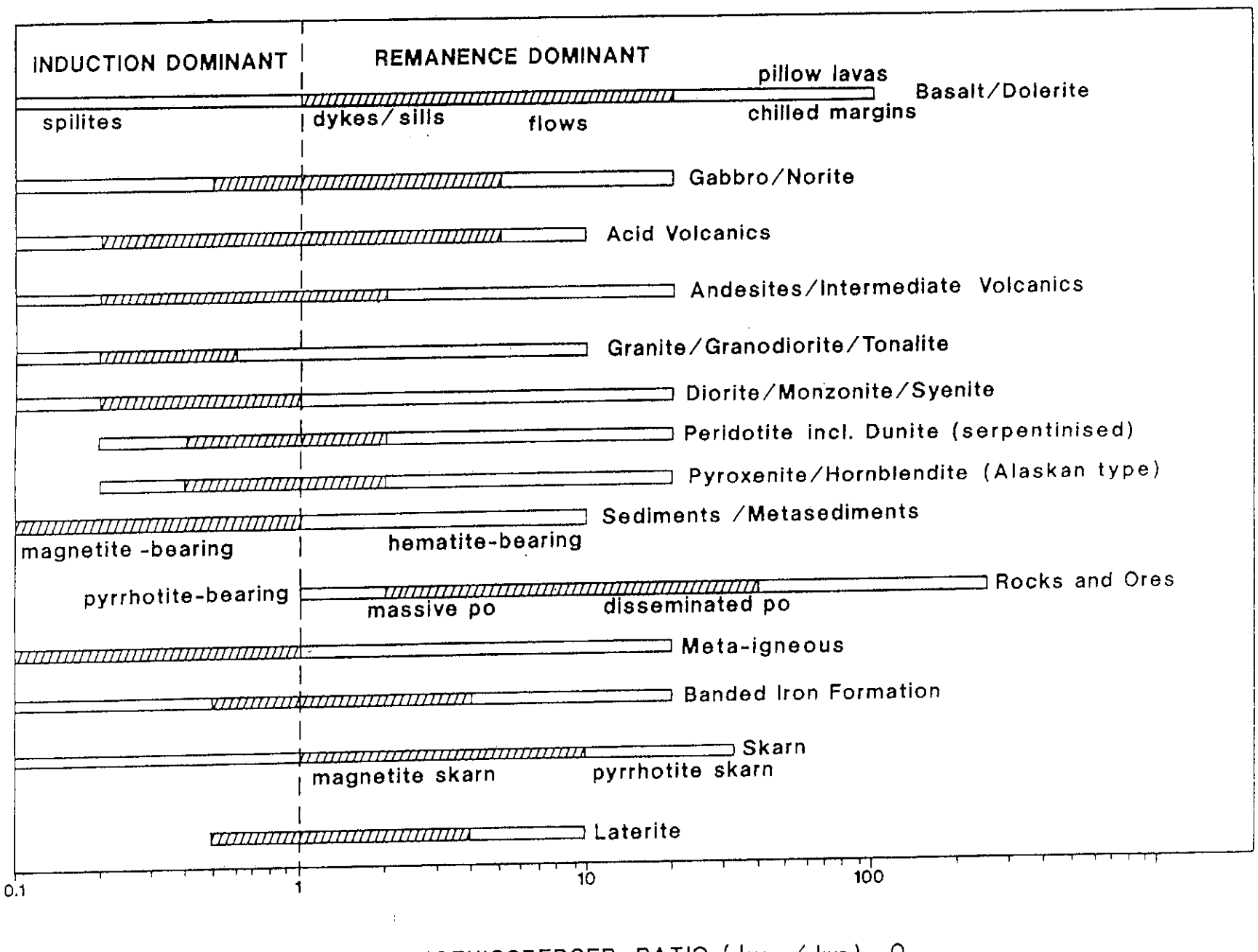
INDUCTION DOMINANT
REMANENCE DOMINANT
pillow lavas
Basalt/Dolerite
spilites
dykes/ sills
flows
chilled margins
Gabbro/Norite
Acid Volcanics
Andesites/Intermediate Volcanics
Granite/Granodiorite/Tonalite
Diorite/Monzonite/Syenite
Peridotite incl. Dunite (serpentinised)
Pyroxenite/Hornblendite (Alaskan type)
Sediments /Metasediments
magnetite -bearing
hematite-bearing
pyrrhotite-bearing
Rocks and Ores
massive po
disseminated po
Meta-igneous
Banded Iron Formation
Skarn
magnetite skarn
pyrrhotite skarn
Laterite
0.1
1
10
100
KOENIGSBERGER RATIO (JNRM / JIND) Qn

FIG. 42

terrains using a hand-held susceptibility meter or a magnetometer and provide a good example of the utility of categories based on magnetics. More generally, bimodal susceptibility distributions represent distinct subpopulations within each rock type for which ferromagnetic minerals are absent and present respectively. Iron in the weakly magnetic subpopulation is incorporated into paramagnetic silicate minerals, predominantly as Fe^{2+}, whereas similar rocks that are moderately to strongly magnetic contain significant Fe^{3+}, which is incorporated into magnetite. Very highly oxidised rocks, however, tend to contain hematite rather than magnetite and are therefore also weakly magnetic. Within each magnetic subpopulation susceptibility tends to increase with basicity. The greater abundance of paramagnetic mafic minerals in rocks with lower SiO_2 increases the paramagnetic contribution to the susceptibility. This produces a small, but systematic difference, in the susceptibilities of paramagnetic acid and basic rocks. The increasing sensitivity of modern magnetometers and the trend to more detailed magnetic surveys suggests that magnetic mapping may become useful even in very weakly magnetic terrains, where the rocks would hitherto have been classified as "non-magnetic" on the basis of their apparent flat and featureless magnetic patterns in low resolution surveys.

More commonly, however, the observed magnetic signatures reflect variations in the abundance of ferromagnetic minerals. The overall tendency for magnetite content of ferromagnetic rocks to increase with basicity is somewhat obscured when igneous rocks from different provinces are compared. For consanguinous rocks, in particular, there is a general correlation between susceptibility and basicity. Andesites generally have similar, or slightly lower, susceptibilities than related basalts. Rhyolites have a distinctly bimodal susceptibility distribution. Ferromagnetic rhyolites tend to be somewhat less magnetic than the more basic members of the series, and many rhyolites are paramagnetic. Trachyandesites and trachytes generally have moderate to high susceptibilities, comparable to or somewhat less than susceptibilities of related alkali basalts, but the corresponding phonolites are usually weakly magnetic. Within the ferromagnetic subpopulation of each lithology, magnetic properties can also be related to geochemistry. For tholeiitic rocks in both oceanic and continental settings iron and titanium-rich variants have been found to have substantially higher susceptibilities, reflecting greater modal titanomagnetite, than similar rocks with lower Fe and Ti contents (e.g. Anderson *et al.*, 1975 ; de Boer and Snider, 1979).

"Clean" carbonates and clastic sediments have very low susceptibilities. Some immature sandstones contain significant quantities of detrital magnetite, which may provide an indication of provenance, and are therefore magnetic. Sediments deposited in the presence of metal-bearing solutions, associated with volcanic activity for example, may contain appreciable magnetite, or possibly pyrrhotite, and therefore be magnetic. Such sediments may be transitional to syngenetic massive mineralisation or to banded iron formation. Magnetite- rich banded iron formations are not only strongly magnetic but are characterised by high anisotropy of susceptibility. The susceptibility parallel to bedding is typically greater than the suscptibility normal to bedding by a factor of 2-4. The susceptibility values for banded iron formation shown in Fig. 41 are bulk susceptibilities, i.e. the average of the susceptibilities along any three orthogonal directions. Although almost all rocks exhibit slightly anisotropic magnetic susceptibility, which can be interpreted in terms of petrofabric, the degree of anisotropy is generally insufficient to

significantly influence the form of magnetic anomalies. Exceptions include banded iron formations and some rocks and ores that contain pyrrhotite with a strong preferred orientation.

The iron content of the sediment (generally higher for pelites than for psammites) and the Fe^{3+}/Fe^{2+} ratio, which reflects the redox conditions during deposition and diagenesis, have a major bearing on the capacity of the rock to develop secondary magnetite during metamorphism. Thus magnetic patterns over metasedimentary rocks tend to reflect sedimentary facies variations, as well as metamorphic conditions. These patterns can be very useful for mapping, although the relationship between the magnetic marker units and conventional lithological units may be quite tenuous (McIntyre, 1980). Pyrrhotite is the main magnetic mineral in many metasedimentary rocks, particularly in mineralised areas. Monoclinic (4C) pyrrhotite, which approximates Fe_7S_8 in composition, is the ferromagnetic variety. More iron-rich varieties of pyrrhotite are very weakly magnetic.

Fresh basalts and dolerites have moderate to high susceptibilities. Hydrothermal alteration of these rocks usually reduces the susceptibility. Regional metamorphism to greenschist grade, and *a fortiori* to amphibolite grade, tends to demagnetise basic igneous rocks. Granulite facies metamorphism of these rocks, however, may produce secondary magnetite and produce highly magnetic units. Eclogite facies metamorphism destroys all magnetite and partitions iron into paramagnetic silicates. Gabbros exhibit a bimodal susceptibility distribution, reflecting paramagnetic and ferromagnetic subpopulations. In most provinces, the ferromagnetic group is more prominent. Very fine, generally acicular, (titano)magnetites within pyroxene, olivine and plagioclase grains are largely responsible for the relatively intense and stable remanence carried by many gabbros and other basic intrusives. These grains may be protected by their silicate hosts from metamorphic breakdown, so that gabbros may be somewhat less sensitive to low and medium grade metamorphism than their extrusive and hypabyssal equivalents.

Ultramafic rocks (pyroxenites, hornblendites, serpentinised dunites etc.) in zoned Alaskan-type complexes are generally highly magnetic. The associated mafic and intermediate rocks (gabbro, diorite, monzonite) in these intrusions are also moderately to highly magnetic. Unaltered komatiitic lavas (including spinifex textured peridotite, olivine orthocumulate and adcumulate (dunite) zones) are weakly magnetic. However, komatiites are almost invariably serpentinised, as are alpine-type peridotites. Serpentinisation usually creates substantial quantities of magnetite, accounting for the high susceptibility of serpentinised ultramafic rocks. This magnetite is generally multidomain, well-crystallised, almost pure Fe_3O_4, which is magnetically soft and carries relatively weak remanence ($Q < 1$). The NRM of serpentinites is often dominated by viscous remanence, subparallel to the present field. Prograde metamorphism of serpentinised ultramafics causes increasing substitution of Mg and Al into the magnetite, eventually shifting the composition into the paramagnetic field. Thus metamorphism progressively demagnetises serpentinites, which become paramagnetic at granulite grade. Subsequent retrograde serpentinisation, if it occurs, can produce a magnetic rock again. This is most likely to occur within zones of fracturing, that may therefore be highlighted by magnetics.

The susceptibility of most rocks primarily reflects their magnetite content. Remanence intensity, whilst also correlated with modal magnetite, is sensitive to other factors, particularly grain size and microstructure of magnetic minerals and geological history. The natural remanent magnetisation of rocks is often multicomponent in character, i.e. it represents the sum of remanence components, each carried by a different subpopulation of magnetic grains, acquired at different times and therefore generally with differing directions. Variations in the relative proportions of remanence components throughout a rock unit produce scatter in the remanence direction, as well as variations in intensity. Specific remanent intensity is highest for acicular submicron magnetite grains in the single domain size range. Pseudosingle domain (titano)magnetite grains, up to ~20 μm diameter, also carry relatively intense remanence and are the dominant remanence carriers in many rocks. Larger magnetite grains have relatively weaker remanence, corresponding to Q values less than unity. Granitic rocks and metamorphic rocks with secondary magnetite usually contain relatively coarse grained multidomain magnetite, accounting for the generally low Q values of these rocks. On the other hand, young, rapidly chilled basaltic rocks (e.g. pillow lavas) exhibit very high Koenigsberger ratios, due to the fine grain size of the titanomagnetites. In basaltic rocks the Q value of the primary thermoremanence is essentially a function of cooling rate, being highest for subaqueous chilled margins and small pillows and decreasing with distance from the margin. However, even thick doleritic sills and dykes are characterised by relatively high Q values, typically 1-10, provided the primary remanence has not been substantially modified by thermal or chemical overprints.

Plutonic rocks generally have low Koenigsberger ratios, due to their coarse grain size, with the notable exception of some gabbroic intrusives for which the remanence is dominated by fine (titano)magnetite inclusions in silicate grains. Remanence carried by hematite and monoclinic pyrrhotite is characterised by high Q values, but hematite is only weakly magnetic and therefore hematite-rich rocks are rarely responsible for substantial anomalies. On the other hand, pyrrhotite-bearing rocks often carry a relatively intense remanence, which may be ancient and quite oblique to the present field. The remanence carried by magnetically soft multidomain magnetite, which is the dominant magnetic phase in many rocks, is dominated by viscous magnetisation. This remanence is subparallel to the present field and therefore augments the induced magnetisation, enhancing the effective susceptibility. Thus most anomalies can be interpreted in terms of magnetisation by induction, even when typical Koenigsberger ratios are comparable to unity. However the anomaly amplitudes may be larger, for a given source geometry, than measured susceptibilities indicate, due to the viscous remanent magnetisation. Neglect of remanence may therefore mislead quantitative interpretation, even though the anomaly form is consistent with magnetisation parallel to the present field.

Koenigsberger ratios for viscous remanence carried by multidomain magnetite have an upper limit of approximately unity, but are typically much lower, averaging ~0.2. Rocks containing predominantly somewhat harder multidomain magnetite grains may carry a stable ancient remanence, characterised by a larger Q value. The Koenigsberger ratio of thermoremanence carried by an igneous rock that contains predominantly such multidomain grains is typically ~0.5. In this case the remanence direction records the geomagnetic field direction at the time of initial cooling. This direction can be of either

normal or reversed polarity and may be highly oblique to the present field, depending on the age of the rock.

Estimation of the bulk remanent magnetisation of a rock unit is not straightforward. The scatter of directions must be taken into account, as well as the distribution of intensities. Remanence makes a greater contribution to the anomaly associated with a unit that exhibits a consistent remanence direction and moderate Koenigsberger ratios than a unit that has highly scattered remanence directions on a mesoscopic scale, even though the samples may all have high Q values. Measurements of raw NRMs can also be quite misleading. Surface samples are often affected by lightning, which imparts unrepresentatively high remanent intensities and Q values. Drill core samples may carry spurious remanence imparted by drilling. Estimation of representative remanence vectors requires palaeomagnetic cleaning of samples to remove spurious components and to identify the components that correspond to bulk *in situ* properties. The remanent magnetisations identified in this way should then be analysed statistically as *vectors*, rather than analysing directions and scalar intensities separately.

Magnetic Mineralogy and Rock Magnetisation

Ferromagnetic phases, such as magnetite and monoclinic pyrrhotite, are accessory minerals that do not feature in conventional classification schemes for rocks. This means that there is only a weak correlation between magnetic properties and broad lithological categories. Magnetisation variations and magnetic anomalies in most geological environments predominantly reflect variations in (titano)magnetite contents of the rocks. For rocks in which magnetite is present in minor amounts, but is the only important magnetic mineral, the susceptibility is approximately proportional to the magnetite content. Several workers have determined the relationship between susceptibility and magnetite content of rocks. The results are fairly consistent and enable the susceptibility to be estimated from magnetite content with reasonable accuracy. On average, the susceptibility of a rock containing a volume fraction, f, of magnetite is given by (Puranen, 1990):

$$k = 0.276f \text{ G/Oe} = 3.47f \text{ (SI)}.$$

The proportionality holds for magnetite contents up to about f=0.1, after which the susceptibility increases more rapidly with f, because of the effects of grain interactions. The relationship is not strongly affected by the magnetite grain size or composition, provided the composition is in the ferromagnetic range, because the effective susceptibility of isolated grains of a strongly ferromagnetic material is controlled largely by self-demagnetisation of the grains, rather than by their intrinsic susceptibility.

Monoclinic pyrrhotite has much lower intrinsic susceptibility than magnetite, however, and the susceptibility of pyrrhotite grains accordingly reflects grain size and microstructure to a much greater extent. Large multidomain grains of monoclinic pyrrhotite have susceptibilities of up to 0.1 G/Oe (1.26 SI), whereas micron-sized SD grains have susceptibilities as low as 0.004 G/Oe (0.05 SI).

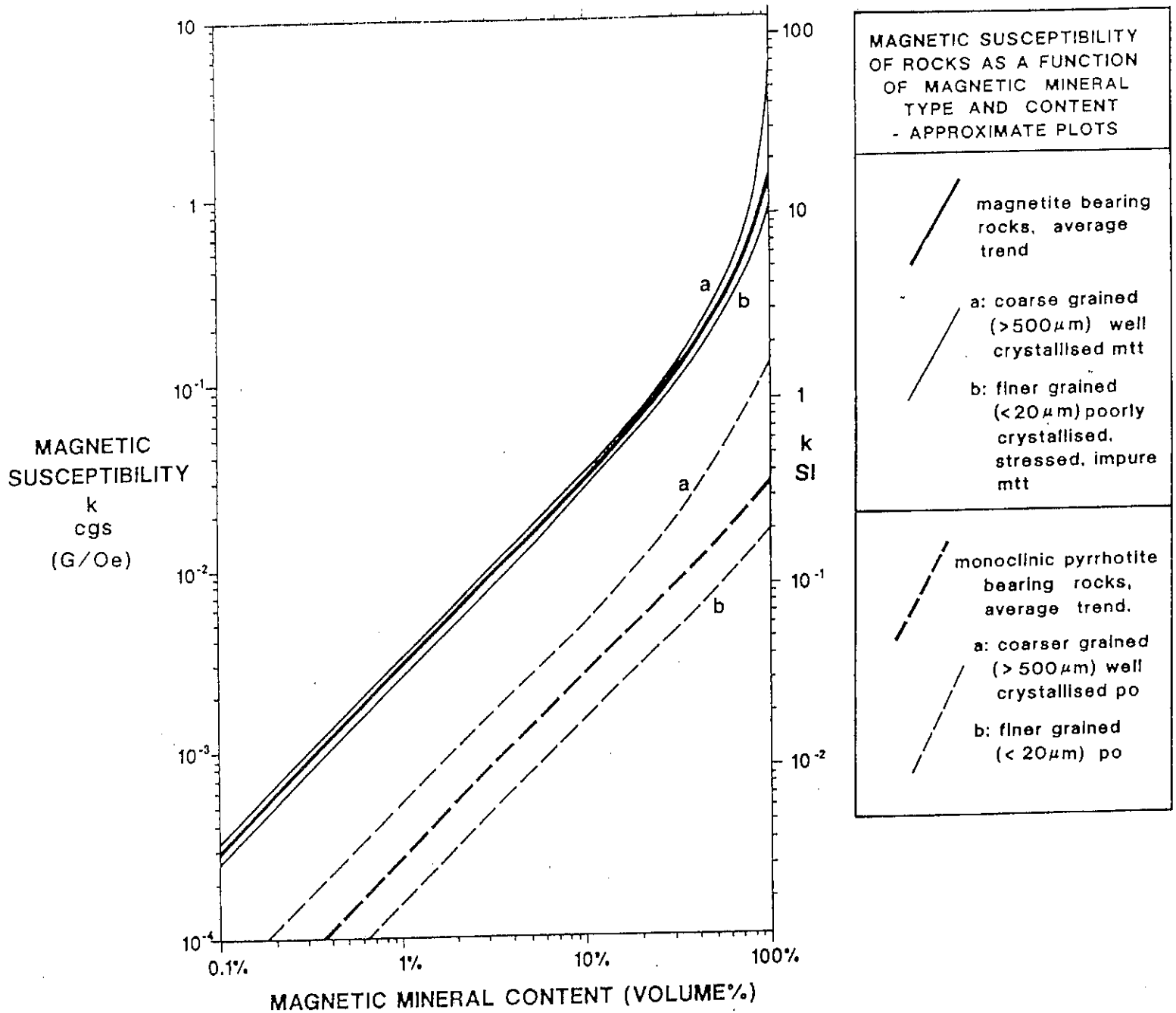
MAGNETIC SUSCEPTIBILITY OF ROCKS AS A FUNCTION OF MAGNETIC MINERAL TYPE AND CONTENT - APPROXIMATE PLOTS
magnetite bearing rocks, average trend
a: coarse grained (>500μm) well crystallised mtt
b: finer grained (<20μm) poorly crystallised, stressed, impure mtt
monoclinic pyrrhotite bearing rocks, average trend.
a: coarser grained (>500μm) well crystallised po
b: finer grained (<20μm) po
MAGNETIC SUSCEPTIBILITY k cgs (G/Oe)
k SI
10
1
10^{-1}
10^{-2}
10^{-3}
10^{-4}
100
10
1
10^{-1}
10^{-2}
a
b
a
b
0.1%
1%
10%
100%
MAGNETIC MINERAL CONTENT (VOLUME%)

FIG. 43

Figure 43 shows the relationships between susceptibility and magnetic mineral concentration for magnetite-bearing and monoclinic pyrrhotite-bearing rocks.

Relationship between Lithology and Magnetic Properties

For each common, broadly defined, rock type there is a very wide range of suceptibilities. Thus the susceptibility of a particular rock unit cannot be reliably inferred from the lithotype, in the absence of other information. Information constraining the possible range of susceptibilities may take the form of direct measurements on accessible portions of the unit, from observed anomalies over well-defined occurrences of the unit, from knowledge of the properties of similar rocks elsewhere within the same geological province or environment, or from information on the mineralogy and petrology of the unit.

When the "global" frequency distributions of susceptibilities for many common rock types are plotted, it is usually found that they exhibit a pronounced bimodal distribution. Figure 44 shows frequency distributions of susceptibility for a variety of rock types, based on very large petrophysical collections in Finland. The two modes of the frequency distribution correspond to distinct paramagnetic and ferromagnetic populations, with a pronounced intervening gap. Within each of the subpopulations, the modal and mean values of susceptibility are much more closely related to rock type than for the total suceptibility distribution. For the paramagnetic subpopulation, in particular, the susceptibility is directly related to the chemical composition, which tends to have a restricted range for each lithology.

The susceptibilities within each of the paramagnetic and ferromagnetic subpopulations are generally lognormally distributed. The total range of susceptibilities is much more restricted for the paramagnetic rocks than for the ferromagnetic rocks. Lognormal distributions arise in nature when the variable in question represents the cumulative multiplicative effect of several factors of comparable importance. The susceptibility of the paramagnetic subpopulation essentially reflects an approximately lognormal distribution of total iron content. For the ferromagnetic subpopulation, the susceptibility reflects, in addition, the partitioning of iron between silicates and oxides, the proportions of paramagnetic and ferromagnetic oxides and the grain size distribution and microstructure of the ferromagnetic minerals. The modal abundance of magnetite is strongly influenced by the ferrous/ferric iron ratio, which in turn depends on a complex interplay of variables such as oxygen fugacity, temperature and bulk composition. Because certain of these variables can amplify the effects of other variables, a lognormal distribution of susceptibilities is a natural consequence of the complex interplay of geological factors. For similar reasons, NRM intensities also tend to be lognormally distributed for the ferromagnetic subpopulation of each rock type. The skewed form of the lognormal distribution, with a long tail at high values, implies that susceptibilities much larger than average occur relatively frequently.

The paramagnetic subpopulation of each lithotype is characterised by a similar range of total iron content as the ferromagnetic subpopulation, but the iron is overwhelmingly partitioned into paramagnetic minerals, particularly silicates, with ferromagnetic minerals either absent, or at most present in trace amounts. This often occurs when the oxidation

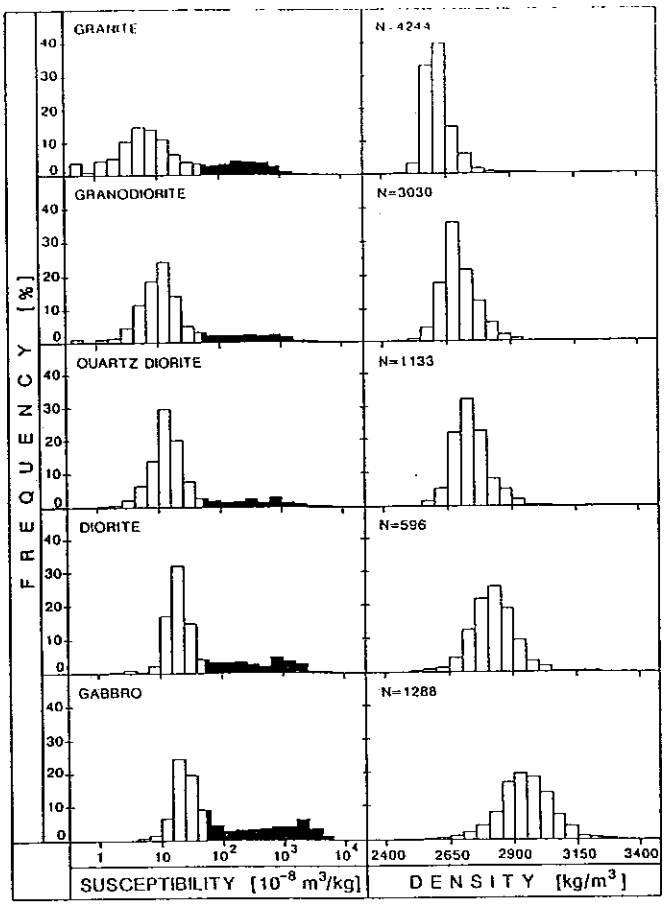

. Frequency distributions of susceptibility and density for igneous rock types.

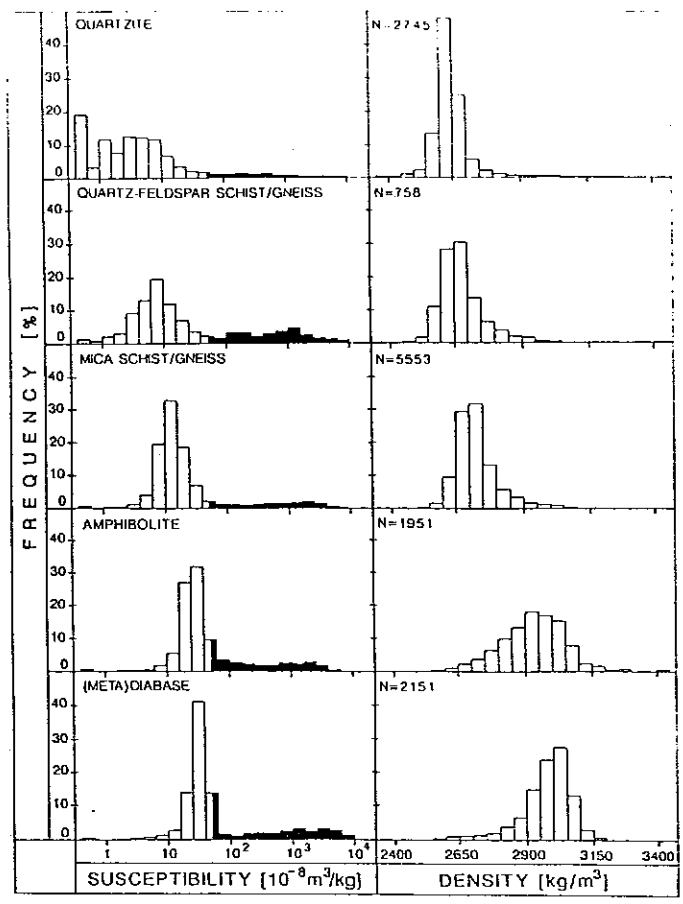

Frequency distributions of susceptibility and density for sedimentogeneous and metamorphic rock types.

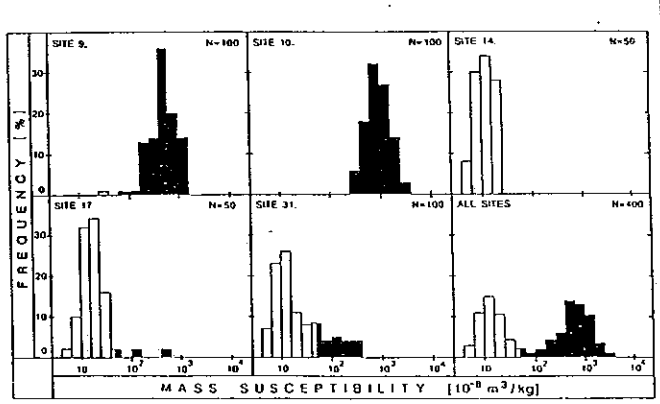

Typical susceptibility distributions from granitoid outcrops in the Hyvinkää area.

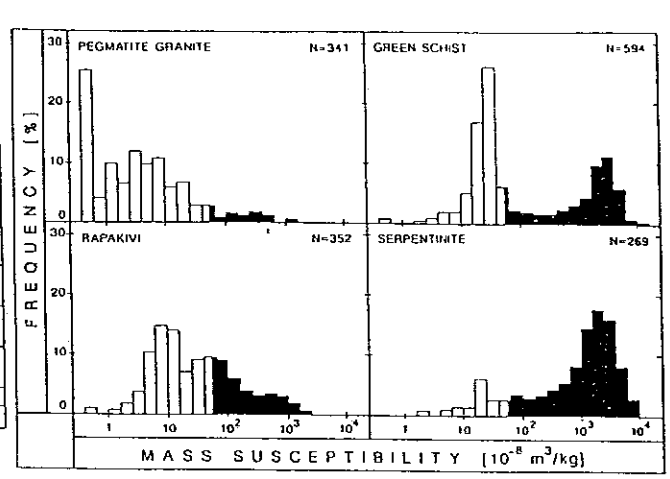

Frequency histograms of susceptibility for magnetically different rock types divided into dia- (grey), para- (white) and ferrimagnetic (black) parts. Susceptibility value 0 separates dia- and paramagnetic parts, and value $50 \cdot 10^{-4}$ m³/kg distinguishes para- and ferrimagnetic parts. Left- and rightmost classes of histograms are open, and N = number of samples.

FIG. 44

state of the iron is sufficiently low, given the overall chemical composition, that the predominantly ferrous iron is incorporated into silicates, ilmenite etc. and the relatively small proportion of ferric iron can be accomodated within paramagnetic phases, such as biotite, amphibole and clinopyroxene, without leaving any excess to form magnetite. On the other hand, when the oxidation state of iron in the rock is too high, e.g. in redbeds and very oxidised lavas, the ferric iron forms hematite excusively, because the relatively small proportion of ferrous iron is all consumed by silicates and none is left to combine with ferric iron to form magnetite. This argument suggests that the oxidation state of the rock is probably the most important geochemical factor influencing the magnetic properties.

For the paramagnetic subpopulation, the susceptibility can be calculated directly from the chemical composition. The paramagnetic cations include ferrous and ferric iron, manganese, chromium, nickel, vanadium etc., but for most rocks the susceptibility mainly reflects iron content. To a reasonable approximation, the paramagnetic susceptibility can be calculated from the total iron content according to:

$$\text{Mass susceptibility } (m^3/kg) = 2.2 \times 10^{-8} \times (\text{wt\% } FeO^T).$$

The SI volume susceptibility can then be calculated by multiplying the mass susceptibility by the rock density in kg/m^3.

The subdivision of each lithotype into paramagnetic and ferromagnetic subpopulations is also reflected in the relationship between rock density and susceptibility. Puranen (1989) has shown that smoothed trends of density versus susceptibility show a very distinctive reversal of slope, which marks the boundary between the paramagnetic and ferromagnetic rocks. Figure 45 illustrates this phenomenon for major rock types in Finland. In each case the smoothed density trend rises monotonically with susceptibility in the paramagnetic range. This trend reflects the positive correlation of both paramagnetic susceptibility and density with iron content. The sudden onset of a decreasing trend of density with susceptibility represents the appearance of small amounts of magnetite in weakly ferromagnetic rocks that have relatively low iron contents, but have oxidation states that favour partitioning of some of this iron into magnetite. The density trend turns upwards again for strongly ferromagnetic rocks, with the appearance of substantial amounts of magnetite, which is dense as well strongly magnetic. The dashed line separating the two distinctive trends in each plot therefore represents a well-defined boundary between the paramagnetic and ferromagnetic populations.

When we consider susceptibility distributions on successively smaller scales, the range of susceptibilities becomes more restricted. Within different geological provinces the relative proportions of paramagnetic and ferromagnetic subpopulations differ from those of other provinces. It is often found that within sufficiently small areas, e.g. within a particular geological environment or simply within a single outcrop, all susceptibilities fall exclusively within one subpopulation. The same may hold when the lithotype is subdivided on the basis of varietal mineralogy. Thus the distinct susceptibility subpopulations reflect differing geological conditions, which are not considered in the primary rock classification schemes. A meaningful magnetic petrological classification scheme therefore needs to relate to mineralogical and geological characteristics that are

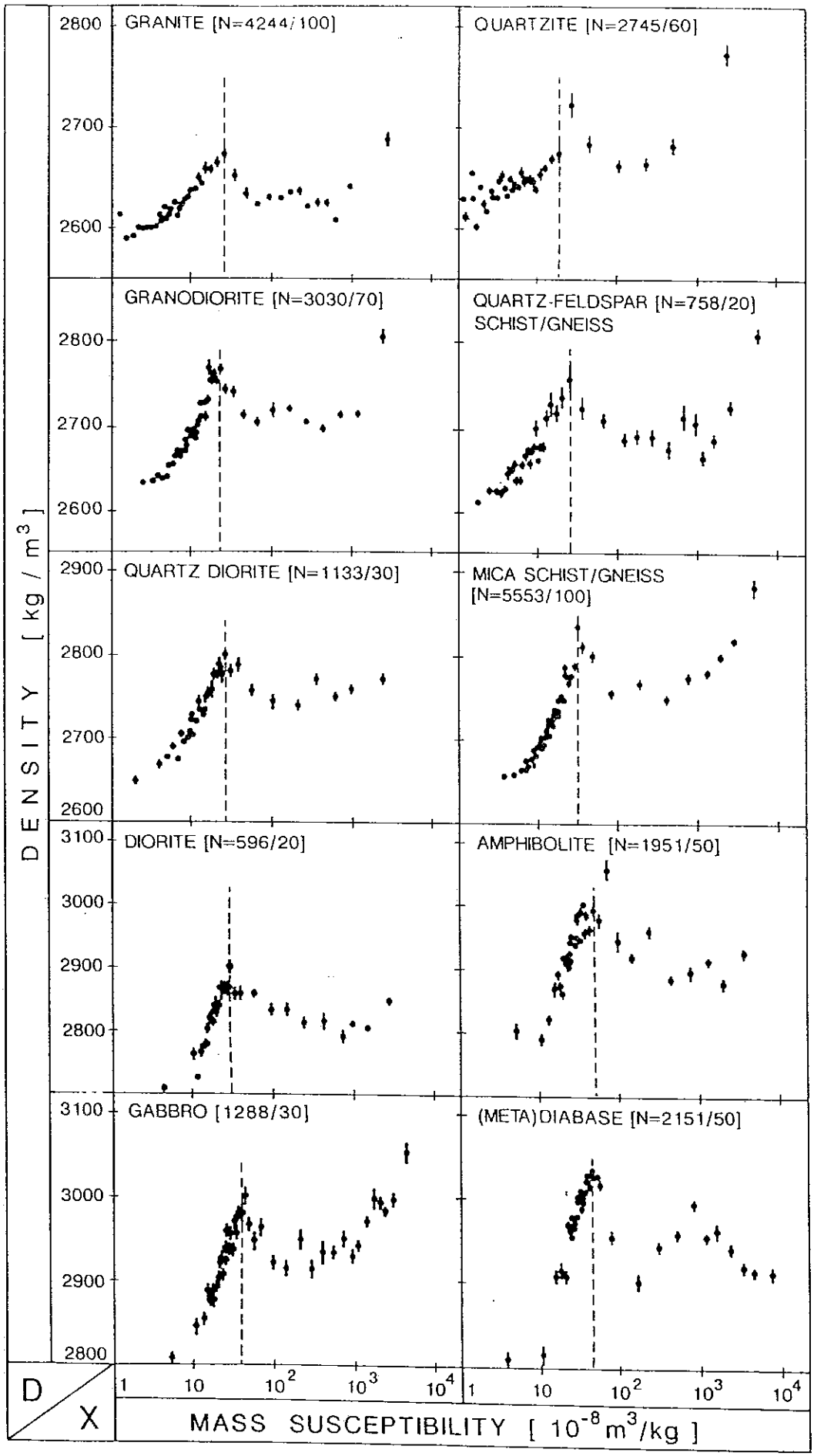

Susceptibility-density diagrams for example rock types. Vertical bars describe standard errors of densities and dashed lines divide data into para- and ferrimagnetic parts. N = number of samples/size of smoothing group.

FIG. 45

much more specific and detailed than rock classification that is based exclusively on relative modal proportions of a few essential minerals. From the viewpoint of magnetic petrology in metamorphic terranes, the common practice of categorising all rocks, for which the primary mineralogy is recognisable, in terms of their protoliths is very misleading, as metamorphic grade and secondary mineralogy affects magnetic properties very strongly.

A Magnetic Petrophysical Classification Scheme

Given the large variation in magnetic properties for each rock type, or even within a single rock unit, it is convenient to construct a simple classification scheme, based on a first order description of the magnetic properties, that can reasonably be correlated with petrological and geological features. Rocks are divided into diamagnetic (DM), paramagnetic (PM), weakly ferromagnetic (WFM), moderately ferromagnetic (MFM), strongly ferromagnetic (SFM) and very strongly ferromagnetic (VSFM) categories on the basis of their susceptibilities:

Classification	Susceptibility
Diamagnetic (DM)	$k < 0$

Diamagnetic rocks have negligible NRM and Koenigsberger ratios of almost zero. They are rocks with very little iron, or other paramagnetic species, and tend to be almost monomineralic quartzites, carbonates, quartz rocks etc.

Paramagnetic (PM)	k = 0-100 μG/Oe = 0-1260 x 10^{-6} SI

Paramagnetic rocks contain less than 0.02 vol% magnetite and their susceptibility is strongly correlated with the total iron content. Unless substantial hematite is present, the NRM is very weak and the Q value is low ($<< 1$).

Weakly Ferromagnetic (WFM)	k = 100-300 μG/Oe = 1260-3770 x 10^{-6} SI

Weakly ferromagnetic rocks are those for which the paramagnetic and ferromagnetic contributions to the susceptibility are comparable, due to the presence of small amounts of ferromagnetic minerals (up to ~0.1 vol% magnetite). If multidomain magnetite is the ferromagnetic phase, the Koenigsberger ratio is low (typically < 0.2-0.3), but it may be greater than unity if pyrrhotite or ilmenohematite is the main ferromagnetic phase.

Moderately Ferromagnetic (MFM)	k = 300-3000 μG/Oe = 3770-37,700 x 10^{-6} SI

The susceptibility of MFM rocks is equivalent to magnetite content of ~0.1-1.0 vol%. NRMs and Q values of these rocks reflect the composition and

grain size of the ferromagnetic minerals, and therefore vary widely. When magnetite is the ferromagnetic phase, Q ≃ 0.2 for felsic igneous rocks and for metamorphic rocks, whereas Q falls in the range 0.2-10 for basic igneous rocks.

Strongly Ferromagnetic (SFM) $k = 3000\text{-}10{,}000\ \mu G/Oe$
$= 37{,}700\text{-}126{,}000 \times 10^{-6}$ SI

The susceptibility of SFM rocks is equivalent to magnetite content of ~1.0-3.3 vol%. NRMs and Q values of these rocks reflect the composition and grain size of the ferromagnetic minerals, and therefore vary widely. When magnetite is the ferromagnetic phase, Q ≃ 0.2 for felsic igneous rocks and for metamorphic rocks, whereas Q falls in the range 0.2-10 for basic igneous rocks.

Very Strongly Ferromagnetic (VSFM) $k > 10{,}000\ \mu G/Oe$
$> 126{,}000 \times 10^{-6}$ SI

The susceptibility of VSFM rocks is equivalent to magnetite content greater than ~4 vol%. Thus magnetite can be considered as a varietal mineral in such rocks, rather than an accessory. NRMs and Q values of these rocks reflect the composition and grain size of the ferromagnetic minerals, and therefore vary widely. When magnetite is the ferromagnetic phase, Q is generally less than unity for serpentinised ultramafics and for hydrothermal and magmatic ores. BIFs may have higher Q values, typically 1-2, and have very anisotropic susceptibility.

The Concept of Oxygen Fugacity

Iron, which is the fourth most abundant element in the Earth's crust, exists in three oxidation states: metallic (Fe^0), ferrous (Fe^{2+}) and ferric (Fe^{3+}) iron. Oxygen fugacity is the variable used to define the propensity for iron to occur in a particular oxidation state. At very low oxygen fugacities, such as in the Earth's core, in some serpentinised ultramafic rocks, and in a few exceptionally reduced lavas that have reacted with carbonaceous material, iron occurs as the native metal. Iron occurs in the divalent ferrous state at higher oxygen fugacities. In silica-bearing systems the ferrous iron is incorporated mainly into silicate minerals. With increasing oxygen fugacity, iron occurs in both the divalent and trivalent states and is incorporated into magnetite as well as silicates. At still higher oxygen fugacities, iron occurs in the ferric state and is incorporated into hematite. This sequence of changes of oxidation state can be represented by a series of reactions:

$$\underset{\text{fayalite}}{Fe_2SiO_4} = \underset{\text{iron}}{2\,Fe^0} + \underset{\text{quartz}}{SiO_2} + O_2 \qquad \text{(QIF)}$$

$$\underset{\text{magnetite}}{2\,Fe_3O_4} + \underset{\text{quartz}}{3\,SiO_2} = \underset{\text{fayalite}}{3\,Fe_2SiO_4} + O_2 \qquad \text{(FMQ)}$$

$$\underset{\text{hematite}}{6\,Fe_2O_3} = \underset{\text{magnetite}}{4\,Fe_3O_4} + O_2 \qquad \text{(MH)}$$

In the system Fe-O-SiO_2, FMQ marks the lower oxygen fugacity limit for the stability of magnetite and MH marks the upper oxygen fugacity limit. Figure 46 shows the stability fields in the Fe-Si-O system for the three oxidation states of iron, in terms of temperature and oxygen fugacity. Oxygen fugacity is measured in units of pressure and is formally defined as the chemical activity of oxygen. The fugacity and partial pressure of a perfect gas are equal, but fugacity takes the place of partial pressure in thermodynamic relations for a real gas, in order to account for departures from ideal behaviour. The two parameters coincide for very dilute concentrations, as in most geological situations.

Each of the reactions above defines an oxygen buffer, i.e. a mineral assemblage that determines the oxygen fugacity uniquely at a given temperature. Thus when, for example, fayalite, magnetite and quartz occur together in any proportions, the oxygen fugacity is constrained to fall on the path FMQ at equilibrium. At fixed temperature any addition of oxygen to the system is immediately consumed by the fayalite to form magnetite and quartz, bringing the fugacity back to the FMQ buffer. The oxygen fugacity can only depart from this buffer curve when all the fayalite has been consumed. From Fig. 46 it is evident that the absolute amounts of free oxygen at even the highest magmatic temperatures are infinitesimal. Thus in a closed system, any excess oxygen, representing a departure upwards from the FMQ buffer, will be completely consumed, with negligible increase in the amount of magnetite and quartz at the expense of fayalite, and the fugacity will return to the equilibrium value. Similarly, a temporary decrease in oxygen fugacity below the buffer curve will cause the FMQ equilibrium to shift slightly to the right, adding oxygen to the system and restoring the fugacity to the buffered value.

Thus, in a closed system only petrologically insignificant quantities of magnetite can be produced by oxidation of fayalite. On the other hand, an open system supplied with substantial amounts of fluid containing free oxygen can create relatively large amounts of magnetite by reactions analogous to FMQ, or replace magnetite with hematite by reaction MH. Many rocks have behaved essentially as closed systems throughout their history and therefore the oxygen fugacity-temperature paths they have followed through their history are determined by their mineralogy, rather than by the environment.

From elementary chemical thermodynamics, the FMQ reaction is characterised by an equilibrium constant at fixed temperature, given by:

$$K_{FMQ} = [Fe_2SiO_4]^3 \times [O_2]/([Fe_3O_4]^2 \times [SiO_2]^3),$$

where the square brackets denote the chemical activity of the enclosed species. The equilibrium constant is related to the free energy change of the FMQ reaction in its standard state, ΔG, by:

$$\log K_{FMQ} = -\Delta G/(2.303RT).$$

$$\therefore \log f(O_2) = -\Delta G/(2.303RT) + 2\log[Fe_3O_4] + 3\log[SiO_2] - 3\log[Fe_2SiO_4],$$

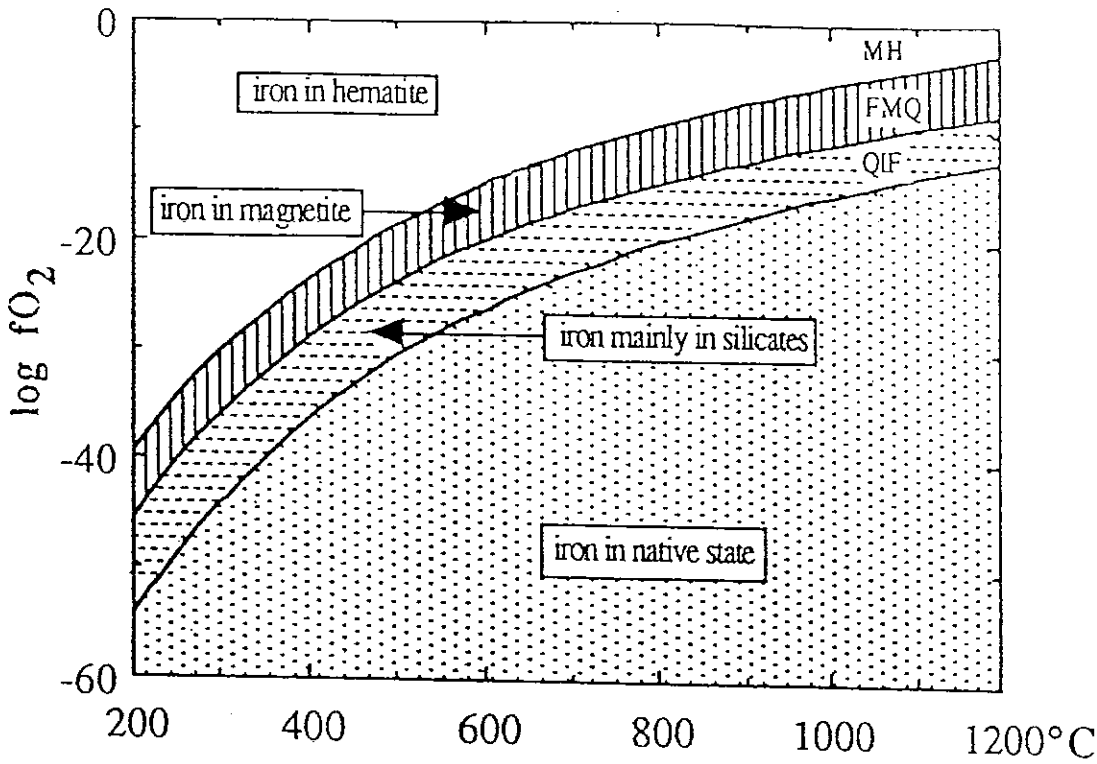

Log oxygen fugacity-T diagram showing the relative stabilities of the various oxidation states of iron in the system Fe-Si-O.

FIG. 46

where the oxygen fugacity of the standard state is one bar, T is the absolute temperature and R is the Universal Gas Constant.

It follows from the above equation that:

(i) for the FMQ buffer curve and related equilibria, log $f(O_2)$ is linear in 1/T, with slope $-\Delta G/2.303R$,

(ii) in the system Fe-Si-Mg-O, the olivine-magnetite-quartz buffer curve is shifted upwards, to higher oxygen fugacity, than the fayalite-magnetite-quartz buffer, because the activity of fayalite is reduced by substitution of Mg for Fe in olivine,

(iii) in the system Fe-Si-Ti-O, the titanomagnetite-fayalite-quartz buffer is shifted down, to lower oxygen fugacity, implying that titaniferous magnetite is stable at lower oxygen fugacities than end-member magnetite,

(iv) in silica-undersaturated rocks, for which the activity of quartz is less than unity, the buffer curve is shifted to lower oxygen fugacity, thereby increasing the stability field of magnetite.

Point (i) above illustrates the principle that, for any oxygen-buffering assemblage, the oxygen fugacity decreases rapidly with falling temperature. It follows that the terms "oxidising" and "reducing" are not absolute, but depend strongly on temperature. Oxidising and reducing conditions are most appropriately expressed relative to an oxygen buffer. The most popular variable for describing redox conditions is Δlog $f(O_2)$, defined as the difference between log $f(O_2)$ for the rock and the corresponding value for the FMQ assemblage. Because oxidation reactions that define oxygen buffers all have similar free energy changes, the slopes of the corresponding buffer curves are all similar.

Point (ii) above illustrates the general principle that substitution of Mg for Fe in silicate minerals stabilises them to higher oxygen fugacity, thereby decreasing the stabilty field of magnetite. Ferrous iron-bearing silicates can even be stable in the presence of hematite, i.e. at high oxygen fugacities, provided they are sufficiently Mg-rich. It should be noted, however, that at high temperatures and oxygen fugacities Mg-rich olivine in the presence of quartz becomes unstable with respect to orthopyroxene + magnetite. Thus for this assemblage at high temperatures the oxygen fugacity is defined by an olivine-orthopyroxene-magnetite buffer curve, which falls below the olivine-magnetite-quartz (displaced FMQ) buffer curve. Similarly, from point (iii), substitution of ferrous iron + titanium for ferric iron in oxides stabilises them with respect to silicates. It should be noted that many igneous rocks follow paths in $f(O_2)$-T space that are subparallel to synthetic buffer curves such as FMQ during their crystallisation history. This merely reflects control of the oxygen fugacity of the rocks by their mineralogical assembages, which have buffer curves with similar slopes to FMQ. Coincidence of the cooling path of a basalt with FMQ, for example, does not imply that fayalite, magnetite and quartz are present in the rock.

In summary, for many rocks which behave essentially as closed systems during their history, the Fe/Mg ratio of the silicates, the Ti content and the ferrous/ferric ratio of the

oxides monitor and, in effect, control the oxygen fugacity. In turn the oxygen fugacity influences the composition of the fluid phase in igneous and metamorphic rocks and the stability of graphite and sulphides.

Compositions of Titanomagnetites in Igneous Rocks

At magmatic temperatures there is complete miscibility between ulvospinel and magnetite. Rapidly cooled lavas often contain quenched homogeneous crystals of titanomagnetite, which have substantially lower Curie Temperature and saturation magnetisation than end-member magnetite, although the susceptibilities are comparable for compositions with ulvospinel contents less than about 75 mole per cent. For example, the typical primary titanomagnetite composition in mid-ocean ridge basalts is ~60% ulvospinel (TM60). A miscibility gap between ulvospinel-rich and magnetite-rich spinels appears at lower temperatures. The form of the solvus curve is not very well known, but the peak is thought to lie at ~500°C and the curve is believed to be somewhat asymmetric towards magnetite, due to the effects of magnetic ordering on the total free energy. Therefore in slowly cooled pluton originally homogeneous intermediate titanomagnetites tend to unmix into magnetite-ulvospinel intergrowths during cooling, increasing the Curie temperature and remanence stability, but decresing the total amount of ferromagnetic material somewhat. Because unmixing predominantly occurs below the Curie point of the exsolved magnetite-rich phase, the remanence acquired during cooling may have the character of a CRM, rather than representing a pure TRM.

It is more common, however, to find granules and "exsolution" lamellae of ilmenite within magnetite grains, although solid solution between the spinels and rhombohedral oxides is minimal. This reflects deuteric oxidation of titanomagnetite, according to:

$$\underset{\text{in Ti-mt}}{6\ Fe_2TiO_4} + O_2 = \underset{\text{ilmenite}}{6\ FeTiO_3} + \underset{\text{magnetite}}{2\ Fe_3O_4}.$$

The above reaction shows that the equilibrium titanium content of titanomagnetite varies with temperature and oxygen fugacity.

High ulvospinel contents are favoured by high temperatures and low oxygen fugacity. Conversely, low titanium content in magnetite is favoured by lower temperatures and relatively high oxygen fugacity. Similarly, the composition of ilmenohematite is controlled by temperature and oxygen fugacity according to the shifted MH reaction:

$$\underset{\text{in Ti-mt}}{4\ Fe_3O_4} + O_2 = \underset{\text{in rhom ox}}{6\ Fe_2O_3}.$$

Because the slopes of titanomagnetite and ilmenohematite isopleths are different, the compositions of co-existing titanomagnetite and hemoilmenite in equilibrium define a unique point in $f(O_2)$-T space. Figure 47 shows the stable titanomagnetite and hemoilmenite compositions as functions of temperature and oxygen fugacity. This forms the basis of the Buddington and Lindsley (1964) magnetite-ilmenite geothermometer. Note that the slopes of the titanomagnetite isopleths are significantly steeper than the buffer curves, such as FMQ, whereas the hemoilmenite isopleths are subparallel to the

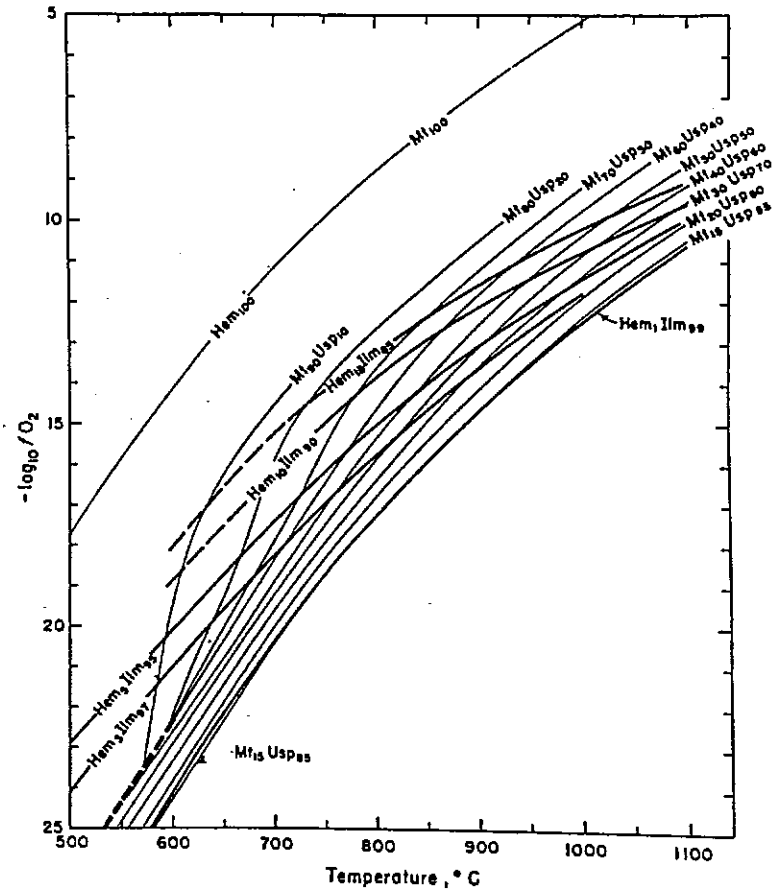
Mt100
Mt80Usp20
Mt70Usp30
Mt60Usp40
Mt50Usp50
Mt40Usp60
Mt30Usp70
Mt20Usp80
Mt15Usp85
Hem100
Mt80Usp20
Hem80Ilm20
Hem60Ilm40
Hem40Ilm60
Hem20Ilm80
Hem15Ilm85
Hem1Ilm99
Mt15 Usp85
-log10 fO2
Temperature, °C
500
600
700
800
900
1000
1100
5
10
15
20
25

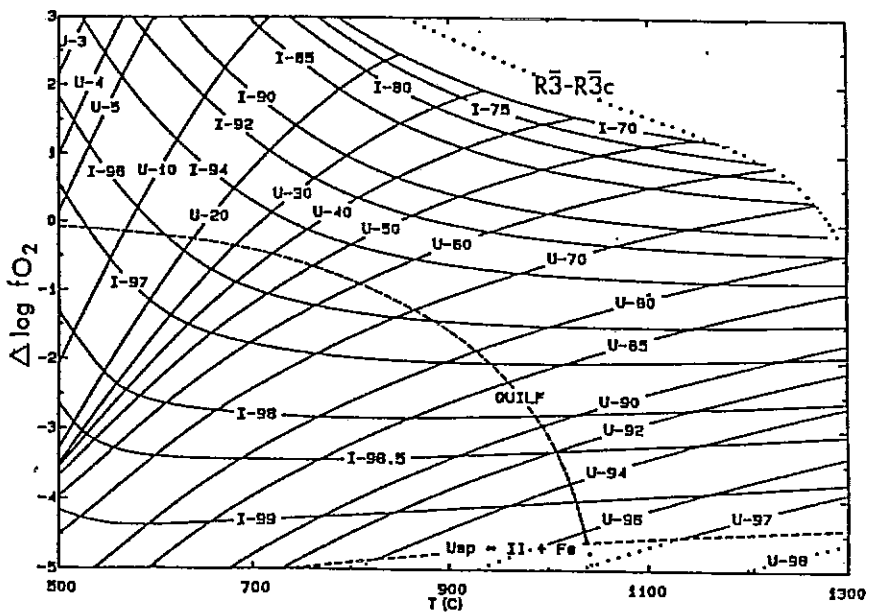
R3̄-R3̄c
I-85
I-80
I-75
I-70
I-90
I-92
I-94
I-96
I-97
I-98
I-98.5
I-99
U-3
U-4
U-5
U-10
U-20
U-30
U-40
U-50
U-60
U-70
U-80
U-85
U-90
U-92
U-94
U-96
U-97
U-98
QUILF
Usp = Il + Fe
Δ log fO2
T (C)
500
700
900
1100
1300

FIG. 47

buffer curves. This implies that re-equilibration of titanomagnetite composition on slow cooling produces progressively more magnetite-rich compositions, until kinetics intervenes to halt further change.

The ilmenite-magnetite geothermometer may also be represented in terms of the exchange equilibrium:

Fe_2TiO_4 +	Fe_2O_3 =	Fe_3O_4 +	$FeTiO_3$,
ulvospinel	hematite	magnetite	ilmenite

which is strongly temperature sensitive.

Figure 48 shows selected titanomagnetite and hemoilmenite isopleths with respect to the FMQ and MH buffer curves. If we consider Fe-Ti oxides crystallising at point A, at a temperature of ~1000°C and oxygen fugacity about one log unit above FMQ, the titanomagnetite composition is 50%Usp50% Mt and the ilmenite contains 15 mole% hematite. Quenching produces Fe-Ti oxide compositions typical of many basaltic volcanics. Slow cooling with oxygen fugacity following a path subparallel to FMQ, along the Ilm85% isopleth, to point B (~600°C) leaves the ilmenite composition unchanged, but greatly modifies the titanomagnetite composition to 10%Usp90%Mt.

Figure 48 shows the typical fields in $f(O_2)$-T space for Fe-Ti oxide crystallisation for acid and basic extrusives with respect to the FMQ and MH buffers. The dashed line indicates the boundary between titanomagnetite compositions that are ferromagnetic and paramagnetic at room temperature. Assuming early crystallisation of Fe-Ti oxides, the equilibrium compositions at ~1100°C in a magma with oxygen fugacity about one log unit below FMQ are Usp85%Mt15% and Ilm99%Hm1%. Quenching of these compositions would result in a paramagnetic rock. Two different scenarios for magmatic evolution, corresponding to differing tectonic settings are considered. A tholeiitic magma (e.g. in a layered gabbro) is assumed to evolve subparallel to the FMQ buffer, with re-equilibration of the Fe-Ti oxide compositions down to ~650°C. In spite of the relatively reduced nature of the magma, the final titanomagnetite composition is ferromagnetic and quite magnetite-rich (20%Usp80%Mt). The ilmenite composition is only slightly more hematite-rich than the initial composition. A calc-alkaline magma, associated with orogenic andesites in a subduction zone, follows a distinctly more oxidising trend and the Fe-Ti oxides evolve accordingly to more oxidised compositions (10%Usp90%Mt and Ilm85%Hm15%).

Typical titanomagnetite compositions of common extrusive and intrusive rocks (Fig. 49) show a systematic trend to more magnetite-rich compositions for more felsic compositions, which are associated with lower temperature, and generally more oxidised, magmas. There is also a clear tendency for lower Ti contents in titanomagnetites from intrusive rocks than for their extrusive analogues, reflecting greater re-equilibration during cooling for the intrusives.

DEPENDENCE OF Fe–Ti OXIDE COMPOSITIONS ON OXYGEN FUGACITY AND TEMPERATURE

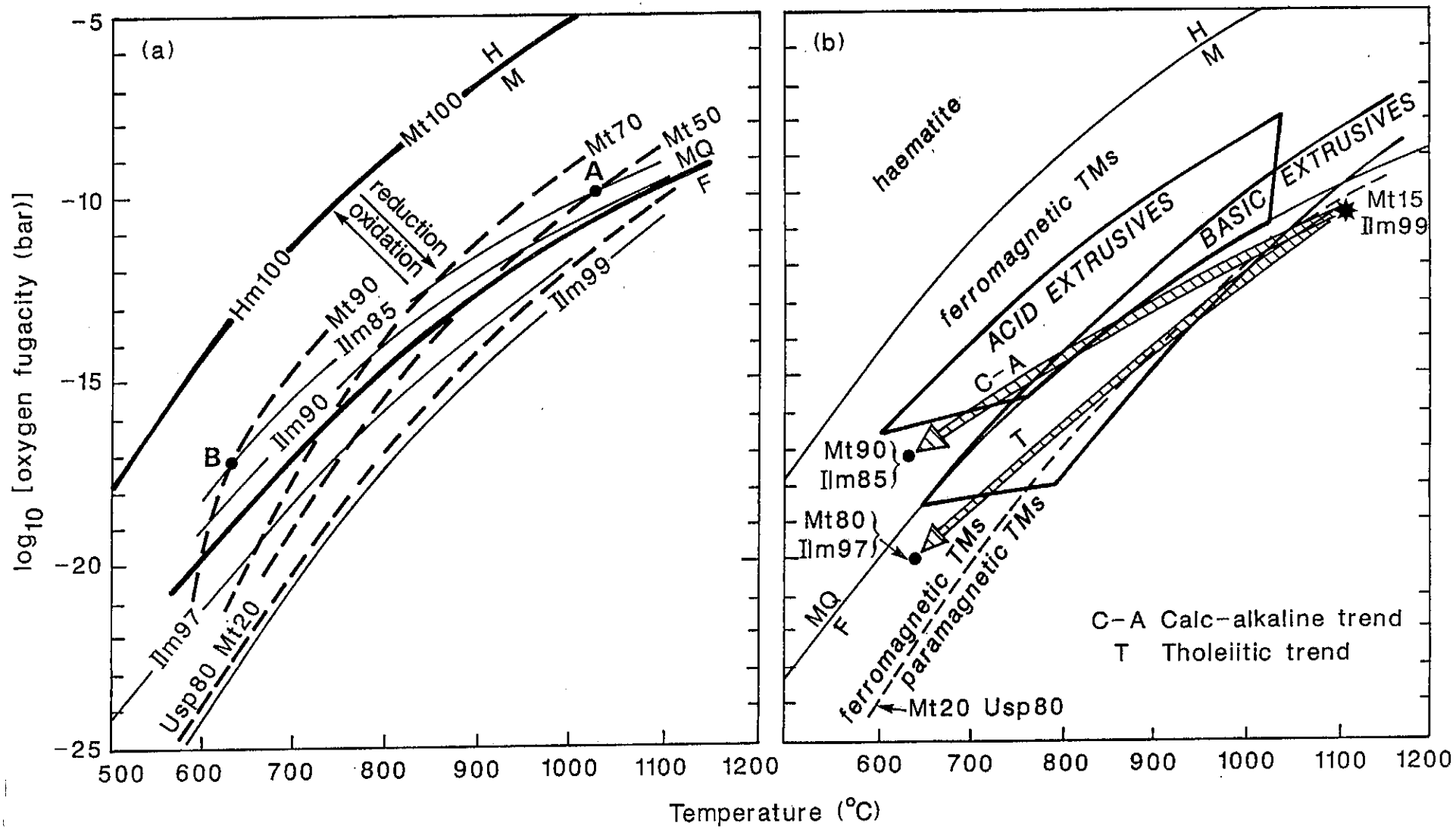

FIG. 48

TITANOMAGNETITES IN IGNEOUS ROCKS

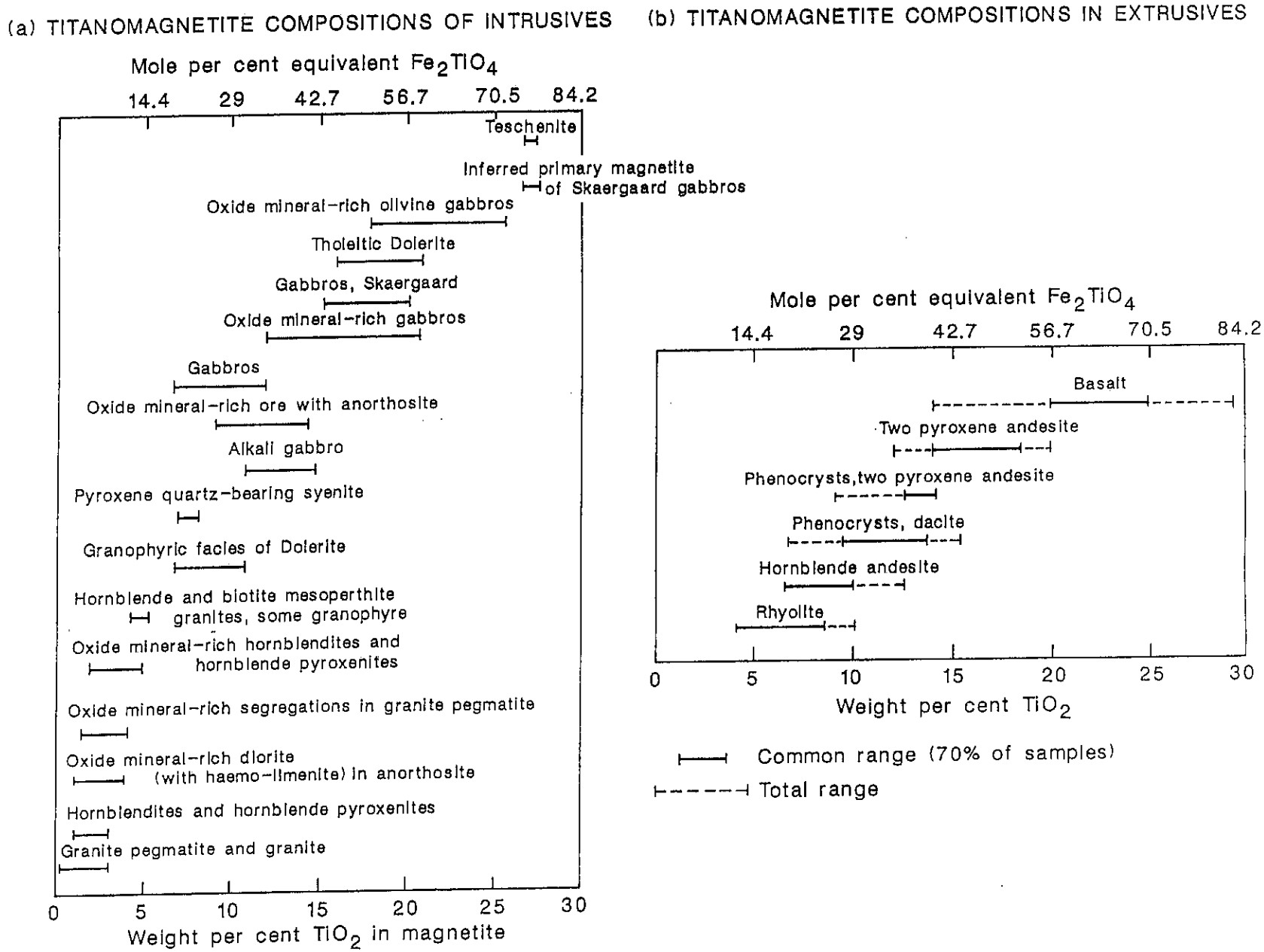

FIG. 49

Feldspar Compositions and Bulk Rock Chemistry

Feldspars are the commonest minerals in igneous rocks, in which they constitute more than 50%, on average. The end-member components of the feldspars are:

orthoclase $K_2Al_2i_6O_{16}$	or $K_2O.Al_2O_3.6SiO_2$
albite $Na_2Al_2Si_6O_{16}$	or $Na_2O.Al_2O_3.6SiO_2$
anorthite $CaAl_2Si_2O_8$	or $CaO.Al_2O_3.2SiO_2$.

From the molecular formulae, it is apparent that alumina occurs in a 1:1 ratio with oxides of the alkali metals or alkaline earth elements in feldspars. Thus departures from this ratio cannot be accomodated by varying the feldspar compositions or relative proportions, but must be expressed in the varietal mineralogy.

Peraluminous rocks are oversaturated with respect to alumina, i.e. molar Al_2O_3 exceeds the sum of $Na_2O + K_2O + CaO$, and are characterised by aluminous minerals, such as corundum (rarely), andalusite, sillimanite or kyanite, almandine garnet or, most commonly, muscovite. Peralkaline rocks, on the other hand, contain insufficient alumina to consume all of the sodium and potassium in feldspars, i.e. molecular Al_2O_3 is less than $Na_2O + K_2O$. Such rocks are characterised by minerals of the aegirine, riebeckite, arfvedsonite or aenigmatite classes. Metaluminous rocks are intermediate in alumina saturation, such that all the alumina, soda and potash can be accomodated in feldspars, with excess calcium appearing in the norm as diopside and in the mode as calcium-bearing pyroxene, amphibole etc. In summary, the classification according to the alumina saturation index (A/CNK) is:

Peraluminous	A/CNK > 1
Metaluminous	A/CNK < 1 and A/NK > 1
Peralkaline	A/NK < 1,

where A/CNK = mol $Al_2O_3/(Na_2O + K_2O + CaO)$ and
A/NK = mol $Al_2O_3/(Na_2O + K_2O)$.

Peraluminous chemistry may result either from high Al content, or from low levels of Na, K or Ca. For example, mature sediments, their metamorphic equivalents, and granitic rocks derived from partial melting of the metasediments are peraluminous because of the severing of the nexus between alumina and Na+Ca during the sedimentary cycle. Sodium is partitioned strongly into seawater and calcium into carbonates, leaving the sediment with excess alumina.

Quartz is a major constituent of many igneous rocks, and its presence or absence is a very significant petrological characteristic. Many minerals exhibit a clear sympathetic or antipathetic association with quartz. Oversaturated rocks contain free quartz, together with oversaturated (compatible) minerals and undersaturated rocks contain undersaturated minerals that are antipathetic to quartz. Common examples of each mineral type are listed below:

Oversaturated Minerals	Undersaturated Minerals
Al- and Ti-poor pyroxenes	magnesian olivine
feldspars	nepheline
amphiboles	sodalite, hauyne, nosean
micas	leucite
fayalitic olivine	melanite garnet
spessartine-almandine	perovskite
sphene	melilite
zircon	corundum
tourmaline	augite (Al- and Ti-rich)
magnetite	
ilmenite	
apatite	

The abundance of Na and K exerts a strong influence on the silica saturation state. Referring above to the molecular formulae for the feldspars, it is clear that every molecule of soda or potash in feldspars consumes six molecules of silica. Thus alkaline rocks, with relatively high Na and/or K for their silica content, have no excess silica to form a free silica phase and are undersaturated. The thermodynamic paramater, silica activity, is strongly dependent on the alkali content for this reason. As an example, alkali basalts are silica undersaturated and are characterised chemically by normative nepheline (an undersaturated mineral). Undersaturated magnesian olivine is relatively abundant in these basalts, whereas tholeiitic basalts are silica saturated, with hypersthene in the norm, and olivine, if present, is in a reaction relationship to ferromagnesian pyroxene and therefore was out of equilibrium with the tholeiitic magma.

Classification of Plutonic Rocks

The internationally accepted IUGS classification of mafic to felsic plutonic rocks is simply based upon the relative proportions of three major rock forming minerals: plagioclase (> An5), alkali feldspar (K-feldspar and albite), and either quartz (in oversaturated rocks) or a feldspathoid mineral, most commonly nepheline, in the case of an undersaturated rock. Figure 50 shows the fields and rock names on the QAPF double triangle. Ultramafic rocks, for which mafic minerals constitute 90-100% of the rock, are classified separately.

Given the fact that, in extreme cases, up to 90% of the mineral content of the rock may be ignored in the first-order classification, it is little wonder that magnetite abundance, for instance, is weakly correlated with rock name. It is also clear that there can be no unique correlation between rock name and bulk chemistry, given the wide range and variety of minor minerals that can be present within any one of the rock type fields. Of course, the classification is so useful and widely accepted because there are coherent patterns of mineralogical and chemical variation among plutonic rocks.

IUGS CLASSIFICATION OF PLUTONIC ROCKS

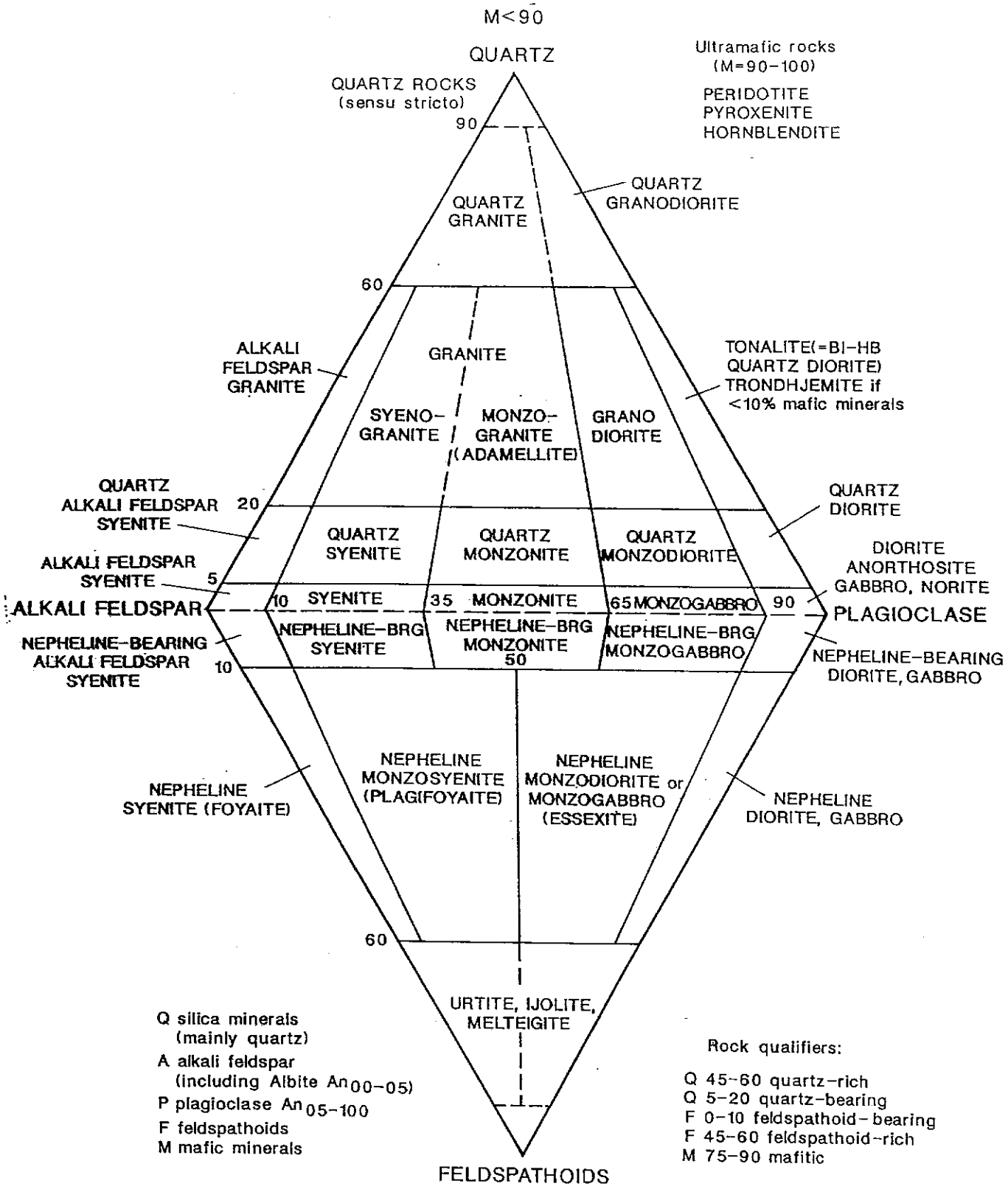

FIG. 50

A generalised plot of mineral composition for the full range of plutonic rock types is shown in Fig. 51(a). Figure 51(b) shows average trends in plagioclase composition, mafic mineral contents and hornblende/biotite ratio in granitoid rocks, showing systematic variation with position in the QAP diagram. Spatially related plutonic rock series show clear mineralogical and chemical correlations with tectonic environment and relative time of emplacement, as shown in Fig. 52. These various rock associations are characterised by different metallogeny and can be related to magnetic petrology much more reliably than to the broad IUGS rock names. This has implications for exploration, as use of magnetics for locating granitoid-hosted or granitoid- related mineralisation requires better understanding of the relationship between rock magnetisation and the geological factors that influence mineralisation.

An important geochemical classification of igneous rock series is based upon Peacock's alkali-lime index (ALI), which is a measure of the relative alkalinity of a rock series derived by igneous differentiation from a parental magma. With increasing differentiation, accompanied by increasing silica content, CaO decreases while Na^2O and K_2O increase. There is a value of silica content, therefore, where the trend of CaO plotted against SiO_2 intersects the trend of Na_2O+K_2O versus SiO_2. This SiO_2 value (in weight per cent) is the alkali-lime index, and is lower for more alkaline rock series. Rock series are classified on the basis of their alkali-lime index into one of four categories: alkalic (ALI < 51), alkali-calcic (ALI = 51-56), calc-alkalic or calc-alkaline (ALI = 56-61) and calcic (ALI > 61), as shown in Fig.53.

Examples of igneous rock series representing each of the ALI categories include: tholeiitic basalts (calcic); basalt-andesite-rhyolite series (calc-alkalic); alkali basalt-phonolite series (alkali calcic); and alkali syenite complexes (alkalic). The ALI provides a measure of the maturity of volcanic arcs, with igneous rock series tending to evolve from early mantle-derived, calcic magmatism, through calc-alkalic and orogenic magmatism, reflecting crust-mantle interactions, to post-orogenic alkali-calcic or anorogenic alkalic magmatism.

Fig. 53 also shows a major difference in the behaviour of iron during differentiation of tholeiitic and calc-alkaline magmas. On a ternary plot of MgO, total iron and alkalis (AFM diagram) tholeiitic magmas show a pronounced iron enrichment trend, reflecting early crystallisation of Mg-rich olivine and pyroxenes. This trend is typical of many layered mafic complexes (e.g. the Skaergaard, Stillwater and Bushveld Complexes), for which the parental mantle-derived magma is anhydrous and relatively reduced.

Calc-alkaline series, typified by orogenic andesites, and minor related mafic and silicic rocks, show a quite different trend, with early depletion in iron and pronounced silica enrichment. This is thought to reflect more hydrous magmas associated with crust-mantle interactions in a subduction zone, with more oxidised parental magma and early, and continuing, crystallisation of Fe-Ti oxides and hydrous phases, such as hornblende. This leads to a pronounced depletion in iron in the more evolved members of a calc-alkaline series, whereas fractionated rocks derived from tholeiitic magma are relatively iron-rich. While calc-alkaline magmas are subduction-related, tholeiitic magmas are associated with a variety of tectonic settings. These mostly, but not always, correspond to tensional regimes and include: mid-ocean ridges; mantle plume-related intraplate

MINERAL COMPOSITION OF MAJOR PLUTONIC ROCK TYPES

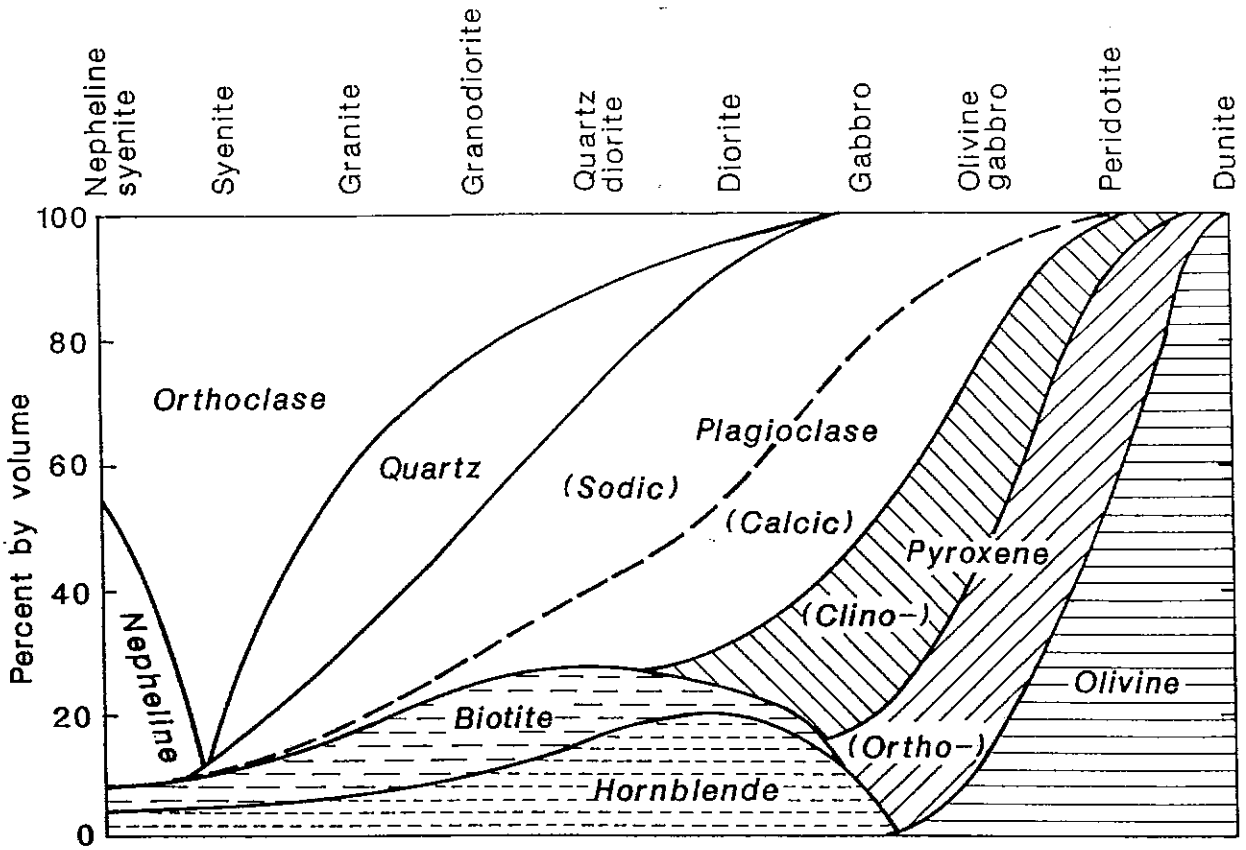

MINERALOGICAL VARIATIONS WITH GRANITOID ROCK TYPE

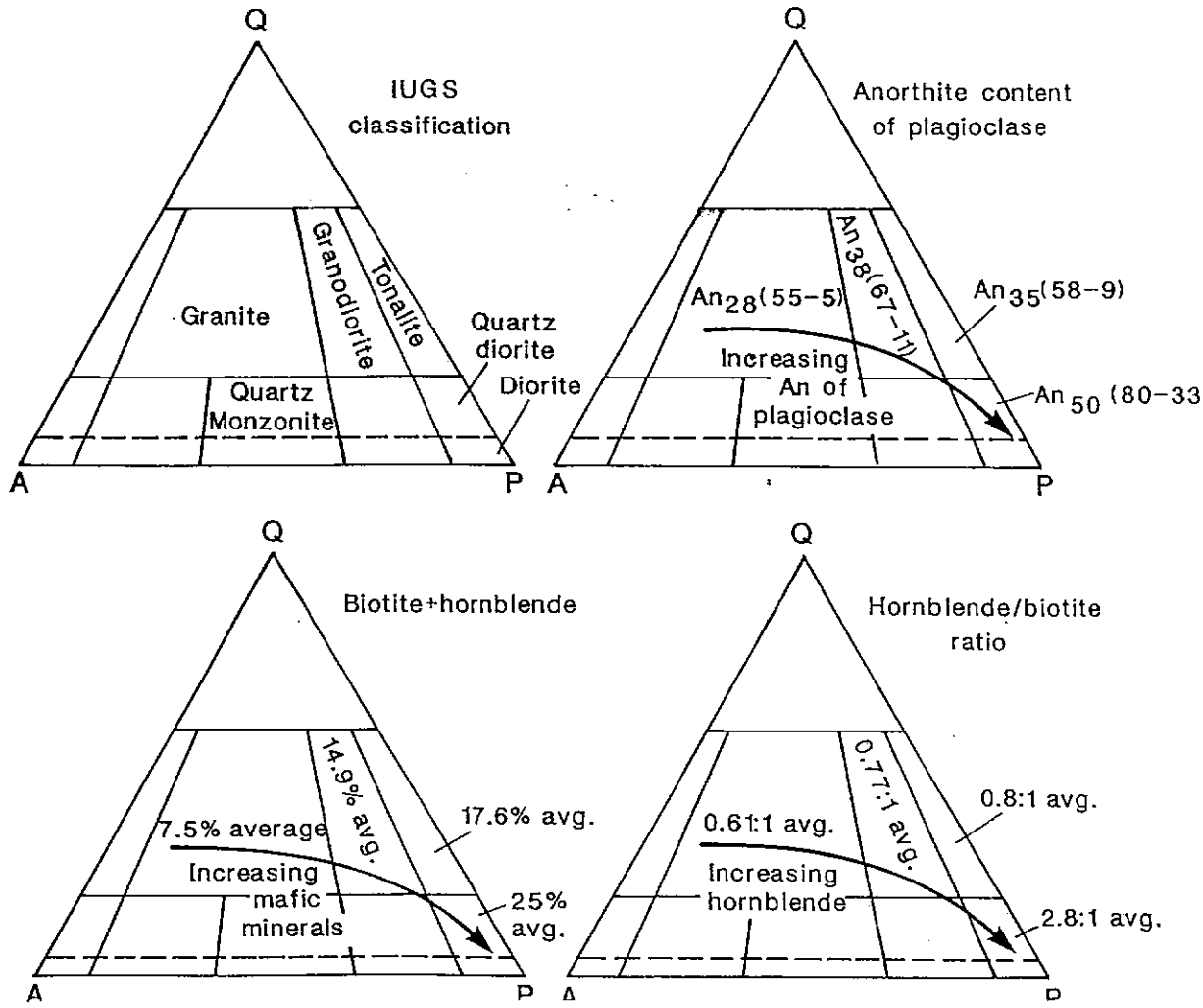

FIG. 51

QAP FIELDS OF GRANITOID SERIES

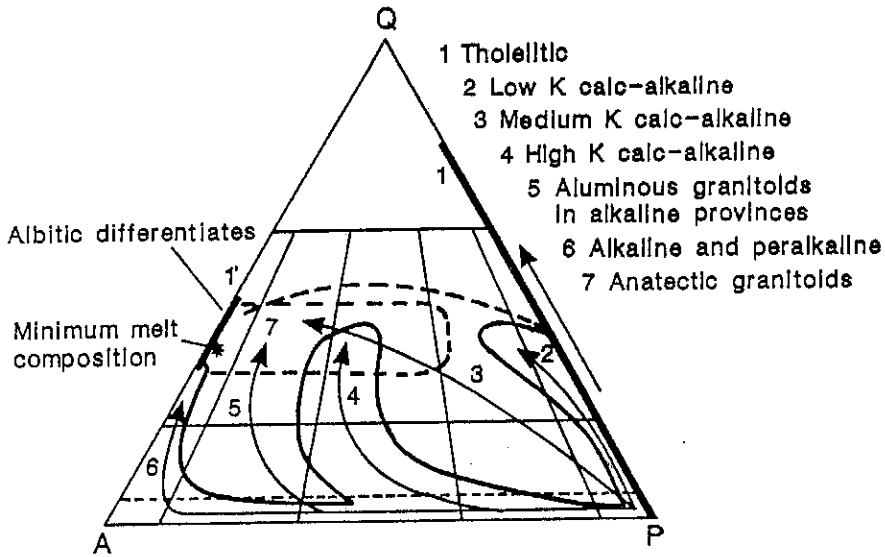

THREE MAJOR CALC-ALKALINE TRENDS

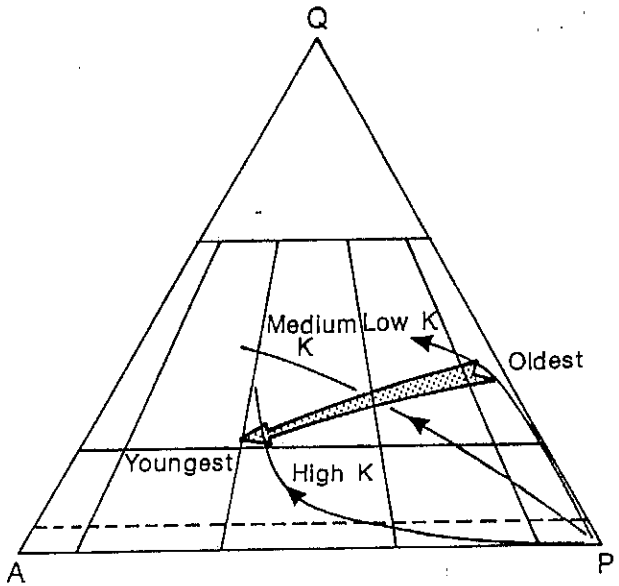

PERALKALINE AND T-GRANITOIDS

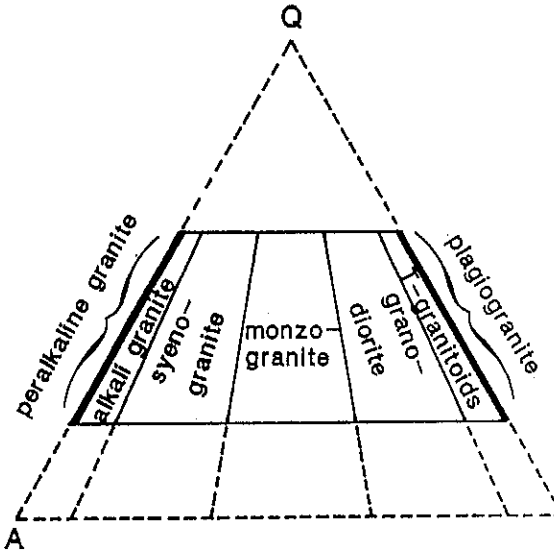

QAP MINERALOGY OF A-, S-, AND I- TYPES

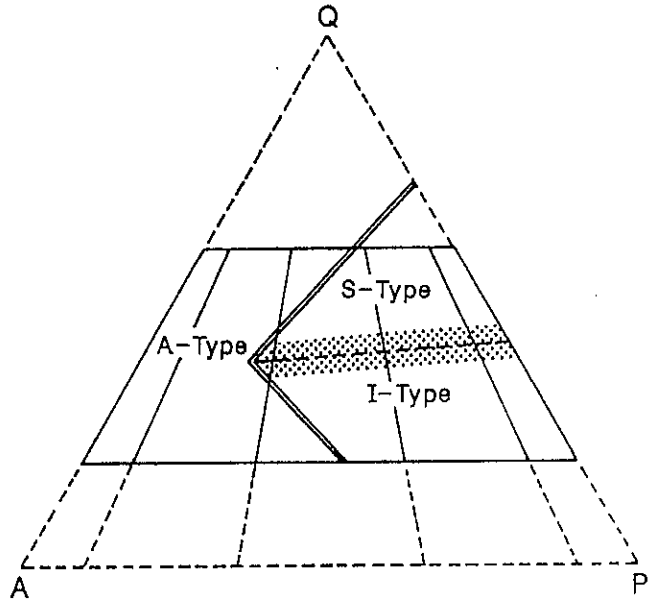

FIG. 52

CONTRASTING THOLEIITIC AND CALC-ALKALINE TRENDS

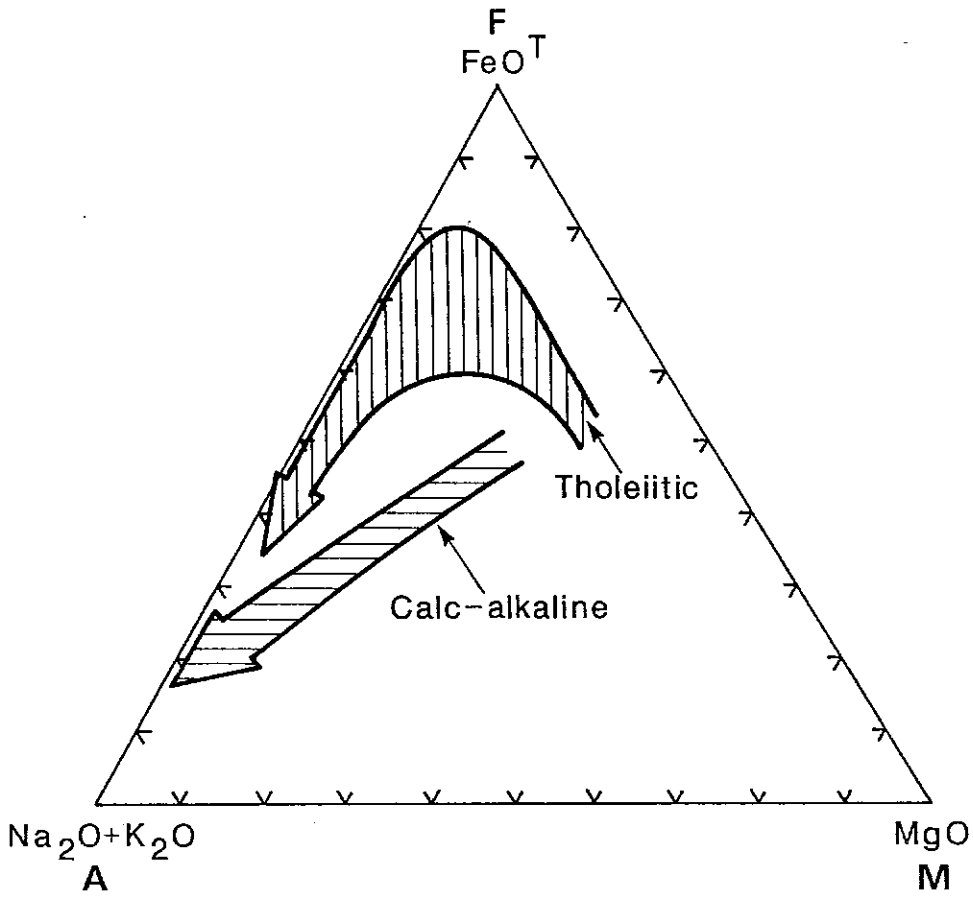

DEFINITION OF PEACOCK'S ALKALI-LIME INDEX

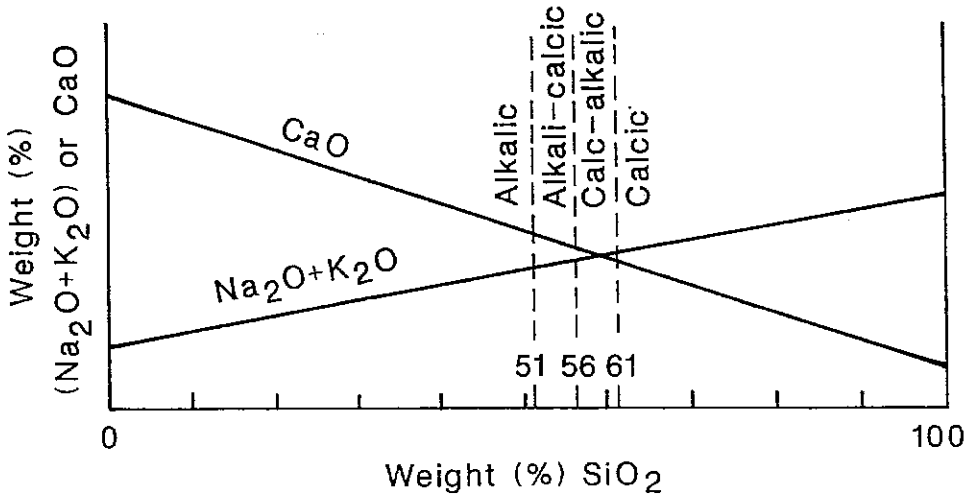

FIG. 53

oceanic islands; and anorogenic continental settings, including flood basalts, major dolerite dyke or sill swarms and layered gabbroic complexes.

Source Rock Classification of Granitoids

Chappell and White (1974) noted the existence of two categories of calc-alkaline granitoids with very distinctive mineralogical, chemical and geological features, which were interpreted as reflecting different source rocks. S-type granitoids are derived from partial melting of (meta)sedimentary rocks, and I-type granitoids from igneous source material. S may also stand for "Supracrustal" and I may represent "Infracrustal". S-type granitoids are characterised by metasedimentary inclusions (microgranitoid enclaves), whereas I-types contain hornblende-rich, mafic inclusions of igneous appearence.

These inclusions are interpreted by Chappell and White as "restite", i.e. as residual source material, and linear inter-element variation trends are regarded as due to restite unmixing. Other workers (e.g. Vernon *et al*, 1988), however, regard the I-type enclaves as quenched globules of mafic magma and linear inter-element variation as reflecting magma mixing. This first order classification based on source rock has been extended to include M-type (mantle-derived) granitoids and A-type (anorogenic, alkaline and anhydrous) granitoids, with distinctive characteristics. The chemistry, lithology, mineralogy and tectonic setting characteristic of these granitoid types are summarised in Table 1. Compositional fields for S-, I- and A-type granitoids in the QAP diagram are also shown in Fig. 52.

S-type and I-type granitoids are the most extensively studied, particularly in the Lachlan Fold Belt, which constitutes the type area for this classification. Detailed chemical characteristics of S- and I-type granitoids are summarised in Table 2 and corresponding mineralogical characteristics are given in Table 3. The predominantly metaluminous chemistry of I-type granitoids is reflected in the characteristic presence of hornblende, whereas the presence of peraluminous minerals, such as muscovite and cordierite, in S-type granitoids conforms to their strongly peraluminous chemistry (A/CNK > 1.1). This difference in alumina saturation arises from the low Na and Ca of S-types, which reflects extraction of these elements from their source rocks during the sedimentary cycle.

From the viewpoint of magnetic petrology, the most important features of Tables 2 and 3 is the generally higher ferric/ferrous iron ratio for I-type granitoids, and the corresponding more frequent occurrence of accessory magnetite. Thus I-type granitoids are usually ferromagnetic, whereas S-type granitoids are generally paramagnetic. The relatively reduced nature of S-type granitoids probably reflects the organic carbon content of the sedimentary source rocks.

Granitoid Classification Based on Tectonic Setting

Maniar and Piccolli (1989) have recently proposed an independent granitoid classification scheme, based on tectonic setting. A first order orogenic category is subdivided into island arc granitoids (IAG), continental arc granitoids (CAG), continental collision granitoids (CCG) and post-orogenic granitoids (POG). Anorogenic granitoids fall into three categories: Rift-Related Granitoids (RRG), Continental Epeirogenic Uplift Granitoids (CEUG) and Oceanic Plagiogranites (OP). Although the occurrence and

TABLE 1. THE SIAM (SOURCE ROCK BASED) GRANITOID CLASSIFICATION

	S-TYPE	I-TYPE	A-TYPE	M-TYPE
Chemistry				
1. Alumina Saturation				
	str. peraluminous	metaluminous to weakly peraluminous	peralkaline to peraluminous	metaluminous
	A/CNK > 1.1	1<A/NK; A/CNK<1.1	A/NK<1 to A/CNK>1	1<A/NK; A/CNK<1
2. Alkali-lime index				
	Alkali-calcic	Calc-alkalic to alkali-calcic	Alkalic to alkali-calcic	Calcic
3. Silica Content (wt%)				
	65-74	53-76	60-63;70-78	45-78
Lithology				
	Relatively quartz-rich monzogranites, granodiorites and tonalites (predominantly biotite granites/granodiorites and two-mica granites)	Relatively quartz-poor monzogranites, granodiorites and tonalites (hornblende-bearing)	Syenogranites, alkali granites and qtz syenites	Gabbros, diorites, quartz-diorites and tonalites

TABLE 2. CHEMICAL CHARACTERISTICS OF I AND S-TYPE GRANITOIDS

I-TYPE	S-TYPE
Metaluminous to weakly peraluminous (A/NK > 1; A/CNK < 1.1)	Strongly peraluminous (A/CNK > 1.1)
Normative diopside or < 1% normative corundum	> 1% normative corundum
Sodium rich ($Na_2O \geq 3.2\%$ for felsic varieties, decreasing to ~2.2% in more mafic varieties)	Sodium poor ($Na_2O < 3.2\%$ in rocks with $K_2O \simeq 5\%$, $Na_2O < 2.2\%$ for $K_2O \simeq 2\%$)
Molar $Na_2O \geq K_2O$	Molar $Na_2O < K_2O$
$SiO_2 < 65\%$ most common	$SiO_2 > 65\%$ most common
Broad range of compositions (mafic to felsic) (SiO_2 = 53-76%)	Restricted to high SiO_2 types (65-74%)
Regular inter-element variations within plutons (linear or near-linear variation diagrams)	Variation diagrams more irregular
Mafic varieties are Ca-rich	Low in calcium and strontium
TiO_2 relatively high	TiO_2 relatively low
$Fe_3^+/(Fe^{2+} + Fe^{3+})$ high (usually > 0.2)	$Fe^{3+}/(Fe^{2+} + Fe^{3+})$ low (usually < 0.2)

A/NK = molar $Al_2O_3/(Na_2O+K_2O)$ = Al/(Na+K);
A/CNK = molar $Al_2O_3/(CaO+Na_2O+K_2O)$ = Al/(Na+K+Ca/2)

TABLE 3. MINERALOGICAL CHARACTERISTICS OF I AND S-TYPE GRANITOIDS

I-TYPE	S-TYPE
Hornblende present, except in most felsic varieties (hornblende-bearing enclaves common)	Hornblende absent; red biotite common; (up to 30% biotite in some examples)
Minor muscovite or garnet in rare peraluminous varieties	Muscovite common, sometimes abundant
Cordierite, andalusite and sillimanite absent	Cordierite, garnet, andalusite and sillimanite may be present
Low to moderate colour index; varietal mafic minerals: Mg-biotite ± clinopyroxene + hornblende	Low colour index; biotite is Fe^{2+} and Al-rich (annite and siderophyllite rich)
Common accessories: magnetite, allanite and sphene; sulphides uncommon, but may contain pyrite; ilmenite, zircon, apatite may be present	Common accessories: ilmenite, cassiterite and tourmaline; sulphides common; zircon, monazite, apatite, pyrrhotite, mullite, aluminosilicate, corundum, topaz and spinel may be present
Calcic plagioclase (labradorite); irregular cores and intermediate rim composition	Corroded plagioclase cores uncommon; sodic or intermediate plagioclase
K-feldspar generally interstitial	K-feldspar megacrysts common

TABLE 4. GRANITOID MINERALOGY AND TECTONIC SETTING (AFTER MANIAR AND PICCOLI, 1989)

	Orogenic				Anorogenic		
	IAG	CAG	CCG	POG	RRG	CEUG	OP
Feldspar type							
	2 feldspar perth<plag	2 feldspar perth<plag	2 feldspar perth~plag	2 feldspar perth≥plag	1 feldspar perth ± Ab	1 feldspar perth ± Ab	1 feldspar perth + Ab
Perthite composition							
	> Or75	> Or75	> Or75	> Or75	≤ Or50	≤ Or50	–
Plagioclase composition							
	Oligoclase -andesine	Oligoclase	Oligoclase	Oligoclase	Albite	Albite	Oligoclase - andesine
Varietal minerals							
	Biotite ± hbld ± pyx	Biotite ± hbld ± epid	Biotite muscovite ± tour ± cord ± sill	Biotite ± hbld or ± musc	Biotite ± hbld ± pyx or alkali amph ± biotite ± hbld ± pyx		Hbld ± pyx

	Orogenic				Anorogenic		
	IAG	CAG	CCG	POG	RRG	CEUG	OP
H^+/B^+							
	$\lesssim$0.2-2.5	$\lesssim$0.2-2.5	$\lesssim$0.2-2.5	$\lesssim$0.2-2.5	$\gtrsim$2.0-2.5	$\gtrsim$2.0-2.5	$\gtrsim$2.0-2.5
M^+/B^+							
	-	$\lesssim$1.3	$\gtrsim$1.3	$\lesssim$1.3	-	-	-

H^+/B^+ = (Hbld + pyx + ol)/(biotite + epid)

M^+/B^+ = (musc + cord + gnt + tour + sill)/(biotite + epid)

IAB = Island Arc Granitoid
CAG = Continental Arc Granitoid
CCG = Continental Collision Granitoid
POG = Post-orogenic Granitoid
RRG = Rift-related Granitoid
CEUG = Continental Epeirogenic Uplift Granitoid
OP = Oceanic Plagiogranite

TABLE 5. GRANITOID CHEMISTRY AND TECTONIC SETTING (AFTER MANIAR AND PICCOLI, 1989)

	Orogenic			Anorogenic		
IAG	CAG	CCG	POG	RRG	CEUG	OP
Silica range (wt%)						
50-68	62-76	70-76	70-78	72-78 60-63	71-77 60-62	61-78
unimodal	unimodal	unimodal	unimodal	bimodal	bimodal	unimodal
Alkali-lime index						
C to C-A	C-A	C-A to A-C	A-C	A	A	C
Alumina saturation						
Predom. metalum.	Metalum. peralum.	Peralum.	Peralum. metalum. (peralk.)	Metalum. peralk. (peralum.)	Metalum. peralk. (peralum.)	Peralum. metalum.
Na_2O/CaO (wt%)						
~1	≤ 4	~2-10	~2-18	~2-25	~1-12	≤ 4
Na_2O/K_2O (wt%)						
~0.4-3.0	~0.4-2.0	~0.4-1.5	~0.6-1.2	~0.7-1.0	~0.6-1.0	0.0-50.0
MgO/FeO^T (wt%)						
0.3-0.85	0.1-0.5	0.05-0.6	0.02-0.2	0.0-7.5	0.0-0.12	0.0-0.7

	Orogenic			Anorogenic		
IAG	CAG	CCG	POG	RRG	CEUG	OP
MgO/MnO (wt%)						
12-28	2-38	2-45	2-18	0.0-7.5	0.0-7.5	0.0-50
$Al_2O_3/[Na_2O+K_2O]$ (molar)						
>1.5	>1.1	>1.1	0.9-1.4	<1.15	<1.15	>1.0

IAG = Island Arc Granitoid
CAG = Continental Arc Granitoid
CCG = Continental Collision Granitoid
POG = Post-orogenic Granitoid
RRG = Rift-related Granitoid
CEUG = Continental Epeirogenic Uplift Granitoid
OP = Oceanic Plagiogranite

abundance of magnetite was not noted by these authors, the detailed information on chemistry and mineralogy allows broad conclusions on likely magnetite contents to be inferred by comparison with other studies.

Granitoid Classification Based on Fe-Ti Oxide Mineralogy

Ishihara (1977) instigated a descriptive classification of calc-alkaline granitoids into a magnetite-series and an ilmenite-series, based on their characteristic iron-titanium oxide mineralogy. This classification can be directly related to magnetic properties and has important exploration implications, because of the association between metallogeny and the magnetite-series/ilmenite-series classification (Ishihara, 1981). The characteristic accessory mineralogy of the two categories of granitoid are:

Magnetite-series	Ilmenite-series
0.1-2 vol% magnetite	magnetite absent
±ilmenite	ilmenite (< 0.1 vol%)
hematite, pyrite, sphene, epidote, oxidised/Mg-rich biotite	pyrrhotite, graphite, muscovite, reduced/Fe-rich biotite

Thus magnetite-series granitoids are ferromagnetic (MFM to SFM), with susceptibilities in the approximate range 300-6000 μG/Oe (3800-75,000 x 10^{-6} SI), whereas ilmenite-series granitoids are paramagnetic. Magnetite-series granitoids are significantly more oxidised than ilmenite-series granitoids. This is thought to reflect upper mantle/lower crustal generation of the magnetite-series , with minimal interaction with carbonaceous material, whereas the ilmenite-series is interpreted to have been generated in the mid-to lower crust and to be significantly contaminated by C-bearing crustal rocks.

Figure 54(a) shows the correlation between opaque mineral content and susceptibility for Japanese granitoids and gabbroids, showing an essentially proportional relationship (Ishihara, 1981). This reflects the dominance of magnetite over other opaque phases in magnetite-series plutons. Ilmenite-series granitoids have very low opaque mineral contents (< 0.1 vol%). Figure 54(b) indicates that there is a wide range of susceptibilities for mafic magnetite-series granitoids, with many strongly ferromagnetic examples, but the maximum magnetite content, and hence the maximum susceptibility, decreases linearly with increasing (quartz + K-feldspar), so that the most felsic members of the series (syenogranites) are only weakly to moderately ferromagnetic. Even so, there is still a distinctly higher average susceptibility for the magnetite-series syenogranites than for their ilmenite-series equivalents. There is also a general trend to decreasing paramagnetic susceptibility in more felsic ilmenite-series granitoids, as expected.

Figure 54(c) shows the relationships between susceptibility, lithology and varietal mineralogy for granitoids from central Australia (Mutton and Shaw, 1979). This confirms the decrease in maximum susceptibility for more felsic rocks, and the association of magnetite with pyroxene and hornblende (indicative of M- or I-type

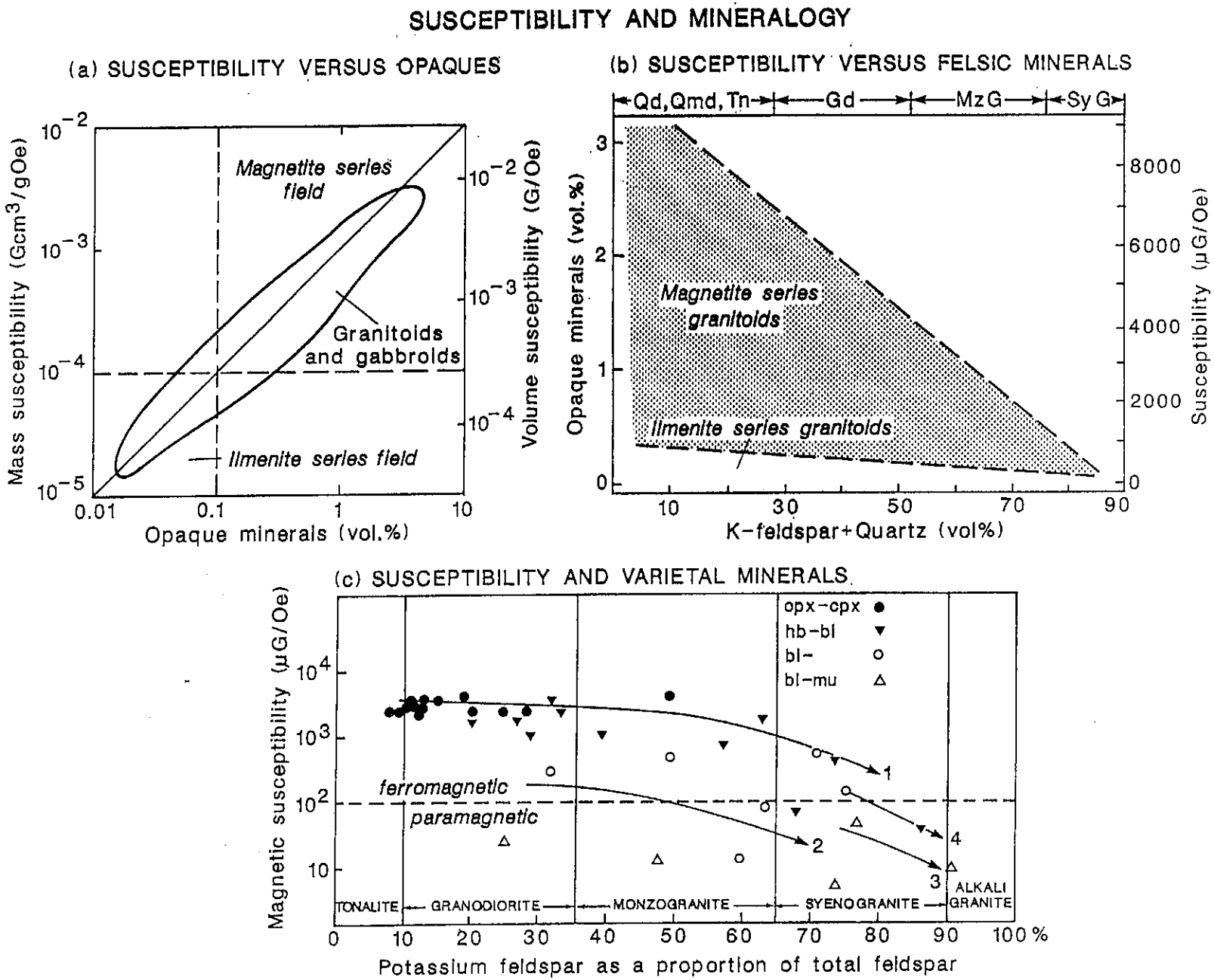
SUSCEPTIBILITY AND MINERALOGY
(a) SUSCEPTIBILITY VERSUS OPAQUES
Mass susceptibility (Gcm³/gOe)
Volume susceptibility (G/Oe)
Magnetite series field
Granitoids and gabbroids
Ilmenite series field
Opaque minerals (vol.%)
(b) SUSCEPTIBILITY VERSUS FELSIC MINERALS
Qd, Qmd, Tn
Gd
MzG
Sy G
Opaque minerals (vol.%)
Susceptibility (μG/Oe)
Magnetite series granitoids
Ilmenite series granitoids
K-feldspar+Quartz (vol%)
(c) SUSCEPTIBILITY AND VARIETAL MINERALS
Magnetic susceptibility (μG/Oe)
opx-cpx
hb-bi
bi-
bi-mu
ferromagnetic
paramagnetic
TONALITE
GRANODIORITE
MONZOGRANITE
SYENOGRANITE
ALKALI GRANITE
Potassium feldspar as a proportion of total feldspar

FIG. 54

affinities) and the apparent antipathetic relationship of magnetite with muscovite, which is a mineral characteristic of peraluminous, usually S-type, granitoids.

Fershtater *et al* (1978) and Fershtater and Chashchukhina (1979) have devised a "Ferrofacies Classification" of granitoids, which can be related to Ishihara's classification. The ferrofacies concept has been applied to a wide range of granitoids from the CIS and can be regarded as an extension of the magnetite-series and ilmenite-series classification. The categories in this classification are: the magnetite ferrofacies, the magnetite-bearing ferrofacies, the magnetite-"free" ferrofacies and the titanomagnetite ferrofacies. The characteristics of each of these categories are summarised below.

Titanomagnetite Ferrofacies Granitoids retain primary titaniferous magnetite either as homogeneous grains (generally with 6-10% TiO_2) or, more commonly, with oxyexsolution lamellae or granules of ilmenite within the titanomagnetite. Some of their characteristic features include:

- they are moderately to strongly ferromagnetic,

- the f ratio (FeO^T/MgO) of amphibole and biotite is relatively high (for biotite f > 0.5), with f generally higher for amphibole than for biotite,

- the titanomagnetite is often partially replaced by biotite, and particularly amphibole,

- they are relatively rare compared to granitoids with post-magmatic, low-Ti magnetite. Titanomagnetite facies granitoids occur in two main settings:

(i) gabbro-plagiogranite associations in ophiolite complexes (M-type granitoids, tectonic classification OP), and

(ii) some anorogenic associations, including some rapakivi complexes and gabbro/granite series that terminate an orogenic cycle.

Magnetite Ferrofacies Granitoids (more appropriately called magnetite-rich granitoids) contain > 2 vol% of iron oxides, mainly low Ti magnetite, and are therefore strongly to very strongly ferromagnetic. Other features include:

- the susceptibility is greater than ~5000 μG/Oe (0.063 SI),

- f(amphibole) < f(biotite) < 0.5, and f is either constant or decreases with increasing differentiation,

- much of the magnetite is post-magmatic, derived from breakdown of amphibole and biotite by late-stage oxidation, and ilmenite occurs as discrete grains, rather than as lamellae within a magnetite host,

- only 10-40% of the total iron content in the rock is incorporated in amphibole and biotite, with the remainder occurring in the oxide phases,

- the proportion of magnetite decreases as the rock compositions become more felsic,

- magnetite and its oxidation products (hematite, maghemite) dominates the opaque mineralogy,

- these magnetite-rich intrusives occur in several associations:

(i) epizonal/subvolcanic gabbro-granite series,

(ii) a minority group of the hornblende-biotite monzogranite-syenogranite associations, generally epizonal, relatively anhydrous intrusions.

Magnetite-bearing Granitoids are those granitoids containing moderate amounts (between 0.75% and 2%) of low Ti magnetite. Thus they are moderately to strongly ferromagnetic. Other features include:

- the susceptibility lies in the approximate range 2000-6000 μG/Oe (0.026-0.063 SI),

- f for biotite and amphibole falls in the range 0.45-0.55 in tonalites and granodiorites, rising to 0.55-0.60 in terminal syenogranites,

- the proportion of silicate iron is 40-70%, decreasing with more felsic composition,

- the proportion of magnetite may increase in the more felsic compositions, along with f in the hydrous silicates, because the the mafic silicate content drops rapidly with differentiation,

- magnetite and its oxidation products (hematite, maghemite) dominates the opaque mineralogy,

- much of the magnetite is post-magmatic, derived from breakdown of amphibole and biotite by late-stage oxidation, and ilmenite occurs as discrete grains, rather than as lamellae within a magnetite host,

- these magnetite-series granitoids occur in several associations:

(i) mesozonal/epizonal hornblende-biotite monzogranite-syenogranite series,

(ii) mesozonal hornblende-biotite tonalite-granodiorite series.

Magnetite-free Ferrofacies (more appropriately termed magnetite-poor granitoids), contain less than 0.75 vol% magnetite, but more usually less than 0.1%. Thus they are usually paramagnetic to weakly ferromagnetic. Other features are:

- f(biotite) has a restricted range (0.55-0.65),

- hornblende is absent,

- the proportion of silicate iron is 70-90% in the biotite syenogranites, which have 2-2.3% total iron, decreasing to 60-70% in the most evolved leucogranites, which contain 1.2-1.5% total iron,

- the compositional range of the rocks is restricted, being dominated by biotite syenogranites,

- these granitoids are predominantly hydrous, catazonal, palingenic granites, peraluminous monzogranite-syenogranite series, and some tonalite-granodiorite associations that have undergone greenschist facies alteration.

Much of the magnetite in granitoids is secondary and results from breakdown of mafic silicates. Examples of relevant reactions include:

$$\underset{\text{in biotite}}{2KFe_3AlSi_3O_{10}(OH)_2} + O_2 = \underset{\text{in feldspar}}{2KAlSi_3O_8} + \underset{\text{magnetite}}{2Fe_3O_4} + \underset{\text{fluid}}{H_2O}$$

$$\underset{\text{in hornblende}}{2Ca_2Fe_5Si_8O_{22}(OH)_2} + 2O_2 = \underset{\text{in augite}}{4CaFeSi_2O_6} + \underset{\text{magnetite}}{2Fe_3O_4} + \underset{\text{quartz}}{8SiO_2} + \underset{\text{fluid}}{H_2O}$$

Thus the stability of biotite, hornblende and other mafic silicates is reduced at higher oxygen fugacities. The oxygen fugacity-temperature conditions of magnetite generation in the four basic granitoid ferrofacies are shown schematically in Fig. 55(a). The magnetite ferrofacies field is regarded as approximately bounded by the MH buffer, the dry granite solidus and the upper stability limit of biotite (f=0.5) with respect to oxidation. The magnetite-"free" ferrofacies is bounded by the FMQ buffer and the upper limit for the stability of spessartine-almandine garnet, whereas the titanomagnetite ferrofacies field lies above the granite solidus.

The granitoid ferrofacies can be subdivided into subfacies, based on accessory mineral parageneses (Fig. 55(b). Magnetite-poor granitoids can be classed as:

(i) ilmenite subfacies, which has a characteristic assemblage of biotite + ilmenite + almandine,

(ii) the less common pyrite-ilmenite subfacies, which has the assemblage: biotite + almandine + pyrite + ilmenite + rutile, where the rutile, if present, is derived from ilmenite,

(iii) garnet-free granitoids of the pyrite-sphene subfacies, which have biotite + pyrite + sphene, without ilmenite.

Magnetite and magnetite-bearing ferrofacies can be subdivided into ilmenite-magnetite and sphene-magnetite subfacies. The sphene-magnetite paragenesis is generally later than the ilmenite-magnetite paragenesis, and reflects more oxidising conditions. The latter subfacies is more common in calcic granitoids.

STABILITY FIELDS OF GRANITOID FERROFACIES

A

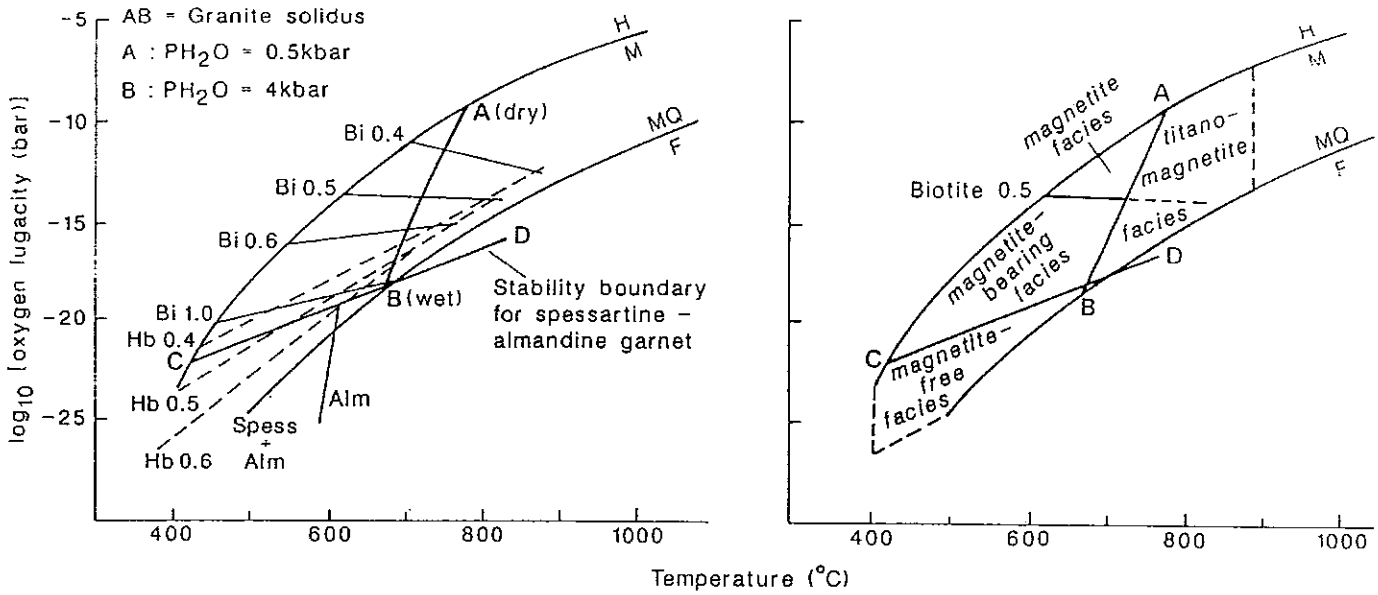

MINERAL PARAGENESES

B

MAGNETITE-FREE FACIES

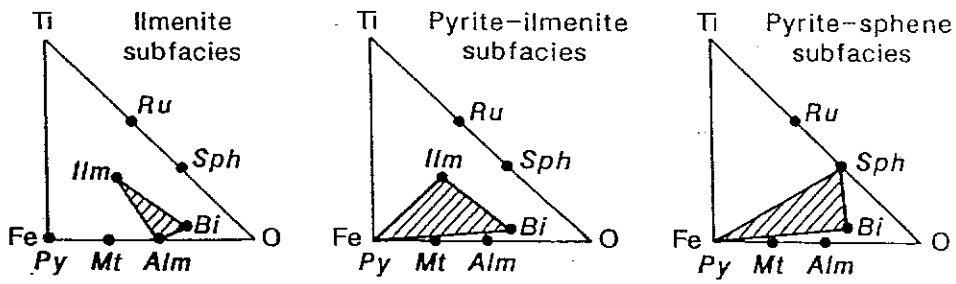

MAGNETITE FACIES

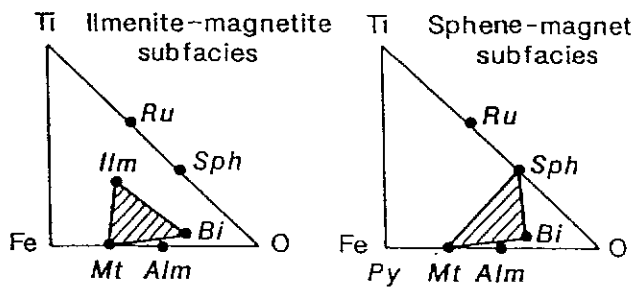

FIG. 55

Geological Factors Controlling Magnetisation of Granitoids

Many petrological studies of granitoids have been made that are relevant to the problem of defining the geological controls on magnetic properties in these rocks. This section attempts to synthesise this body of knowledge, without detailed citation. Readers are referred to the extensive bibliography at the end of these notes. Data on geochemical and mineralogical associations with magnetite in granitoids are summarised in Tables 6 and 7, respectively. Other geological factors that are demonstrably related to magnetic petrology are listed in Table 9. In fact, there are many correlations between geological, chemical and mineralogical characteristics of granitoids, on the one hand, and magnetic properties on the other hand. These patterns arise directly in some cases, e.g. the correlation between oxidation ratio and magnetite content, but in many cases they are indirect. One example is the strong overlap between paramagnetic ilmenite-series granitoids and S-type granitoids, where the reduced character arises from incorporation of crustal carbon.

Iron Content and Oxidation Ratio

To a good approximation, the susceptibility of granitoid rocks is simply proportional to their magnetite content. The directly relevant chemical parameters are the total iron content of the rock, which constrains the theoretical maximum attainable susceptibility, and the oxidation ratio (ferric/total iron), which essentially determines the partitioning of iron between silicates and oxides (mainly magnetite, in fresh igneous rocks). Figure 56 shows the typical trend for major elements with increasing silica for a series of igneous rocks derived from a basic parental magma. The total iron tends to decrease steadily, but it is important to note that even the most evolved rocks contain sufficient iron to make them at least moderately to strongly ferromagnetic, provided all the iron was contained in magnetite.

In fact, much of the iron is always sequestered within paramagnetic silicate minerals. If the rocks are paramagnetic, the susceptibility decreases monotonically with increasing silica content. This occurs if the oxidation ratio of the rocks is low, particularly in the more evolved rocks. Then the predominantly ferrous iron is taken up by silicates and the relatively small amounts of ferric iron can also be accomodated in silicates, mainly in hydrous phases. As the oxidation ratio of the rocks increases, the silicates are obliged initially to take up more ferric iron. Once the oxidation ratio exceeds a certain limit, however, the maximum amount of ferric iron that can be accomodated in silicates is reached and the excess ferric iron is forced to appear as magnetite.

Figure 56 shows how the oxidation ratios of hornblende and biotite are correlated with oxidation ratio of the whole rock, showing that these phases become essentially saturated with ferric iron at rock oxidation ratios above ~20%. When this ratio is exceeded, there is a steady increase in magnetite content, until it constitutes ~20% of the mafic minerals, as the oxidation ratio increases up to ~70%. Above this value, the whole rock ferric iron would be in surplus for forming magnetite, especially when the large proportion of ferrous iron in silicates is considered, and hematite or maghemite would appear.

PARTITIONING OF IRON BETWEEN MAGNETITE AND SILICATES

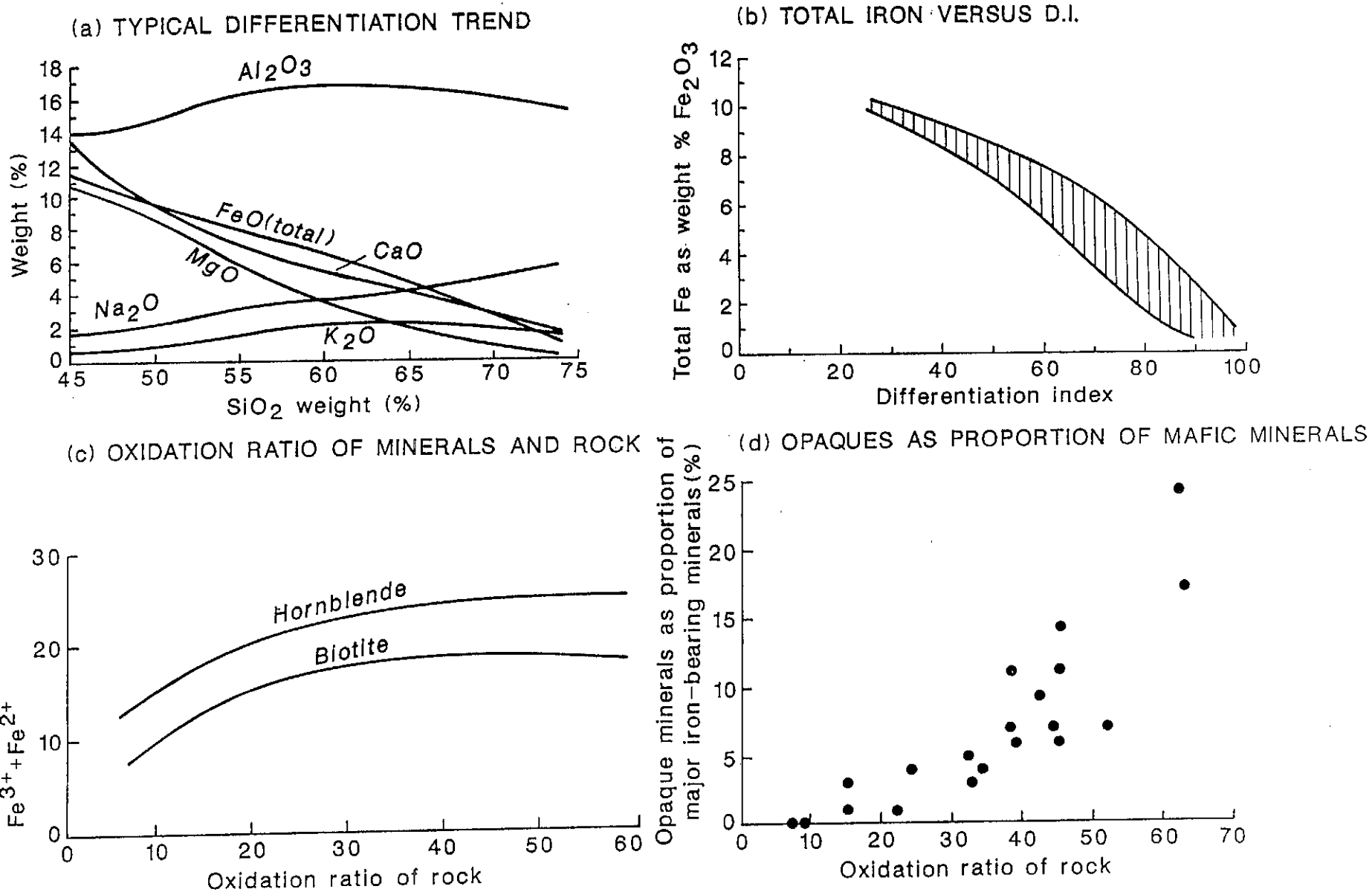

FIG. 56

In basic, anhydrous rocks without amphibole or mica, however, the anhydrous silicates can accommodate much less ferric iron than hornblende and biotite, and magnetite appears in such rocks at lower oxidation ratios. This explains why many gabbros and norites are strongly magnetic, in spite of lower oxidation ratios than for the granitoids considered in Fig. 56. Figure 57(a) shows ferrous and ferric iron contents versus silica content of average igneous rocks (values from Clark, 1982). While ferrous iron decreases rapidly, from ~10 wt% to ~3 wt%, as silica increases from 43 to 60 wt%, and thereafter more slowly, ferric iron is almost constant at ~2.5 wt% over this silica range. Thus basic igneous rocks tend to have much lower oxidation ratios than intermediate rocks, but may nevertheless have abundant magnetite. The maximum ferromagnetic susceptibility, assuming all ferric iron occurs as magnetite, and the minimum susceptibility, assuming all iron occurs as paramagnetic species are plotted, together with total iron and oxidation ratio, in Fig. 57(b). Intermediate rocks are seen to be *potentially* as magnetic as basic rocks, with a decrease in maximum susceptibility in silicic rocks.

More specific data on intrusive rocks from Finland, taken from Puranen (1989) are plotted in Fig. 58. Figure 58(a) shows the average total iron, oxidation ratio, and percentage of ferromagnetic rocks for gabbros, diorites, quartz diorites, granodiorites and granites. There is a systematic increase in oxidation ratio with silica content, offsetting the decrease in total iron. This produces an increased proportion of ferromagnetic rocks at the felsic end of the spectrum, with a slight increase in average susceptibility for granites, compared to granodiorites, as a result (Fig. 58(b)). Note that these data refer to all sampled units within the appropriate QAP field, irrespective of geological setting, metamorphic grade, varietal mineralogy etc. Thus systematic trends tend to be smoothed out by this variability, and the fact that a clear correlation between chemistry and magnetic petrology is evident suggests that there are strong underlying trends, when specific geological provinces, tectonic settings, geochemical characteristics or mineralogical varieties are considered.

Geochemical and Mineralogical Associations with Magnetite

The clearest correlation with magnetite content is that with oxidation ratio and iron content. The occurrence and abundance of magnetite is clearly correlated with other geochemical characteristics, however. Metaluminous granitoids are much more likely to be ferromagnetic than peraluminous or peralkaline granitoids, and igneous rocks with extreme alumina saturation are almost always paramagnetic. Within each Ishihara series, there is a general correlation of decreasing susceptibility with increasing silica content.

Hornblende + pyroxene or olivine in mafic varieties is favourable for the presence of magnetite, as is hornblende + biotite in more felsic rocks. Mg-rich hornblende and biotite indicate relatively oxidising conditions, with removal of iron into magnetite and consequent enrichment of the mafic silicates in magnesium. When ilmenite is present, its composition is correlated with magnetite content. Granitoids without magnetite have relatively reduced ilmenite (< 8 mol% Fe_2O_3), whereas magnetite-bearing granitoids have more oxidised ilmenite or Mn-rich ilmenite. Figure 59 shows the variation in ilmenite composition within a zoned tonalitic pluton, where the composition has evolved from metaluminous magnetite-bearing tonalites to peraluminous tonalites with little or no magnetite.

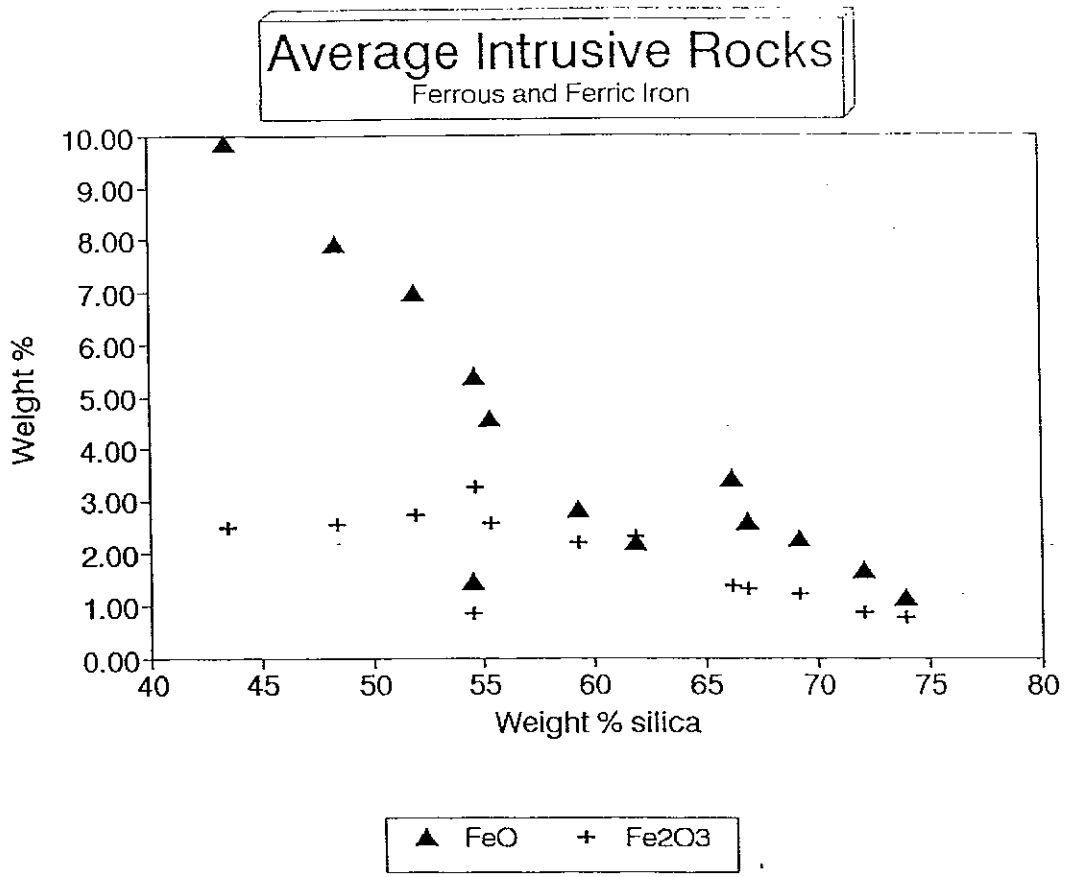
Average Intrusive Rocks
Ferrous and Ferric Iron
A
Weight %
10.00
9.00
8.00
7.00
6.00
5.00
4.00
3.00
2.00
1.00
0.00
40
45
50
55
60
65
70
75
80
Weight % silica
FeO
Fe2O3

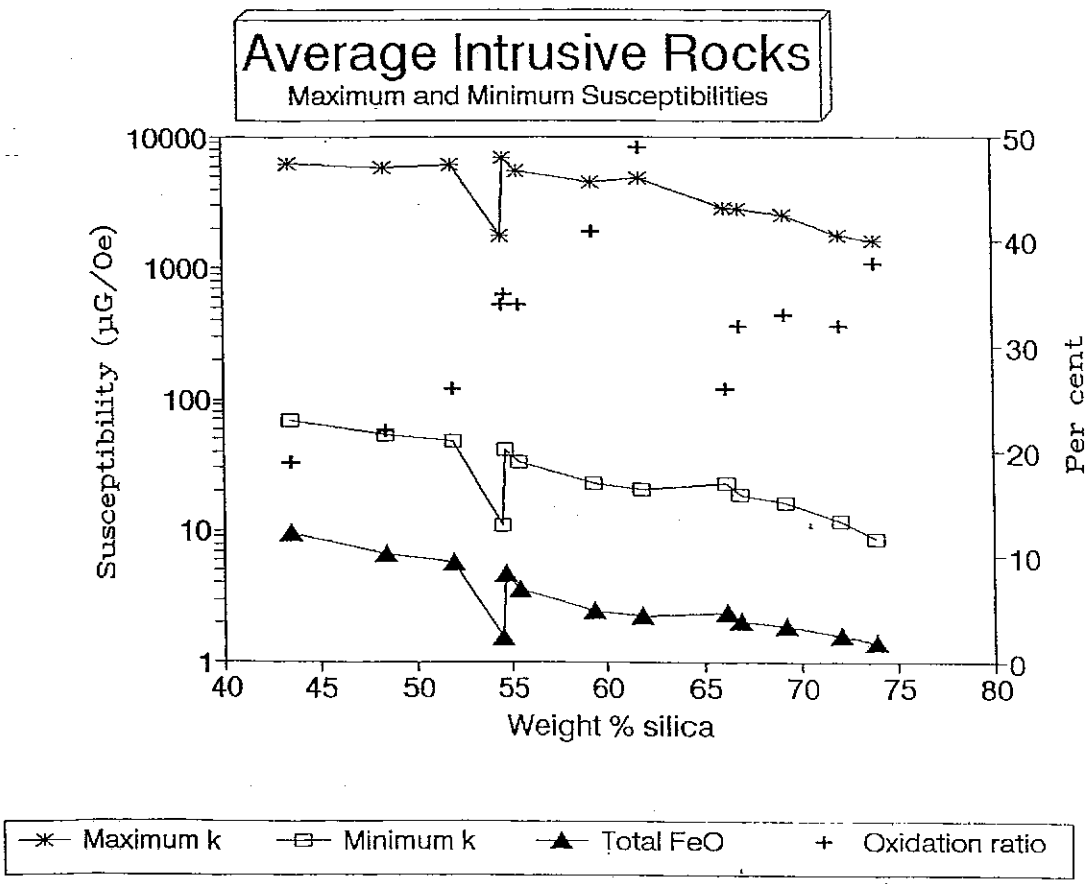
Average Intrusive Rocks
Maximum and Minimum Susceptibilities
B
Susceptibility (μG/Oe)
10000
1000
100
10
1
Per cent
50
40
30
20
10
0
40
45
50
55
60
65
70
75
80
Weight % silica
Maximum k
Minimum k
Total FeO
Oxidation ratio

FIG. 57

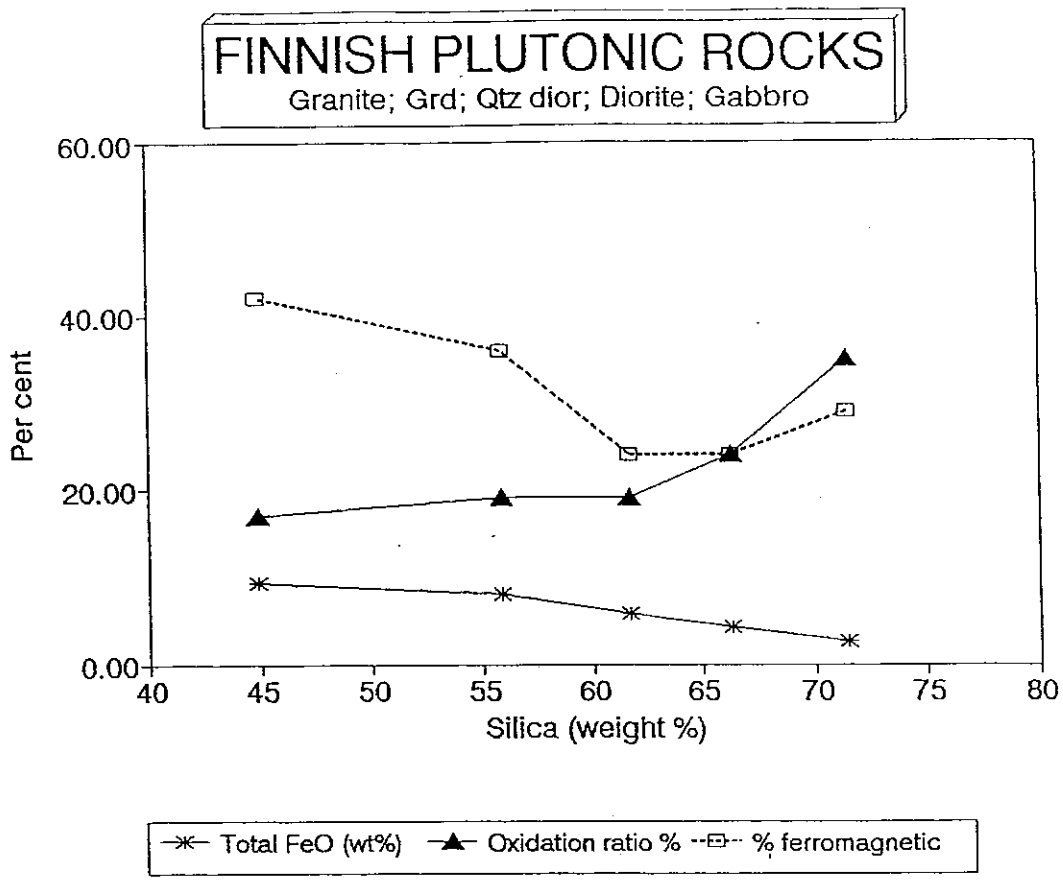
FINNISH PLUTONIC ROCKS
Granite; Grd; Qtz dior; Diorite; Gabbro
A
60.00
40.00
20.00
0.00
Per cent
40
45
50
55
60
65
70
75
80
Silica (weight %)
Total FeO (wt%)
Oxidation ratio %
% ferromagnetic

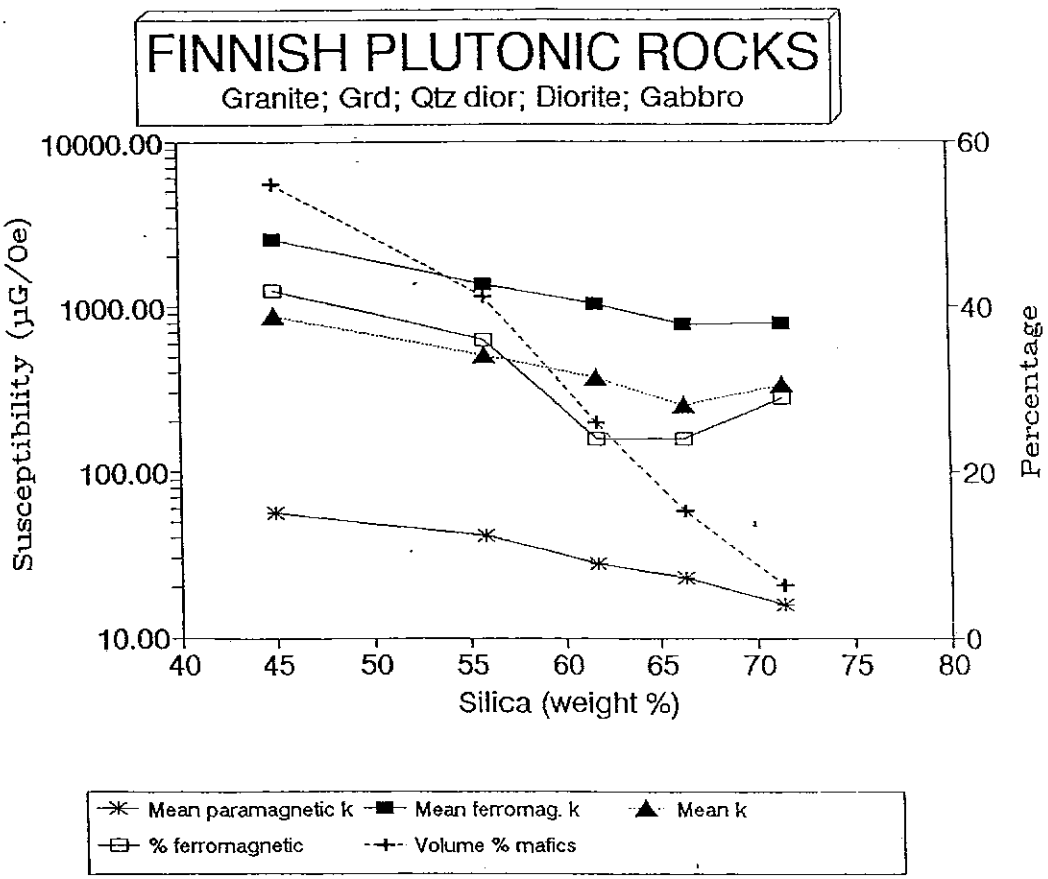
FINNISH PLUTONIC ROCKS
Granite; Grd; Qtz dior; Diorite; Gabbro
B
10000.00
1000.00
100.00
10.00
Susceptibility (µG/Oe)
60
40
20
0
Percentage
40
45
50
55
60
65
70
75
80
Silica (weight %)
Mean paramagnetic k
Mean ferromag. k
Mean k
% ferromagnetic
Volume % mafics

FIG. 58

Fe–Ti OXIDE COMPOSITIONS

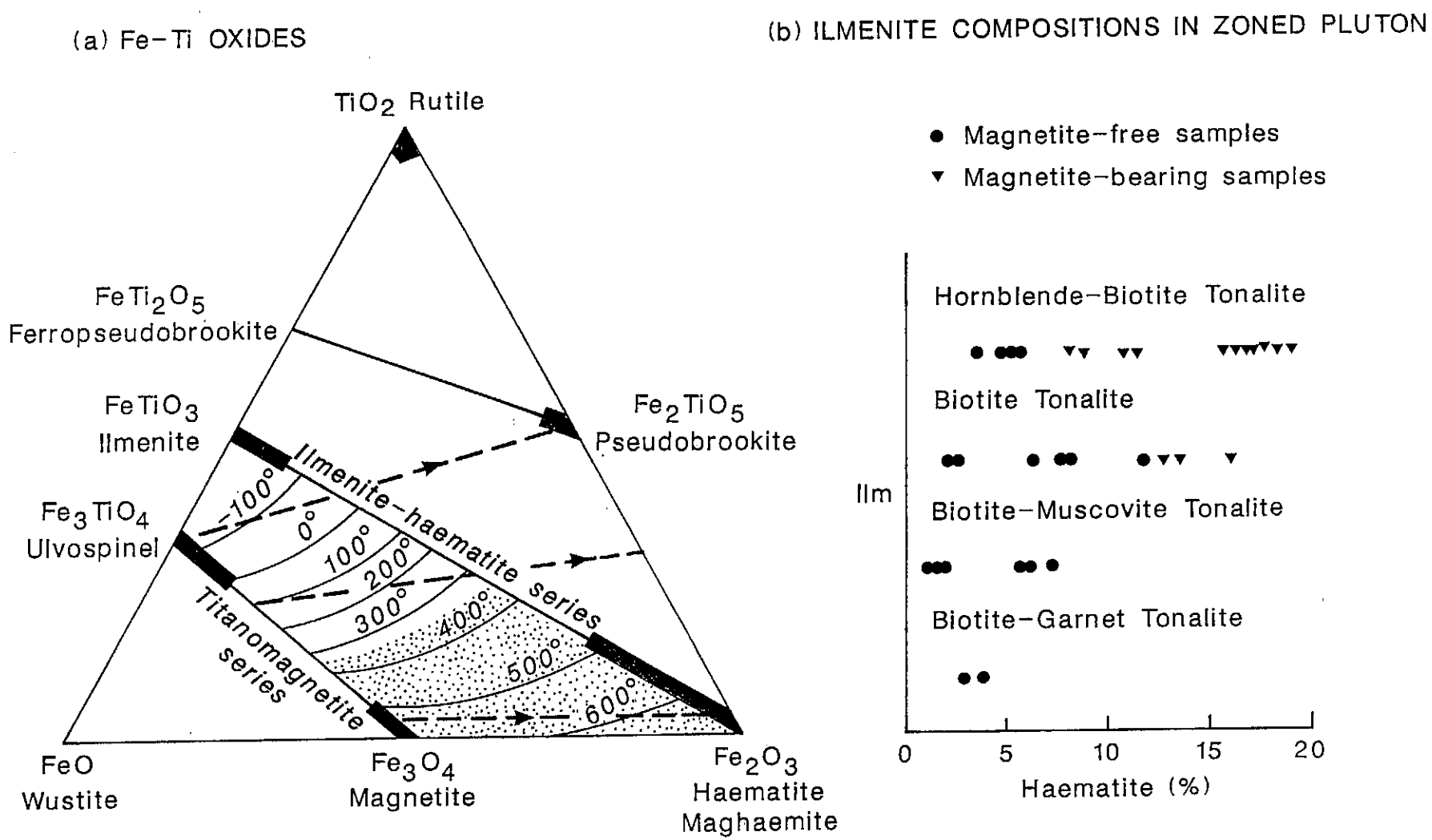

FIG. 59

TABLE 6. MAGNETITE IN GRANITOIDS: GEOCHEMICAL ASSOCIATIONS

Granitoids with Magnetite	Granitoids without Magnetite
Predominantly metaluminous (weakly peralkaline to weakly peraluminous), particularly mafic varieties	Strongly peraluminous; strongly peralkaline; or highly differentiated (silica-rich) metaluminous
$0.9 \leq A/NK < A/CNK \leq 1.1$, particularly with $SiO_2 < 70\%$	$A/CNK > 1.1$ or $A/NK < 0.9$ or $A/CNK \approx 1$ and $SiO_2 > 70\%$
Normative (diopside ± olivine ± acmite) plus > 1 wt% magnetite ± haematite	Normative acmite + sodium metasilicate; or normative corundum
$Fe_2O_3 > 0.8$ weight % (typically 1-3 weight %)	Fe_2O_3 usually < 1 weight %
Mean Fe^{3+}/Fe^{2+} ranges from 0.6 at 60% SiO_2 to 0.9 at 75% SiO_2	Mean Fe^{3+}/Fe^{2+} ranges from 0.1 at 60% SiO_2 to 0.4 at 75% SiO_2
i.e. $Fe^{3+}/(Fe^{2+}+Fe^{3+})$ ranges from 0.4 to 0.5	$Fe^{3+}/(Fe^{2+}+Fe^{3+})$ ranges from 0.1 to 0.3
Molar $Fe_2O_3/(FeO+Fe_2O_3) = 0.2$-$0.3$	Molar $Fe_2O_3/(FeO+Fe_2O_3) = 0.05$-$0.2$

A/NK = molar $Al_2O_3/(Na_2O+K_2O) = Al/(Na+K)$;
A/CNK = molar $Al_2O_3/(CaO+Na_2O+K_2O) = Al/(Na+K+Ca/2)$

TABLE 7. MAGNETITE IN GRANITOIDS: MINERALOGICAL ASSOCIATIONS

Magnetite-bearing Granitoids	Magnetite-free Granitoids
Calc-alkaline rocks	
Biotite ± hornblende in felsic varieties or hornblende ± pyroxene ± olivine in more mafic metaluminous rocks. Biotite is Fe^{3+} and Mg-rich (phlogopite-rich). (Biotite colour is brown, black or olive green.	Biotite + muscovite, cordierite, garnet or aluminosilicate in peraluminous rocks. Biotite is Fe^{2+} and Al-rich (annite-siderophyllite rich). Biotite has "foxy" red colour.
Sphene ± haemoilmenite ± epidote ± allanite ± pyrite as accessories	"Reduced" ilmenite ± pyrrhotite (predominantly hex po) ± spinel. Primary sphene is absent.
Haemoilmenite (8-20 mole % Fe_2O_3) or Mn-rich ilmenite (up to ~30 mole % $MnTiO_3$)	"Reduced" ilmenite (<8% Fe_2O_3), usually with low Mn content
Tholeiitic rocks	
Intermediate to Fe-rich olivine and pyroxenes + intermediate to sodic plagioclase ± hornblende ± apatite in upper ± middle zones of layered basic intrusions	Mg-rich olivine and pyroxenes, calcic plagioclase ± chromite in lower to middle zones of layered basic intrusions
Zoned plagioclase (> 60%) + quartz + biotite and/or hornblende in M-type oceanic/ophiolitic plagiogranites	
Serpentine minerals (after olivine and pyroxene) + brucite + chromite in alpine-type (ophiolitic) peridotites and in ultramafic basal sections of layered mafic/ultramfic intrusions	

Alkaline rocks

Nepheline + alkali feldspar + plagioclase + calcic pyroxene + hastingsite + biotite in silica undersaturated metaluminous (miaskitic) rocks

Quartz + alkali feldspar + sodic pyroxene and/or sodic amphibole ± aenigmatite ± astrophyllite ± biotite in oversaturated peralkaline (ekeritic) rocks

Nepheline + alkali feldspar + sodic pyroxene and amphibole ± biotite without aenigmatite or astrophyllite in mildly peralkaline undersaturated rocks.

Nepheline + sodic pyroxene + aenigmatite ± astrophyllite in silica undersaturated peralkaline (agpaitic) rocks

TABLE 8. MINERALOGICAL COMPATIBILITY WITH MAGNETITE

Sympathetic Minerals	**Antipathetic Minerals**
HORNBLENDE (partic. Mg-rich, Al-poor Hb)	MUSCOVITE
Mg and Fe^{3+}-RICH BIOTITE	HIGH Al AND Fe/Mg BIOTITE
CLINOPYROXENE	CORDIERITE
ORTHOPYROXENE	GARNET
OLIVINE (except fayalite)	FAYALITE
SPHENE	SILLIMANITE
EPIDOTE	ANDALUSITE
ALLANITE	CASSITERITE
SODIC PYROXENE	TOURMALINE
RIEBECKITE-ARFVEDSONITE	AENIGMATITE
"OXIDISED" ILMENITE	ASTROPHYLLITE
	"REDUCED" ILMENITE

Figure 60 shows the variations in mineral abundances along a traverse through a typical zoned pluton, showing, in particular the sympathetic variation of magnetite with hornblende and sphene. Figure 61 shows the correlation between normative and modal magnetite along this traverse. Note the clear positive correlation between the theoretical magnetite content and the actual content, but that the norm significantly overestimates the magnetite content, because all ferric iron in rocks of this broad composition is allocated to magnetite. In fact a substantial proportion of ferric iron occurs in the hydrous silicates, which are not considered in the normative calculation.

Similar studies can be summarised by a list of minerals that are either sympathetic or antipathetic to magnetite (Table 8).

Source Rock

Mantle-derived (M-type) and I-type granitoids derived from mafic crustal underplates or second generation I-types derived from relatively oxidised igneous rocks are generally magnetite-series. I-type granitoids derived from reduced source rocks within specific basement terranes, on the other hand, are ilmenite-series. Local reduction of I-type magmas by assimilation of carbonaceous wall rocks is also known to produce rocks that are free of magnetite. S-type granitoids derived from graphitic metasediments, generally pelitic, are reduced and have little or no magnetite.

Lithology

The overall proportion of ferromagnetic rocks within a given geological province or within a particular igneous rock series decreases from gabbro through to granite. Mafic to felsic and intermediate to felsic associations are much more likely to be magnetite-series throughout, than compositionally restricted felsic associations. Alkaline intrusive rocks are often magnetite-series, with the exception of extreme compositions, such as peralkaline granites and agpaitic (peralkaline) nepheline syenites. In tholeiitic layered complexes, less evolved lower gabbros are paramagnetic to weakly ferromagnetic, whereas sufficiently evolved upper ferrogabbros and ferrodiorites, and associated granophyres, are usually strongly ferromagnetic.

Emplacement Depth

Pecherskiy (1963) noted the strong correlation between shallow emplacement depth and occurrence of magnetite in granitoids. Figure 62 shows the percentage of moderately and strongly ferromagnetic granitoids versus estimated depth of emplacement for a large number of plutons in the CIS. The ferromagnetic proportion rises to 70% for subvolcanic/epizonal granitoids. The paramagnetic "granitoids" at 200 m depth refers to a single occurrence of sill-like felsic rocks that are probably hypabyssal analogues of S-type volcanics, such as those in the Lachlan Fold Belt. Apart from this aberration, there is a systematic decrease in ferromagnetic proportion with increasing depth of emplacement. Czamanske *et al* (1981) explain a similar correlation in Japan by invoking onset of second boiling in the residual melt in epizonal plutons. Dissociation of water and preferential diffusion of hydrogen out of the pluton into fractured country rock is the

MODAL MINERALOGY FOR A TRAVERSE
ACROSS A TYPICAL ZONED PLUTON

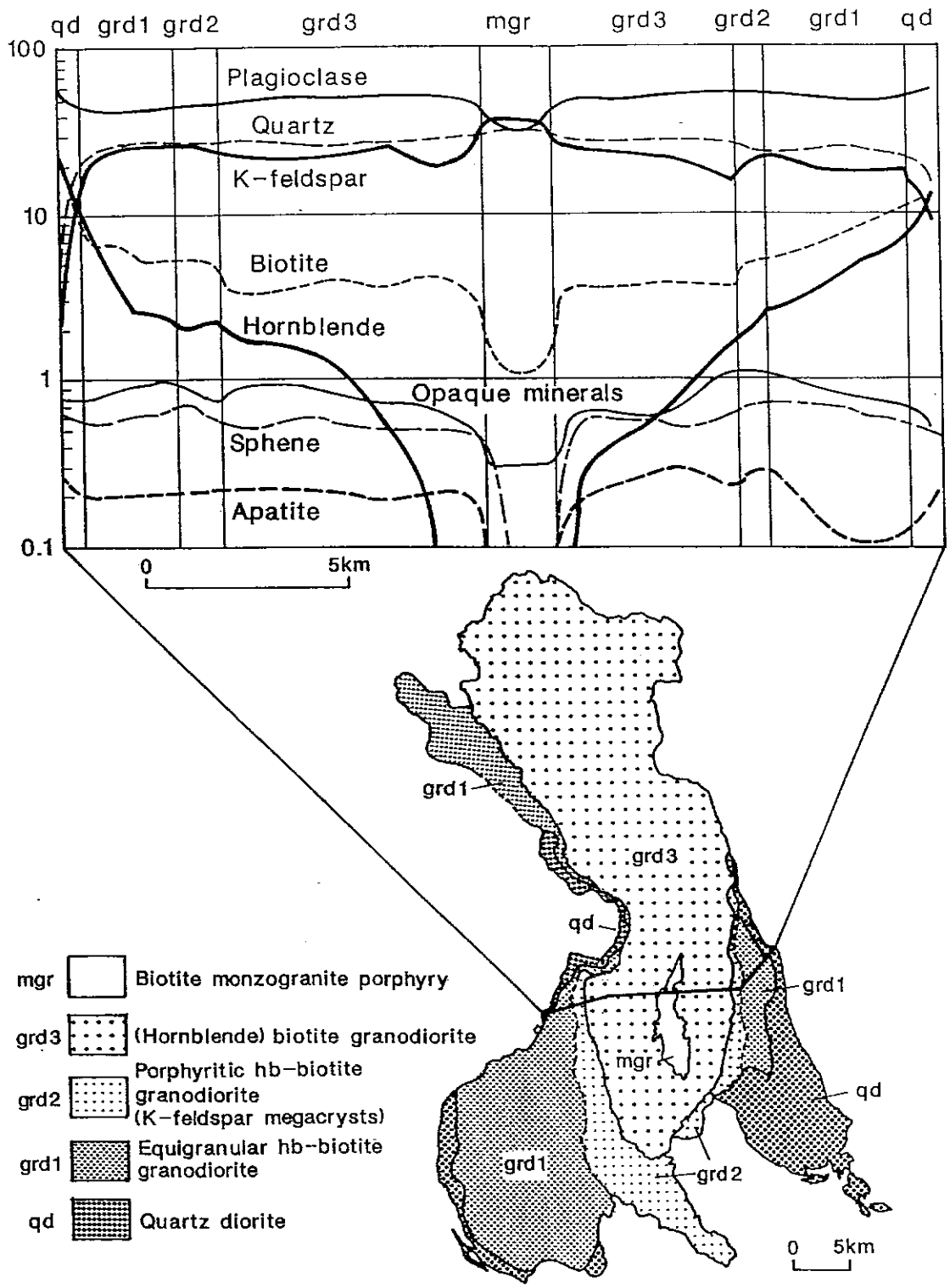

FIG. 60

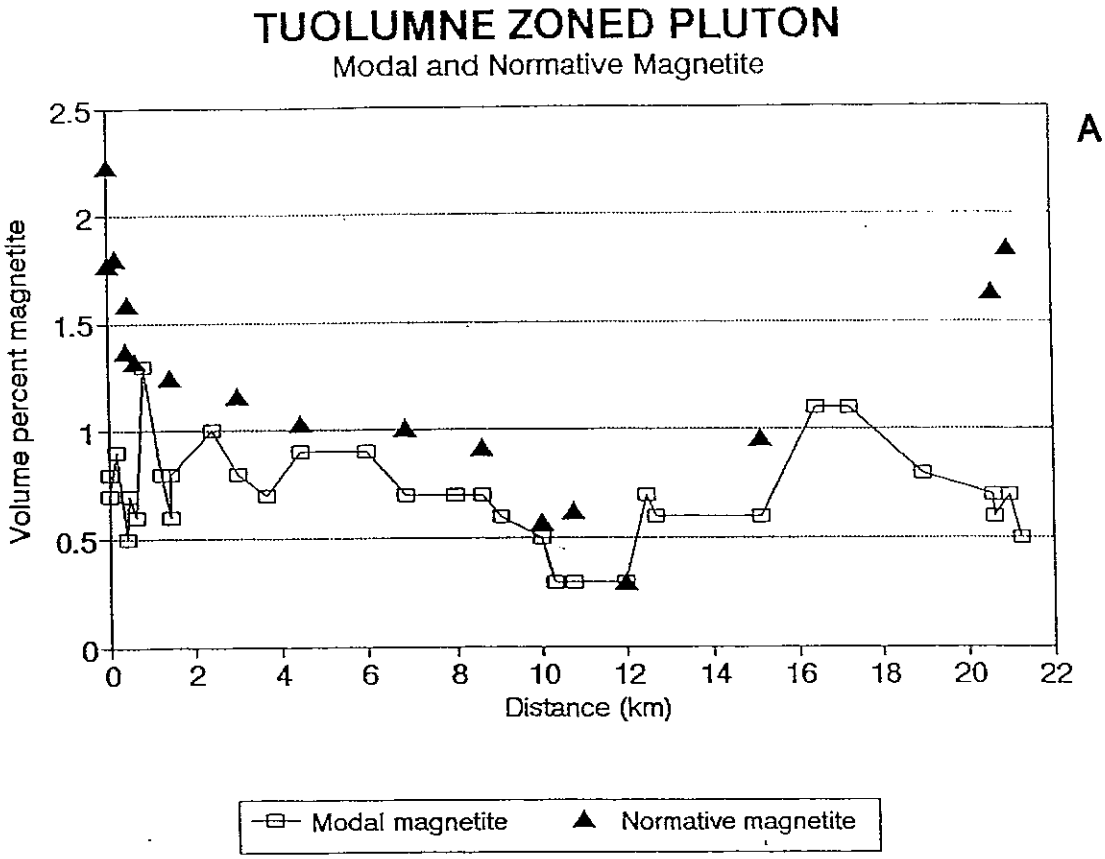
TUOLUMNE ZONED PLUTON
Modal and Normative Magnetite
A
Volume percent magnetite
2.5
2
1.5
1
0.5
0
0
2
4
6
8
10
12
14
16
18
20
22
Distance (km)
Modal magnetite
Normative magnetite

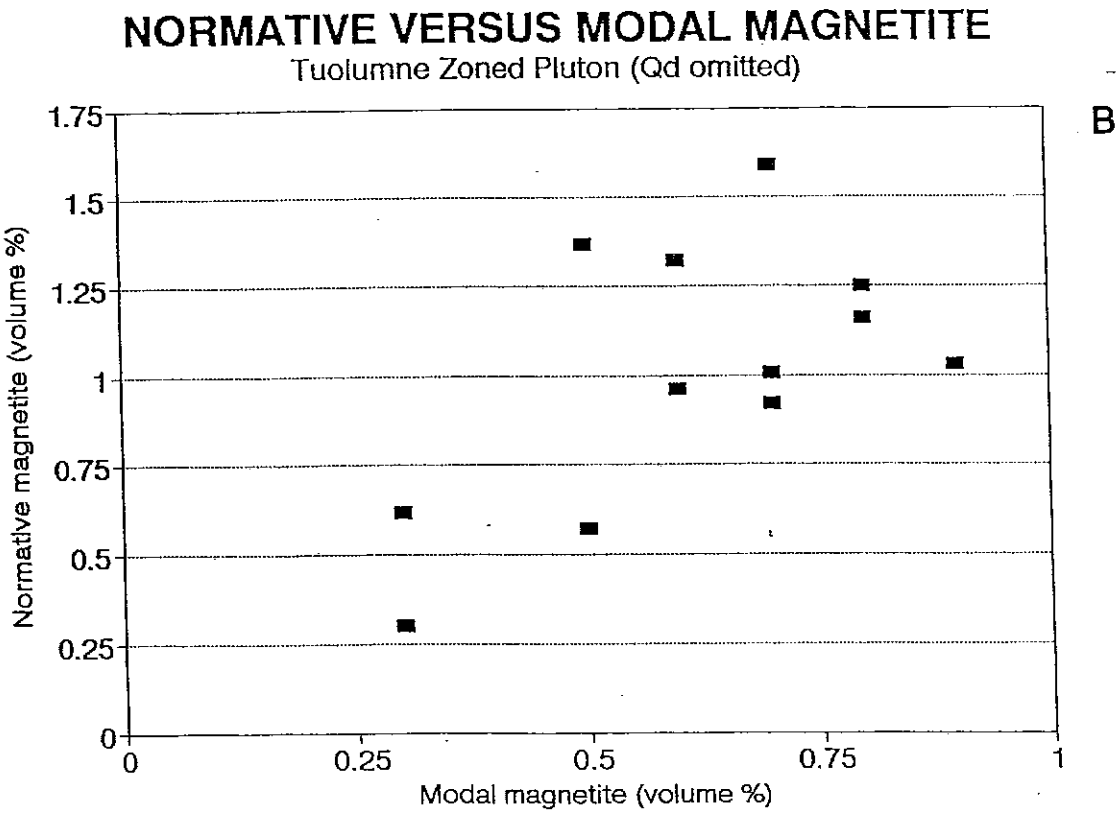
NORMATIVE VERSUS MODAL MAGNETITE
Tuolumne Zoned Pluton (Qd omitted)
B
Normative magnetite (volume %)
1.75
1.5
1.25
1
0.75
0.5
0.25
0
0
0.25
0.5
0.75
1
Modal magnetite (volume %)

FIG. 61

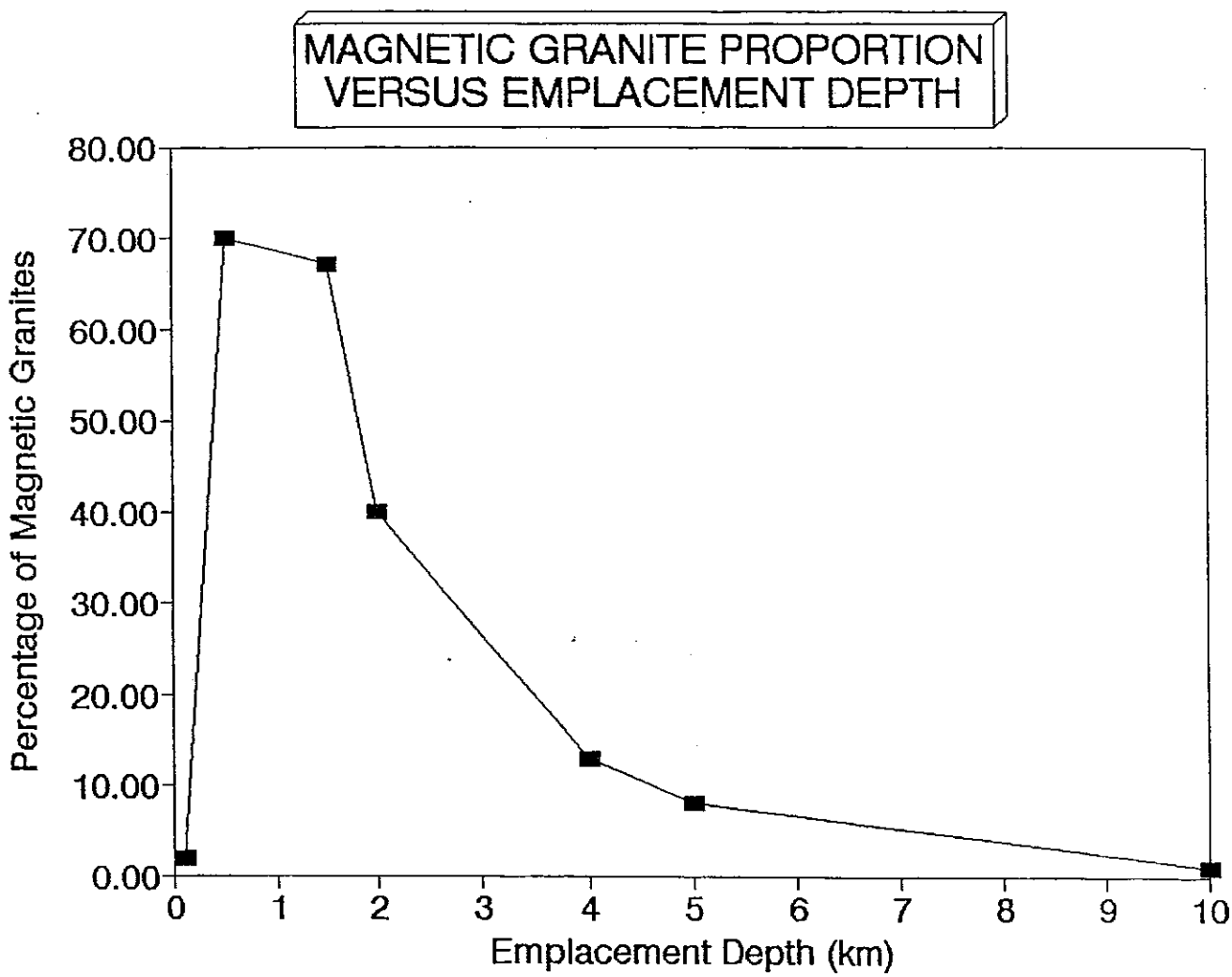
MAGNETIC GRANITE PROPORTION
VERSUS EMPLACEMENT DEPTH
Percentage of Magnetic Granites
80.00
70.00
60.00
50.00
40.00
30.00
20.00
10.00
0.00
0
1
2
3
4
5
6
7
8
9
10
Emplacement Depth (km)

FIG. 62

TABLE 9. GEOLOGICAL FACTORS AFFECTING MAGNETISATION OF GRANITOIDS

Ferromagnetic Granitoids	**Paramagnetic Granitoids**
SOURCE ROCK	
Mantle Mafic crustal underplate Oxidised felsic igneous rocks	Metasediments (particularly pelites) Reduced felsic igneous rocks
LITHOLOGY	
Gabbro > diorite > tonalite > granodiorite > granite	Predominantly granite and granodiorite
Hornblende ± biotite granitoids and biotite granites with high Mg, low Al biotite	Muscovite and two mica granitoids, most leuco-granites, some biotite granites
Pyroxene ± hornblende granitoids	Cordierite, corundum or aluminosilicate-bearing granitoids
Most monzonites, quartz-monzonites, syenites, quartz-syenites and miaskitic nepheline syenites	Peralkaline granites and syenites, agpaitic nepheline syenites
Most alkali gabbros, essexites ijolites etc.	
Serpentinised peridotites	Unserpentinised peridotites
Upper gabbros in layered complexes	Lower gabbros in layered complexes
CHEMISTRY	
Predominantly metaluminous, but also weakly peraluminous or weakly peralkaline granitoids	Strongly peraluminous and strongly peralkaline granitoids, some metalum. granitoids

Ferromagnetic Granitoids	**Paramagnetic Granitoids**
Moderate to high ferric iron	Low ferric iron
and	or
Moderate to high total iron	Very low total iron
and	or
Moderate oxidation ratio	Low oxidation ratio
Relatively anhydrous	Relatively hydrous
EMPLACEMENT DEPTH	
Predominantly epizonal, particularly subvolcanic; some mesozonal and catazonal	Predominantly mesozonal or catazonal, some epizonal
ASSOCIATED ROCKS	
Associated volcanics common	Associated volcanics uncommon
Gabbro-diorite-tonalite-trondhjemite associations	Syenogranite-monzogranite-granodiorite associations
(Gabbro)-diorite-granodiorite monzogranite associations	Quartz syenite-syenogranite-associations
Diorite-monzonite-quartz monzonite-monzogranite associations	
Syenite-alkali syenite-alkali granite associations	
TECTONIC SETTING	
Andinotype (subduction of oceanic plate beneath continental margin - generating Cordilleran I-type batholiths)	Hercynotype (continental collision - e.g. Himalayan and Hercynian leucogranites)
Island arc plagiogranites, gabbros and quartz diorites	Encratonic ductile shear belts with thickened continental crust

Ferromagnetic Granitoids	Paramagnetic Granitoids
Alpinotype (tectonically emplaced serpentinised peridotites, gabbros and plagiogranites)	Late tectonic/post tectonic catazonal migmatites and d mesozonal granitoids associated with regional metamorphism
Caledonian-type post-closure uplift with major faulting	Compressional regimes
Post-orogenic tensional and uplift with major faulting	Anorogenic, rifting associated highly evolved magmas
Anorogenic, rifting associated moderately evolved magmas	

oxidation process that is considered to produce the high magnetite contents of these plutons.

There is also a general correlation between the source rock, depth of generation and depth of emplacement of granitoids. Deep-seated, high temperature, anhydrous magmas rise to shallow crustal levels, whereas lower temperature, hydrous magmas (produced by partial melting of muscovite-rich pelitic metasediments, for example) do not rise very far from their source regions, producing catazonal granitoids. The former type of magma is more likely to produce magnetite-series granitoids, whereas the latter generally produces ilmenite-series granitoids, for reasons already explained.

Tectonic Setting

Referring to Maniar and Piccoli's (1989) classification, most island arc and oceanic plagiogranites, and more mafic continental arc granitoids, are ferromagnetic. Nearly all continental collision and post-orogenic granitoids are paramagnetic. Rift-related granitoids and continental epeirogenic uplift granitoids have a bimodal distribution of magnetite contents, with the mafic compositions tending to be ferromagnetic and the felsic compositions generally paramagnetic.

Magnetic Petrology and Metallogeny of Granitoids

Ishihara (1981) noted the important correlation between his magnetite- and ilmenite-series granitoid classification and granitoid-related mineralisation. For example, copper and molybdenum porphries are almost always magnetite-series, whereas tin granites are invariably ilmenite-series. This relationship is not just empirically based, but can, in some cases, be related to redox conditions in the magma. Ishihara's data on metallogenic associations with granitoid series and with susceptibility are reproduced in Fig. 63.

Tin occurs in two oxidation states in magmas: stannous (Sn^{2+}) and stannic (Sn^{4+}). The oxidised stannic species fits easily into the structures of minerals such as magnetite and sphene, and is therefore dispersed throughout an oxidised granitoid. On the other hand, the reduced stannous ion is too large to be accomodated readily within mineral structures and is accordingly concentrated in the original melt. Thus reduced, and therefore paramagnetic, granitoids are potential sources of tin mineralisation, whereas magnetite-bearing granitoids are too oxidised to be associated with tin deposits.

Khitrunov (1985) has attempted a general explanation of the empirical relationships between oxidation state of granitoids and associated Cu, Mo, W or Sn mineralisation, concluding that magmatic conditions are progressively more reduced for Mo, Cu, W and Sn mineralisation. Cameron and Hattori have pointed out the association between oxidised felsic magmas and Archaean gold deposits, and have given a detailed discussion of the factors favouring incorporation of gold from sulphide minerals in source rocks, concentration into a CO_2-rich melt and deposition after development of an immiscible fluid phase. Sillitoe (1979) pointed out the association between gold-rich porphyry copper deposits and oxidised, magnetite-rich plutons with a magnetite-rich potassic alteration zone. Kwak and White (1982) distinguished between reduced porphyry tin and

MINERALISATION ASSOCIATED WITH MAGNETITE AND ILMENITE SERIES GRANITOIDS

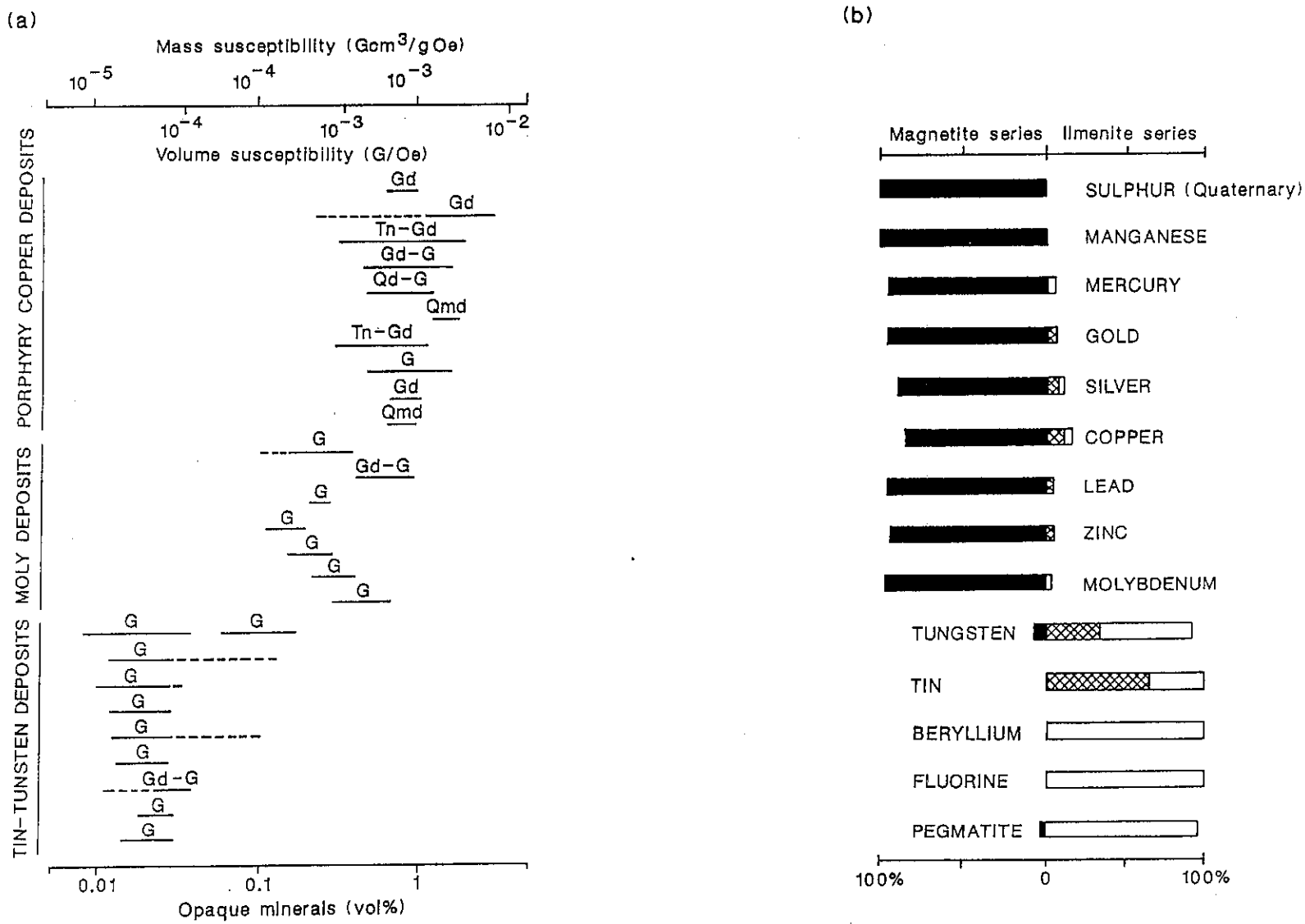

FIG. 63

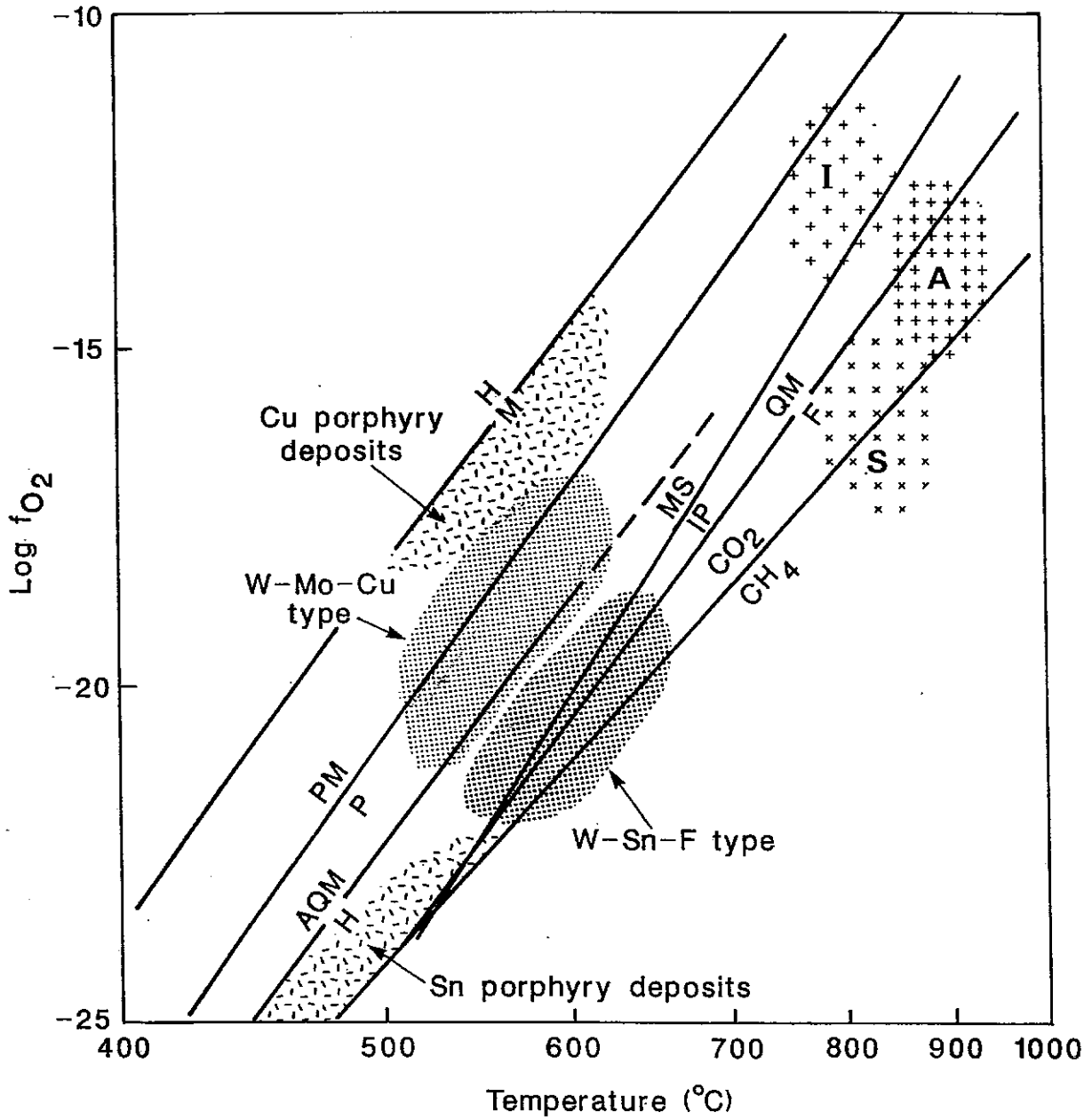
-10
-15
-20
-25
Log f_{O_2}
400
500
600
700
800
900
1000
Temperature (°C)
Cu porphyry deposits
W-Mo-Cu type
W-Sn-F type
Sn porphyry deposits
H
M
P
H
PM
AQM
MS
IP
QM
F
CO_2
CH_4
I
A
S

FIG. 64

TABLE 10. MINERALISATION AND OXIDATION STATE OF GRANITOIDS

Strongly ferromagnetic	**Paramagnetic**
MOST OXIDISED	MOST REDUCED
Au → Mo → Cu → W → Sn	
Mineralisation	**Magnetic Petrological Classification**
Au-rich porphyry Cu (> 0.4 g/T)	SFM granitoid (M or I-type) + SFM potassic alteration zone
Porphyry Cu	MFM to SFM granitoid ± SFM potpotassic alteration zone
Porphyry Mo	MFM to SFM granitoid
Au-scheelite-quartz exo-granitic plutonic vein. Scheelite contains Mo.	WFM to MFM granitoid
W-Mo-Cu skarn	MFM to SFM granitoid
W-Cu-Sn veins. Tungsten mineral is wolframite or Mo-free scheelite.	PM granitoid
W-Sn-F skarn	PM granitoid
Sn-W greisen	PM granitoid
Cr, PGEs in lower levels of layered basic complex	PM to WFM gabbros overlying MFM to SFM serpentinised ultramafics
Ti, V in upper levels of layered basic complex	SFM gabbros
Sn-W, Be, Li and U mineralisation associated with peraluminous two-mica granites	PM granitoids
Nb-Ta, REE mineralisation associated with peralkaline anorogenic ring complexes	PM granitoids

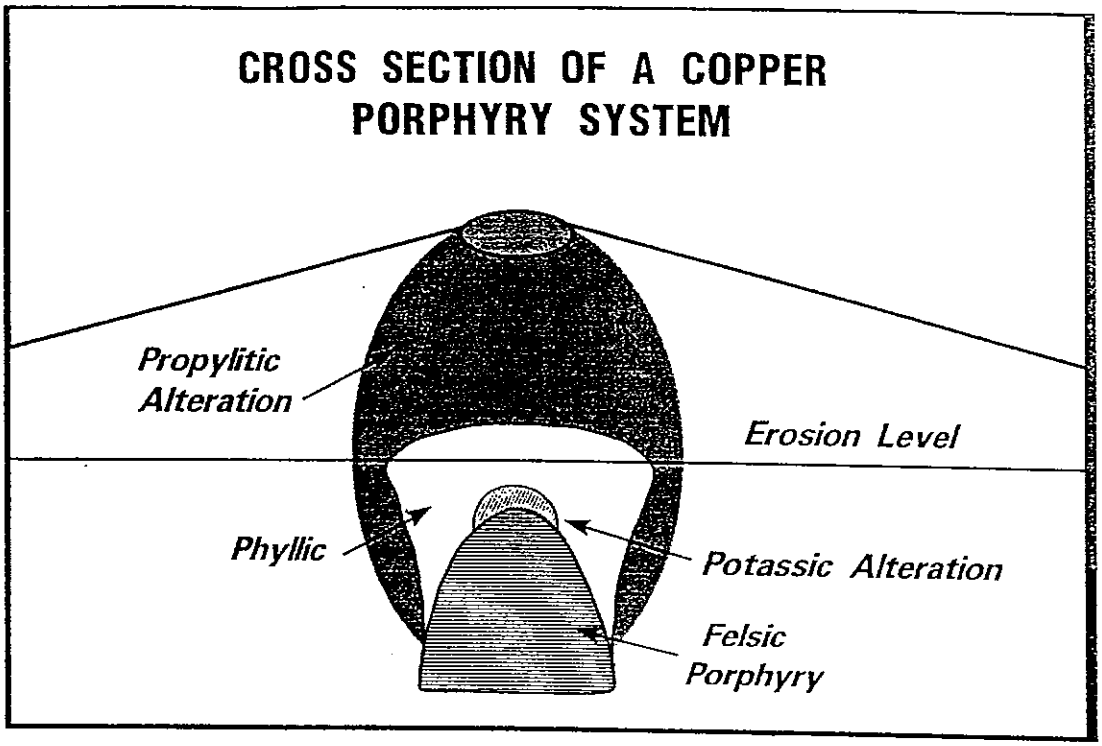
CROSS SECTION OF A COPPER PORPHYRY SYSTEM
A
Propylitic Alteration
Erosion Level
Phyllic
Potassic Alteration
Felsic Porphyry

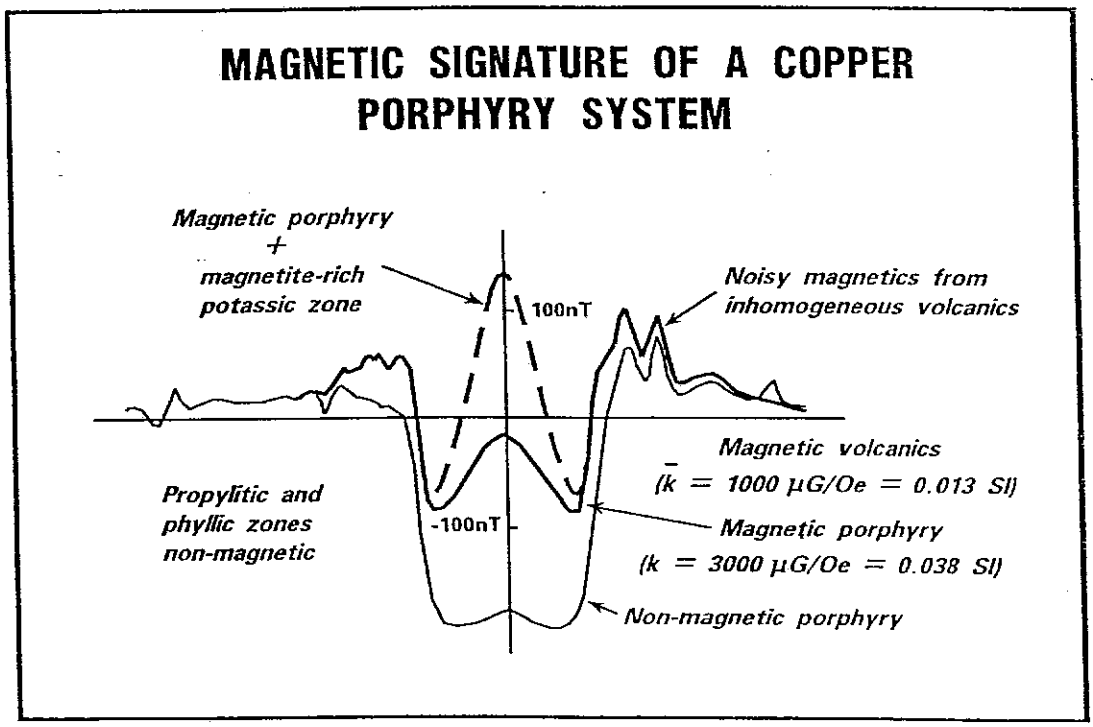
MAGNETIC SIGNATURE OF A COPPER PORPHYRY SYSTEM
B
Magnetic porphyry + magnetite-rich potassic zone
100nT
Noisy magnetics from inhomogeneous volcanics
Magnetic volcanics (k = 1000 μG/Oe = 0.013 SI)
Propylitic and phyllic zones non-magnetic
-100nT
Magnetic porphyry (k = 3000 μG/Oe = 0.038 SI)
Non-magnetic porphyry

FIG. 65

W-Sn-F skarn deposits and more oxidised W-Mo-Cu skarn deposits and Cu porphyries (Fig. 64).

In summary, the association between magmatic redox state, magnetic properties and type of associated mineralisation is well established and obviously has major implications for exploration. As an example Fig. 65(a) shows an idealised cross-section through a copper porphyry system, showing concentric potassic, phyllic and propyltic alteration zones. The magnetic signature over the such a system, emplaced within a sequence of magnetic volcanics, is shown in Fig. 65(b). The extensive propylitic and phyllic zones within the host volcanics are paramagnetic due to destruction of magnetite originally present within the volcanics. This produces a smooth, broad low zone in the magnetics, which contrasts with the busy magnetic pattern over the unaltered volcanics. The felsic porphyry is usually moderately to strongly ferromagnetic, producing a local magnetic high within the alteration signature. An Au-Cu porphyry is likely to be associated with a strongly magnetic potassic zone, as well as a magnetic pluton, and produces a sharp magnetic high as shown.

Magnetic Signatures of Layered Mafic/Ultramafic Complexes

Layered mafic/ultramafic complexes have been intensively studied because of the insights they offer into magmatic differentiation processes, and because of their great economic importance. The Bushveld Complex of South Africa, for example, contains the most significant collection of magmatic ore deposits in the world. The PGE mineralisation of the Merensky Reef and the Cr mineralisation of the main chromite band are particularly notable, but gold, copper, nickel, vanadium-titanium and tin deposits are all associated with particular zones within the Complex. Understanding of the magnetic petrology of such layered intrusions has substantial benefits in terms of applying magnetic surveys to mapping the "stratigraphy" of layered intrusions and locating favourable horizons for mineralisation.

Figure 66 shows the phase petrology of the Bushveld Complex, which serves as a type example of a layered mafic/ultramafic complex, characterised by zones with pronounced rhythmic layering and by cryptic layering from the base to the top. The lower levels of the complex contain no primary tianomagnetite. The early crystallising spinel phase in tholeiitic magmas is chromite, which is abundant in the lower levels and forms a number of cumulus bands. However, the olivine in the basal zone is serpentinised, with the formation of secondary magnetite. Above the olivine-out level, however, there is negligible magnetite, until the upper half of the main zone is reached, where intercumulus magnetite makes its first appearance and gradually increases in abundance towards the upper zone. The abrupt appearance of cumulus magnetite, marking the base of the upper zone, produces a strongly ferromagnetic assemblage of upper ferrogabbros/ferrodiorites.

Figure 67 shows the inferred magnetic stratigraphy in relation to the lithological and mineralogical variation and to the mineralisation. This magnetic stratigraphy was used to infer type magnetic signatures over a Bushveld-type intrusion. Figure 68(a) shows the case of an intrusion tilted on edge, and Fig. 68(b) considers the case of a shallowly dipping intrusion. The calculated anomalies are reduced to the pole, to eliminate the effects of geomagnetic field direction on the anomaly form. An example of a magnetic

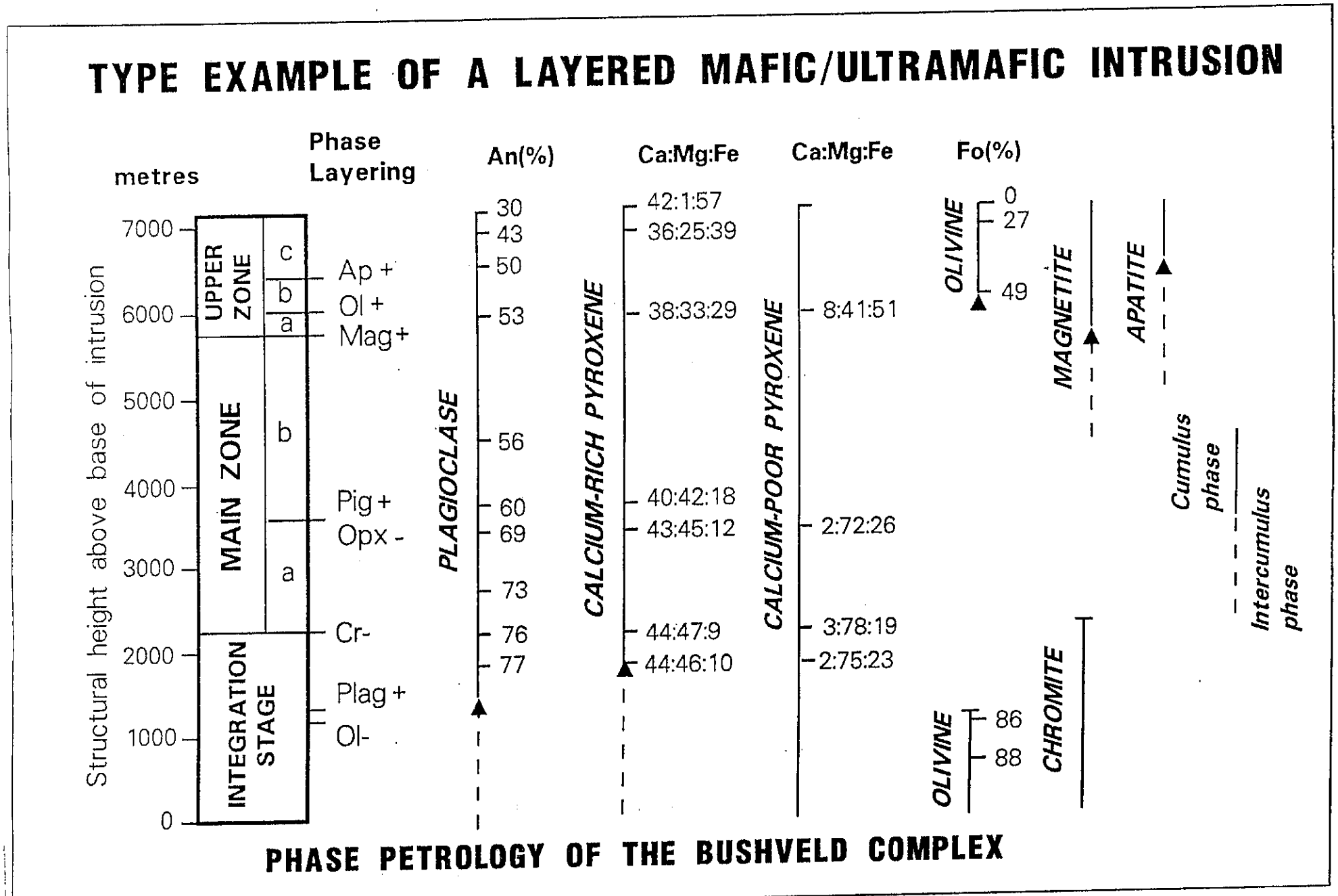
TYPE EXAMPLE OF A LAYERED MAFIC/ULTRAMAFIC INTRUSION
metres
Phase Layering
An(%)
Ca:Mg:Fe
Ca:Mg:Fe
Fo(%)
Structural height above base of intrusion
7000
6000
5000
4000
3000
2000
1000
0
UPPER ZONE
MAIN ZONE
INTEGRATION STAGE
c
b
a
b
a
Ap +
Ol +
Mag+
Pig +
Opx -
Cr-
Plag +
Ol-
PLAGIOCLASE
30
43
50
53
56
60
69
73
76
77
CALCIUM-RICH PYROXENE
42:1:57
36:25:39
38:33:29
40:42:18
43:45:12
44:47:9
44:46:10
CALCIUM-POOR PYROXENE
8:41:51
2:72:26
3:78:19
2:75:23
OLIVINE
0
27
49
OLIVINE
86
88
MAGNETITE
CHROMITE
APATITE
Cumulus phase
Intercumulus phase
PHASE PETROLOGY OF THE BUSHVELD COMPLEX

FIG. 66

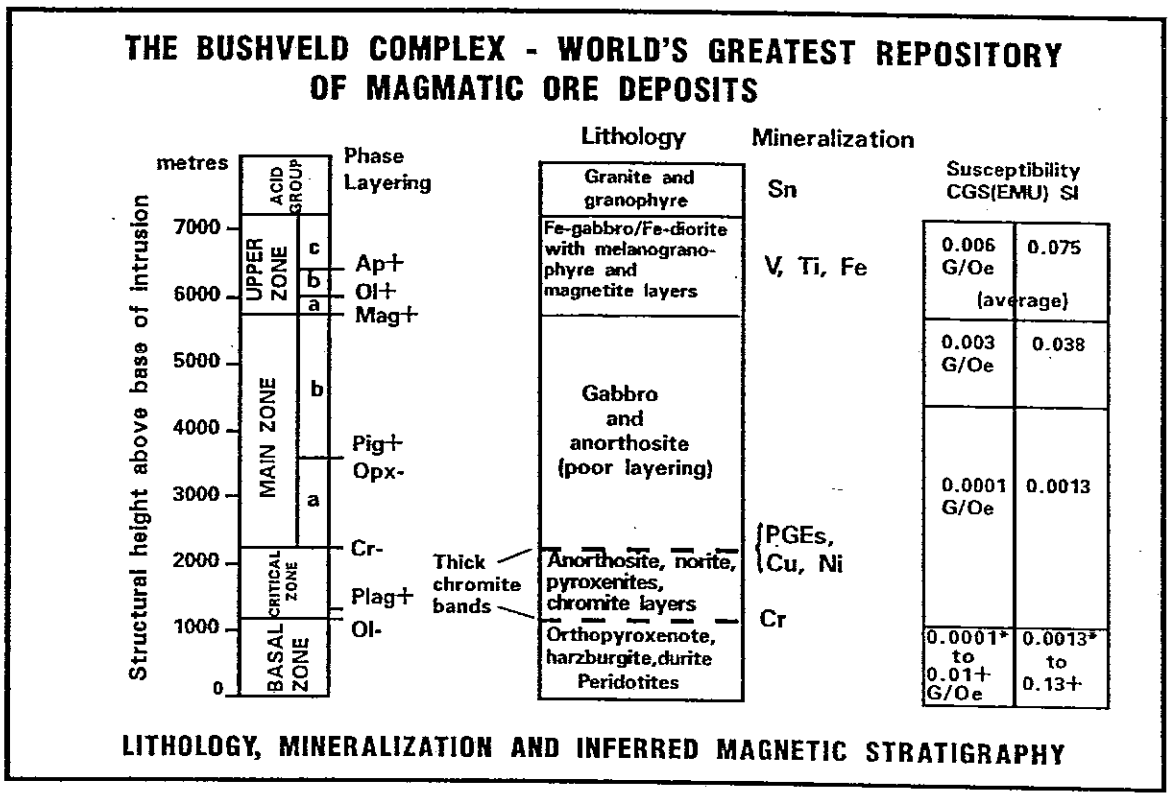
THE BUSHVELD COMPLEX - WORLD'S GREATEST REPOSITORY OF MAGMATIC ORE DEPOSITS
Structural height above base of intrusion
metres
7000
6000
5000
4000
3000
2000
1000
0
ACID GROUP
UPPER ZONE
MAIN ZONE
CRITICAL ZONE
BASAL ZONE
c
b
a
b
a
Phase Layering
Ap+
Ol+
Mag+
Pig+
Opx-
Cr-
Plag+
Ol-
Lithology
Mineralization
Granite and granophyre
Sn
Fe-gabbro/Fe-diorite with melanogranophyre and magnetite layers
V, Ti, Fe
Gabbro and anorthosite (poor layering)
PGEs, Cu, Ni
Thick chromite bands
Anorthosite, norite, pyroxenites, chromite layers
Cr
Orthopyroxenote, harzburgite, durite Peridotites
Susceptibility CGS(EMU) SI
0.006 G/Oe
0.075
(average)
0.003 G/Oe
0.038
0.0001 G/Oe
0.0013
0.0001* to 0.01+ G/Oe
0.0013* to 0.13+
LITHOLOGY, MINERALIZATION AND INFERRED MAGNETIC STRATIGRAPHY

FIG. 67

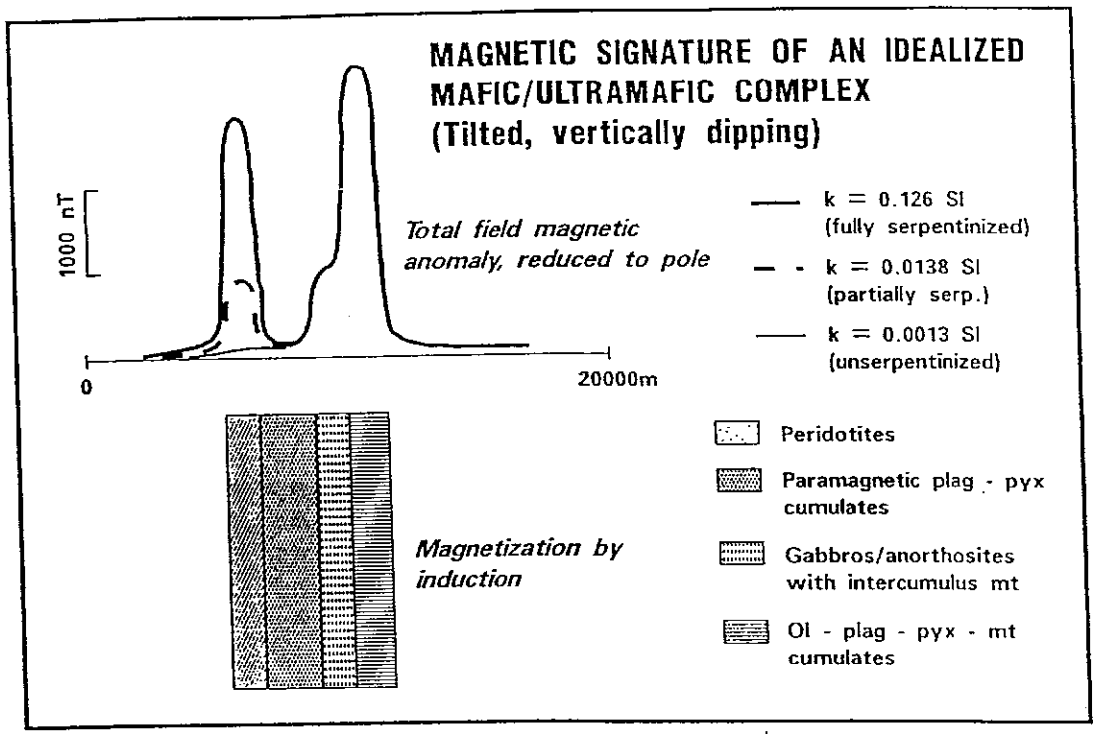
MAGNETIC SIGNATURE OF AN IDEALIZED
MAFIC/ULTRAMAFIC COMPLEX
(Tilted, vertically dipping)
A
1000 nT
Total field magnetic
anomaly, reduced to pole
0
20000m
k = 0.126 SI
(fully serpentinized)
k = 0.0138 SI
(partially serp.)
k = 0.0013 SI
(unserpentinized)
Magnetization by
induction
Peridotites
Paramagnetic plag - pyx
cumulates
Gabbros/anorthosites
with intercumulus mt
Ol - plag - pyx - mt
cumulates

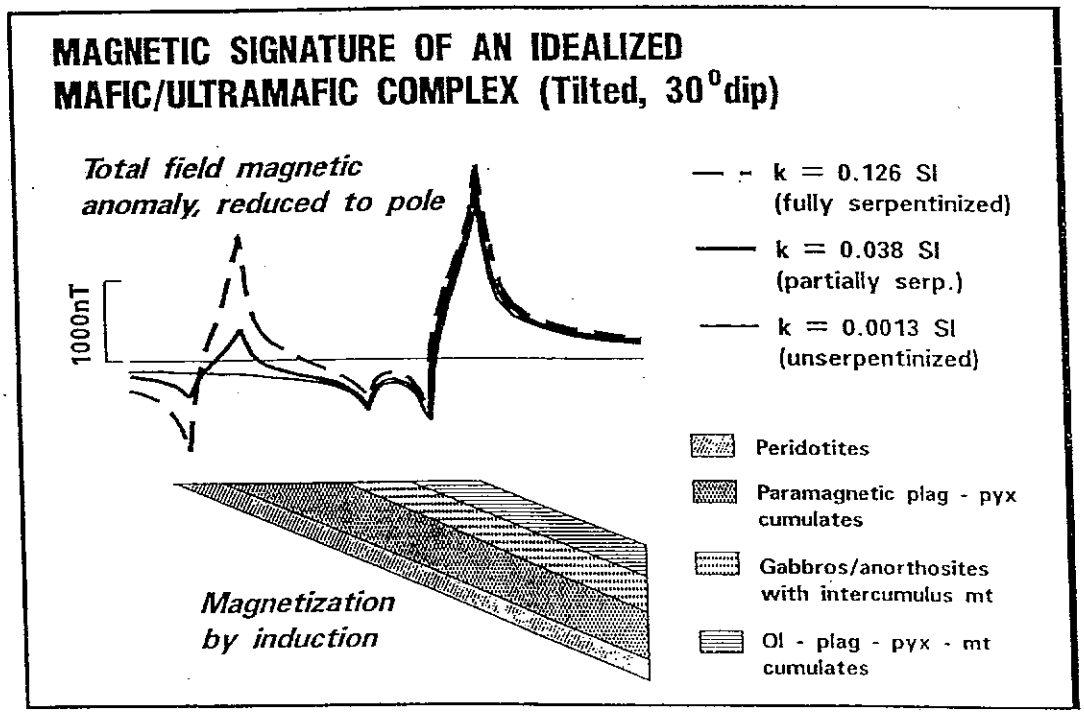
MAGNETIC SIGNATURE OF AN IDEALIZED
MAFIC/ULTRAMAFIC COMPLEX (Tilted, 30°dip)
B
Total field magnetic
anomaly, reduced to pole
1000nT
k = 0.126 SI
(fully serpentinized)
k = 0.038 SI
(partially serp.)
k = 0.0013 SI
(unserpentinized)
Peridotites
Paramagnetic plag - pyx
cumulates
Gabbros/anorthosites
with intercumulus mt
Ol - plag - pyx - mt
cumulates
Magnetization
by induction

FIG. 68

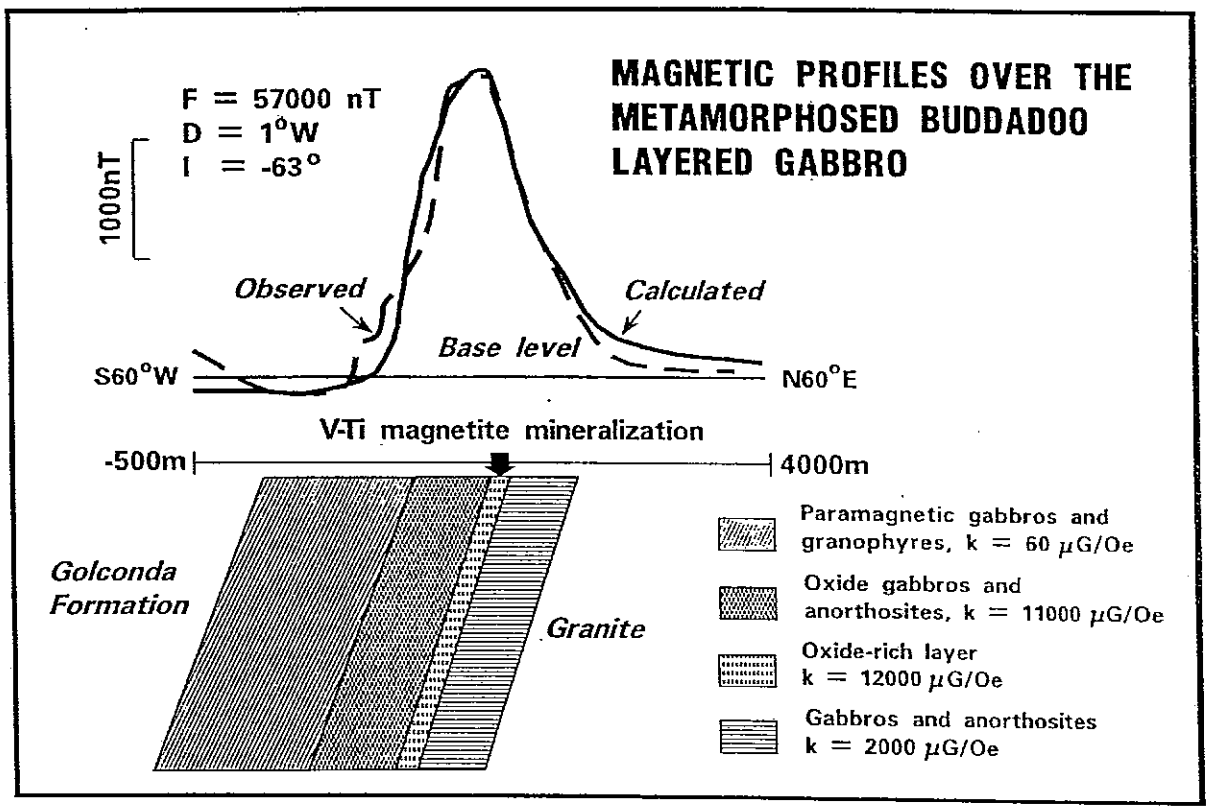
MAGNETIC PROFILES OVER THE METAMORPHOSED BUDDADOO LAYERED GABBRO
F = 57000 nT
D = 1°W
I = -63°
1000nT
Observed
Calculated
Base level
S60°W
N60°E
V-Ti magnetite mineralization
-500m
4000m
Golconda Formation
Granite
Paramagnetic gabbros and granophyres, k = 60 μG/Oe
Oxide gabbros and anorthosites, k = 11000 μG/Oe
Oxide-rich layer k = 12000 μG/Oe
Gabbros and anorthosites k = 2000 μG/Oe

FIG. 69

profile over a layered complex that was sampled during the course of Project P96C, the Buddadoo Metagabbro, is shown in Fig. 69. This is a recrystallised layered complex, within the Gullewa Greenstone Belt of the southern Murchison Province. The lower layers of the complex have been removed by granite intrusions, but the upper layers are preserved and are associated with a large magnetic high, with an amplitude of ~2700 nT. The anomaly occurs over only part of the upper zone, however, including a band of vanadiferous titanomagnetite (now martite at the surface) that is several metres thick. The anomaly is far too large and broad to be caused by the cumulus magnetite band alone, and is clearly related to a thick stratigraphic interval of elevated magnetite content.

To the west, however, the stratigraphically higher gabbros and granophyres are paramagnetic and the anomaly is very subdued. Although magnetite was almost certainly originally present in these levels of the intrusion, it appears to have been replaced by sphene-ilmenite-rutile during metamorphism. This is typical of greenschist and amphibolite grade metamorphism of gabbroic rocks with normal magnetite contents. The preservation of substantial magnetite content in the stratigaphic interval around the main magnetite layer suggests that the elevated magnetite content of this zone led to self-buffering. The suggested analogue is banded iron formation, which resists alteration of its finely interlayered oxide bands during metamorphism.

Study of the Ravenswood Batholith, North Queensland - Summary

The Charters Towers region lies in the Lolworth-Ravenswood Block (Fig. 70). The block is bound on the north by the Broken River Province, with pre-Cambrian Inliers to the northwest (Georgetown) and south (Anakie). The Drummond and Bowen Basins define the southern boundary. The block lies within the Tasman Fold Belt. This study deals with the Ravenswood Igneous Complex, which is in the east of the block.

The geology of the Charters Towers area consists of pre-batholithic basement rocks which have been intruded by Mid-Ordovician to Early Devonian I-Type granitoid plutons of the composite Ravenswood Batholith. Final igneous activity occurred in the Late Carboniferous - Early Permian with extrusion of rhyolitic lavas and pyroclastics associated with high level intrusive complexes (Fig. 71).

The pre-batholithic rocks are divided into two groups, (1), the Seventy Mile Range Group which consists of the Puddler Creek Formation, Mt Windsor Volcanics and the Trooper Creek Formation, (2), the Charters Towers Group which consists of the high grade Charters Towers Metamorphics and undifferentiated basement complex which are intruded by mafic bodies and granitoid intrusives. There are three groups of mafic intrusives: (1) small plutons (e.g. Stannett Creek Gabbro), (2) stratabound bodies (e.g. Buckland Hill Diorite) and (3) crosscutting diorite dykes. As well, several small pre-batholithic plutons (e.g. Mount Leyshon Granite, Fig. 71) occur. The pre-batholithic rocks are pre-Middle Ordovician in age.

The Mid-Ordovician batholithic granitoids are generally monzogranite to granodiorite, biotite dominant in the west and hornblende dominant in the Ravenswood area. The Siluro-Devonian granitoids are usually hornblende-bearing tonalite orgranodiorite. Carboniferous and Permian age igneous rocks (e.g. Tuckers Range Igneous Complex) are

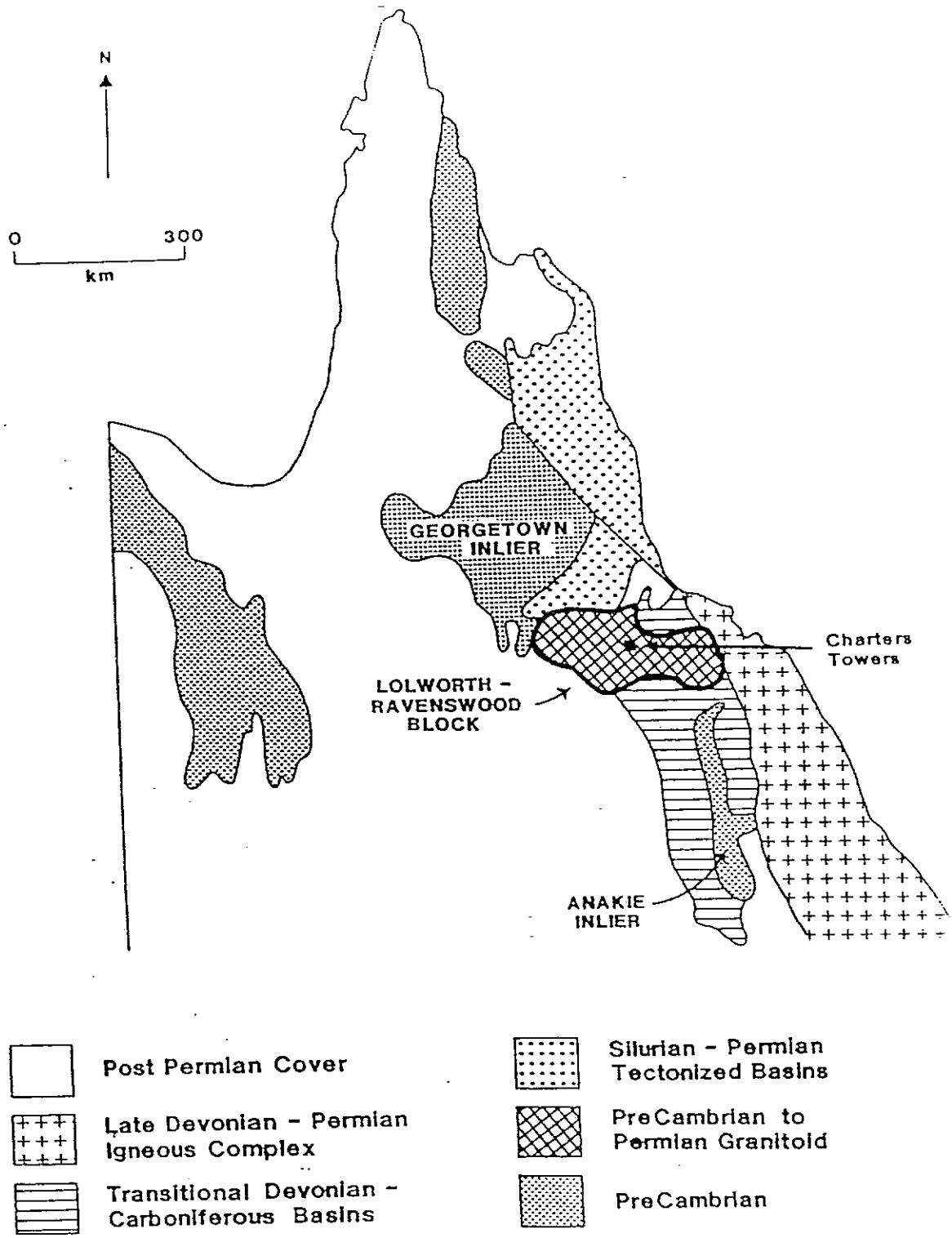

FIG. 70 Main structural divisions of North Queensland.

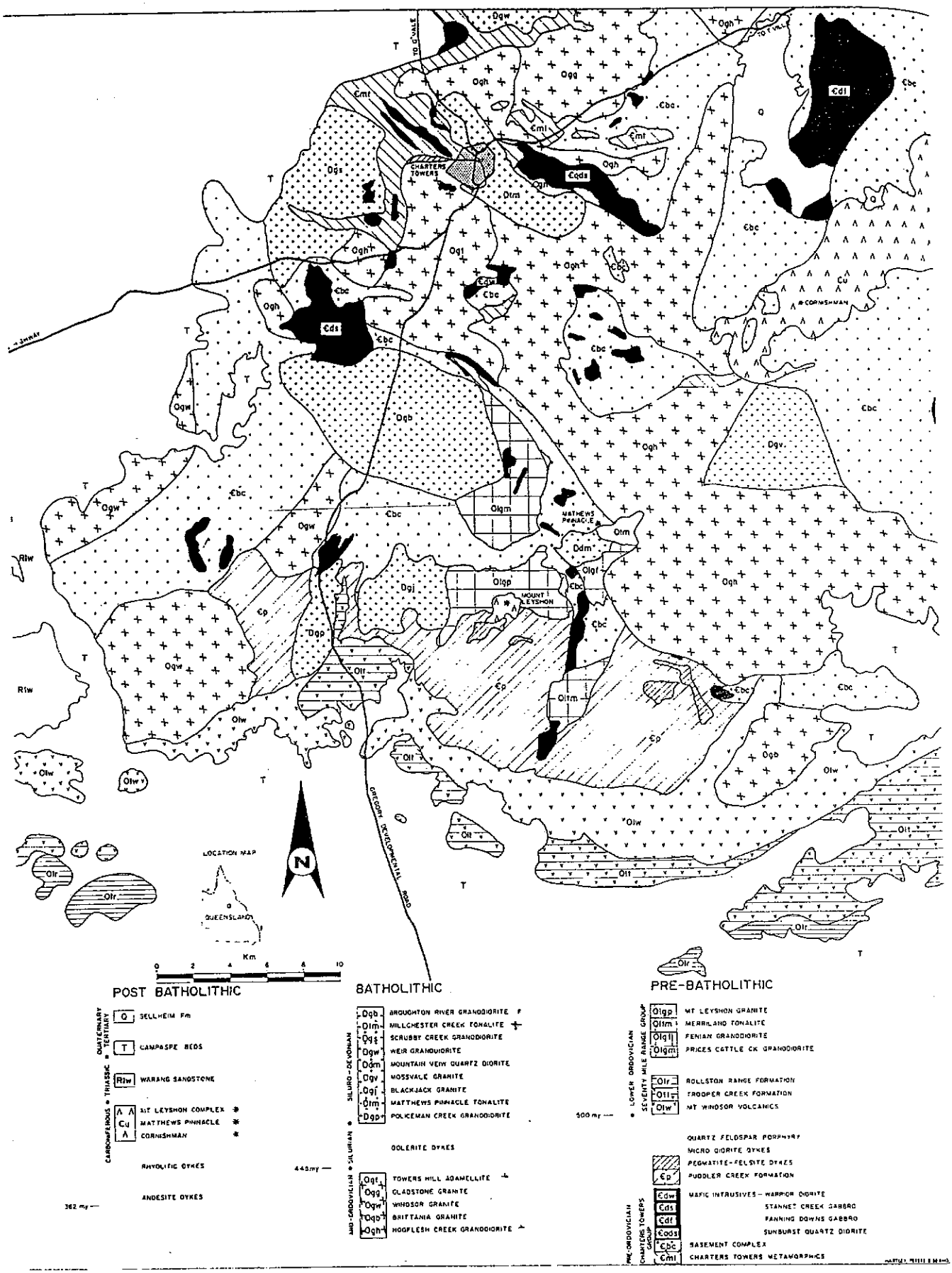

FIG. 71 Geological Elements in the Charters Towers Area

concentrated in the eastern and northern parts of the Lolworth-Ravenswood Block. All the batholithic plutons are classified as I-type.

The aeromagnetic signature of the batholith is one of a busy magnetic high with its southern boundary well delineated. Figure 72 shows reprocessed BMR aeromagnetics for the Charters Towers 1:250,000 Sheet, which shows the batholith in the north and the Drummond Basin in the south, with the Seventy Mile Group wrapping around the southern and western margins of the batholith. The magnetic intensity is variable across the batholith with the plutons around Charters Towers to Mount Leyshon having a lower intensity than the plutons to the east around the Ravenswood area. The Charters Towers metamorphic Group has a low magnetic signature, although the pre-batholith mafic plutons generally have an associated positive anomaly. The magnetics delineates specific plutons (e.g. Broughton River Granodiorite) and the zones of basement complex. The anomalies associated with the Permian Tuckers Range Complex and Boori Igneous Complex are also very distinct.

The main conclusions from the study were:

(i) Susceptibilities of the Batholith plutons ranges from weak (~100 μG/Oe [0.0012 SI]) to strong (> 4000 μG/Oe [0.05 SI]). However, most susceptibilities are greater than 1000 μG/Oe [0.0126 SI] (Fig. 73). Thus these plutons are magnetite-series, most belonging to the magnetite-bearing ferrofacies.

(ii) The mean susceptibility of the Ordovician plutons increases across the Batholith from west to east (Fig. 74). Plutons in the Charters Towers area (i.e. Hogsflesh Creek Granodiorite, Towers Hill Granodiorite) have susceptibilities less than 2000 μG/Oe [0.025 SI] while those to the east of the Tuckers Igneous Complex can have susceptibilities greater than 3000 μG/Oe [0.038SI]. The reduction in susceptibility westwards is reflected in the magnetic base level which decreases in the west. This regional change in magnetisation is interpreted to reflect regional compositional variation in the source region, similar to that observed in the Sierra Nevada and Peninsular Ranges Batholiths of the western USA.

(iii) The susceptibility variation correlates with change in granodiorite character, where granodiorites in the Ravenswood area are hornblende dominant, while those in the Charters Towers region are biotite dominant.

(iv) The susceptibility of the Ordovician plutons is related to the petrology of the plutons. In general, tonalites have higher susceptibilities than granodiorites, which in turn have markedly higher susceptibilities than granites (Fig. 73).

(v) The Devonian plutons have moderate to high susceptibilities in the range 1000 μG/Oe [0.0125 SI] to 3000 μG/Oe [0.038 SI]. This range of susceptibilities is recorded in both granodiorites and tonalites.

(vi) The small mafic plutons of the Charters Towers Group have high susceptibilities (e.g. Warrior Diorite (~2000 μG/Oe [0.025SI])). This agrees with the aeromagnetic response of these mafic bodies which is distinct and positive in character.

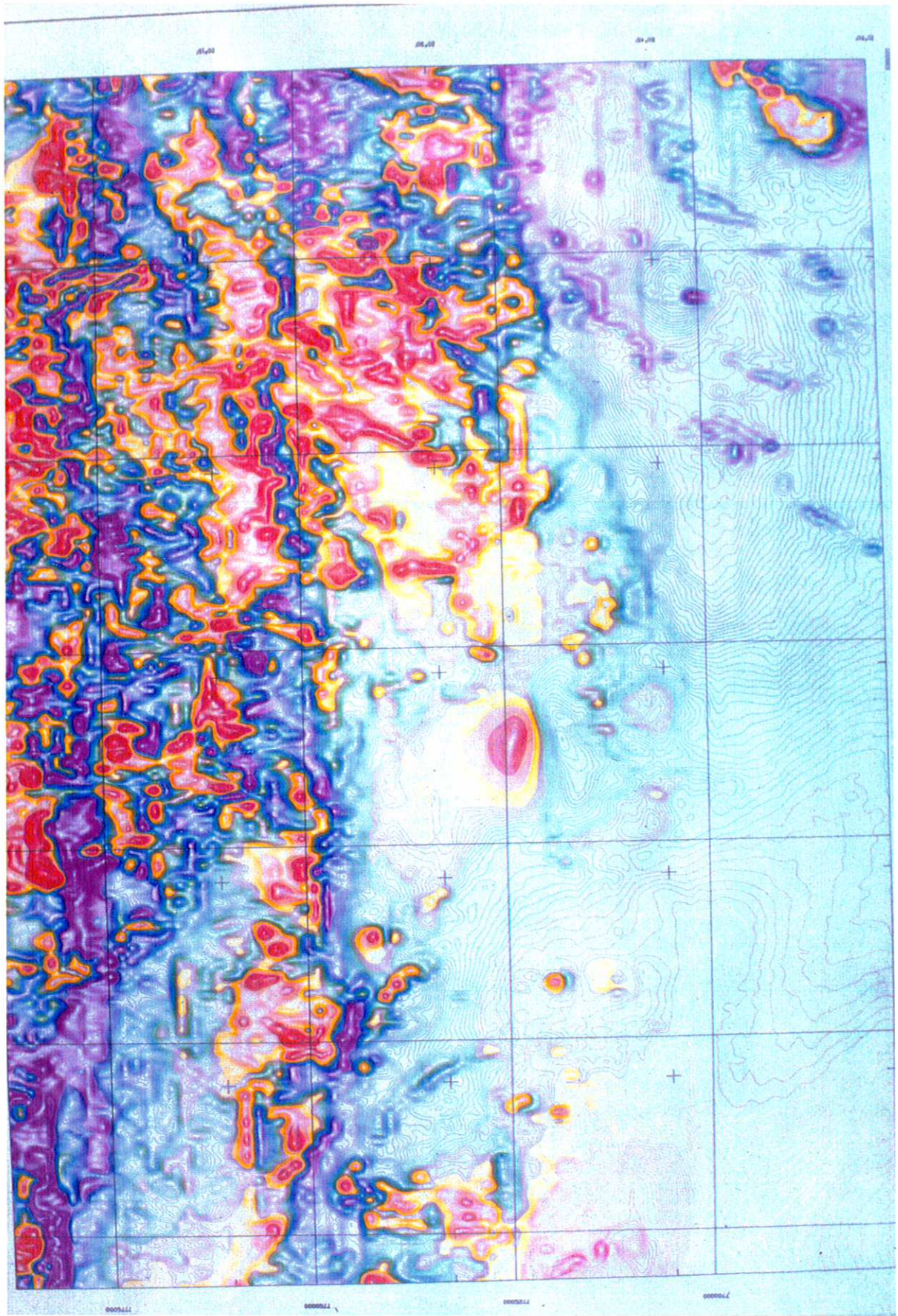

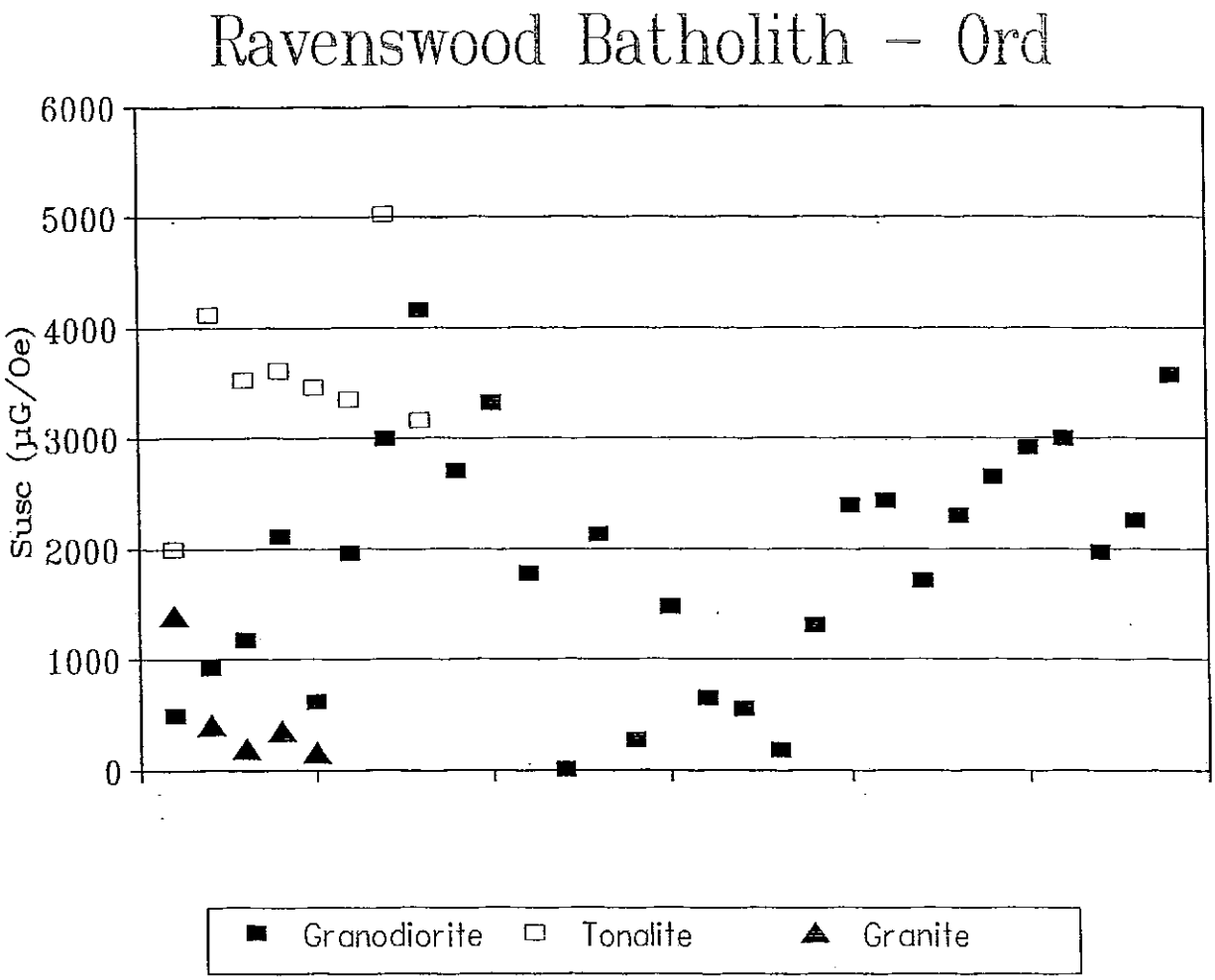
Ravenswood Batholith – Ord
6000
5000
4000
3000
2000
1000
0
Susc (µG/Oe)
Granodiorite
Tonalite
Granite

FIG. 73

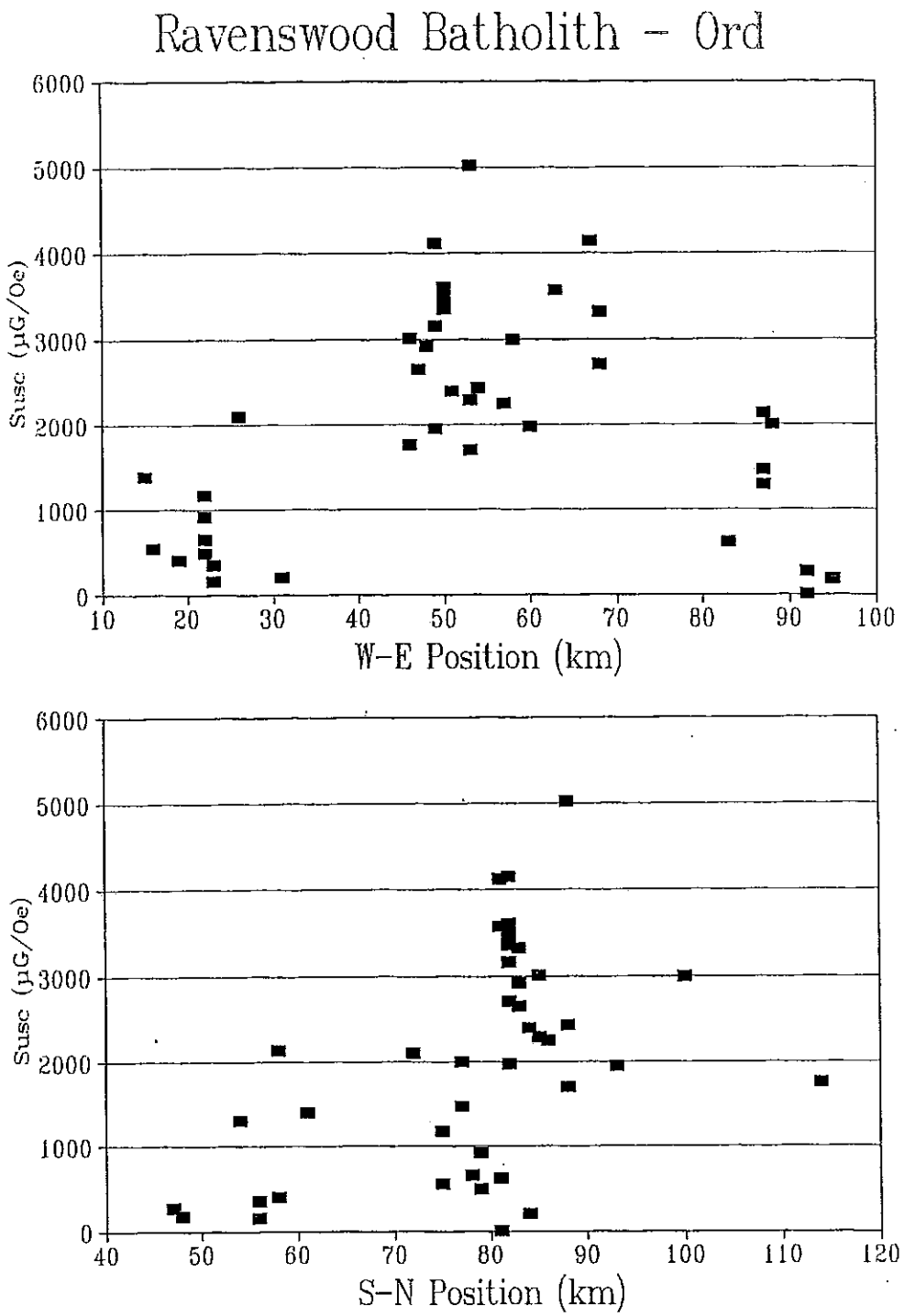
Ravenswood Batholith - Ord
Susc (μG/Oe)
6000
5000
4000
3000
2000
1000
0
10
20
30
40
50
60
70
80
90
100
W-E Position (km)
Susc (μG/Oe)
6000
5000
4000
3000
2000
1000
0
40
50
60
70
80
90
100
110
120
S-N Position (km)

FIG. 74

(vii) Rocks of the Charters Towers Metamorphics generally have low susceptibilities with the exception of some stratabound mafics. This is reflected in the aeromagnetics.

(viii) Rocks of the Permian Tuckers Range Igneous Complex have high (~4000 μG/Oe [0.05 SI] susceptibilities. This is reflected in the aeromagnetics which shows a distinct magnetic high. Where a strong magnetic low is observed over part of the complex, this results from mafic plutons retaining a strong remanence (Q >1.0) which is steep and down and thus results in a reversed resultant magnetization. The stable remanence carried by all phases in the complex is a primary Permian thermoremanence of reversed polarity.

(ix) Ordovician and Devonian plutons in the Charters Towers area show no consistent remanence. Thus the effective Q value is low and magnetization by induction can safely be assumed for these relatively felsic intrusives.

(x) Mafic rocks of the Charters Towers Group have a remanence which is west and shallow up in direction (Fig. 75(a)). Siluro-Ordovician granodiorites and tonalites in the Tuckers Range area also show the same direction after thermal cleaning (Fig. 75(b)). The thermal demagnetisation initially removes a steep down Permian overprint, which is present in varying degrees in these rocks, depending on proximity to the Tuckers Range Complex. This overprint direction is also shown in Fig. 75(b). This indicates that the age of the stable remanence in the mafic rocks of the Charters Towers Group is Siluro-Ordovician. The palaeomagnetic poles obtained from the Charters Towers Group and Siluro-Ordovician plutons are shown on a plot of the Australian APWP (Fig. 76). The APWP from the Cambrian to Early Devonian is not well defined but the Ravenswood Block poles agree with data from central Australia, suggesting that the block was concordant with Australia during the Siluro-Ordovician, in spite of its cross-cutting trend within the meridional Tasman Fold Belt.

(xi) The magnetization of the rocks of the Tuckers Igneous Complex is steep and down in direction (Fig. 75(b)), consistent with the overprint direction found in the contact aureole. This direction is consistent with the Early-Permian age of the complex. The pole obtained from the Tuckers Range Complex (TR) is indistinguishable from those obtained from the Mount Leyshon Complex (MTL) and from the volcanics of the Conway-Bimurra area (DCV) (Fig. 76).

(xii) In the north of the Batholith the Alex Hill Shear Zone cuts east-west across the Batholith. This is clearly reflected in the aeromagnetics with a prominent linear zone of lower response observed. The susceptibilities of the granites in this area are distinctly lower than in other parts of the Batholith (~400 μG/Oe [0.005 SI], reflecting destruction of magnetite due to increased permeability within the shear zone.

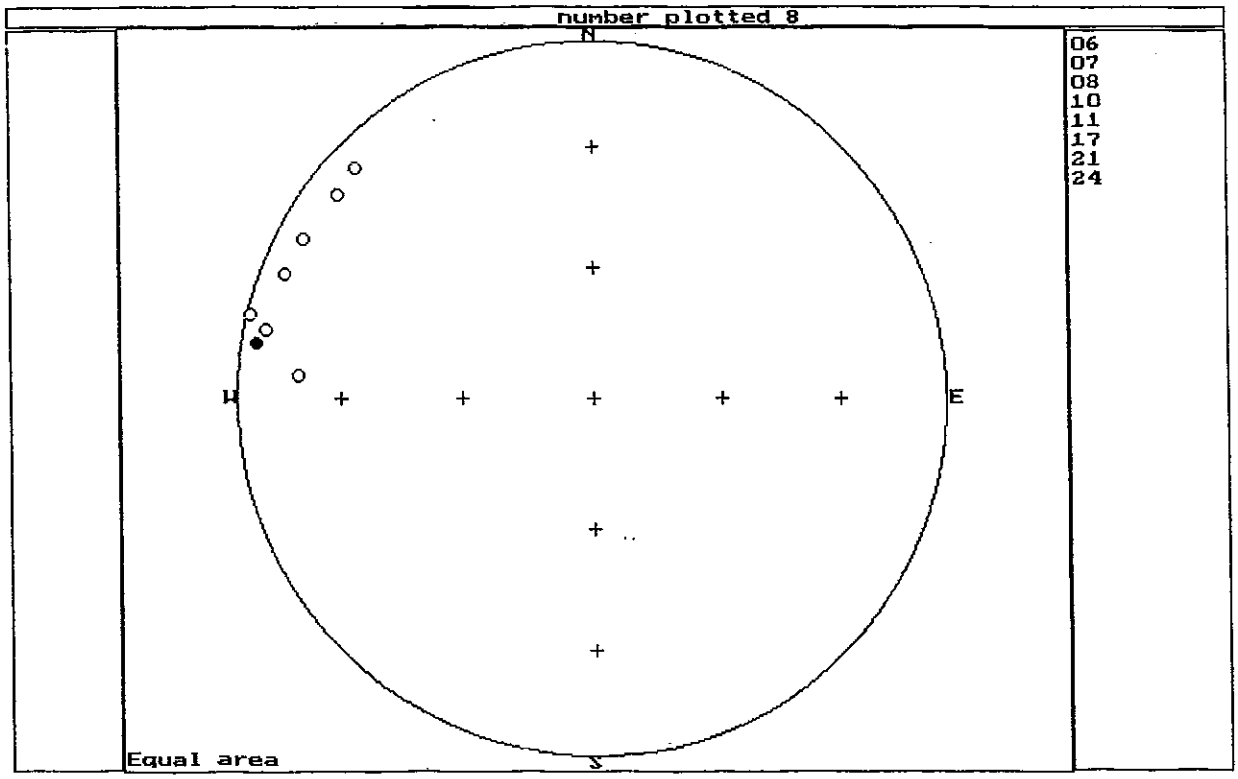
number plotted 8
N
W
E
S
Equal area
06
07
08
10
11
17
21
24

A

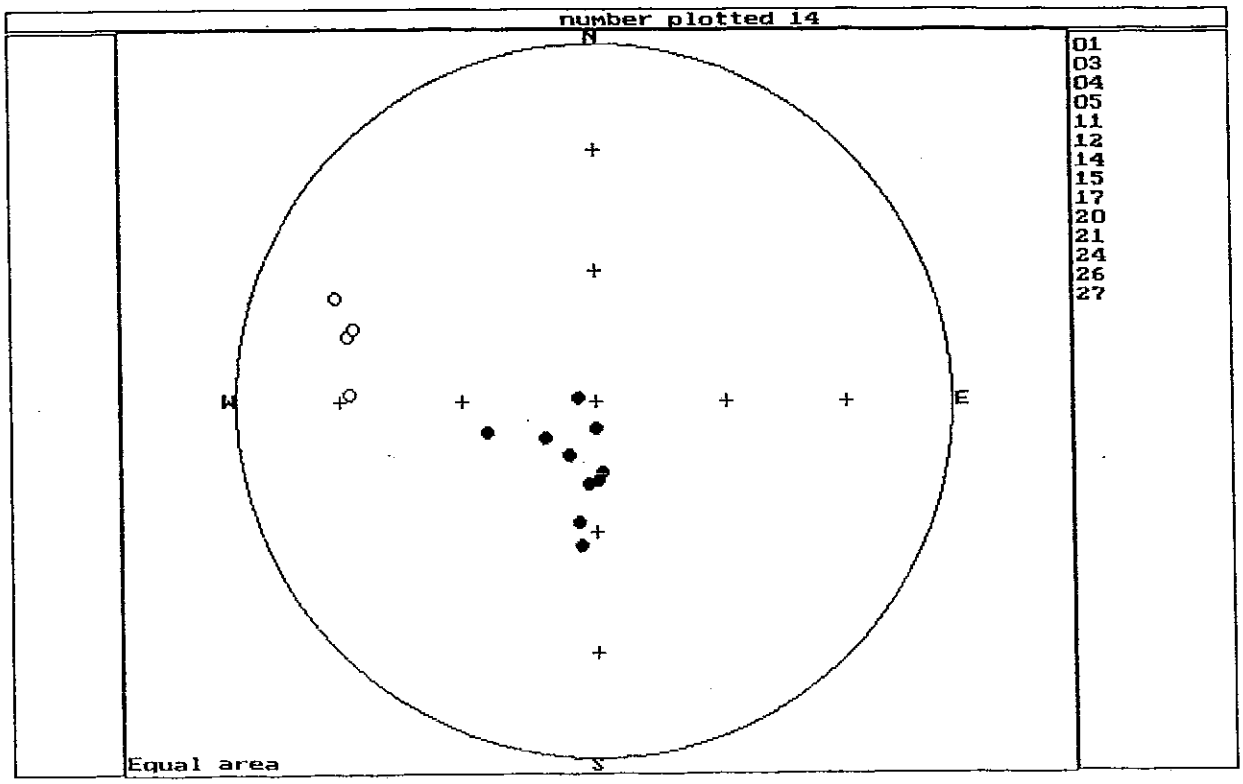
number plotted 14
N
W
E
S
Equal area
01
03
04
05
11
12
14
15
17
20
21
24
26
27

B

FIG. 75

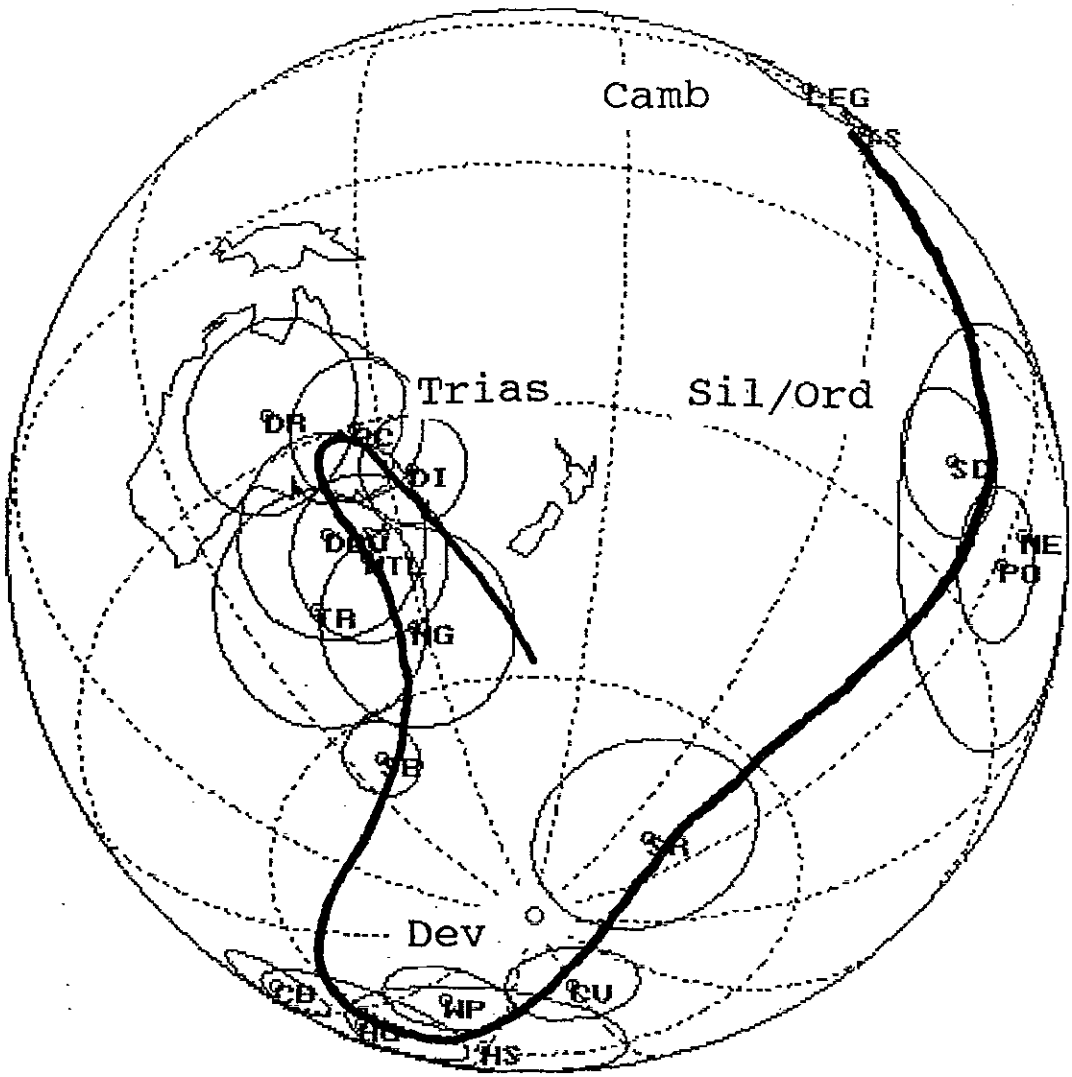

FIG. 76

Study of the Mount Leyshon Complex - Summary

The regional geology of the Mount Leyshon area has been described above. Figure 77 shows the local geology. The Mount Leyshon Complex is a large breccia pipe formed by shallow level emplacement of felsic porphyries. The age is ~280 Ma. Gold mineralisation is hosted by breccias, porphyry plugs and basement rocks within the complex. The magnetic expression of the complex is weak, but a large, intense magnetic low (~ 4 km^2, up to -2000 nT), flanked by a minor high to the south, occurs adjacent to the complex (Fig. 78). The form of the anomaly implies a source with strong reversed remanence, suggesting a Permo-Carboniferous intrusive with primary thermoremanence as the cause of the anomaly. This study was directed at establishing the cause of the Mount Leyshon anomaly, and the relationship between the source of the anomaly and the gold mineralisation. Extensive sampling of a wide range of lithologies from within and around the complex was carried out for this purpose.

The main conclusions of the study were:

(i) The Mount Leyshon anomaly is not an alteration low, reflecting local destruction of magnetic minerals within highly magnetic country rocks, but must arise from a source with reversed remanence.

(ii) Acid-sulphate type hydrothermal alteration within and around the complex has resulted in extensive magnetite destruction in originally magnetic country rocks, such as dolerites, and complete thermochemical overprinting of remanence carried by country rocks. Alteration initially reduces the magnetite grain size, producing a stable thermochemical remanence. Continuing alteration replaces the magnetite with sphene + rutile, and finally rutile.

(iii) Magnetite is the dominant magnetic mineral in all the lithologies sampled, maghemite and hematite being of secondary importance. k-T curves for the dolerites are variable and this reflects the degree of alteration which may be of recent origin or related to Permian mineralization. End-member magnetite is observed in the trachytic porphyries and some of the trachy-andesite dykes.

(iv) Magnetic susceptibility of the majority of the diatreme lithologies is relatively low (< 250 μG/Oe [0.006 SI]) with the exception of some dolerites, skarns and a trachyandesite dyke.

(v) Stable remanence is shown only by those samples which have had the primary magnetite partially altered to sphene during a Permian alteration event. Some dolerites and skarns show high (~5) Q values. Diatreme complex units usually have a low (< 1.0) Q value. The dominant remanence carrier is magnetite and, less commonly, hematite. The stable remanent magnetization of all rock types sampled in and around the diatreme is southerly and steep down in direction. The remanence of the Cambrian Puddler Creek Formation has been overprinted and also shows a steep down direction. This direction and consequent palaeomagnetic southpole are consistent with the mid-Permian (~280 Ma) age of the diatreme and associated mineralisation.

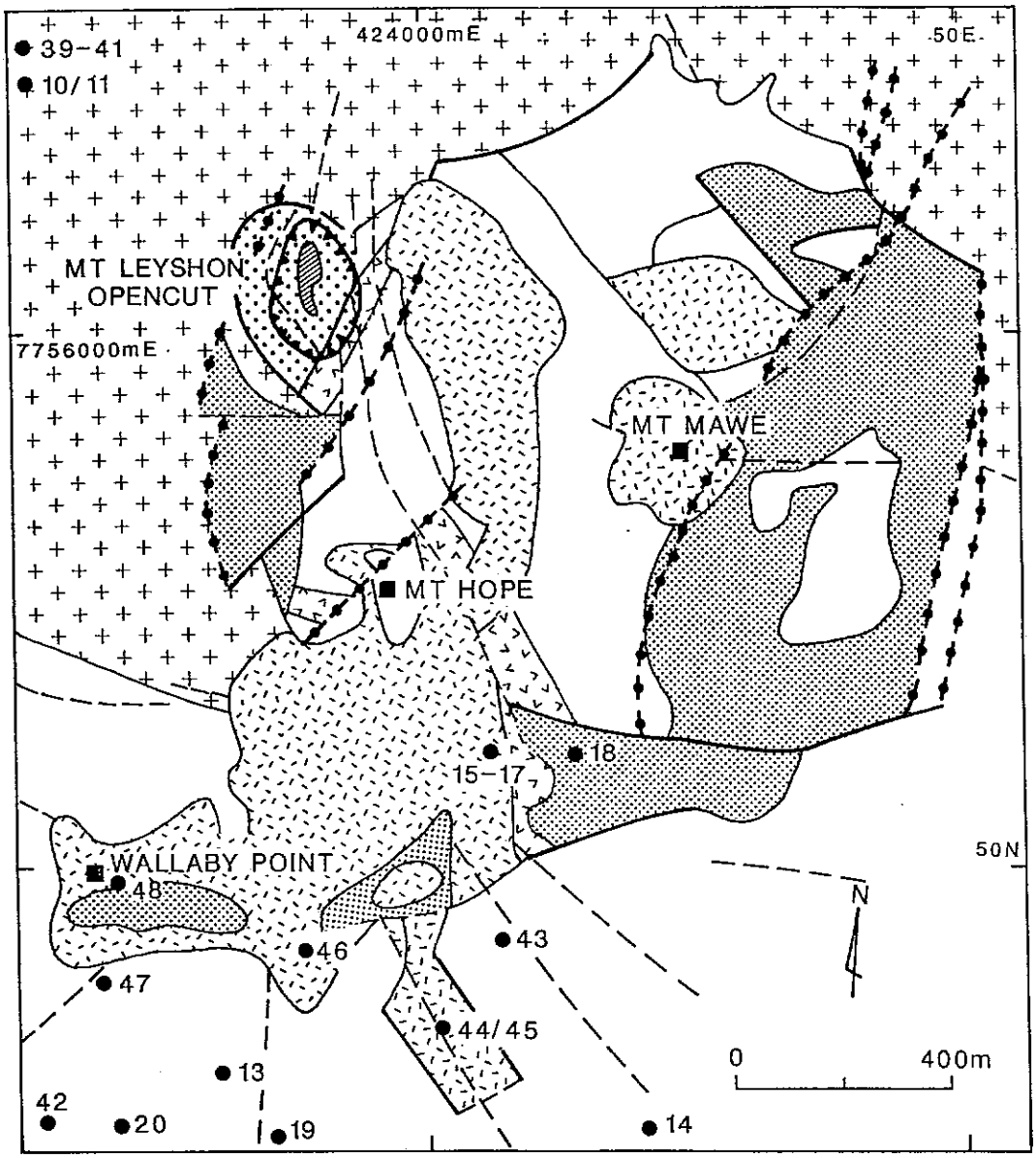

P Mt Leyshon Complex

- Milled breccia
- Mt Leyshon breccia
- Main Pipe breccia
- Lapilli tuff
- Dykes: early, late
- Porphyry plugs

O–D Ravenswood batholith

- Granite

Є Puddler Ck Fm

- Metasediments
- Faults

FIG. 77

AUSTIREX DATA PROCESSING FACILITIES

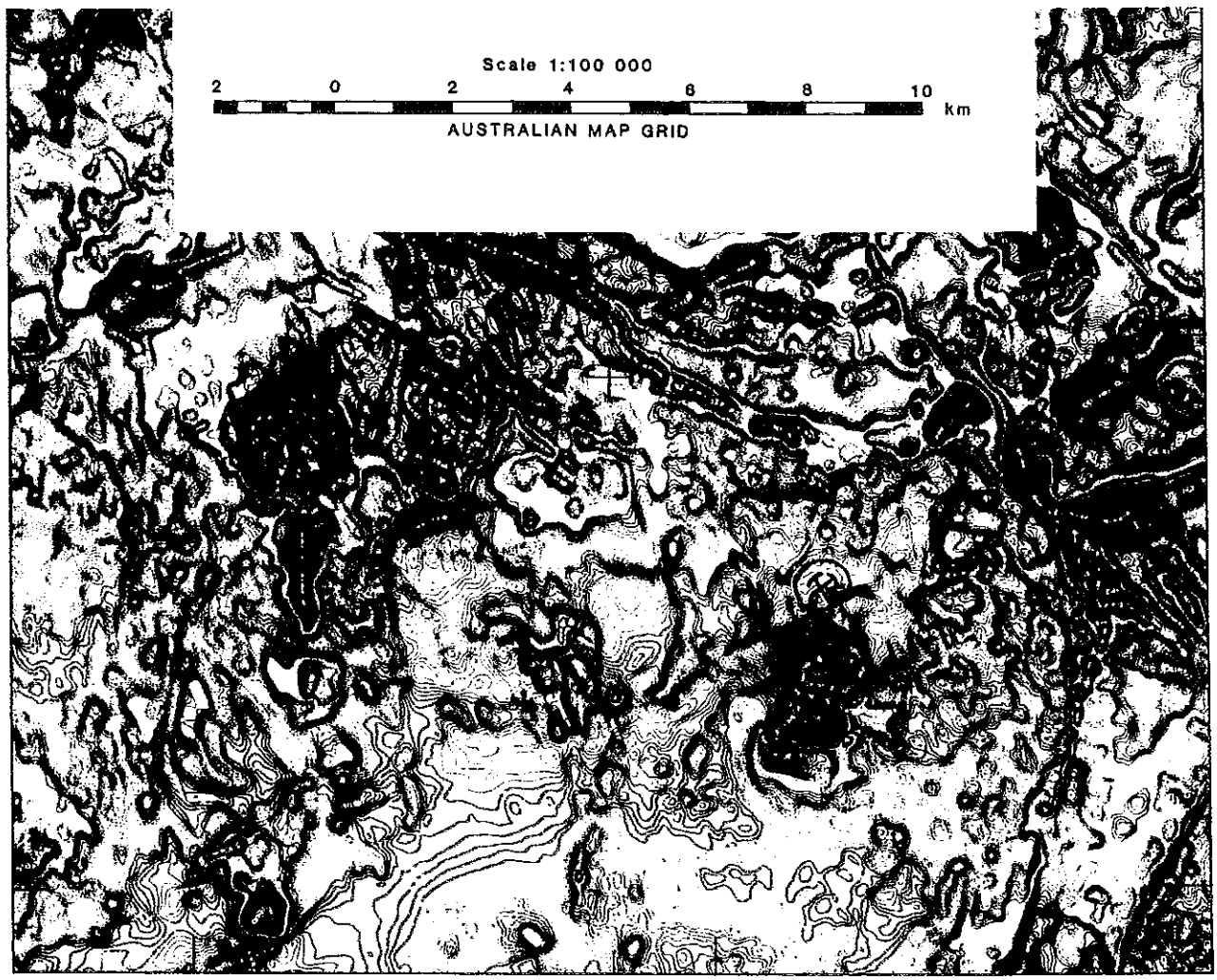

AEROMAGNETIC CONTOURS - LINE SPACING 200m

FIG. 78

(vi) Modelling of the distinctive aeromagnetic anomaly immediately south of the Mount Leyshon mine using the measured remanence direction indicates that the body causing the anomaly consists of a large intrusion at depth from which apophyses rise towards the surface (Fig. 79). The depth to the top of the large body is ~550 m and the body has a diameter of ~1700 m. The apophyses rise to ~80 m below the current surface and could be modelled as small separate cylinders (~200 m diam.) or as larger E-W elongated bodies. Remanence of the larger body is modelled as ~5000 μG while the remanences of the apophyses can be higher with values up to 14,000 μG.

(vii) The aeromagnetic modelling and the pervasive remagnetisation throughout the area suggest that an intrusive, probably gabbroic, plug is present at depth. The plug, its apophyses and the Mount Leyshon complex formed in the mid-Permian. The evidence suggests a genetic relationship between the source of the Mount Leyshon anomaly and the mineralised Mount Leyshon Complex. The distinctive magnetic signature of mid-Permian intrusions can indicate the presence of similar sub-surface bodies that may be associated with Mount Leyshon-type mineralisation.

(viii) The Fenian Gabbro, which lies 3-4 kilometres from the Mount Leyshon Complex, is suggested as an analogue of the unexposed source of the Mount Leyshon anomaly. This intrusion is characterised by a strong, stable rversed remanence and an associated magnetic low, and is close in age to the Mount Leyshon Complex, based on the similarity in palaeomagnetic directions.

Effects of Hydrothermal Alteration on Magnetic Properties

Hydrothermal alteration of rocks has profound effects on their magnetic properties through destruction of magnetic minerals, or changes in their grain size, composition and microstructure, or sometimes through creation of new magnetic minerals. Some generalisations about these processes are given below:

(i) Zeolite-grade hydrothermal alteration of mafic to silicic igneous rocks tends to decrease the susceptibility of these rocks according to the degree of development of zeolites. Zeolite-rich rocks are generally paramagnetic, even when derived from strongly magnetic protoliths.

(ii) Regional hydrothermal alteration of volcanic piles produces progressive demagnetisation from zeolite grade to green schist grade. For example, primary titanomagnetite and ilmenomagnetite in basalts progressively develops ferrirutile granules at~150°C, with sphene replacing ilmenite lamellae by ~250°C, and polycrystalline titanohematite replacing titanomagnetite above 300°C.

(iii) Both major types of alteration associated with epithermal systems, acid-sulphate and adularia-sericite alteration, demagnetise volcanic rocks through replacement of magnetite by paramagnetic phases.

(iv) Propylitic and phyllic alteration around porphyry intrusions destroy magnetic minerals in the surrounding rocks.

(v) Around oxidised magnetic felsic plutons, the potassic alteration zone may be magnetite-rich. This is commonly observed for Au-rich porphyry copper systems.

(vi) Serpentinisation is the characteristic hydrothermal alteration process for ultramafic rocks, particularly those rich in olivine. At low grades, initial serpentinisation of olivine produces Fe-lizardite + brucite. With further serpentinisation, the maximum iron content of lizardite is exceeded, and magnetite is produced, along with lizardite, chrysotile and brucite. There is there an inverse relationship between density, which decreases with degree of serpentinisation, and susceptibility. Weakly (~10%) serpentinised peridotites are weakly magnetic (k ~100 μG/Oe = 1260 x 10^{-6} SI). Partially (~55%) serpentinised peridotites are moderately ferromagnetic (k ≈ 700 μG/Oe = 0.0088SI) and fully serpentinised peridotites are substantially more magnetic (k ≈ 3000 μG/Oe = 0.038 SI).

(vii) Carbonate alteration of serpentinised ultramafics initially redistributes magnetite, but does not destroy it, and has little effect on susceptibility. Extreme talc-carbonate alteration, on the other hand, consumes the magnetite, with the iron entering magnesite, and demagnetises the rock.

Hydrothermal Alteration of Acid Volcanics, Conway-Bimurra Area

At Conway-Bimurra Late Devonian acid volcanics, which are prospective for epithermal gold, are difficult to distinguish from non-prospective Late Carboniferous acid volcanics. On a regional scale the aeromagnetics show a reasonable correlation with the mapped geology (Fig. 80). Discrepancies in detail between aeromagnetics and the BMR geology map in several cases arise from misidentification of units during mapping. Other discrepancies simply reflect magnetic signatures arising from shallow, unexposed intrusives, illustrating the utility of magnetics for looking at the third dimension as well as a tool for surficial mapping. The Carboniferous units tend to be distinctly more magnetic and can therefore be distinguished using aeromagnetics. There is a pervasive propylitic alteration in both the Carboniferous and Devonian volcanic suites, the intensity greater in the latter.

The main conclusions from the study are summarised below:

(i) Within the Devonian volcanics intense adularia-sericite alteration centres show up as very smooth, flat magnetic zones, reflecting magnetite destruction (Fig. 81). Within these centres, titanomagnetite is replaced by sphene in the intense propylitic zone and by rutile in the phyllic zone. The susceptibilities of rocks from the intense alteration zones of the prospects are very low (weakly paramagnetic, <10 μG/Oe [0.00013 SI], or diamagnetic), indicating that any magnetic minerals pre-dating the alteration have almost been completely erased.

(ii) Outside the zones of intense alteration, the background susceptibilities of the silicic Devonian volcanics are generally in the strong paramagnetic range (<~ 100 μG/Oe). However, variations in paramagnetic iron contents and in the trace amounts of ferromagnetic minerals produce sufficient differences in magnetization

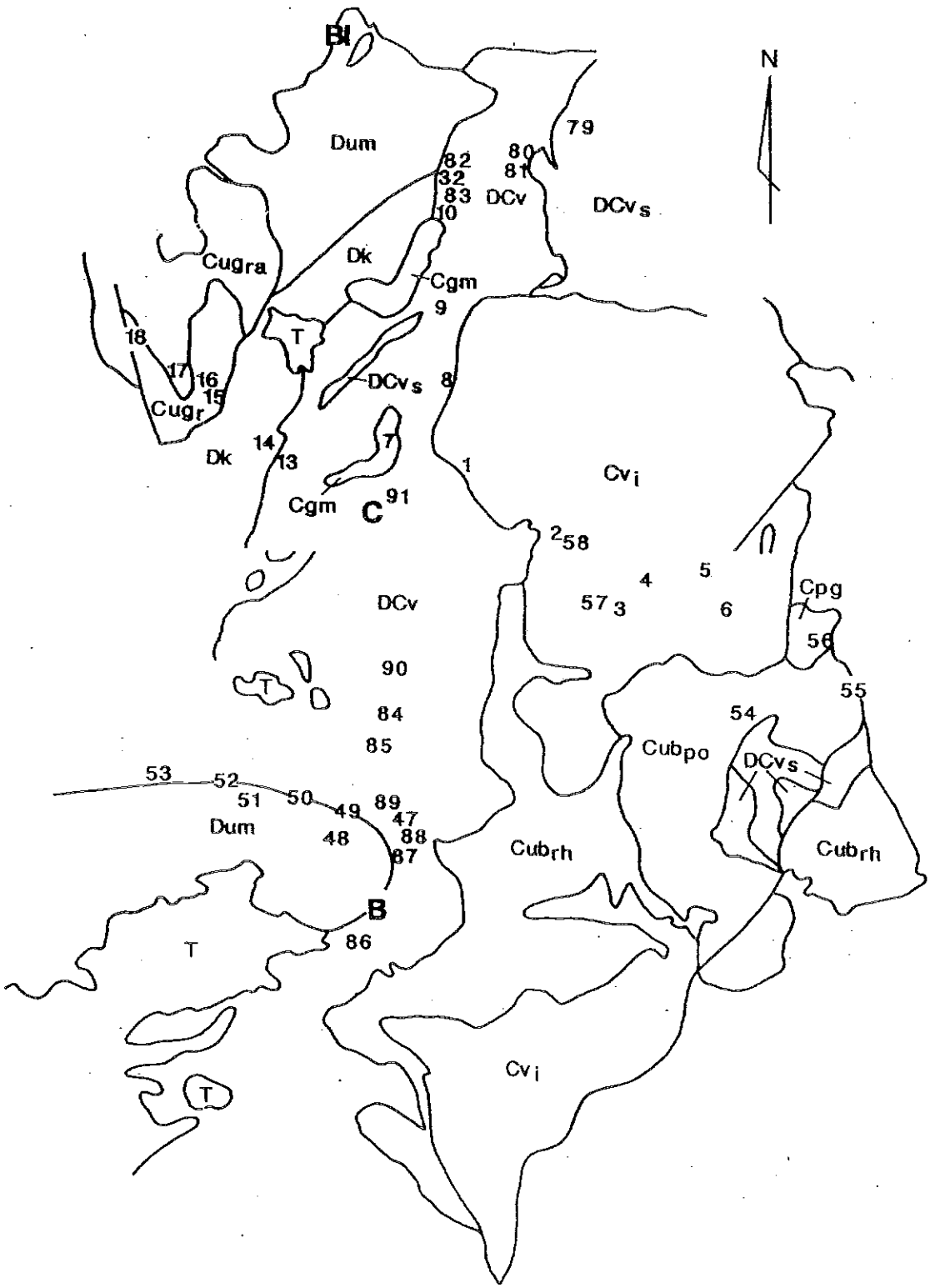
Bl
N
Dum
79
80
81
82
32
83
10
DCv
DCvs
Cugra
Dk
Cgm
9
T
18
17
16
15
Cugr
DCvs
8
14
13
7
Dk
Cgm
C
91
1
Cvi
2
58
4
5
57
3
6
Cpg
56
55
DCv
90
84
85
T
54
Cubpo
DCvs
53
52
51
50
49
89
47
88
87
48
Dum
Cubrh
Cubrh
B
86
T
Cvi
T

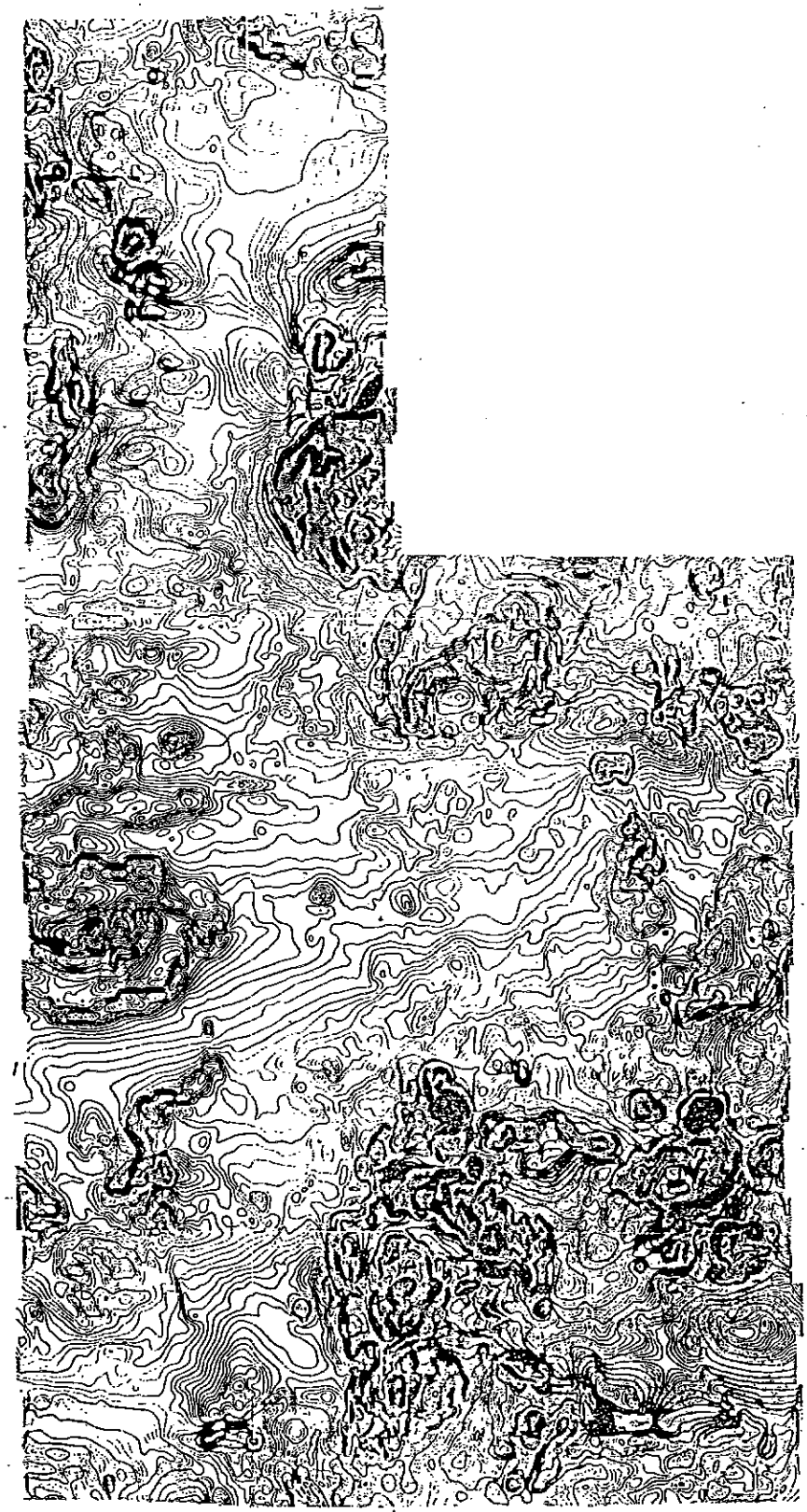

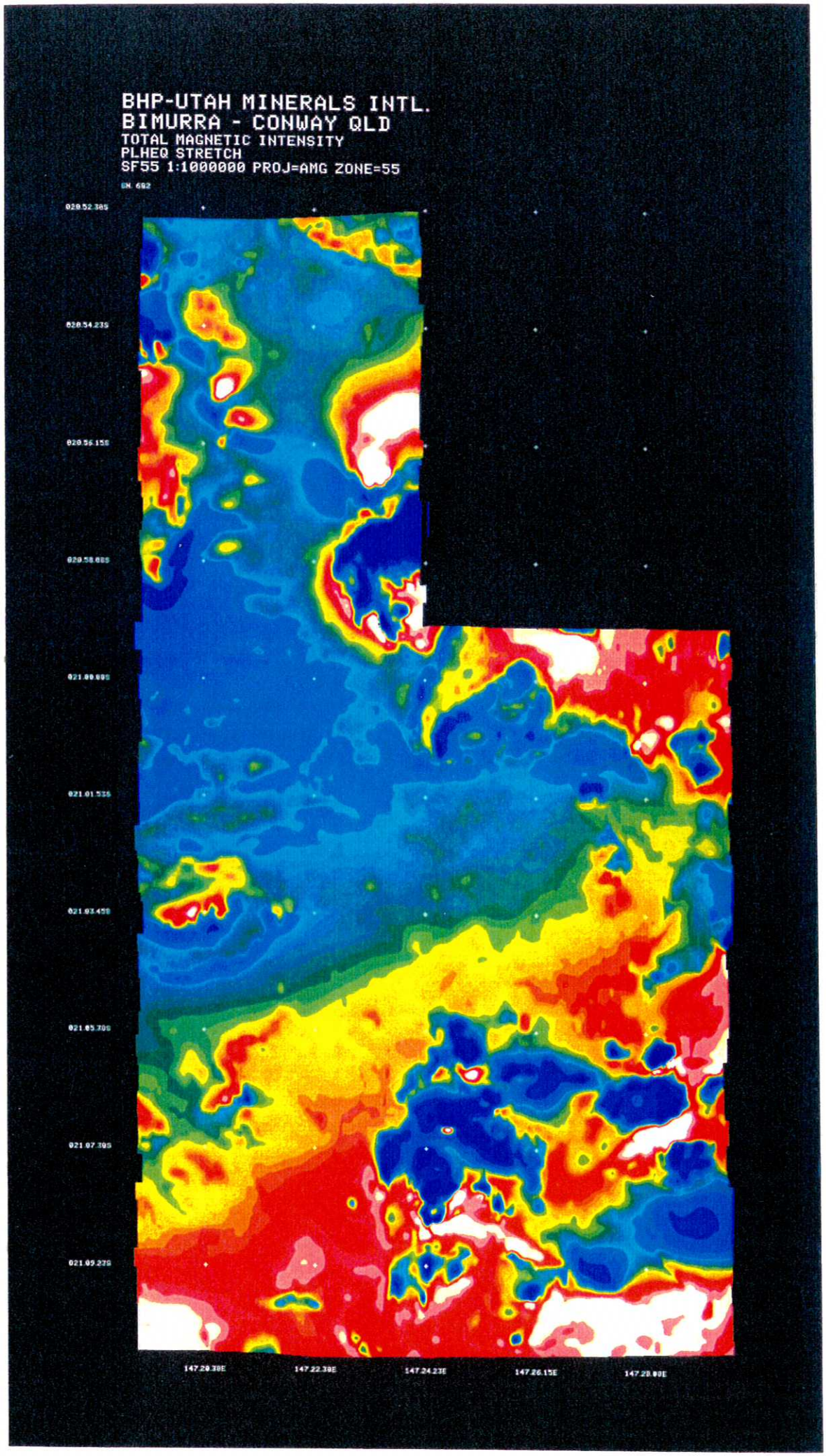
BHP-UTAH MINERALS INTL.
BIMURRA - CONWAY QLD
TOTAL MAGNETIC INTENSITY
PLHEQ STRETCH
SF55 1:1000000 PROJ=AMG ZONE=55
020.52.38S
020.54.23S
020.56.15S
020.58.08S
021.00.00S
021.01.53S
021.03.45S
021.05.30S
021.07.38S
021.09.27S
147.20.30E
147.22.38E
147.24.23E
147.26.15E
147.28.00E

FIG. 80

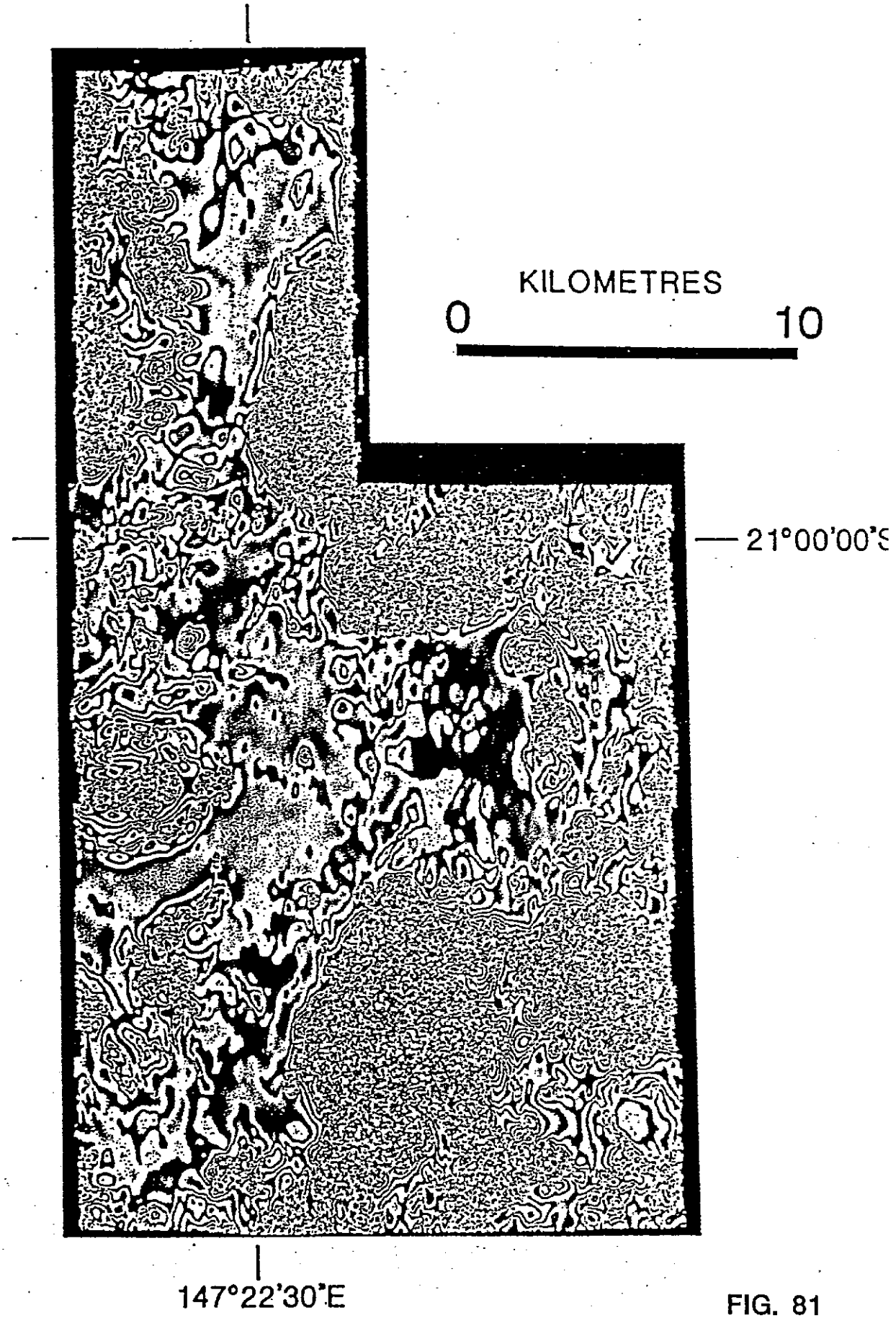

FIG. 81

to produce a texture in the aeromagnetic anomalies that is clearly distinguishable from the smooth flat response associated with the epithermal alteration systems.

(iii) A busy magnetic pattern associated with the Carboniferous volcanics reflects variations in susceptibility, which mainly reflects magnetite content, and Q value, which is dependent on grain size. Major shifts in magnetic base level reflect varying Q values, with reversed remanence overwhelming induced magnetization and producing magnetic lows when Q is greater than unity. Susceptibilities of Carboniferous volcanics range from ~2000 μmG/Oe [0.025 SI] for andesitic flow units, to ~40 μG/Oe [0.0005 SI] for rhyolitic units. The susceptibility of the Devonian volcanics is probably lower because of a combination of initial bulk-rock chemistry (a preponderance of rhyolitic compositions) and the more intense pervasive propylitic alteration.

(iv) The oxide mineralogy is a function of the primary bulk-rock compositions and severity of alteration. Within each volcanic suite, susceptibility tends to decrease in the order andesite, dacite, rhyolite. The pervasive propylitic alteration reduces magnetization by partially replacing magnetic minerals, thereby reducing magnetic grain size and consequently increasing the stability of remanence as the susceptibility and remanence intensity decrease. Figs. 82-85 illustrate the effects of alteration on Fe-Ti oxides.

(v) The Late Carboniferous units record a Permo-Carboniferous remanence direction, directed south and steep down, which dominates the NRM of these units. Most Late Devonian units have NRMs that are dominated by a Permo-Carboniferous overprint, indistinguishable in direction from the primary remanence of the Late Carboniferous rocks, which dominates the NRM of these units.

(vi) Some Late Devonian units retain, in addition to the Late Carboniferous overprint, an underlying primary Late Devonian remanence, directed SW and shallow down. Recognition of this characteristic Late Devonian remanence in some units, that have been mapped as Carboniferous, shows that they are in fact of Devonian age. Ubiquitous Carboniferous overprinting of remanence in Devonian rocks suggests that the regional alteration is penecontemporaneous with the eruption of the Carboniferous volcanics.

(vii) There is as as a strong, noisy, positive aeromagnetic anomaly associated with andesitic units mapped by the BMR asDCv_A. Samples from this area have high susceptibilities, suggesting that the exposed units are responsible for the observed anomaly pattern. No trace of a Devonian remanence component underlying the Carboniferous magnetization is found during demagnetization of the samples. The samples are less altered than typical DCv rocks and the susceptibilities are higher than those of Devonian andesites that are interbedded with the Ukalunda Beds. These characteristics are more consistent with a Carboniferous age, suggesting that this may be a Late Carboniferous unit.

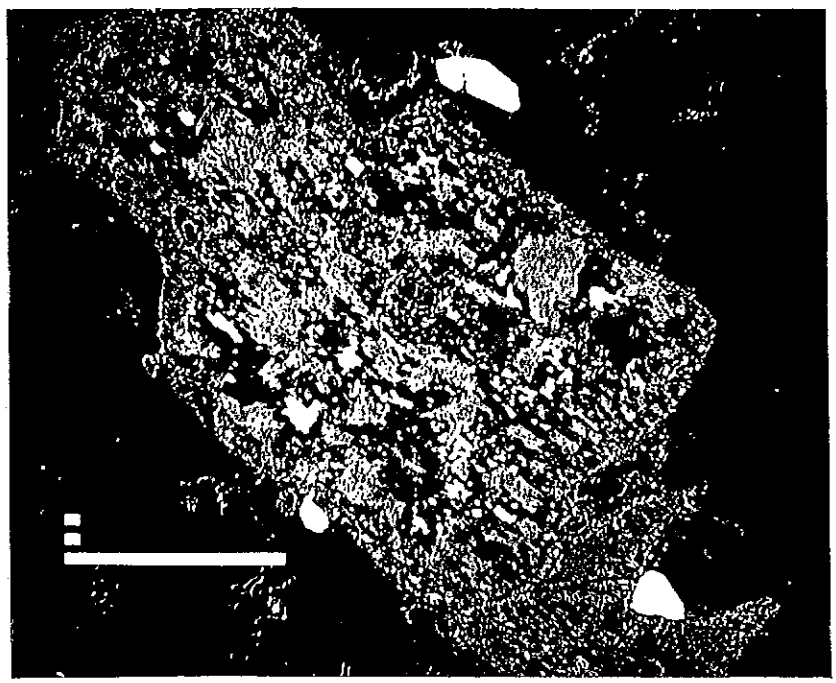

FIG. 82. Back-scattered electron image of altered ilmenite in Upper Carboniferous intrusive rhyolite. Small, bright relics of ilmenite are enclosed in light grey rutile and darker sphene. Length of scale bar is 100um.

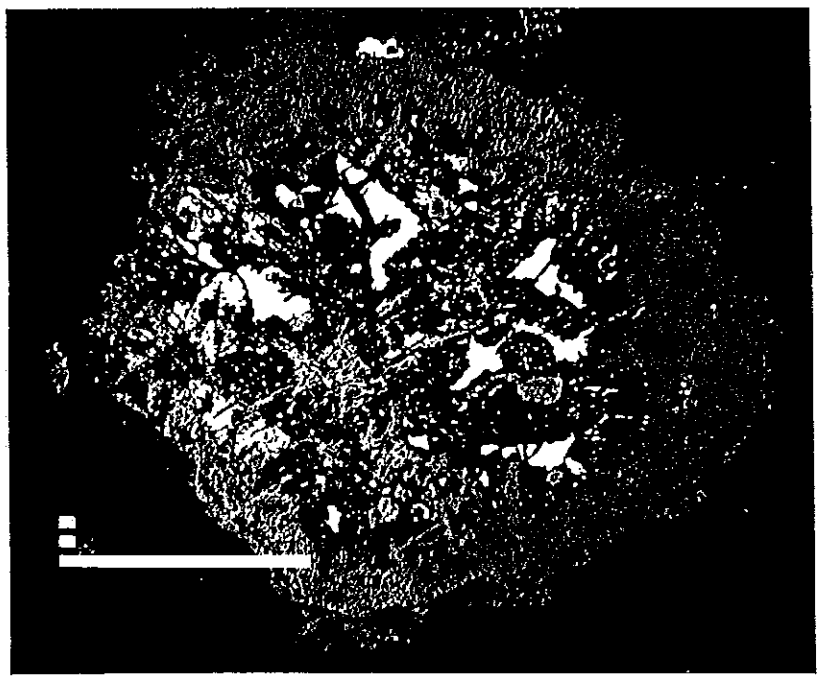

FIG. 83 Back-scattered electron image of altered titanomagnetite in the Locharwood Rhyolite. Primary titanomagnetite (bright) has been replaced by titanomaghemite (slightly darker), then both replaced by calcite (dark grey) and marginal zoned siderite (mid grey). Rare rutile (light grey) is also present. Length of scale bar is 100um.

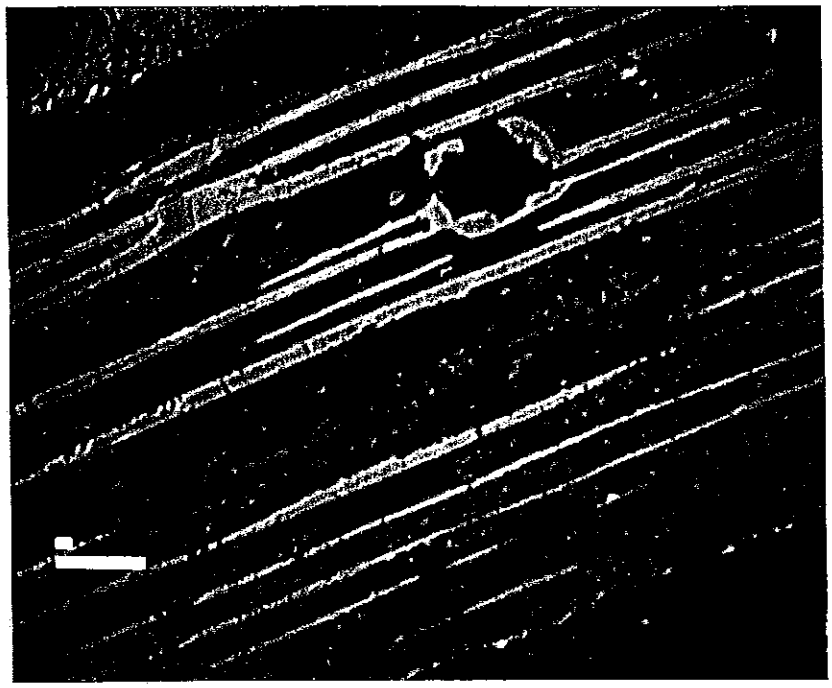

FIG. 84 Back-scattered electron image of altered ilmenite in porphyritic andesite from the Stones Creek Formation. Bright titanomaghenmite lamellae are set in a matrix of light-grey relict ilmenite altering to rutile (mid grey) and darker sphene. Length of scale bar is 10 um.

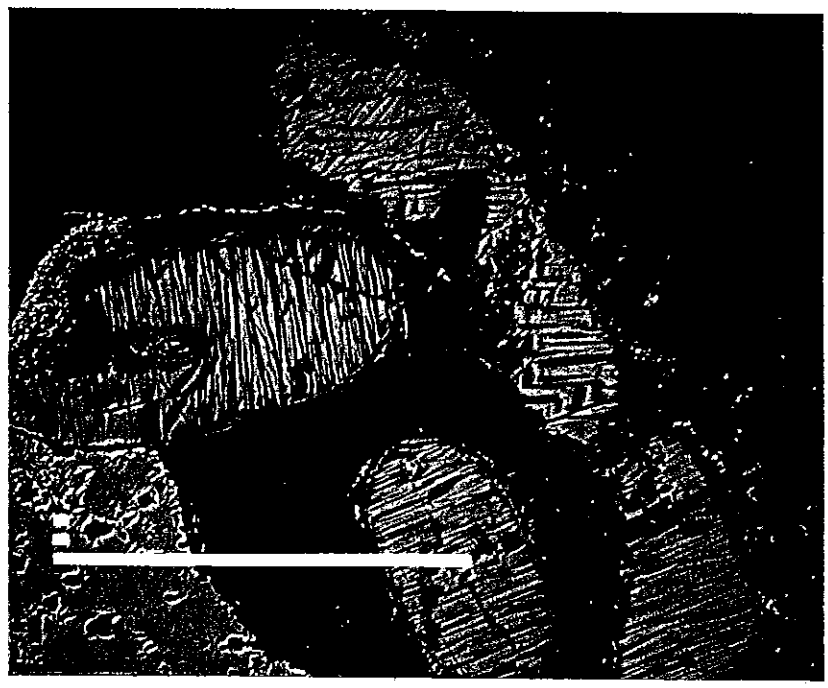

FIG. 85 Back-scattered electron image of altered titanomagnetite in a rhyolitic ash-flow tuff from the Stones Creek Formation. Primary titanomagnetite has been replaced by titanomaghemite (light grey) which in turn is being replaced by rutile (dark grey). Length of scale bar is 100um.

Effects of Metamorphism on Magnetic Properties of Igneous Rocks

Metamorphism is one of the most important controls on themagnetic properties of rocks. Some generalisations follow:

(i) Unmetamorphosed mafic volcanics, hypabyssal rocks and evolved tholeiitic intrusives are usually MFM to SFM. Silicic igneous rocks have bimodal susceptibility distributions reflecting distinct paramagnetic and ferromagnetic populations. For example hornblende/biotite-bearing rhyolites are often ferromagnetic, whereas reduced fayalite rhyolites and peralkaline rhyolites are paramagnetic.

(ii) Burial metamorphism of igneous rocks to zeolite or prehnite-pumpellyite grade does not demagnetise them, in the absence of circulating hydrothermal fluids.

(iii) Low temperature hydrothermal alteration starts to reduce susceptibility by 150°C and replaces primary titanomagnetite or ilmenomagnetite by titanohematite-sphene-rutile by 300°C.

(iv) Extensive development of zeolites, prehnite, epidote etc. is accompanied by a substantial reduction in susceptibility of ferromagnetic rocks. Greenschist grade hydrothermal alteration produces PM to WFM rocks.

(v) Contact metamorphism of hydrothermally altered, demagnetised rocks may produce secondary magnetite.

(vi) Greenschist grade regional metamorphism usually destroys magnetic minerals in volcanic and basic plutonic rocks. Felsic plutons and iron-enriched mafic rocks seem to be more resistant to this process.

(vii) Amphibolite grade metamorphism produces more heterogeneous magnetic properties with bimodal susceptibilities, although dominated by PM/WFM rocks. At this grade FM basic rocks are much more common than FM silicic rocks.

(viii) Chlorite and/or biotite-bearing amphibolites tend to be weakly magnetic. Hornblende-rich amphibolites may have high susceptibilities.

(ix) Granulite grade metamorphism of basic rocks frequently produces metamorphic magnetite and a substantial increase in susceptibility.

(x) Metamorphic magnetite is associated with low Q values and unstable, predominantly viscous, remanence.

(xi) Within the ferromagnetic population of metaigneous rocks, basic rocks tend to have higher susceptibilities than acid rocks at each metamorphic grade.

(xii) High pressure granulites and eclogites are generally paramagnetic, reflecting incorporation into clinopyroxene and garnet.

(xiii) At all metamorphic grades the ferromagnetic proportion is greater for basic than for acid protoliths.

(xiv) Magnetite breakdown in high pressure granulites/eclogites occurs between ~10 kbars and ~20 kbars (lower for undersaturated basaltic rocks than for quartz tholeiites, lower for low Mg/Fe, higher for oxidised rocks).

(xv) Decompression of high pressure granulites during rapid uplift can produce fine-grained magnetite by breakdown of garnetand clinopyroxene. This can carry strong and stable remanence.

(xvi) The magnetite-in isograd for basic rocks reflects P-T-t conditions:
- within lower granulite facies (above orthopyroxene isograd) for prograde metamorphism, followed by isobaric cooling.
- within upper amphibolite facies (above biotite isograd) for retrograde metamorphism or for isothermal decompression due to rapid uplift.

(xvii) Ferric iron in metabasites is redistributed during progressive metamorphism. Ferric iron originally present in magnetite goes largely into hematite during greenschist grade metamorphism, then into biotite and hornblende in the amphibolite facies, whence into metamorphic magnetite in the granulite facies and finally into clinopyroxene and garnet in eclogite facies.

(xviii)The stable spinel composition in serpentinised peridotites varies systematically with progressive metamorphism. Initially pure magnetite and Cr-magnetite produced during serpentinisation, incorporate progressively more Cr. In the amphibolite facies Mg and Al start to enter the spinel phase and a progressively greater proportion of the spinels enter the paramagnetic field (Fig. 86), thus reducing the susceptibility of the rock (Fig. 87). At granulite grade the rock contains only Mg-Al spinel and is paramagnetic, unless subsequently subjected to retrogressive serpentinisation.

Metamorphism of Mafic and Ultramafic Rocks, Agnew-Wiluna Greenstone Belt

Figure 88 shows the distribution of metamorphic facies in the Agnew-Wiluna Belt of the Yilgarn. There is an increase in grade from prehnite-pumpellyite facies in the north to upper amphibolite facies in the south. This is accompanied by a distinct decrease in the anomaly associated with the major ultramafic unit of the belt, which hosts major nickel deposits (Figs. 89-90). Most of this decrease in anomaly amlitude occurs within the southern part of the belt, at higher grades, and reflects the changing spinel compositions with higher grade in serpentinites. The basalts and gabbros also show a distinct decrease in susceptibility, from prehnite-pumpellyite grade to greenschist grade and above (Fig. 91).

SPINEL COMPOSITIONS IN METAMORPHOSED SERPENTINITES

(a) Ferrimagnetic & paramagnetic fields

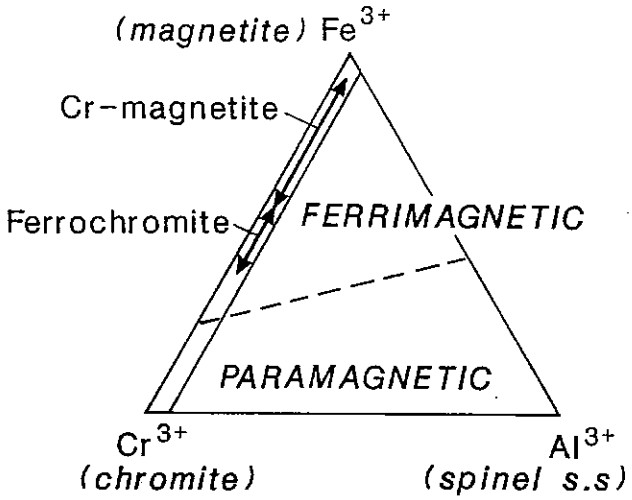

(b) Diopside + olivine + antigorite

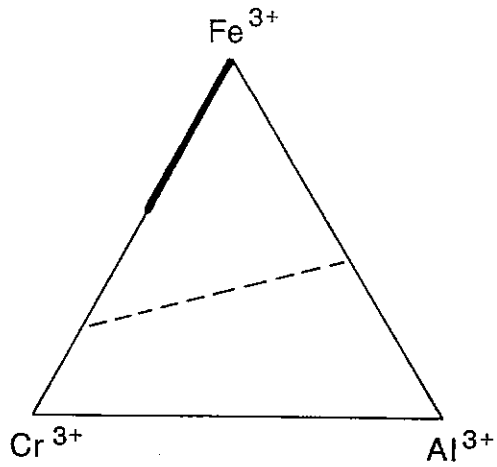

(c) Tremolite + olivine +antigorite

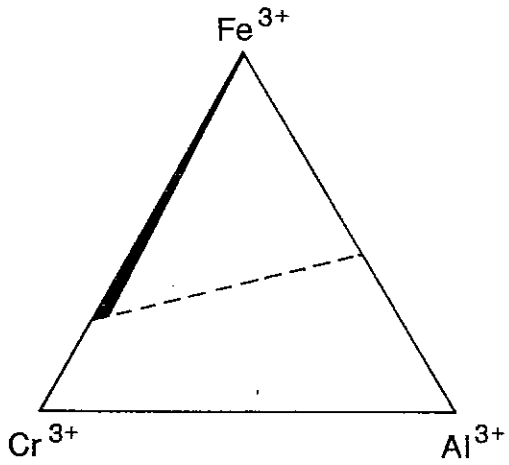

(d) Talc + olivine

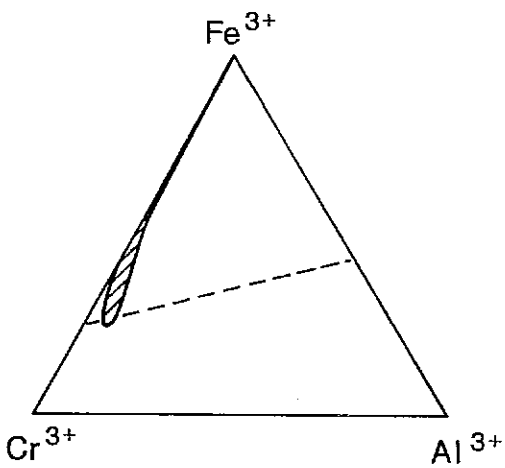

(e) Ca-poor amphibole + olivine

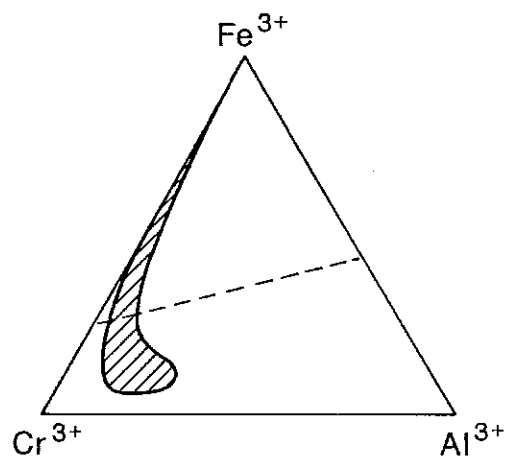

(f) Chlorite + enstatite + olivine

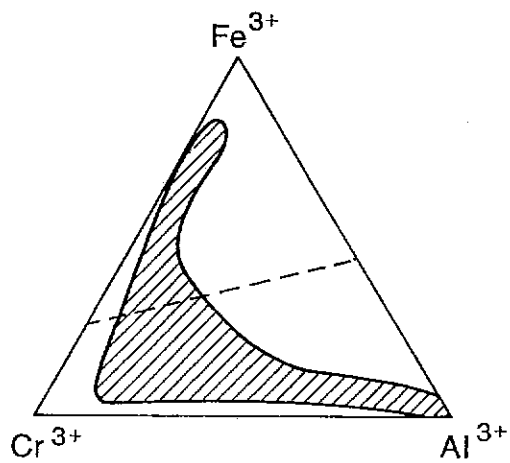

FIG. 86

SUSCEPTIBILITY OF METAMORPHOSED SERPENTINITES

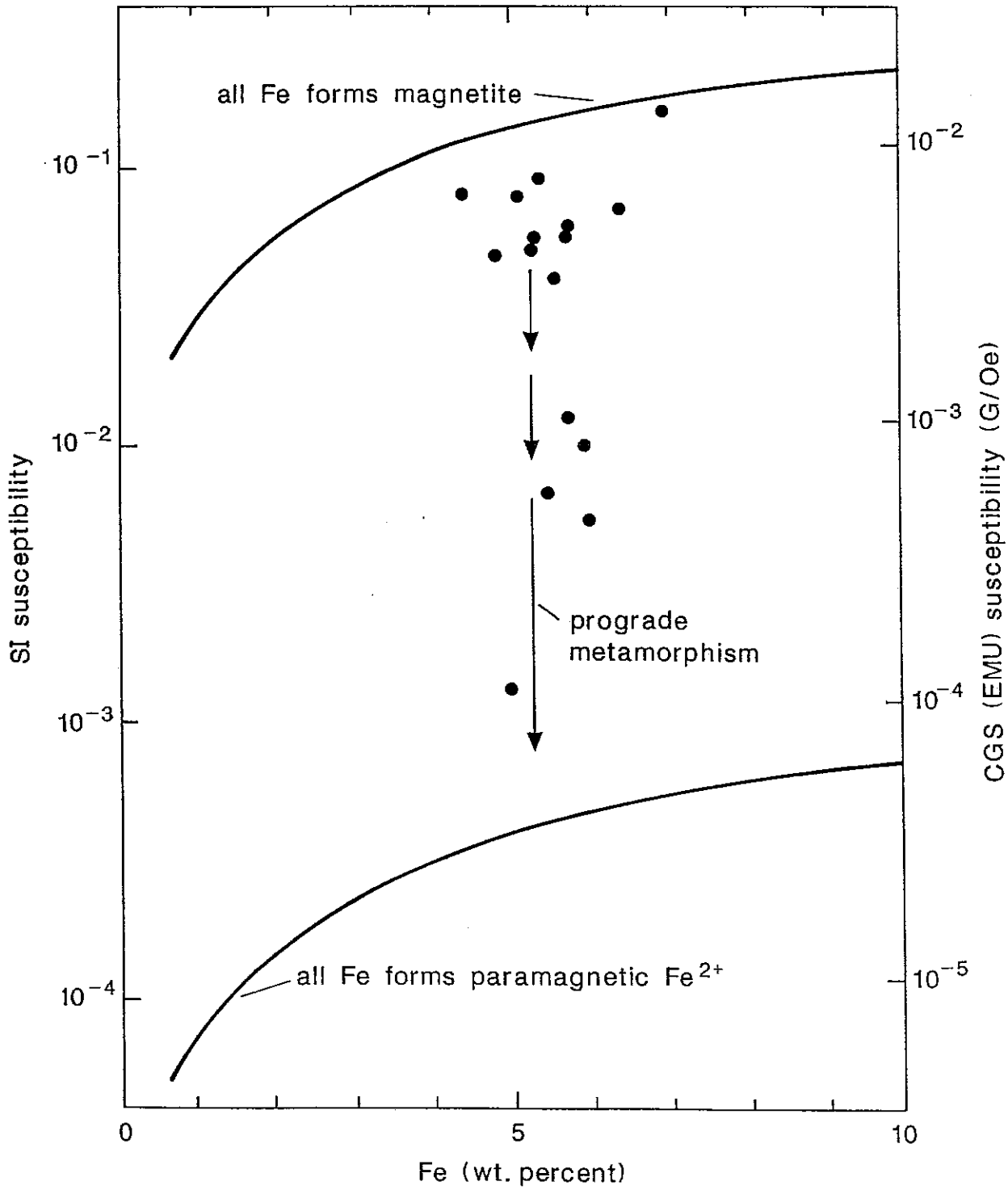

FIG. 87.

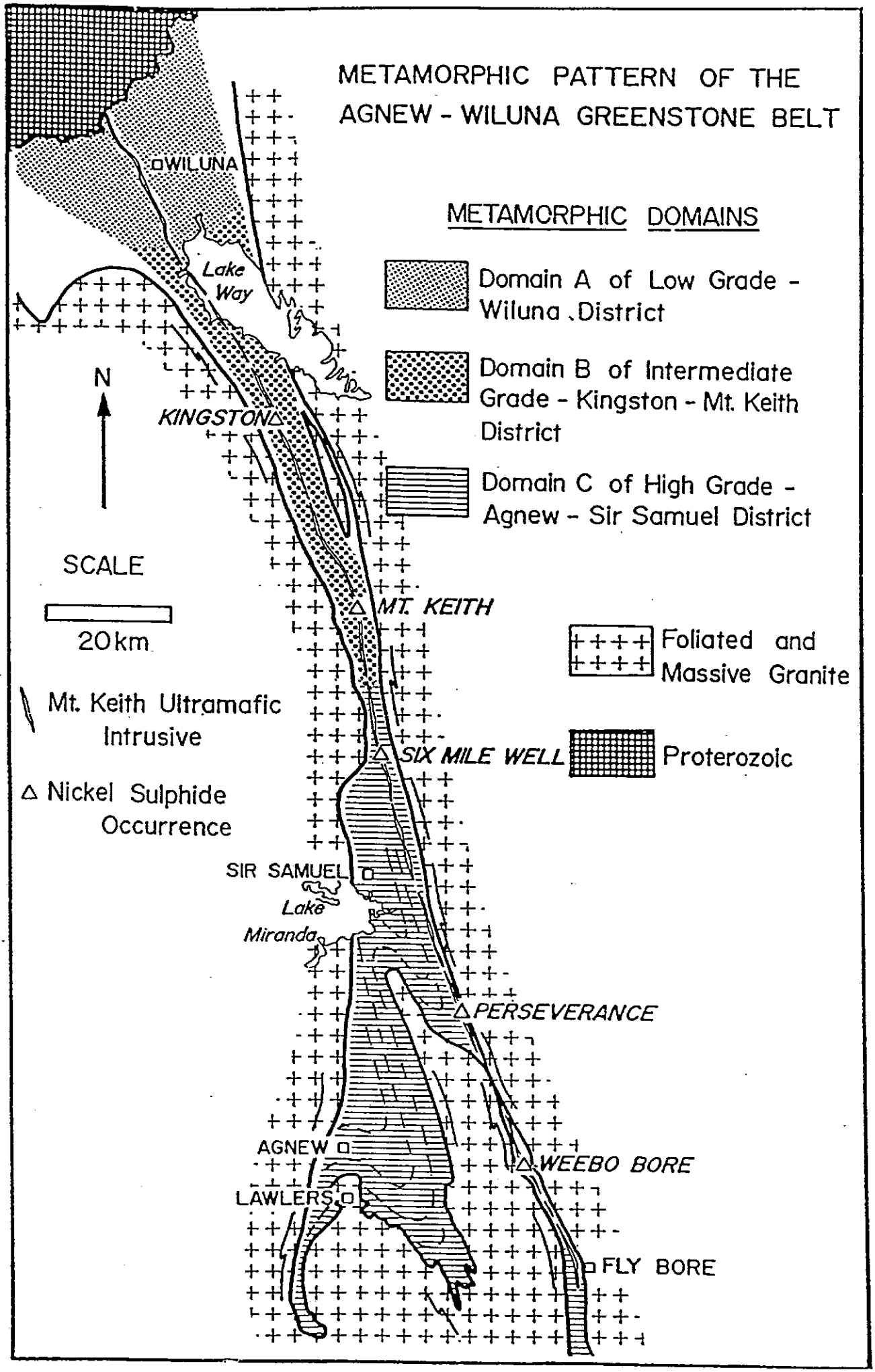
METAMORPHIC PATTERN OF THE
AGNEW - WILUNA GREENSTONE BELT
METAMORPHIC DOMAINS
Domain A of Low Grade - Wiluna District
Domain B of Intermediate Grade - Kingston - Mt. Keith District
Domain C of High Grade - Agnew - Sir Samuel District
Foliated and Massive Granite
Proterozoic
Mt. Keith Ultramafic Intrusive
Nickel Sulphide Occurrence
SCALE
20km
N
WILUNA
Lake Way
KINGSTON
MT. KEITH
SIX MILE WELL
SIR SAMUEL
Lake Miranda
PERSEVERANCE
AGNEW
WEEBO BORE
LAWLERS
FLY BORE

FIG. 88

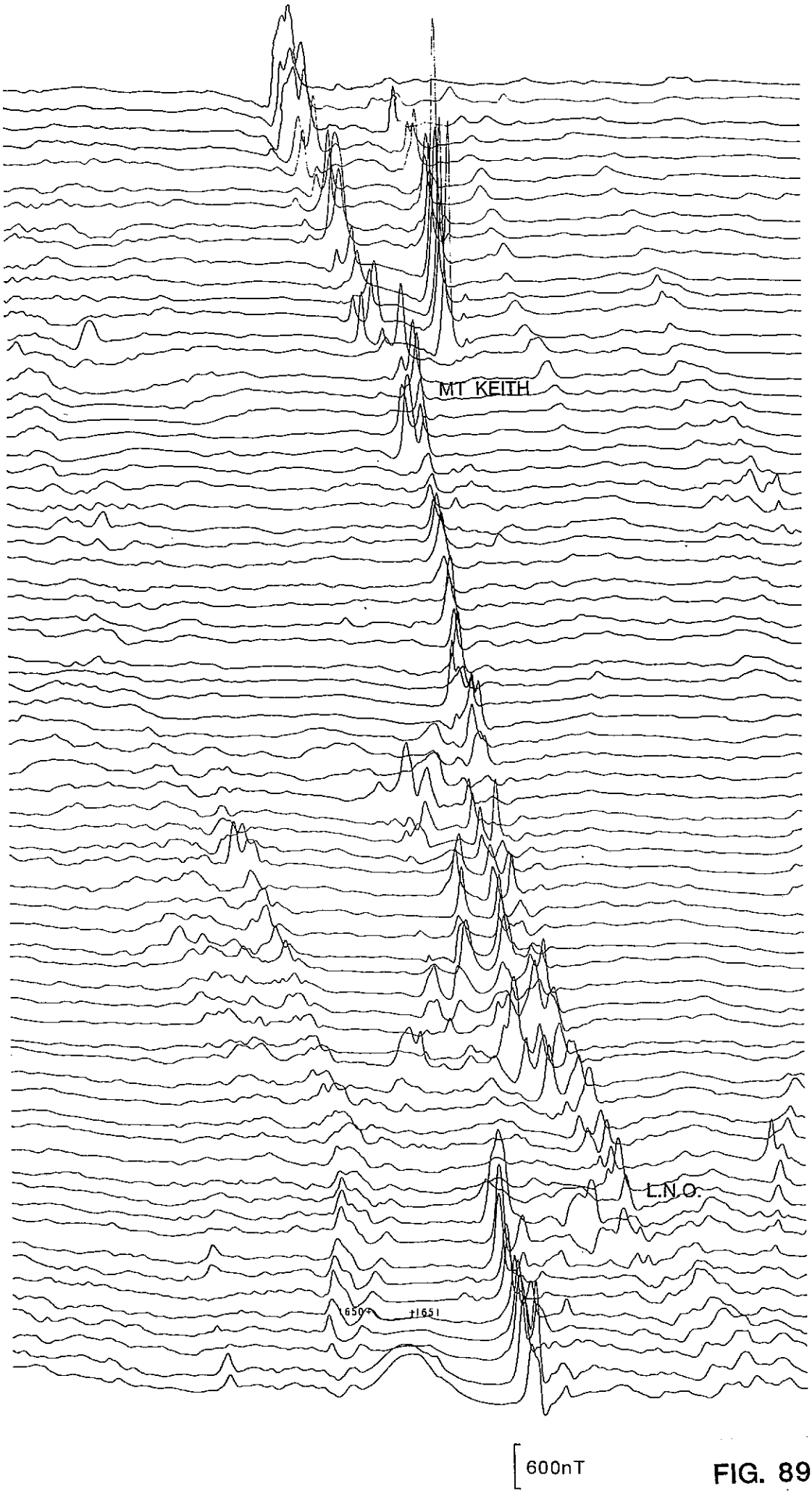

FIG. 89

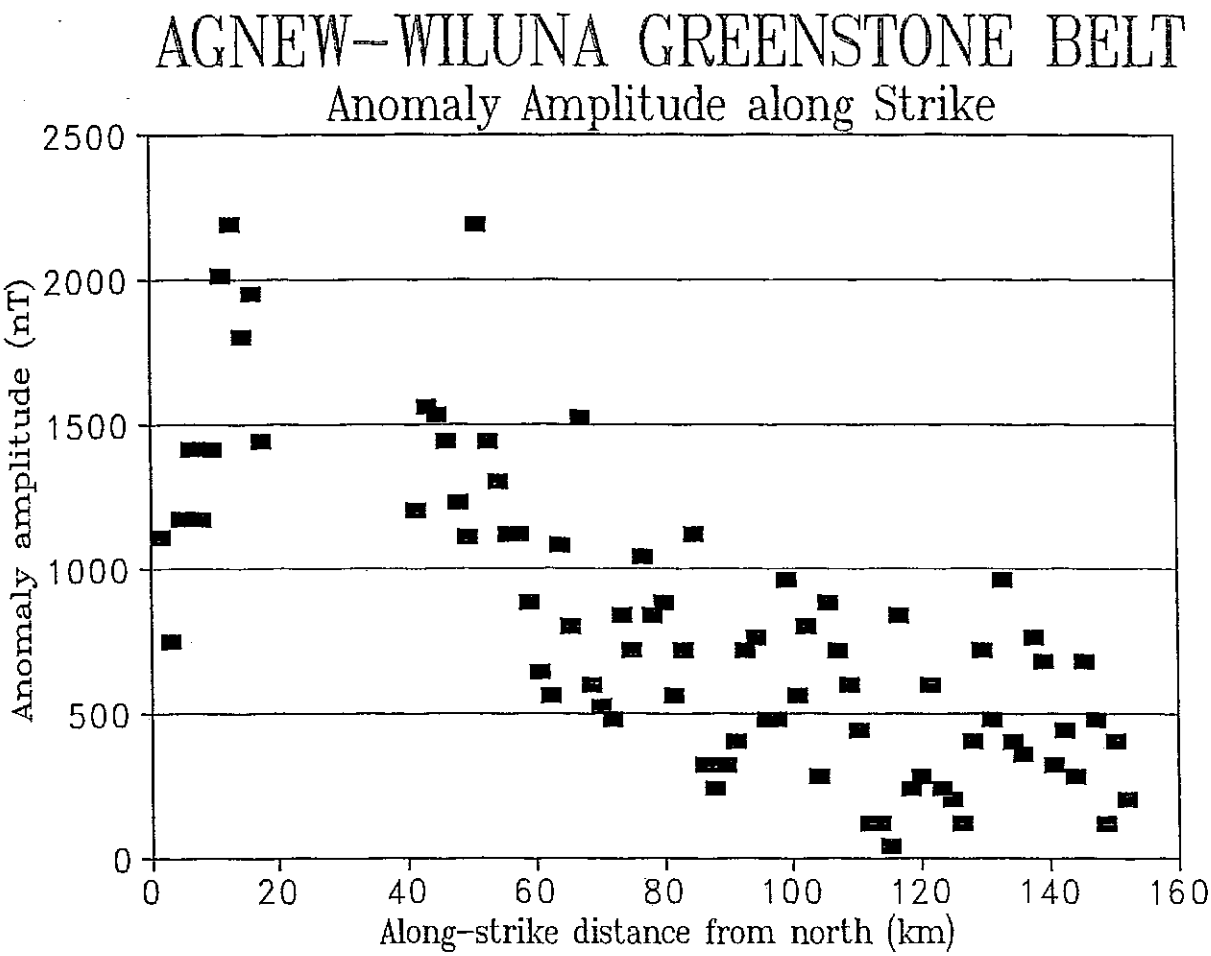
AGNEW–WILUNA GREENSTONE BELT
Anomaly Amplitude along Strike
Anomaly amplitude (nT)
2500
2000
1500
1000
500
0
0
20
40
60
80
100
120
140
160
Along–strike distance from north (km)

FIG. 90

METABASIC ROCKS
Norseman–Wiluna Greenstone Belt

A

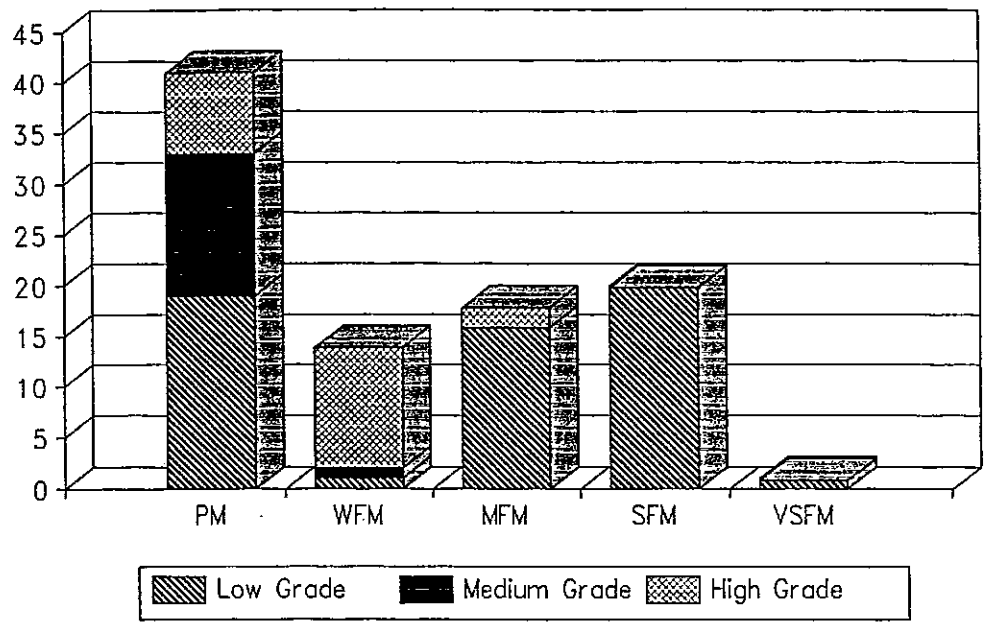

METABASALTS AND METAGABBROS
Norseman–Wiluna Greenstone Belt

B

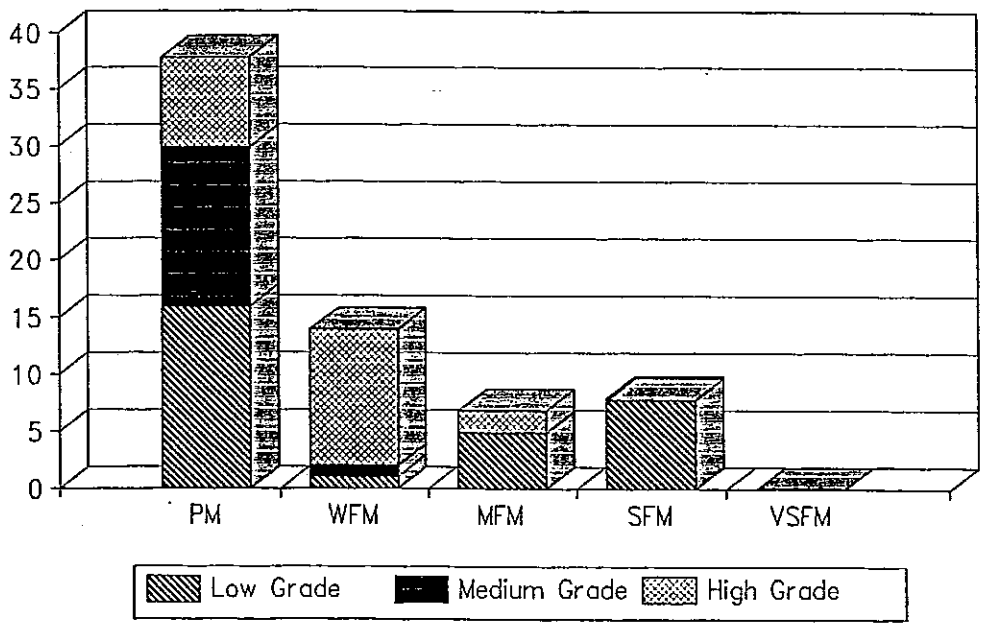

Fig.91

Magnetisation of Metasediments

Magnetic patterns in high grade sedimentary terranes are often broadly conformable and are related to bulk composition, including total iron content, and oxidation state, which is controlled, in many cases, from the depositional environment. McIntyre (1980) and Frost (t (1991c, 1991d) have given extensive discussions of magnetite formation in metasediments. Some general principles are summarised below.

(i) Organic-rich sediments produce reduced graphitic metasediments, which are magnetite-free, but commonly contain pyrrhotite above greenschist grade.

(ii) Red (hematite-bearing) sediments produce intermediate redox metasediments, which may be magnetite-bearing. Hematite goes to magnetite in the biotite or lower garnet zones for these rocks.

(iii) Magnetite formation is favoured by high total iron, and therefore tends to be associated with metapelites more frequently than with metapsammites.

(iv) Magnetite formation is favoured by intermediate redox state or oxidation ratio. Low oxidation states are associated with ilmenite and very high oxidation states with hematite.

(v) Substantial chemical input (exhalative metal-bearing solutions, including iron) increases the potential for magnetite formation during subsequent metamorphism.

(vi) Very iron oxide-rich assemblages, for example BIFs, are sel-buffered during metamorphism, preserving fine layering with magnetite-and hematite-rich bands.

(vii) The maximum ferromagnetic proportion in meta sediments generally occurs at granulite grade.

(viii) Magnetite-rich BIFs have singular magnetic properties, including very high susceptibiltiy anisotropy (A = 3-4) and moderate Q values, typically 1-2.

Magnetic Properties of Precambrian Rocks from the Eyre Peninsula

The regional aeromagnetics over a large part of the Eyre Peninsula is shown in Fig. 92, with geology overlain. Sampling included 10 traverses across heterogeneous metamorphic terranes of the Sleaford Complex, the Lincoln Complex and the Hutchison Group. Banded mafic/felsic gneiss from the mylonite zone at Port Neill (locality 01) is extremely magnetic, as is the mafic gneiss of the Lincoln Complex at Cape Donington (locality 03). Foliated granite of the Lincoln Complex outcropping within the Hutchison Group at Sleaford Bay (locality 06) is moderately magnetic. Most other Hutchison Group units at locality 06 are too weathered to be representative, although the Cook Gap Schist from locality 13 is very magnetic. A fresh drill core sample thought to be from the Hutchison Group supplied by SADME proved to be moderately magnetic (Table II). Other moderately magnetic rocks include some metadolerite dykes. Generally the amphibolite dykes are low to weakly magnetic.

Three characteristic remanent components have been isolated. The A component directed to the southeast is present in mafic gneiss from the Kalinjala Mylonite Zone and in mafic and felsic granulites from Bratten Cairn, a few km north. The most prevalent component, the B component directed upward to the northeast, is observed in the Lincoln Complex gneiss (at Cape Donington, Port Lincoln and Salt Creek), in amphibolite dykes (near Port Neill and Salt Creek), and in the Gawler Range Volcanics to the north. A third component, the C component, is observed in the Lincoln Complex gabbro-norite and amphibolite dykes (Cape Donington and Cape Colbert), and metadolerite dykes, the latter thought to be late stage intrusions of low metamorphic grade. The C magnetization, downward to the west, is almost though not exactly 180° reversed from the B magnetisation, and is extremely stable in the some metadolerite dykes, e.g. samples from locality 16 are only partially demagnetised by 1000 Oe (Appendix 1). The remanent components may represent a craton-wide tectonic event post-dating the Gawler Range Volcanics (~1600 Ma).

A simple model of retrograde metamorphism accompanied by a geomagnetic field reversal (normal to reversed) can explain the occurrence of different polarity remanence at different localities. The C component is similar to magnetizations seen in dolerite dykes from central Australia and may be of similar age (~1050 Ma). The B component is not seen in the metadolerite dykes which suggests that the retrograde metamorphism is bracketted between 1600 Ma and 1050 Ma. Notwithstanding their different polarities, the magnetic axes of the two components are close, although not exactly the same, which further suggests that the magnetic components are of similar age, that is the B component is not very much older that 1050 Ma.

The results have important implications for Australia's Precambrian apparent polar wander path. Firstly, the present pole path does not recognise the possibility that the 1050 Ma Stuart Dykes of the Arunta Block may belong to the same swarm as the GB dykes from the Gawler Craton, i.e. the Gairdner Dykes. With similar characteristic directions of reversed polarity this must be considered a possibility, particularly since the Kulgera Dykes from the intervening Musgrave Block also possess similar directions (Schmidt, 1991). This would require replotting the GB pole near the Stuart Dykes and the Kulgera Dykes poles, not 180° away. The implication of this is that the Gawler, Musgrave and Arunta Blocks have not rotated significantly with respect to each other since 1050 Ma. Secondly, the Gawler Range Volcanics pole (GR) is derived from overprint magnetisations and can no longer be treated as a key pole for 1590 Ma. Thirdly, reversals of the Earth's field at about 1100 Ma have been shown in other studies, e.g. the Keweenawan Volcanics (Pesonon and Nevanlinna, 1981), to be oblique and not 180°. This suggests that the normal polarity and reversed polarity magnetisations found in all kinds of rock types from the Eyre Peninsula may be more closely related temporally than has been thought previously. Many of the poles plotted around the 1.65 Ga to 1.5 Ga segment of the pole path ought to be plotted near the 1.1 Ga segment about 180° away.

If this model of retrograde metamorphism during a time that the geomagnetic field switched polarity is substantially correct, basement rocks may be remanently magnetised in stripes analogous to the sea-floor. This may be discernible as base level jumps in magnetic surveys.

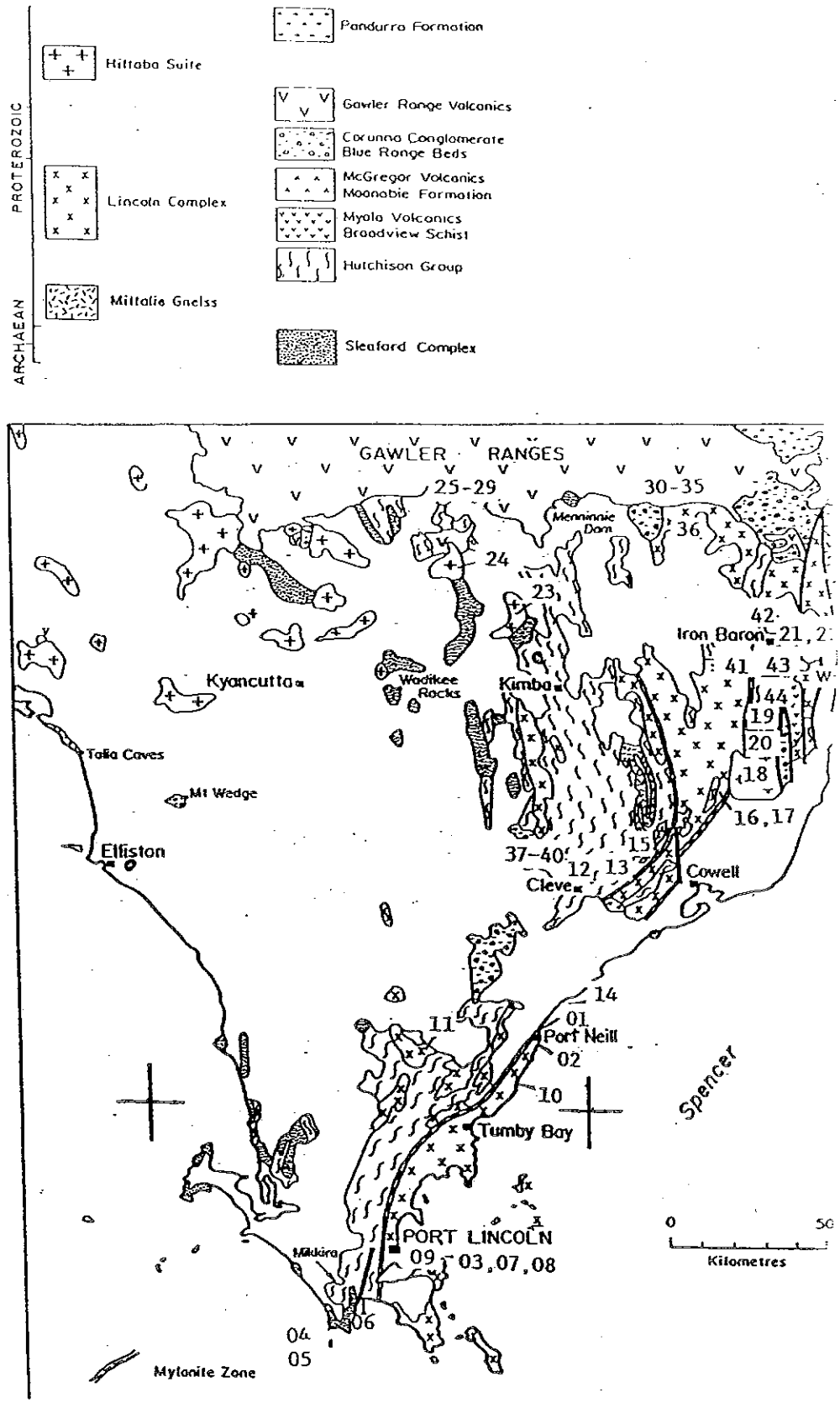
PROTEROZOIC
ARCHAEAN
Hiltaba Suite
Lincoln Complex
Miltalie Gneiss
Pandurra Formation
Gawler Range Volcanics
Corunna Conglomerate
Blue Range Beds
McGregor Volcanics
Moonabie Formation
Myola Volcanics
Broadview Schist
Hutchison Group
Sleaford Complex
GAWLER RANGES
25-29
30-35
Menninnie Dam
36
24
23
42
Iron Baron
21, 2
41
43
44
19
20
18
16,17
15
37-40
12, 13
Cowell
Cleve
Kyancutta
Wudikee Rocks
Kimba
Tulla Caves
Mt Wedge
Elliston
14
11
01
Port Neill
02
10
Tumby Bay
Spencer
PORT LINCOLN
09
03, 07, 08
Mikkira
06
04
05
Mylonite Zone
0
50
Kilometres

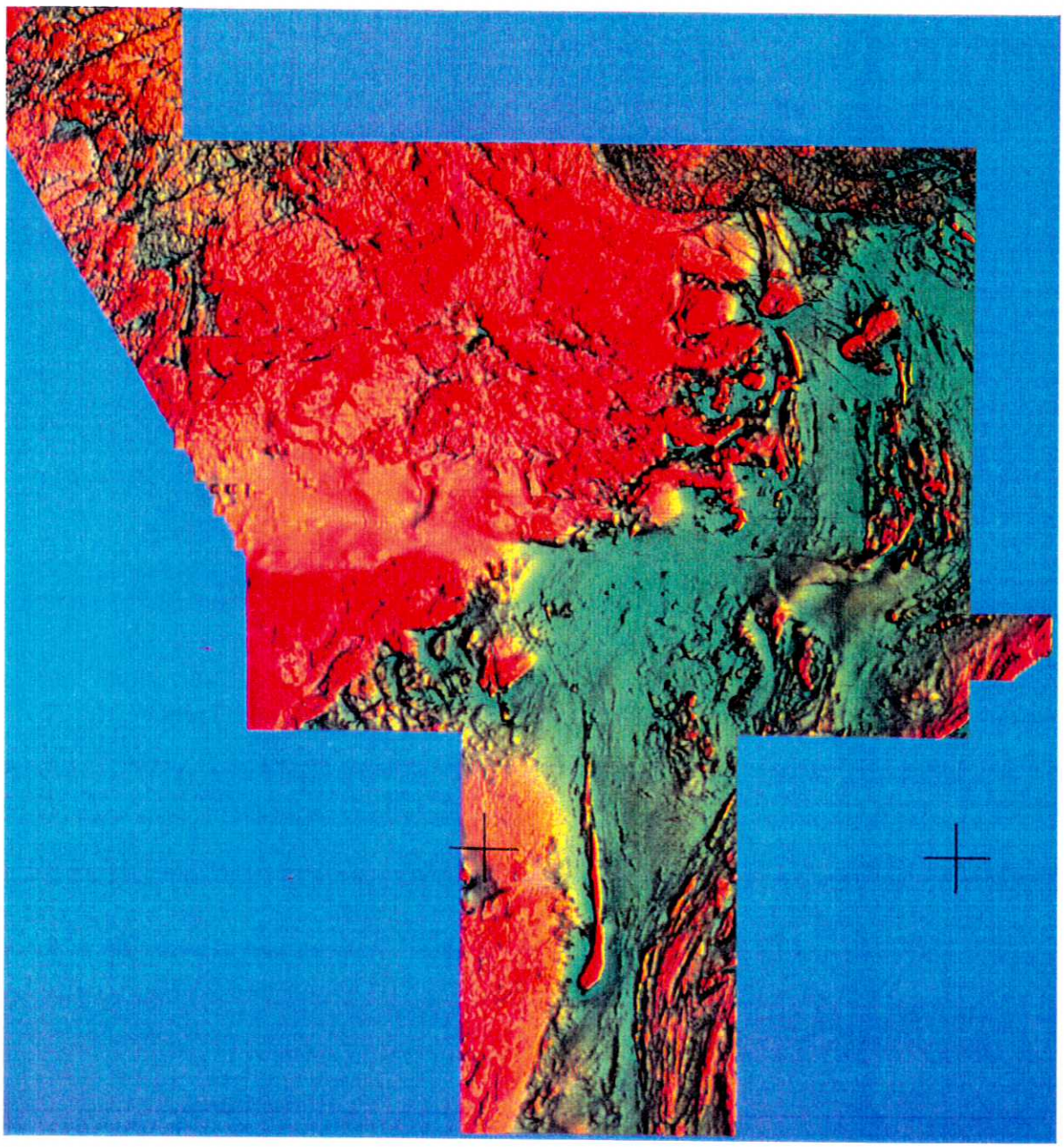

Fig. 92

Magnetic Properties of Rocks from the Golden Grove Area

This study area contrasts with the other main Yilgarn Block study area of this project, the Agnew-Wiluna Greenstone Belt, in the importance of felsic volcanic sequences, chemical sediments and banded iron formations, and the relative scarcity of ultramafic rocks. These features are characteristic of the supracrustal sequences of the Murchison Province, which are probably somewhat older than those of the Eastern Goldfields and Southern Cross Provinces, in which ultramafics are much more prominent. In particular, the volcanigenic massive sulphide mineralisation of the Golden Grove area and its environment afford a good opportunity to investigate the processes responsible for the creation, alteration and destruction of magnetic minerals during the deposition, hydrothermal alteration and metamorphism of the volcanic, volcaniclastic, epiclastic and exhalative chemical units.

The geology and mineralisation of the Murchison Province have been described by Watkins (1990) and Watkins and Hickman (1990). Most of the samples in this study were collected from the eastern portion of the YALGOO 1:250,000 Sheet, for which Explanatory Notes are available (Muhling and Low, 1977).

The oldest supracrustal sequences of the Luke Creek Group were deposited on unidentified basement at about 3.0 Ga. The Luke Creek Group comprises four laterally extensive formations, which form a layered stratigraphy about 10 km thick. Syngenetic base metal mineralisation in the Golden Grove area occurs within the Gabanintha Formation of the Luke Creek Group.

Subhorizontal monzogranite and granodiorite sheets intruded the base of the Luke Creek Group at about 2920 Ma. The earliest deformational/metamorphic event (D1) produced major recumbent folds and thrusts and converted the granitoid sheets into pegmatite-banded gneiss.

The greenstones of the Mount Farmer Group were deposited, probably unconformably, on top of the Mount Luke greenstones and pegmatite-banded gneisses. Unlike the Mount Luke Group, the Mount Farmer Group consists of nine penecontemporaneous sequences associated with volcanic centres and one epiclastic sedimentary sequence, the Mougoodera Formation. Each of these sequences has limited lateral extent and, with one exception, is confined to a single greenstone belt.

In the present study area the Mount Farmer Group is represented by the Yalgoo Subgroup in the north, the Singleton Basalt in the south and the Mougoodera Formation in the core of the Warriedar Fold Belt. The Murchison Supergroup overall is dominated by mafic volcanic and intrusive rocks, which comprise about 70% of both its groups. Felsic volcanic/volcaniclastic rocks make up about 20% of each group. The remainder of the Luke Creek Group consists of ~5% ultramafic rocks and ~5% BIF, whereas the Mount Farmer Group contains ~4% ultramafics and ~6% epiclastic sediments.

Deposition of the Mount Farmer Group was followed by intrusion of thick, subhorizontal sheets of monzogranite into the base of the Murchison Supergroup, at about 2690 Ma. Concordant and subconcordant mafic and ultramafic sills are abundant within all basalt sequences in the greenstone belts. Gabbroic sills also selectively intrude the BIF-rich

Golconda and Windaning Formations. D2 produced tight east-trending upright folding of pegmatite-banded gneiss, recrystallised monzogranite and the entire Murchison Supergroup, including the mafic/ultramafic sills. A more intense deformation, D3, produced tight to isoclinal north to northeast-trending upright folds of granitoids and greenstones. This deformation was followed by regional metamorphism of pegmatite-banded gneiss, recrystallised monzogranite and greenstones, mostly in the greenschist facies. Most gold deposits formed soon after the peak of regional metamorphism, between about 2680 and 2620 Ma. Gold mineralisation is mostly epigenetic, is preferentially hosted by BIF and by ultramafic and mafic rocks in the lower part of the stratigraphy, and is closely related to major faults and shear zones in the greenstones.

Post-folding granitoids intruded the deformed and metamorphosed greenstones and greenstone-granitoid contacts at about 2630 Ma. These plutons can be divided into two suites on the basis of petrology and geochemistry. Suite I plutons comprise tonalites, trondhjemites, granodiorites and monzogranites, derived from mafic crustal rocks, and are confined mainly to the northern Murchison Province. Suite II consists of quartz-rich monzogranites and syenogranites, derived from siliceous granulite, and is confined mainly to the southern part of the Murchison Province, including the present study area.

East-west compression produced D4 shearing and faulting along northeast to northwest, but dominantly NNE, trends towards the end of F3. At about 2400 Ma an extensive set of east to ENE- trending dolerite dykes intruded the greenstones and granitoids.

The earliest metamorphic event was contact metamorphism of greenstones by mafic intrusions, producing generally narrow high-grade aureoles. M2 represents contact metamorphism associated with intrusion of pre-folding granitoids and is also developed only locally. M3 regional metamorphism of supracrustal rocks, pegmatite-banded gneiss and recrystallised monzogranite ranges from prehnite-pumpellyite grade to granulite grade, but over most of the exposed areas is in the greenschist facies. Margins of the greenstone belts are generally of upper greenschist grade, decreasing to lower greenschist grade in the cores of the belts. Regional metamorphism took place between about 2680 Ma and 2640 Ma.

Clifford (1987) has described the detailed stratigraphy of the Warriedar Fold Belt, which represents the central portion of the Yalgoo-Singleton Greenstone Belt of Watkins and Hickman (1990). Clifford's (1987) Gossan Hill Group and Thundelarra Group correspond to the lower and upper portions of the Gabanintha Formation respectively.

The felsic volcaniclastics and lavas of the Gossan Hill Group host the Zn-Cu-Pb-Ag-Au VMS deposits of the Golden Grove area, in particular the copper-rich Gossan Hill mineralisation and the zinc-rich Scuddles mineralisation. The mineralised horizon consists of a sulphidic, cherty exhalative sequence that is commonly magnetite-rich. The thickness of the mineralised horizon varies from 10 to 80 metres. Ashley et al. (1988) have described the Scuddles mineralisation and Frater (1983, 1985a,b) has given a detailed account of the "Golden Grove" mineralisation, now known as the Gossan Hill deposit.

Figure 93 shows detailed aeromagnetic contours over the Golden Grove area, with sampling localities indicated. This coverage, supplied by ACM Pty Ltd, and the regional BMR aeromagnetics enable a general aeromagnetic stratigraphy for the Southern Murchison Province to be devised, which is summarised below:

MAGNETIC STRATIGRAPHY OF THE SOUTHERN MURCHISON PROVINCE

LITHOLOGY	ANOMALY AMPLITUDE
BIF	1000-9000 nT, average ~3000 nT over most of YALGOO Sheet. Locally up to 12,000 nT in low-level survey. Linear highs, with slight assymetry that is persistent along strike.
Felsic/intermediate volcanics and volcaniclastics + epiclastics, except for mineralised horizon	< 10 nT
Mineralised horizon, away from mineralisation	~ 50 nT
Zn-rich sulphides + magnetite mineralisation at Scuddles	~ 100 nT
Mineralised horizon, approaching Gossan Hill	~ 250 nT
Massive magnetite + Cu-rich sulphide mineralisation at Gossan Hill	1200-4500 nT
Basalts and gabbros	generally < 100 nT
Oxide-rich zone of Buddadoo metagabbro	1500-3500 nT
Proterozoic dolerite dykes	~ 100 nT
Granitoids	generally smooth variations, typical amplitude +100 nT; locally up to ~ 500 nT. E-W symmetry of highs indicates subvertical contacts.
Hornblende monzogranite (mafic phase of post-folding granitoid, with Mo mineralisation), Gullewa	500-1750 nT

The main conclusions from the Southern Murchison Province study are:

(i) Banded iron formations are responsible for the most prominent magnetic anomalies in the Murchison Province. The anomalies are linear or curvilinear highs, generally of great strike extent. In the case of linear highs, the asymmetry of the anomaly form is quite persistent along strike, suggesting very consistent dips. In fact, this feature is attributable to suppression of the normal dip dependence of anomaly shape as a result of the high susceptibility anisotropy of the BIFs. The induced magnetisation is deflected strongly towards the bedding plane, producing magnetic poles that lie predominantly on the upper edge of the sheet-like unit, so that varying dips correspond to similar "line of pole" anomalies. Anomaly forms around fold noses show features, such as reversals of anomaly sign, that imply strong anisotropy effects and, in some cases, the presence of pre-folding remanence.

(ii) the susceptibility of fresh BIFs is ~0.1 G/Oe (~1 SI) in the bedding plane and the susceptibility anisotropy is typically 2-4.

(iii) Remanent magnetisation carried by BIFs generally lies close to the bedding plane, with typical Q values of 1-2.

(iv) In the Golden Grove area, the felsic/intermediate stratigraphy is paramagnetic, except for the mineralised horizon. Greenschist grade metamorphism appears to be responsible for the low susceptibility of the andesitic and dacitic volcanics, which were probably magnetic originally.

(v) Exhalations of metal-bearing solutions created conditions favourable for sulphide mineralisation and formation of diagenetic magnetite. Along strike from massive sulphide zones the mineralised horizon contains minor magnetite, which becomes very abundant in massive sulphides.

(vi) The mineralised horizon can be traced within the stratigraphy using detailed aeromagnetics. Because of the large regional gradient arising from the very strong magnetic influence of the BIF units across strike, filtering of the raw aeromagnetics, such as calculation of derivative anomalies, is necessary to accurately define the anomaly associated with the mineralised horizon.

(vii) Magnetite-rich syngenetic mineralisation produces local bullseye anomalies within the linear magnetic ridge corresponding to the mineralised horizon. The magnetite content of the copper-rich mineralisation at Gossan Hill is greater than that of the zinc-rich mineralisation at Scuddles. Magnetite replaced a primary hematite-goethite assemblage that formed on or just below the sea-floor, probably during diagenesis or a late hydrothermal-autometamorphic phase (Frater, 1985a).

(viii) The magnetisation of the Scuddles and Gossan Hill orebodies is predominantly due to magnetite. Minor pyrrhotite is present, but makes only a small contribution to the magnetic properties. The magnetisation is predominantly induced and the remanence is dominated by soft viscous remanence subparallel to the present field.

Fig.93

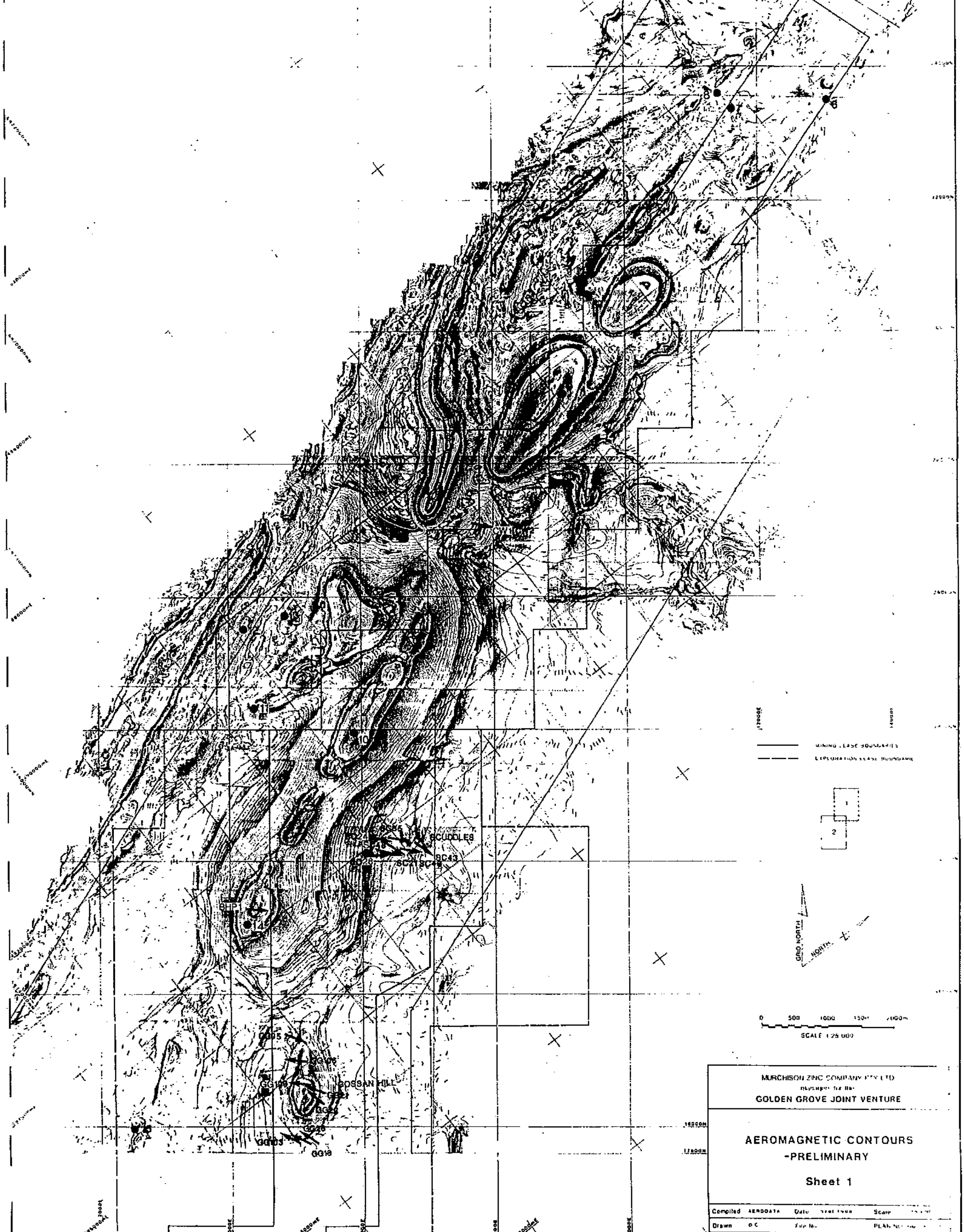
SCUDDLES
BHP
GOSSAN HILL
GRID NORTH
NORTH
MINING LEASE BOUNDARIES
EXPLORATION LEASE BOUNDARIES
0 500 1000 2000m
SCALE 1:25 000
GOLDEN GROVE JOINT VENTURE
AEROMAGNETIC CONTOURS
-PRELIMINARY
Sheet 1
Compiled AERODATA
Date
Scale
Drawn
PLAN

BIBLIOGRAPHY

Ade-Hall, J.M., Palmer, H.C. and Hubbard, T.P., 1971. The magnetic and opaque petrological response to regional hydrothermal alteration. Geophys. J. R. Astron. Soc., 24, 137- 174.

Ague, J.J. and Brimhall, G.H., 1987. Granites of the batholiths of California: products of local assimilation and regional-scale crustal contamination. Geology, 15, 63-66.

Ague, J.J. and Brimhall, G.H., 1988a. Regional variations in bulk chemistry, mineralogy and the compositions of mafic and accesory minerals in the batholiths of California. Geol. Soc. Am. Bull., 100, 891-911.

Ague, J.J. and Brimhall, G.H., 1988b. Magmatic arc asymmetry and distribution of anomalous plutonic belts in the batholiths of California: effects of assimilation, crustal thickness, and depth of crystallization. Geol. Soc. Am. Bull., 100, 912-927.

Aguirre, L., 1974. Andean magmatism: its paleogeographic and structural setting in the central part (30°-35°S) of the Southern Andes. Pacific Geology, 8, 1-38.

Aguirre, L., 1983. Granitoids in Chile in J.A. Roddick (Ed.), Circum-Pacific Plutonic Terranes. Geol. Soc. Am. Memoir 159, 293-316 .

Airo, M.-L., 1991. Geological Survey of Finland Report of Investigation.

Allis, R.G., 1990. Geophysical anomalies over epithermal systems. J. Geochem. Explor., 36, 339-374.

Alva-Valdivia, L.M., Urrutia-Fucugauchi, J., Bo"hnel, H. and Moran-Zenteno, D.J., 1991. Aeromagnetic anomalies and paleomagnetism in Jalisco and Michoachan, southern Mexico continental margin. Tectonophysics, 192, 169-190.

Andersen, R.N., Clague, D.A., Klitgord, K.D., Marshall, M. and Hishimori, R.K., 1975. Magnetic and petrologic variations along the Galapagos Spreading Center and their relation to the Galapagos Melting Anomaly. Geol. Soc. Am. Bull., 86, 683-694.

Anderson, A.T., 1968. Oxidation of the Lablanche Lake titaniferous magnetite deposit, Quebec. J. Geol., 76, 528-547.

Anderson, J.L., 1980. Mineral equilibria and crystallization conditions in the Late Precambrian Wolf River rapakivi massif, Wisconsin. Am. J. Sci., 280, 289-332.

Anderson, J.L. and Bender, E.E., 1989. Nature and origin of A- type granitic magmatism in the southwestern United States of America. Lithos, 23, 19-52.

Anderson, J.L. and Cullers, R.L., 1978. Geochemistry and evolution of the Wolf River Batholith, a Late Precambrian rapakivi massif in North Wisconsin, U.S.A. Precam. Res., 7, 287- 324.

Anderson, J.L. and Rowley, M.C., 1981. Synkinematic intrusion of peraluminous and associated metaluminous granitic magmas, Whipple Mountains, California. Can. Mineral., 19, 83-101.

Anderson, J.L., Cullers, R.L. and Van Schmus, W.R., 1980. Anorogenic metaluminous and peraluminous granitic plutonism in the mid-Proterozoic of Wisconsin, U.S.A. Contrib. Mineral. Petrol., 74, 311-328.

Anderson, R.G., 1985. An overview of some Mesozoic and Tertiary plutonic suites and their associated mineralization in the northern Canadian Cordillera in R.P. Taylor and D.F. Strong (eds), Granite-related Mineral Deposits, Geology, Petrogenesis and Tectonic Setting, CIM Geology Division.

Andersson, U.B., 1989. Evidence of plutonic magma-mixing, southern Sweden. Rend. Soc. Ital. Mineral. Petrol., 43, 831-839.

Andersson, U.B., 1991. Granitoid episodes and mafic-felsic magma interaction in the Svecofennian of the Fennoscandian Shield, with main emphasis on the ~1.8 Ga plutonics. Precam. Res., 51, 127-149.

Arndt, N.T., Naldrett, A.J, and Pyke, D.R.,1977. Komatiitic and iron-rich tholeiitic lavas of Munro Township, Northeast Ontario. Journ. Petrol., v.18, pp319-369.

Arth, J.G., Barker, F., Peterman, Z.L. and Friedman, I., 1978. Geochemistry of the gabbro-diorite-tonalite-trondhjemite suite of southwest Finland and its implications for the origin of tonalitic and trondhjemitic magmas. J. Petrology, 19, 289-316.

Asami, N. and Britten, R.M., 1980. The porphyry copper deposits at the Frieda River Prospect, Papua New Guinea. Mining Geology Special Issue, 8, 117-139.

Ashley, P.M., 1975. Opaque mineral assemblage formed during serpentinization in the Coolac Ultramafic Belt, New South Wales. J. Geol. Soc. Aust., 22, 91-102.

Ashley, P.M., Dudley, R.J., Lesh, R.H., Marr, J.M. and Ryall, A.W., 1988. The Scuddles Cu-Zn prospect, an Archean volcanogenic massive sulfide deposit, Golden Grove district, Western Australia. Econ. Geol., 83, 918-951.

Atherton, M.P. and Tarney, J., 1979 (eds). Origin of Granite Batholiths. Shiva Publishing, 148 pp.

Balsey, J.R. and Buddington, A.F., 1958. Iron-titanium oxide minerals, rocks, and aeromagnetic anomalies of the Adirondack area, New York. Econ. Geol., 53, 777-805.

Barink, H.W., 1982. Decrease of cation-deficiency in rock-forming minerals as the cause of the retrogressive oxidation of accessory Fe-Ti oxides in deep-seated rocks; a new approach. N. Jb. Miner. Mh., H.1, 29-44.

Barker, F., 1981. Introduction to special issue on granites and rhyolites: a commentary for the nonspecialist. J. geophys. Res., 86, 10,131-10,135.

Barker, F., Wones, D.R., Sharp, W.N. and Desborough, G.A., 1975. The Pikes Peak batholith, Colorado Front Range, and a model for the origin of the gabbro-anorthosite-syenite-potassic granite suite. Precamb. Res., 2, 97-160.

Barnes, S.J., Gole, M.J. and Hill, R.E.T., 19 .The Agnew Nickel Deposit, Yilgarn BLock, Western Australia: Stratigraphy, Structure, Geochemistry and Origin. WAMPRI Project 38, Final Report.

Barnes, S.J., Gole, M.J. and Hill, R.E.T., 1988a. The Agnew nickel deposit, Western Australia: Part I. Structure and stratigraphy. Econ. Geol., 83, 524-536.

Barnes, S.J., Gole, M.J. and Hill, R.E.T., 1988b. The Agnew nickel deposit, Western Australia: Part II. Sulfide geochemistry with emphasis on the platinum-group elements. Econ. Geol., 83, 537-550.

Barrett, F.M., Groves, D.I. and Binns, R.A., 1976. Importance of metamorphic processes at the Nepean nickel deposit, Western Australia. Trans. Inst. Min. Metall., 85, B252-B273.

Bateman, P.C., 1983. A summary of critical relations in the Sierra Nevada batholith, California, U.S.A. in J.A. Roddick (Ed.), Circum-Pacific Plutonic Terranes. Geol. Soc. Am. Memoir 159, 241-254.

Bateman, P.C. and Chappell, B.W., 1979. Crystallization, fractionation, and solidification of the Tuolumne Intrusive Series, Yosemite National Park, California. Geol. Soc. Am. Bull., 90, 465-482.

Bateman, P.C. and Dodge, F.C.W., 1970. Variations of major chemical constituents across the central Sierra Nevada batholith. Geol. Soc. Am. Bull., 81, 409-420.

Bateman, P.C., Dodge, F.C.W. and Kistler, R.W., 1991. Magnetic susceptibility and relation to initial $^{87}Sr/^{86}Sr$ for granitoids of the central Sierra Nevada, California. J. Geophys. Res., 96, 19,555-19,568.

Beane, R.E. and Titley, S.R., 1981. Porphyry copper deposits. Part II. Hydrothermal alteration and mineralization. Econ. Geol., 75th Anniversary Volume, 235-269.

Belluso, E., Bino, G. and Lanza, R., 1990. New data on the rock magnetism in the Ivrea-Verbano Zone (northern Italy) and its relationship to magnetic anomalies. Tectonophysics, 182, 79-89.

Berner, R., 1970. Iron in Handbook of Geochemistry, Springer- Verlag, Berlin.

Bideau, D., Hebert, R., Hekinian, R. and Cannat, M., 1991. Metamorphism of deep-seated rocks from the Garret ultrafast transform (East Pacific Rise near 13°25'S). J. Geophys. Res., 96, 10,079-10,099.

Bina, M.M. and Henry, B., 1990. Magnetic properties, opaque mineralogy and magnetic anisotropies of serpentinized peridotites from ODP Hole 670A near the Mid-Atlantic Ridge. Phys. Earth Planet. Inter., 65, 88-103.

Binns, R.A.,, Gunthorpe, R.J. and Groves, D.I., 1976. Metamorphic patterns and development of greenstone belts in the Eastern Yilgarn Block in B.F. Windley (ed), The Early History of the Earth, Wiley, London, pp. 303-313.

Blais, S. and Auvray, B., 1990. Serpentinization in the Archean komatiitic rocks of the Kuhmo Greenstone Belt, eastern Finland. Can. Mineral., 28, 55-66.

Bleil, U. and Petersen, N., 1982. Magnetic properties of minerals in G. Angenheister (ed), Physical Properties of Rocks, Landolt-Bornstein Numerical Data and Functional Relationships in Science and Technology, Group V, Volume 1b. Springer-Verlag, Berlin.

Blevin, P.L. and Chappell, B.W., 1991. Relationships between granites and mineral deposits in the Lachlan Fold Belt.

Blevin, P.L. and Chappell, B.W., 1991. Some fundamental parameters in granitoid metallogeny: an eastern Australian perspective in Second Hutton Symposium on Granites and Related Rocks, BMR Record 1991/25, 10.

Bliss, N.W. and Maclean, W.H., 1975. The paragenesis of zoned chromite from central Manitoba. Geochim. Cosmochim. Acta, 39, 973-990.

Böhnel, H. and Negedank, J.F.W., 1988. Paleomagnetism of the Puerta Vallarta intrusive complex and the accretion of the Guerrero terrain, Mexico. Phys. Earth Planet. Inter., 52, 330- 338.

Böhnel, H. and Negedank, J.F.W., 1988. Paleomagnetism and ore petrology of three Cretaceous-Tertiary batholiths of southern Mexico. N. Jb. Geol. Palaont. Mh., 2, 97-127.

Bonin, B. and Giret, A., 1984. The plutonic alkaline series: the problem of their origin and differentiation, the role of their mineralogical assemblages. Phys. Earth Planet. Inter., 35, 212- 221.

Borisov, A.A. and Shapkin, A.I., 1990. A new empirical equation relating Fe^{3+}/Fe^{2+} in magmas to their composition, oxygen fugacity and temperature. Geochemistry International, 6, 111-116.

Bouchez, J.L., Gleizes, G., Djouadi and Rochette, P., 1990. Microstructure and magnetic susceptibility applied to emplacement kinetics of granites: the example of the Foix pluton (French Pyrenees). Tectonophysics, 184, 157-171.

Bowden, P., 1982. Magmatic evolution and mineralization in the Nigerian Younger Granite Province in Metallization Associated with Acid Magmatism, A.M. Evans (Ed.), Wiley.

Bowden, P., Batchelor, R.A., Chappell, B.W., Didier, J. and Lameyre, J., 1984. Petrological, geochemical and source criteria for the classification of granitic rocks: a discussion. Phys. Earth Planet. Inter., 35, 1-11.

Bowles, J.F.W., 1976. Distinct cooling histories of troctolites from the Freetown layered gabbro. Mineral. Mag., 40, 703-714.

Bowles, J.F.W., 1977. A method of tracing the temperature and oxygen-fugacity histories of complex magnetite-ilmenite grains. Mineral. Mag., 41, 103-109.

Brewster, D. and O'Reilly, W., 1988. Magnetic properties of synthetic analogues of the altered olivines of igneous rocks. Geophys. J., 95, 421-432.

Brown ,G.C., 1979. The changing pattern of batholith emplacement during Earth history in Atherton, M.P. and Tarney, J., 1979 (eds). Origin of Granite Batholiths. Shiva Publishing, pp. 106- 115.

Brown, G.C., Thorpe, R.S. and Webb, P.C., 1984. The geochemical characteristics of granitoids in contrasting arcs and comments on magma sources. J. Geol. Soc. London, 141, 413-426.

Buddington, A.F., 1951. Chemical petrology of some metamorphosed Adirondack gabbroic, syenitic and quartz syenitic rocks. Am J. Sci., Bowen Volume, 37-84.

Buddington, A.F. and Lindsley, D.H., 1964. Iron-titanium oxide minerals and synthetic equivalents. J. Petrology, 5, 310-357.

Burkhard, D.J.M., 1991. Temperature and redox path of biotite- bearing intrusives: a method of estimation applied to S- and I- type granites from Australia. Earth Planet. Sci. Lett., 104, 89- 98.

Burnham, C.W. and Ohmoto, H., 1980. Late stage processes of felsic magmatism. Mining Geology Special Issue, 8, 1-11.

Cameron, E.M. and Carrigan, W.J., 1987. Oxygen of Archean felsic magmas: relationship to gold mineralization. Geol. Surv. Canada, Paper 87-1A, 281-298.

Cameron, E.M. and Hattori, K., 1987. Archean gold mineralization and oxidised hydrothermal fluids. Econ. Geol., 82, 1177-1191.

Candela, P.A., 1986. The evolution of aqueous vapour from igneous melts: effect on oxygen fugacity. Geochim. Cosmochim. Acta, 50, 1205-1211.

Candela, P.W., 1991. Controls on metal ratios in granite-related ore systems: an experimental and computational approach in Second Hutton Symposium on Granites and Related Rocks, BMR Record 1991/25, 10.

Carmichael, I.S.E., 1967. The iron-titanium oxides of salic volcanic rocks and their associated ferromagnesian silicates. Contrib. Mineral. Petrol., 14, 36-64.

Carmichael, I.S.E., 1972. The occurrence of magnesian pyroxene and magnetite in porphyritic acid glasses.

Carmichael, I.S.E., 1991. The redox states of basic and silicic magmas: a reflection of their source regions. Contrib. Mineral. Petrol., 106, 129-141.

Carmichael, I.S.E. and Ghiorso, M.S., 1986. Oxidation-reduction relations in basic magma - a case for homogeneous equilibria. Earth Planet. Sci. Lett., 78, 200-210.

Carmichael, I.S.E. and Ghiorso, M.S., 1990. The effect of oxygen fugacity on the redox state of natural liquids and their crystallizing phases. Rev. Mineral.,24, 192-212.

Carmichael, I.S.E. and Nicholls, J., 1967. Iron-titanium oxides and oxygen fugacities in volcanic rocks. J. Geophys. Res., 62, 4665-4687.

Clark D.A. and Schmidt P.W. 1982. Theoretical analysis of thermomagnetic properties, low-temperature hysteresis and domain structure of titanomagnetites. Phys. Earth Planet. Int. 30, 300- 316.

Clark, D.A. and Schmidt, P.W., 1986. Geological structure and magnetic signatures of Hamersley BIFs. CSIRO Restricted Investigation Report 1639R.

Clark, D.A. and Emerson, D.W., 1992. Notes on rock magnetization characteristics in applied geophysical studies. Explor. Geophys., 22, 547-555.

Clark, D.A. and Tonkin, C., 1987. Magnetic properties of ironstones and host rocks from the Tennant Creek area. CSIRO Restricted Investigation Report 1691R.

Clark, K.A., 1982. Mineral composition of rocks in R.S. Carmichael (ed), CRC Handbook of Physical Properties of Rocks, Volume I, pp. 1-215.

Clarke, D.B., 1981. The mineralogy of peraluminous granites: a review. Can. Mineral., 19, 3-17.

Clifford, B.A., 1987. A field guide to the geology of the Gossan Hill Group at Golden Grove, W.A. ACM Ltd.

Coleman, M.L., 1986. Isotopic analysis of trace sulphur from some S- and I-type granites: heredity or environment? in M.P.Coward and A.C. Ries (eds), Collision Tectonics, Geol. Soc. Spec. Pub., 19, 129-133.

Coleman, R.G., 1971. Petrologic and geophysical nature of serpentinites. Geol. Soc. Am. Bull., 82, 897-918.

Collins, W.J., Beams, S.D., White, A.J.R. and Chappell, B.W., 1982. Nature and origin of A-type granites with particular reference to southeastern Australia. Contrib. Mineral. Petrol., 80, 189-200.

Cooper, J.A., Nesbitt, R.W., Platt, J.P., and Mortimer, G.E., 1978. Crustal development in the Agnew Region, Western Australia, as shown by Rb/Sr isotopic and geochemical studies. Precamb. Res., v.7, pp31-59.

Cornwell, J.D., 1975. The magnetization and densities of Precambrian rocks and iron-ores of northern Sweden. Geoexploration, 13, 201-214.

Cox, A., Doell, R.R. and Thompson, G., 1964. Magnetic properties of serpentinite from Mayaguez, Puerto Rico in A Study of Serpentinite: the AMSOC core hole near Mayaguez, Puerto Rico. National Academy of Siences - National Research Council, Washington, Publication No. 1188.

Crawford, M.B. and Windley, B.F., 1990. Leucogranites of the Himalaya/Karakoram: implications for magmatic evolution within collisional belts and the study of collision-related leucogranite petrogenesis.

Criss, R.E. and Champion, D.E., 1984. Magmatic properties of rocks from the southern half of the Idaho batholith: influences of hydrothermal alteration and implications for aeromagnetic interpretation. J. Geophys. Res., 89, 7061-7076.

Cuney, M., Sabate, P., Vidal, P., Marinho, M.M. and Conceicao, H., 1990. The 2 Ga peraluminous magmatism of the Jacobina- Contendas Mirante belt (Bahia, Brazil): major and trace-element geochemistry and metallogenic potential. J. Volcan. Geother. Res., 44, 123-141.

Cunneen, J.P. and Wellman, P., 1987. The use of airborne geophysics and ground gravity surveys in understanding the geology of the Eastern Goldfields of Western Australia. Explor. Geophys., 18, 22-25.

Currie, K.L. and Pajari, G.E., 1981. Anatectic peraluminous granites from the Carmanville area, northeastern Newfoundland. Can. Mineral., 19, 147-161.

Currie, K.L., Eby, G.N. and Gittins, J., 1986. The petrology of the Mont Saint Hilaire Complex, southern Quebec: an alkaline gabbro-peralkaline syenite association. Lithos, 19, 65-81.

Czamanske, G.K. and Dillet, B., 1988. Alkali amphibole, tetrasilicic mica, and sodic pyroxene in peralkaline siliceous rocks, Questa Caldera, New Mexico. Am. J. Sci., 288-A, 358-392.

Czamanske, G.K. and Mihalik, P., 1972. Oxidation during magmatic differentiation, Finnamarka Complex, Oslo area, Norway: Part 1, the opaque oxides. J. Petrology, 13, 493-509.

Czamanske, G.K. and Wones,D.R., 1973. Oxidation during magmatic differentiation, Finnamarka Complex, Oslo area, Norway: Part 2, the mafic silicates. J. Petrology, 14, 349-380.

Czamanske, G.K., Wones, D.R. and Eichelberger, J.C., 1977. Mineralogy and petrology of the intrusive complex of the Pliny Range, New Hampshire. Am. J. Sci., 277, 1073-1123.

Czamanske, G.K., Ishihara, S. and Atkin, S.A., 1981. Chemistry of rock-forming minerals of the Cretaceous-Paleocene batholith in southwestern Japan and implications for magma genesis. J. Geophys. Res., 86, 10431-10469.

Dall'agnol, R., 1989. Proterozoic granitoids of the Carajas-Rio Maria Province, eastern Amazonian region, Brazil in I. Haapala and Y. Kahkonen (eds). Symposium Precambrian Granitoids. Geol. Surv. Finland Spec. Paper 8, 34.

Davis, K.E., 1981. Magnetite rods in plagioclase as the primary carrier of stable NRM in ocean floor gabbros. Earth Planet. Sci. Lett., 55, 190-198.

Davison, F.C. and Ellwood, B.B., 1983.Thermomagnetic characteristics in late orogenic granites and gneisses of the southern Appalachian Piedmont. Earth Planet. Sci. Lett., 64, 117-122.

Desborough, G.A., Ludington, S.D. and Sharp, W.N., 1980. Redskin Granite: a rare-metal-rich Precambrian pluton, Colorado, USA. Min. Mag., 43, 959-966.

Dickenson, M.P. and Hess, P.C., 1981. Redox equilibria and the structural role of iron in alumino-silicate melts. Contrib. Mineral. Petrol., 78, 352-357.

Dickenson, M.P. and Hess, P.C., 1986. The structural role and homogeneous redox equilibria of iron in peraluminous, metaluminous and peralkaline silicate melts. Contrib. Mineral. Petrol., 92, 207-217.

Dodge, F.C.W., 1972. Variation of ferric-ferrous ratios in the central Sierra Nevada batholith, U.S.A. 24th IGC, Section 10, 12-19.

Dodge, F.C.W., Smith, V.C. and Mays, R.E., 1969. Biotites from granitic rocks of the central Sierra Nevada batholith, California. J. Petrology, 10, 250-271.

Donaldson, M.J., 1981. Redistribution of ore elements during serpentinization and talc-carbonate alteration of some Archean dunites, Western Australia. Econ. Geol., 76, 1698-1713.

Donaldson, M.J. and Bromley, G.J., 1981. The Honeymoon Well nickel sulfide deposits, Western Australia. Econ. Geol., 76, 1550-1564.

Drummond, S.E. and Ohmoto, H., 1985. Chemical evolution and mineral deposition in boiling hydrothermal systems. Econ. Geol., 80, 126-147.

DuBois, R.L., 1963. Remanent, induced and total magnetism of a suite of serpentine specimens from the Sierra Nevada, California. J. Geophys. Res., 68, 267-278.

Dunlop, D.J., 1990. Developments in rock magnetism. Rep. Prog. Phys., 53, 707-792.

Dunlop, D.J. and Prevot, M., 1982. Magnetic properties and opaque mineralogy of drilled submarine intrusive rocks. Geophys. J. R. astron. Soc., 69, 763-802.

Eales, H.V., Wilson, A.H. and Reynolds, I.M., 1988. Complex unmixed spinels in layered intrusions within an obducted ophiolite in the Natal-Namaqua mobile belt. Mineral. Deposita, 23, 150-157.

Eby, G.N., 1990. The A-type granitoids: a review of their occurrence and chemical characteristics and speculations on petrogenesis. Lithos, 26, 115-134.

Eckstrand, O.R., 1972. Redox control of the formation of nickeliferous opaque mineral assemblages in a serpentinite. 24th IGC, Abstracts with Programs, Section 10, 25.

Eckstrand, O.R., 1975. The Dumont serpentinite: a model for control of nickeliferous opaque mineral assemblages by alteration reactions in ultramafic rocks. Econ. Geol., 70, 183- 201.

Einaudi, M.T., Meinert, L.D. and Newberry, R.J., 1981. Skarn deposits. Econ. Geol., 75th Anniversary Volume, 317-391.

Elliott, R.B., 1973. The chemistry of gabbro/amphibolite transitions in south Norway. Contrib. Mineral. Petrol., 38, 71- 79.

Ellwood, B.B., 1981. Weathering effects on the magnetic properties of the Milledgeville granite, Georgia. Earth Planet. Sci. Lett., 55, 311-316.

Ellwood, B.B. and Wenner, D.B., 1981. Correlation of magnetic susceptibility with 18O/16O data in late orogenic granites of the southern Appalachian Piedmont. Earth Planet. Sci. Lett., 54, 200-202.

Elo,S. and Tuomi, A., 1989. Gravimetric, magnetic and seismic interpretations of rapakivi massifs in southeastern Finland in I. Haapala and Y. Kahkonen (eds). Symposium Precambrian Granitoids. Geol. Surv. Finland Spec. Paper 8, 45.

Emerson, D.W., Embleton, B.J.J. and Clark, D.A., 1979. The Petrophysical and petrologic characteristics of the magnetic igneous intrusion at Mt Derriwong, N.S.W. Bull. Aust. Soc. Explor. Geophys., 10,67-78.

Emerson, D.W. and Welsh, H.K., 1987. Some physical property characteristics of zeolitic rock - preliminary results. Explor. Geophys., 18, 393-400.

Emslie, R.F., 1991. Granitoids of rapakivi granite-anorthosite and related associations. Precam. Res., 51, 173-192.

Engel, A.E.J. and Engel, C.G., 1962. Progressive metamorphism of amphibolite, northwest Adirondack mountains, New York. Am. J. Sci., Buddington Volume, 37-62.

Eugster, H.P., 1959. Oxidation and reduction in metamorphism in P.H. Abelson (ed), Researches in Geochemistry, Wiey, New York, 397-426.

Eugster, H.P., 1972. Reduction and oxidation in metamorphism (II). 24th IGC, Abstracts with Programs, Section 10, 3-11.

Evans, B.W. and Frost, B.R., 1975. Chrome-spinel in progressive metamorphism - a preliminary analysis. Geochim. Cosmochim. Acta, 39, 959-972.

Ewart, A., 1976. Mineralogy and chemistry of some modern orogenic lavas - some statistics and implications. Earth Planet. Sci. Lett., 31, 417-432.

Ewart, A., 1981. The mineralogy and chemistry of the anorogenic Tertiary silicic volcanics of S.E. Queensland and N.E. New South Wales, Australia. J. Geophys. Res., 86, 10,242-10,256.

Fershtater, G.B. and Chashchukhina, V.A., 1979. Granitoid mineral parageneses in various ferrofacies. Geochemistry International, 3, 48-61.

Fershtater, G.B., Borodina, N.S. and Chashchukhina, V.A., 1978. Granitoid ferrofacies. Geochemistry International, 2, 91-102.

Flohr, M.J.K. and Ross, M., 1990. Alkaline igneous rocks of Magnet Cove, Arkansas: mineralogy and geochemistry of syenites. Lithos, 26, 67-98.

Flood, R.H. and Shaw, S.E., 1975. A cordierite-bearing granite suite from the New England batholith, N.S.W., Australia. Contrib. Mineral. Petrol., 52, 157-164.

Flood, R.H. and Shaw, S.E., 1991. A pressure-quench cumulate origin for microgranitoid enclaves in Second Hutton Symposium on Granites and Related Rocks, BMR Record 1991/25, 10.

Forster, H.-J., Tischendorf, G. and Thomas, R., 1989. Geochemical and physicochemical comparison of Precambrian and Phanerozoic tin-specialized granitic rocks - the Proterozoic anorogenic rapakivi granites of Finland and the Hercynian late orogenic granite complexes of the Erzgebirge, GDR in I. Haapala and Y. Kahkonen (eds). Symposium Precambrian Granitoids. Geol. Surv. Finland Spec. Paper 8, 52.

Fox, P.J. and Opdyke, N.D., 1973. Geology of the oceanic crust: magnetic properties of oceanic rocks. J. Geophys. Res., 78, 5139-5154.

Frater, K.M., 1985a. Mineralization at the Golden Grove Cu-Zn deposit, Western Australia. I: Premetamorphic textures of the opaque minerals. Can. J. Earth Sci., 22, 1-14.

Frater, K.M., 1985b. Mineralization at the Golden Grove Cu-Zn deposit, Western Australia. II: Deformation textures of the opaque minerals. Can. J. Earth Sci., 22, 15-26.

Frost, B.R., 1985. On the stability of sulfides, oxides and native metals in serpentinite. J. Petrology, 26, 31-63.

Frost, B.R., 1988. A review of graphite-sulfide-oxide-silicate equilibria in metamorphic rocks. Rend. Soc. Ital. Mineral. Petrol., 43, 25-40.

Frost, B.R., 1991a. Introduction to oxygen fugacity and its petrologic importance in D.H. Lindsley (ed), Oxide Minerals: petrologic and magnetic significance. Rev. Mineral., 25, 1-9.

Frost, B.R., 1991b. Stability of oxide minerals in metamorphic rocks in D.H. Lindsley (ed), Oxide Minerals: petrologic and magnetic significance. Rev. Mineral., 25, 469-488.

Frost, B.R., 1991d. Magnetic petrology: factors that control the occurrence of magnetite in crustal rocks in D.H. Lindsley (ed), Oxide Minerals: petrologic and magnetic significance. Rev. Mineral., 25, 489-509.

Frost, B.R. and Lindsley, D.H., 1991. Occurrence of iron-titanium oxides in igneous rocks in D.H. Lindsley (ed), Oxide Minerals: petrologic and magnetic significance. Rev. Mineral., 25, 489-509.

Frost, B.R., Lindsley, D.H. and Andersen, D.J., 1988. Fe-Ti oxide-silicate equilibria: assemblages with fayalitic olivine. Am. Mineral., 73, 727-740.

Frost, T.P. and Mahood, G.A., 1987. Field, chemical, and physical constraints on mafic-felsic magma interaction in the Lamarck Granodiorite, Sierra Nevada, California. Geol. Soc. Am. Bull., 99, 272-291.

Fudali, R.F., 165. Oxygen fugacities of basaltic and andesitic magmas. Geochim. Cosmochi. Acta, 29, 1063-1075.

Gaucher, E.H.S., 1965. Quantitative interpretation of the "Montagne du Sorcier" magnetic anomaly, Chibougamau, Quebec. Geophysics, 30, 762-782.

Ghiorso, M.S. and Sack, R.O., 1991. Fe-Ti oxide geothermometry: thermodynamic formulation and the estimation of intensive variables in silicic magmas. Contrib. Mineral. Petrol., 108, 484-510.

Goad, B.E. and Cerny, P., 1981. Peraluminous pegmatitic granites and their pegmatite aureoles in the Winnipeg River District, southeastern Manitoba. Can. Mineral., 19, 177-194.

Godoy, E. and Kato, T., 1990. Late Paleozoic serpentinites and mafic schists from the Coast Range accretionary complex, central Chile: their relationship to aeromagnetic anomalies. Geol. Rund., 79, 121-130.

Goellnicht, N.M., Groves, D.I. and McNaughton, N.J., 1989. Granitoids as indicators of tectonic setting of the Telfer District, Paterson Province, Western Australia.

Goellnicht, N.M., Groves, D.I. and McNaughton, N.J., 1991. Late Proterozoic fractionated granitoids of the mineralized Telfer area, Paterson Province, Western Australia. Precam. Res., 51, 375-391.

Golding, H.G. and Bayliss, P., 1968. Altered chrome ores from the Coolac Serpentine Belt, New South Wales, Australia. Am. Mineral., 53, 162-183.

Gole, M.J., Barnes, S.J. and Hill, R.E.T., 1987. The role of fluids in the metamorphism of komatiites, Agnew nickel deposit, Western Australia. Contrib. Mineral. Petrol., 96, 151-162.

Gower, C.F., Heaman, L.M., Loveridge, W.D., Scharer, U. and Tucker, R.D., 1991. Grenvillian magmatism in the eastern Grenville Province, Canada. Precam. Res., 51, 315-336.

Grant, F.S., 1985a. Aeromagnetics, geology and ore environments, I. Magnetite in igneous, sedimentary and metamorphic rocks: an overview. Geoexploration, 23, 303-333.

Grant, F.S., 1985b. Aeromagnetics, geology and ore environments, II. Magnetite and ore environments. Geoexploration, 23, 335-362.

Green, D.H. and Ringwood, A.E., 1967. An experimental investigation of the gabbro to eclogite transformation and its petrological applications. Geochim. Cosmochim. Acta, 31, 767- 833.

Griscom, A., 1964. Magnetic properties and aeromagnetic interpretation of serpentinite from southwest Puerto Rico in A Study of Serpentinite: the AMSOC core hole near Mayaguez, Puerto Rico. National Academy of Sciences - National Research Council, Washington, Publication No. 1188.

Groves, D.I. and Keays, R.R., 1979. Mobilization of ore-forming elements during alteration of dunites, Mt Keith-Betheno, Western Australia. Can. Mineral., 17, 373-389.

Groves, D.I., Hudson, D.R. and Hack, T.B.C., 1974. Modification of iron-nickel sulfides during serpentinization and talc- carbonate alteration at Black Swan, Western Australia. Econ. Geol., 69, 1265-1281.

Groves, D.I., Barrett, F.M., Binns, R.A. and McQueen, K.G., 1977. Spinel phases associated with metamorphosed volcanic-type iron-nickel sulfide ores from Western Australia. Econ. Geol., 72, 1224-1244.

Guidotti, C.V. and Dyar, M.D., 1991. Ferric iron in metamorphic biotite and its petrologic and crystallochemical implications. Am. Mineral., 76, 161-175.

Gwinn and Hess, 1989. Iron and titanium in peraluminous and peralkaline rhyolitic liquids. Contrib. Mineral. Petrol., 101, 326-338.

Haapala, I., 1974. Some petrological and geochemical characteristics of rapakivi granite varieties associated with greisen-type Sn, Be and W mineralization in the Eurajoki and Kymi areas, southern Finland in Metallization Associated with Acid Magmatism, Geol. Surv. Czechoslovakia, Prague, pp. 159-169.

Haapala, I. and Kahkonen, Y., 1989 (eds). Symposium Precambrian Granitoids. Geol. Surv. Finland Spec. Paper 8.

Haapala, I. and Lindh, A., 1989. The postorogenic and anorogenic Proterozoic granites of the Fennoscandian Shield in I. Haapala and Y. Kahkonen (eds). Symposium Precambrian Granitoids. Geol. Surv. Finland Spec. Paper 8, 63.

Haapala, I., Front, K., Rantala, E. and Vaarma, M., 1987. Petrology of Nattanen-type granite complexes, northern Finland. Precam. Res., 35, 225-240.

Hageskov, B., 1984. Magnetic susceptibility used in mapping of amphibolite facies recrystallization in basic dykes. Tectonophysics, 108, 339-351.

Haggerty, S.E., 1976a. Oxidation of opaque mineral oxides in basalts in D. Rumble (ed), Oxide Minerals. Mineral. Soc. Amer. Short Course Notes (Rev. Mineral.), 3, Hg-1 - Hg-100.

Haggerty, S.E., 1976b. Opaque mineral oxides in terrestrial igneous rocks in D. Rumble (ed), Oxide Minerals. Mineral. Soc. Amer. Short Course Notes (Rev. Mineral.), 3, Hg-101 - Hg-300.

Haggerty, S.E., 1979. The aeromagnetic mineralogy of igneous rocks. Can. J. Earth Sci., 16, 1281-1293.

Hammarstrom, J.M. and Zen, E-an, 1991. Petrologic characteristics of magmatic epidote-bearing granitoids of the western cordillera of North America in Second Hutton Symposium on Granites and Related Rocks, BMR Record 1991/25, 10.

Hammond, P.A. and Taylor, L.A., 1982. The ilmenite/titano- magnetite assemblage: kinetics of re-equilibration. Earth Planet. Sci. Lett., 61, 143-150.

Harding, K.L., Morris, W.A., Balch, S.J., Lapointe, P. and A.G. Latham, 1988. A comparison of magnetic character and alteration in three granite drill cores from eastern Canada. Can. J. Earth Sci., 25, 1141-1150.

Harris, N.B.W., Pearce, J.A. and Tindle, A.G., 1986. Geochemical characteristics of collision zone magmatism in M.P.Coward and A.C. Ries (eds), Collision Tectonics, Geol. Soc. Spec. Pub., 19, 67-81.

Harrison, T.N., Parsons, I. and Brown, P.E., 1990. Mineralogical evolution of fayalite-bearing rapakivi granites from the Prins Christians Sund pluton, South Greenland. Min. Mag., 54, 57-66.

Hattori, K., 1987. Magnetic felsic intrusions associated with Canadian Archean gold deposits. Geology, 15, 1107-1111.

Hattori, K., 1991. Archaean gold mineralization and granitoid intrusions in the Superior Province of Canada: a review in Second Hutton Symposium on Granites and Related Rocks, BMR Record 1991/25, 10.

Heitanen, A., 1986. Role of replacement in the genesis of anorthosite in Boehls Butte area, Idaho. Bull. Geol. Soc. Finland, 58, 71-79.

Henkel, H., 1991. Petrophysical properties (density and magnetization) of rocks from the northern part of the Baltic Shield. Tectonophysics, 192, 1-19.

Hill, R. and Roeder,P., 1974. The crystallization of spinel from basaltic liquid as a function of oxygen fugacity. J. Geol., 82, 709-729.

Hill, R.T., Gole, M.J. and Barnes, S.J., 1987. Physical Volcanology of Komatiites. Geol. Soc. Australia (W.A. Div.), Excursion Guide No. 1.

Hine, R., Williams, I.S., Chappell, B.W. and White, A.J.R., 1978. Contrasts between I-type and S-type granitoids of the Kosciusko batholith. J. Geol. Soc. Australia, 25, 219-234.

Hogan, J.P., Gilbert, M.C. and Weaver, B.L., 1991. Textural, mineralogical and chemical variation in shallow, A-type, sheet granites of the Wichita Mountains Igneous Province, Oklahoma, U.S.A. in Second Hutton Symposium on Granites and Related Rocks, BMR Record 1991/25, 10.

Hubbard, F. and Branigan, N., 1987. Late Svecofennian magmatism and tectonism, Aland, southwest Finland. Precam. Res., 35, 241- 256.

Hughes, C.J., 1982. Igneous Petrology. Elsevier, Amsterdam.

Hutchison, C.S., 1982. The various granitoid series and their relationship to W and Sn mineralisation. Tungsten Geology Symposium, Jianxi. Geological Publishing House, Beijing.

Hyndman, D.W., 1981. Controls on source and depth of emplacement of granitic magma. Geology, 9, 244-249.

Hyndman, D.W., 198?. Petrology of Igneous and Metamorphic Rocks (Second edition). McGraw-Hill, New York.

Hyndman, D.W., 1983. The Idaho batholith and associated plutons, Idaho and western Montana in J.A. Roddick (Ed.), Circum-Pacific Plutonic Terranes. Geol. Soc. Am. Memoir 159, 213-240.

Hyndman, D.W. and Foster, D.A., 1988. The role of tonalites and mafic dykes in the generation of the Idaho Batholith. J. Geol., 96, 31-46.

Irvine, R.J. and Robertson, I., 1987. Interpretation of airborne geophysical data over the Ok Tedi porphyry copper-gold orebody using image processing techniques. Explor. geophys., 18, 103- 107.

Ishihara, S., 1977. The magnetite-series and ilmenite-series granitic rocks. Min. Geol., 27, 293-305.

Ishihara, S., 1978. Metallogenesis in the Japanese island arc system. J. Geol. Soc. Lond., 135, 389-406.

Ishihara, S., 1979. Lateral variation of magnetic susceptibility of the Japanese granitoids. J. Geol. Soc. Japan, 85, 509-523.

Ishihara, S., 1981. The granitoid series and mineralization. Econ. Geol., 75th Anniversary Volume, 458-484.

Ishihara, S., 1982. Granitoid series and tungsten deposits in Japan. Tungsten Geology Symposium, Jianxi. Geological Publishing House, Beijing.

Ishihara, S. and Sasaki, A., 1989. Sulfur isotope ratios of the magnetite-series and ilmenite-series granitoids of the Sierra- Nevada batholith - a reconnaissance study. Geology, 17, 788-791.

Ishihara, S. and Terashima, S., 1989. Carbon contents of the magnetite-series and ilmenite-series granitoids of Japan. Geochim. J., 23, 25-36.

Ishihara, S., Sawata, H., Arpornsuwan, S., Busaracome, P. and Bungbrakearti, N., 1979. The magnetite-series and ilmenite- series granitoids and their bearing on tin mineralization, particularly of the Malay Peninsula region. Geol. Soc. Malaysia. Bull., 11, 103-110.

Ishihara, S., Sawata, H., Shibata, K., Terashima, S., Arrykul, S. and Sato, K., 1980. Granites and Sn-W deposits of peninsular Thailand. Min. Geol. Spec. Issue, 8, 223-241.

Ishihara, S., Terashima, S. and Tsukimura, K., 1987. Spatial distribution of magnetic susceptibility and ore elements, and cause of local reduction on magnetite-series granitoids and related ore deposits at Chichibu, central Japan. Min. Geol., 37, 15-28.

Jahren, C.E., 1965. Magnetization of Keweenanan rocks near Duluth, Minnesota. Geophysics, 30, 858-874.

James, R.S., Turnock, A.C. and Fawcett, J.J., 1976. The stability and phase relations of iron chlorite below 8.5 kb PH O. Contrib. Mineral. Petrol., 56, 1-25.

Janassi, V.A. and Ulbrich, H.G.J., 1991. Late Proterozoic granitoid magmatism in the state of Sao Paulo, southeastern Brazil. Precam. Res., 51, 351-374.

Jayananda, M. and Mahabaleswar, B., 1989. Petrology and geochemistry of the southern Closepet Granite: an example of crustal melting during granulite formation in I. Haapala and Y. Kahkonen (eds). Symposium Precambrian Granitoids. Geol. Surv. Finland Spec. Paper 8, 73.

Jover, O., Rochette, P., Lorand, J.P., Maeder, M. and Bouchez, J.L., 1989. Magnetic mineralogy of some granites from the French Massif Central: origin of their low-field suceptibility. Phys. Earth Planet. Inter., 55, 79-92.

Kadushkin, A.P., 1988. Main findings on magnetism and other physical properties of rocks along southeast Asian tin belt in M.M. Purbo Hadiwidjoyo (ed) Application of Geophysics in the Tin Mining Industry, SE Asia Tin Research and Development Centre Technical Publication no. 7.

Kafafy, A.M., 1987. Preliminary results on the use of magnetic techniques on the study of the granite aureoles. J. Geomagn. Geoelectr., 39, 5443-550.

Kanisawa, S., 1983. Chemical characteristics of biotites and hornblendes of Late Mesozoic to Early Tertiary granitic rocks in Japan in J.A. Roddick (Ed.), Circum-Pacific Plutonic Terranes. Geol. Soc. Am. Memoir 159, 129-134.

Kawakatsu, K. and Yamaguchi, Y., 1987. Succesive zoning of amphibole during progressive oxidation in the Daito-Yokota granitic complex, San-in belt, southwest Japan. Geochim. Cosmochim. Acta, 51, 535-540.

Kerrich, R., 1989. Archean gold: relation to granulite formation or felsic intrusions? Geology, 17, 1011-1015.

Khitrunov, A.T., 1985. Oxidation-reduction environment of formation of granitoid rocks with different ore concentrations. Doklady Earth Science Sections, 280, 201-204.

Jolly, W.A., 1982. Progressive metamorphism of komatiites and related Archaean lavas of the Abitibi area, Canada in N.T. Arndt and E.G. Nisbet, Komatiites, George Allen and Unwin, London, 247-266.

Kimball, K.L., 1990. Effects of hydrothermal alteration on the compositions of chromian spinels. Contrib. Mineral. Petrol., 105, 337-346.

Kress, V.C. and Carmichael, I.S.E., 1988. Stoichiometry of the iron oxidation reaction in silicate melts. Am. Mineral., 73, 1267-1274.

Krutikhovskaya, Z.A., Silina, I.M., Bondareva, N.M. and Podolyanko, S.M., 1979. Relation of magnetic properties of the rocks of the Ukrainian Shield to their composition and metamorphism. Can. J. earth Sci., 16, 984-991.

Kuroda, Y., Yamada, T., Takano, O. and Matsuo, S., 1989. D/H study of the magnetite-series granitic plutons from the Kitakami district, northeast Japan. Chem. Geol., 73, 343-352.

Kwak, T.A.P. and White, A.J.R., 1982. Contrasting W-Mo-Cu and W- Sn-F skarn types and related granitoids. Mining Geology, 32, 339-351.

Kwak, T.A.P., Taylor, R.G. and Plimer, I.R., 1982. Australian tungsten deposits. Tungsten Geology Symposium, Jiangxi, China, Geological Publishing House, Beijing, pp. 127-152.

Lackie M.A. 1989. The rock magnetism and palaeomagnetism of granitic and ignimbritic rocks in the Lachlan and New England Fold Belts, N.S.W.. PhD thesis (unpub), Macquarie University, Australia, 154 pp.

Lackie M.A., Clark D.A. and French D.H. 1991. Rock Magnetism and Palaeomagnetism of the Mount Leyshon gold mine in northeast Queensland. CSIRO Restricted Report 217R.

Lackie, M.A., Clark, D.A. and French, D.H., 1992. Magnetic mineralogy of felsic volcanics of the Conway-Bimurra area, northeast Queensland: relationships to aeromagnetic anomalies and hydrothermal alteration. CSIRO Restricted Report 274R.

Lameyre, J. and Bowden, P., 1982. Plutonic rock series: discrimination of various granitoid series and related rocks. J. Volcan. Geotherm. Res., 14, 169-186.

Latham, A.G., Harding, K.L., Lapointe, P., Morris, W.A. and Balch, S.J., 1989. On the lognormal distribution of oxides in igneous rocks, using magnetic susceptibility as a proxy for oxide mineral concentration. Geophys. J., 96, 179-184.

Lauer, H.V. and Morris, R.V., 1977. Redox equilibria of multivalent ions in silicate glasses. J. Amer. Ceram. Soc., 60, 443-451.

Leake, B.E., Brown, G.C. and Halliday, A.N., 1980. The origin of granite magmas: a discussion. J. Geol. Soc. London, 137, 93-97.

Le Bas, M.J. and Streckeisen, A.L., 1991. The IUGS systematics of igneous rocks. J. Geol. Soc. London, 148, 825-833.

Letros,, S., Strangway, D.W., Tasillo-Hirt, A.M., Geissman, J.W. and Jensen, L.S., 1983. Aeromagnetic interpretation of the Kirkland Lake - Larder Lake portion of the Abitibi Greenstone Belt, Ontario. Can J. Earth Sci., 20, 548-560.

Lienert, B.R. and Wasilewski, P.J., 1979. A magnetic study of the serpentinization process at Burro Mountain, California. Earth Planet. Sci. Lett., 43, 406-416.

Lindbergh, B. and Eklund, O., 1988. Interactions between basaltic and granitic magmas in a Svecofennian postorogenic granitoid intrusion, Aland, southwest Finland. Lithos, 22, 13- 23.

Lindsley, D.H. (ed), 1991. Oxide Minerals: petrologic and magnetic significance. Rev. Mineral., 25, 509 pp.

Lϕvlie, R., 1988. Evidence for deuteric magnetization in hydrothermally altered Mesozoic basaltic rocks from East Antarctica. Phys. Earth Planet. Inter., 52, 352-364.

Lowell, G.R., 1991. The Butler Hill Caldera: a mid-Proterozoic ignimbrite-granite complex. Precam. Res., 51, 245-263.

Lowrie W. 1990. Identification of ferromagnetic minerals in a rock by coercivity and unblocking temperature properties. Geophys. Res. Let. 17, 159-162.

Lumbers, S.B., Wu, T, Heaman, V.M. and MacRae, N.D., 1991. Petrology and age of the A-type Mulock granite batholith, northern Grenville Province, Ontario. Precam. Res., 53, 199-231.

Lyakhovich, V.V., 1987. Accessory minerals as an indicator of the evolution of the lithosphere. Int. Geol. Rev., 899-911.

Macdonald, M.A. and Clarke, D.B., 1991. Use of nonparametric ranking statistics to characterize magmatic and post-magmatic processes in the eastern South Mountain Batholith, Nova Scotia, Canada. Chem. Geol., 92, 1-20.

Maniar, P.D. and Piccoli, P.M., 1989. Tectonic discrimination of granitoids. Geol.Soc. Am. Bull., 101, 635-643.

Marsh, J.S., 1975. Aenigmatite stability in silica- undersaturated rocks. Contrib. Mineral. Petrol., 50, 135-144.

Mason, D.R. and McDonald, J.A., 1978. Intrusive rocks and porphyry copper occurrences of the Papua New Guinea - Solomon Islands region: a reconnaissance study. Econ. Geol., 73, 857- 877.

Mathez, E.A., 1984. Influence of degassing on oxidation states of basaltic magmas. Nature, 310, 371-375.

McGuire, A.V., Dyar, M.D. and Nielson, J.E., 1991. Metasomatic oxidation of upper mantle peridotite. Contrib. Mineral. Petrol., 109, 252-264.

McIntyre, J.I., 1980. Geological significance of magnetic patterns related to magnetite in sediments and metasediments - a review. Aust. Soc. Explor. Geophys. Bull., 11, 19-33.

McQueen, K.G., 1981. The nature and metamorphic history of the Wannaway Nickel Deposit, Western Australia. Econ. Geol., 76, 1444-1468.

Merrill, R.T., 1975. Magnetic effects associated with chemical changes in igneous rocks. Geophys. Surv., 2, 277-311.

Mezhvilk, A.A., 1989. Subdivision of metamorphic rocks of the Anbar Shield based on aeromagnetic data. Doklady Earth Science Sections, No. 5, 145-147.

Miller, C.F., Watson, E.B. and Harrison, T,M., 1988. Perspectives on the source, segregation and transport of granitoid magmas. Trans. Roy. Soc. Edinburgh, Earth Sci., 79, 135-156.

Moody, J.M., 1976a. An experimental study of the serpentinization of iron-bearing olivines. Can. Mineral., 14, 462-478.

Moody, J.M., 1976b. Serpentinization: a review. Lithos, 9, 125- 138.

Morse, 1979. Kiglapait geochemistry II: petrography. J. Petrology, 20, 591-624.

Morse, S.A., 1980. Kiglapait mineralogy II: Fe-Ti oxide minerals and the activities of oxygen and silica. J. Petrology, 21, 685- 719.

Mueller, R.F., 1971. Oxidative capacity of magmatic components. Am. J. Sci., 270, 236-243.

Muhling, P.C. and Low, G.H., 1977. Yalgoo 1:250,000 Geological Series Explanatory Notes, Geological Survey of W.A.

Murata, M and Itaya, T., 1987. Sulfide and oxide minerals from S-type and I-type granitic rocks. Geochim. Cosmochim. Acta, 51, 497-507.

Mutton, A.J. and Shaw, R.D., 1979. Physical property measurements as an aid to magnetic interpretation in basement terrains. Bull. Aust. Soc. Explor. Geophys., 10, 79-91.

Naldrett, A.J., and Turner, A.R, 1977. The geology and petrogenesis of a greenstone belt and related nickel sulfide mineralization at Yakabindie, Western Australia. Precamb. Res., v.5, pp43-103.

Nardi, L.V.S. and Bonin, B., 1991. Post-orogenic and non- orogenic alkaline granite associations: the Saibro intrusive suite, southertn Brazil - a case study. Chem. Geol., 92, 197- 211.

Noyes, H.J., Wones, D.R. and Frey, F.A., 1983. A tale of two plutons: petrographic and mineralogic constraints on the petrogenesis of the Red Lake and Eagle Peak plutons, central Sierra Nevada, California. J. Geology, 91, 353-379.

Nozawa, T., 1983. Felsic plutonism in Japan in J.A. Roddick (Ed.), Circum-Pacific Plutonic Terranes. Geol. Soc. Am. Memoir 159, 105-122.

Nurmi, P.A. and Haapala, I., 1986. The Proterozoic granitoids of Finland: granite types, metallogeny and relation to crustal evolution. Bull. Geol. Soc. Finland, 58, 203-233.

Ohlander, B, Hamilton, P.J., Fallick, A.E. and Wilson, M.R., 1987. Crustal reactivation in northern Sweden: the Vettasjarvi Granite. Precam. Res., 35, 277-293.

Olesen, O., Henkel, H., Kaada, K. and Tveten, E., 1991. Petrophysical properties of a prograde amphibolite-granulite facies transition zone at Sigerfjord, Vesteralen, northern Norway. Tectonophysics, 192, 33-39.

Oliver, H.W., 1977. Gravity and magnetic investigations of the Sierra Nevada batholith, California. Geol. Soc. Am. Bull., 88, 445-461.

Onyeagocha, A.C., 1984. Alteration of chromite from the Twin Sisters Dunite, Washington. Am. Mineral., 59, 608-612.

Osborn, E.F., 1959. Role of oxygen pressure in the crystallization and differentiation of basaltic magma. Am. J. Sci., 257, 609-647.

Pagel, M. and Leterrier, J., 1980. The subalkaline potassic magmatism of the Ballons massif (southern Vosges, France): shoshonitic affinity. Lithos, 13, 1-10.

Parsons, I., 1979. The Klokken gabbro-syenite complex, south Greenland: cryptic variation and origin of inversely graded layering. J. Petrology, 20, 653-694.

Parsons, I., 1980. Alkali-feldspar and Fe-Ti oxide exsolution textures as indicators of the distribution and subsolidus effects of magmatic 'water' in the Klokken layered syenite intrusion, south Greenland. Trans. Roy. Soc. Edinburgh: Eart Sci., 71, 1-12.

Pasteris, J.D., 1985. Relationships between temperature and oxygen fugacity among Fe-Ti oxides in two regions of the Duluth Complex. Can. Mineral., 23, 111-127.

Pearce, G.W. and Fueten, F., 1989. An intensive study of magnetic susceptibility anisotropy of amphibolite layers of the Thompson Belt, north Manitoba. Tectonophysics, 162, 315-329.

Pearce, J.A., Harris, N.B.W. and Tindle, A.G., 1984. Trace element discriminaion diagrams for the tectonic interpretation of granitic rocks. J. Petrol., 25, 956-983.

Pecherskiy, D.M., 1963. Statistical analysis of the reasons for the varying magnetization of the granitoids of the Verkhoyansk- Chutotka fold region and the Okhotsk-Chucotka belt. Inter. Geol. Rev., 7,, 1963-1976.

Perring, C.S., Groves, D.I. and Shellabear, J., 1989. The porphyry-gold association in the Yilgarn Block of Western Australia: spatial coincidence or genetic connection? in I. Haapala and Y. Kahkonen (eds). Symposium Precambrian Granitoids. Geol. Surv. Finland Spec. Paper 8, 100-101.

Petersen, N., 1976. Notes on the variation of magnetization within basalt lava flows and dikes. Pure Appl. Geophys., 114, 177-193.

Petersen, J.S., 1980. The zoned Kleivan Granite - an end member of the anorthosite suite in southwest Norway. Lithos, 13, 79-95.

Petersen, N. and Bleil, U., 1982. Magnetic properties of rocks in G. Angenheister (ed), Physical Properties of Rocks, Landolt- Bornstein Numerical Data and Functional Relationships in Science and Technology, Group V, Volume 1b. Springer-Verlag, Berlin.

Phillips, G.N., Wall, V.J. and Clemens, J.D., 1981. Petrology of the Strathbogie batholith: a cordierite-bearing granite. Can. Mineral., 19, 47-63.

Philpotts, A.R., 1967. Origin of certain iron-titanium oxide and apatite rocks. Econ. Geol., 62, 303-315.

Pitcher, W.S., 1979a. The nature, ascent and emplacement of granitic magmas. J. Geol. Soc. London, 136, 627-662.

Pitcher, W.S., 1979b. Comments on the geological environments of granites in Atherton, M.P. and Tarney, J., 1979 (eds). Origin of Granite Batholiths. Shiva Publishing, pp. 1-8.

Pitcher, W.S., 1983. Granite type and tectonic environment in K. Hsu (ed), Mountain Building Processes, Academic Press, London, pp. 19-40.

Popp, R.K., Gilbert, C.M. and Craig, J.R., 1977. Stability of Fe-Mg amphiboles with respect to oxygen fugacity. Am. Mineral., 62, 1-12.

Pridmore, D.F., Coggon, J.H., Esdale, D.J. and Lindeman, F.W., 1984. Geophysical exploration for nickel sulphide deposits in the Yilgarn Block, Western Australia. Western Mining Corporation.

Puffer, J.H., 1972. Iron-bearing minerals as indicators of intensive variables pertaining to granitic rocks from the Pegmatite Points area, Colorado. Am. J. Sci., 272, 273-289.

Puffer, J.H. and Volfert, R.A., 1991. Generation of trondhjemite from partial melting of dacite under granulite facies conditions: an example from the New jersey Highlands, USA. Precam. Res., 51, 115-125.

Puranen, R., 1989. Susceptibilities, iron and magnetite content of Precambrian rocks from Finland. Geol. Surv. Finland Rep. Inv. 90, 45 pp.

Reeves, C.V., 1987. Geophysical mapping of Precambrian granite- greenstone terranes as an aid to exploration. Exploration '87 Proceedings, Geophysical Methods: Advances in the State of the Art, 254-266.

Reynolds, I.M., 1985. The nature and origin of titaniferous magnetite-rich layers in the upper zone of the Bushveld Complex: a review and synthesis. Econ. Geol., 80, 1089-1108.

Richardson, S.W., 1968. The petrology of the metamorphosed syenite in Glen Dossary, Inverness-shire. Q. J. geol. Soc. Lond., 124, 9-51.

Rock, N.M.S., 1978. Petrology and petrogenesis of the Monchique Alkaline Complex, southern Portugal. J. Petrology, 19, 171-214.

Roddick, J.C., Compston, W., and Durney, D.W., 1976. The radiometric age of the Mt Keith granodiorite, a maximum estimate for an Archean greenstone sequence. Precamb. Res., v.3, pp55-78.

Rogers, J.J.W., 1989. Comparison of late-orogenic, postorogenic and anorogenic granites in I. Haapala and Y. Kahkonen (eds). Symposium Precambrian Granitoids. Geol. Surv. Finland Spec. Paper 8, 112.

Rollinson, H.R., 1980. Iron-titanium oxides as an indicator of the role of the fluid phase during the cooling of granites metamorphosed to granulite grade. Min. Mag., 43, 623-631.

Rona, P.A., 1978. Magnetic signatures of hydrothermal alteration and volcanogenic mineral deposits in oceanic crust. J. Volcan. Geotherm. Res., 3, 219-225.

Rossi, P. and Cocherie, A., 1991. Genesis of a Variscan batholith: field, petrological and mineralogical evidence from the Corsica-Sardinia batholith. Tectonophysics, 195, 319-346.

Rottura, A., Bargossi, G.M., Caironi, V., Del Moro, A., Maccarone, E., Macera, P., Paglionico, A., Petrini, R., Piccaretta, G. and Poli, G., 1990. Petrogenesis of contrasting Hercynian granitoids from the Calabrian Arc, southern Italy. Lithos, 24, 97-119.

Rutherford, M.J., 1969. An experimental determination of iron biotite-alkali feldspar equilibria. J. Petrology, 10, 381-408.

Saad, A.H., 1969. Magnetic properties of ultramafic rocks from Red Mountain, California. Geophysics, 34, 974-987.

Sanderson, D.D., 1974. Spatial distribution and origin of magnetite in an intrusive igneous mass. Geol. Soc. Am. Bull., 85, 1183-1188.

Sarkar,S.C., Bhattacharyya, S., Kabiraj. S. and Das, S., 1989. The granitoid-hosted Early Proterozoic copper deposit of Malanjkhand, central India - a study in I. Haapala and Y. Kahkonen (eds). Symposium Precambrian Granitoids. Geol. Surv. Finland Spec. Paper 8, 118.

Sauck, W.A., 1972. Magnetic susceptibility and magnetite content. Econ. Geol., 67, 383-385.

Schlinger, C.M., 1985. Magnetization of lower crust and interpretations of regional magnetic anomalies: example from Lofoten and Vesteralen, Norway. J. Geophys. Res., 11,484-11,504.

Schlinger, C.M. and Veblen, D.R., 1989. Magnetism and transmission electron microscopy of Fe-Ti oxides and pyroxenes in a granulite from Lofoten, Norway. J. Geophys. Res., 94, 14,009-14,026.

Schmidt, P.W., 1986. Magnetic properties and models for Peculiar Knob and Teatree Glen prospects, S.A. CSIRO Restricted Investigation Report 1659R.

Schmidt, P.W., Clark, D.A. and French, D., 1990. Rock magnetism and palaeomagnetism of the greenstone belt in the Mt Keith - Agnew area. CSIRO Div. Explor. Geosci., Restricted Report 189R.

Schmidt, P.W. and Clark, D.A., 1992. Magnetic properties of Archaean and Proterozoic rocks from the Eyre Peninsula. CSIRO Restricted Report 275R.

Schwarz, E.J., 1991. Magnetic expressions of intrusions including magnetic aureoles. Tectonophysics, 192, 191-200.

Shaw, S.E. and Flood, R.H., 1981. The New England Batholith, eastern Australia: geochemical variations in time and space. J. Geophys. Res., 86, 10,530-10,544.

Shearer, C.K. and Robinson, P., 1988. Petrogenesis of metaluminous and peraluminous tonalites within the Merrimack synclinorium: Hardwick Tonalite, central Massachusetts. Am. J. Sci., 288-A, 148-195.

Shi, Y., Yang, S., Guo, L. and Dong, H., 1991. Crustal genesis and plate tectonics. Tectonophysics, 187, 277-284.

Shiga, Y., 1987. Behaviour of iron, nickel, cobalt and sulfur during serpentinization, with reference to the Hayachine ultramafic rocks of the Kamaishi Mining District, northeastern Japan. Can. MIneral., 25, 611-624.

Shive, P.N., 1989. Can remanent magnetization in the deep crust contribute to long wavelength magnetic anomalies? Geophys. Res. Lett., 16, 89-92.

Shive, P.N., 1990. The Ivrea Zone and lower crustal magnetization. Tectonophysics, 182, 161-167.

Shive, P.N. and Fountain, D.M., 1988. Magnetic mineralogy in an Archean crustal cross-section: implications for crustal magnetization. J. Geophys. Res., 93, 12,177-12,186.

Shive, P.N., Frost, B.R. and Peretti, A., 1988. The magnetic properties of metaperidotitic rocks as a function of metamorphic grade: implications for crustal magnetic anomalies. J. Geophys. Res., 93, 12,187-12,195.

Shive, P.N., Houston, R.S. and Blakely, R.J., 1990. Modeling of aeromagnetic data from the Precambrian Lake Owens mafic complex, Wyoming. Geol. Soc. Am. Bull., 102, 1317-1322.

Sillitoe, R.H., 1979. Some thoughts on gold-rich porphyry copper deposits. Mineral. Deposita, 14, 161-174.

Silver, L.T. and Chappell, B.W., 1988. The Peninsular Ranges batholith: an insight into the evolution of the Cordilleran batholiths of southwestern North America. Trans. Roy. Soc. Edinburgh, 79, 105-121.

Sinigoi, S., Antonini, P., Demarchi, G., Longinelli, A., Mazzucchelli, M. Negrini, L. and Rivaletti, G., 1991. Interactions of mantle and crustal magmas in the southern part of the Ivrea Zone, Italy. Contrib. Mineral. Petrol., 108, 385- 395.

Skilbrei, J.R., Skyseth, T. and Olesen, O., 1991. Petrophysical data and opaque mineralogy of high-grade and retrogressed lithologies: implications for the interpretation of aeromagnetic anomalies in northern Vestranden, central Norway. Tectonophysics, 192, 21-31.

Skolotnev, S.G., 1984. Mineral formation during oxidation of iron in basalts of the Klyuchevskaya volcanic group, Kamchatka. Int. Geol. Rev., 29, 727-736.

Sϕrenson, H. (ed), 1974. The Alkaline Rocks. Wiley, London.

Speer, J.A., 1981a. The nature and magnetic expression of isograds in the contact aureole of the Liberty Hill pluton, South Carolina. Geol. Soc. Am. Bull., 92, Part 1, 603-609 and Part 2, 1262-1358.

Speer, J.A., 1981b. Petrology of cordierite- and almandine- bearing granitoid plutons of the southern Appalachian Piedmont, U.S.A. Can. Mineral., 19, 35-46.

Spencer, R., 1989. Interpretation of regional and detailed aeromagnetic data over the Owendale Intrusive Complex, Fifield, New South Wales. N.S.W. Geol. Surv. Quart. Notes, 80, 19-37.

Strong, D.F. and Hanmer, S.K., 1981. The leucogranites of southern Brittany: origin by faulting, frictional heating, fluid flux and fractional melting. Can. Mineral., 19, 163-176.

Studemeister, P.A., 1984. The redox state of iron: a powerful indicator of hydrothermal alteration. Geoscience Canada, 10(4), 189-194.

Stussi, J.-M., 1989. Granitoid chemistry and associated mineralization in the French Variscan. Econ. Geol., 84, 1363- 1381.

Subrahmanyam, C. and Verma, R.K., 1981. Densities and magnetic susceptibilitties of Precambrian rocks of different metamorphic grade (southern Indian Shield). J. Geophys., 49, 101-107.

Sutcliffe, R.H., 1989. Magma mixing in Late Archean tonalitic and mafic rocks of the Lac des Iles area, western Superior Province. Precam. Res., 44, 81-101.

Sutherland, D.S., 1974. Petrography and mineralogy of the peralkaline silicic rocks. Bull. Volcan., 38, 517-547.

Sylvester, A.G., Miller, C.F. and Nelson, C.A., 1978. Monzonites of the White-Inyo Range, California, and their relation to the calc-alkalic Sierra Nevada batholith. Geol. Soc. Am. Bull., 89, 1677-1687.

Takahashi, M., 1989. Neogene granitic magmatism in the South Fossa Magna collision zone, Central Japan. Modern Geology, 14, 127-143.

Takahashi, M., Aramaki, S. and Ishihara, S., 1980. Magnetite- series/ilmenite-series vs. I-type/S-type granitoids. Min. Geol. Spec. Issue, 8, 13-28.

Taylor, R.P., Strong, D.F. and Kean, B.F., 1980. The Topsails igneous complex: Silurian-Devonian peralkaline magmatism in western Newfoundland. Can. J. Eart Sci., 17, 425-439.

Thoa, N.T.K. and Pecherskiy, D.M., 1989. Serpentinites as possible sources of linear magnetic anomalies. Int. Geol. Rev., 1, 239-245.

Thompson, J.B., 1972. Oxides and sulfides in regional metamorphism of pelitic schists. 24th IGC, Section 10, 27-35.

Thy, P., 1982. Titanomagnetite and ilmenite in the Fongen- Hyllingen basic complex, Norway. Lithos, 15, 1-16.

Titley, S.R. and Beane, R.E., 1981. Porphyry copper deposits. Part I. Geologic settings, petrology, and tectogenesis. Econ. Geol., 75th Anniversary Volume, 214-235.

Toft, P.B., Arkani-Hamed, J. and Haggerty, S.E., 1990. The effects of serpentinization on density and magnetic susceptibility: a petrophysical model. Phys. Earth Planet. Inter., 65, 137-157.

Tracy and Robinson, 1988. Silicate-sulfide-oxide-fluid reactions in granulite-grade pelitic rocks, central Massachusetts. Am. J. Sci., 288-A, 45-74.

Tulloch, A.J., 1983. Granitoid rocks of New Zealand - a brief review in J.A. Roddick (Ed.), Circum-Pacific Plutonic Terranes. Geol. Soc. Am. Memoir 159, 5-20.

Urquhart, W.E.S., 1989. Field examples of controls on magnetite content. Explor. Geophys., 20, 93-97.

Vernon, R.H., 1961. Magnetic susceptibility as a measure of total iron plus manganese in some ferromagnesian silicate minerals. Am. Mineral., 46, 1141-1153.

Vernon, R.H., Etheridge, M.A. and Wall, V.J., 1988. Shape and microstructure of micrgranitoid enclaves: indicators of magma mingling and flow. Lithos, 22, 1-11.

Vogt, P.R. and Byerly, G.R., 1976. Magnetic anomalies and basalt composition in the Juan de Fuca - Gorda Ridge area. Earth Planet. Sci. Lett., 33, 185-207.

Vogt, P.R. and De Boer, J., 1976. Morphology, magnetic anomalies and basalt magnetization at the ends of the Galapagos high- amplitude zone. Earth Planet. Sci. Lett., 33, 145-163.

Vyhnal, C.R., McSween, H.Y. and Speer, J.A., 1991. Hornblende chemistry in southern Appalachian granitoids: implications for aluminum hornblende thermobarometry and magmatic epidote stability. Am. Mineral., 76, 176-188.

Wahl, W.G., 1960. An interpretative technique for delimiting mineral potential areas based on the magnetic susceptibility of source rocks. 21st International Geological Congress, Part 2, 200-215.

Wall, V.J., Clemens, J.D. and Clarke, D.B., 1987. Models for granitoid evolution and source compositions. J. Geology, 95, 731-749.

Wallace, G.M., Whalen, J.B. and Martin, R.F., 1990. Agpaitic and miaskitic nepheline syenites of the McGerrigle Plutonic Complex, Gaspe, Quebec: an unusual petrological association. Can. Mineral., 251-266.

Wang, L.C., McNaughton, N.J. and Groves, D.I., 1991. Archean granitoids in the Murchison Province, Western Australia: petrogenetic classification and relations to gold mineralisation in Second Hutton Symposium on Granites and Related Rocks, BMR Record 1991/25, 10.

Wasilewski, P.J., 1987. Magnetic properties of mantle xenoliths and the magnetic character of the crust-mantle boundary in P.H. Nixon (ed), Mantle Xenoliths, Wiley, pp. 577-588.

Wasilewski, P. and Warner, R.D., 1988. Magnetic petrology of deep crustal rocks - Ivrea Zone, Italy. Earth Planet. Sci. Lett., 87, 347-361.

Watkins, K.P. and Hickman, A.H., 1990. Geological evolution and mineralization of the Murchison Province, Western Australia. Geol. Surv. W.A. Bulletin 137.

Webster, S.S., 1984. A magnetic signature for tin deposits in south-east Australia. Explor. Geophys., 15, 15-31.

Webster, S.S. and E. Scheibner, 1984. Introduction to the magnetic properties of New England granitoids. Explor. Geophys., 15, 67-73.

Whalen, J.B. and Chappell, B.W., 1988. Opaque mineralogy and mafic mineral mineral chemistry of I- and S-type granites of the Lachlan Fold Belt, southeast Australia. Am. Mineral., 73, 281- 296.

Whalen, J.B. and Currie, K.L., 1984. The Topsails igneous terrane, western Newfoundland: evidence for magma mixing. Contrib. Mineral. Petrol., 87, 319-327.

Whalen, J.B., Curie, K.L. and Chappell, B.W., 1987. A-type granites: geochemical characteristics, discrimination and petrogenesis. Contrib. Mineral. Petrol., 95, 407-419.

Whitaker, A., Wellman, P and Reith, H., 1987. The use of gravity and magnetic surveys in mapping greenstone terrane near Kalgoorlie, Western Australia. Explor. Geophys., 18, 371-380.

White, A.J.R., 1992. On the origin of peralkaline granites. Geol. Soc. Australia Abstracts No. 32, 202.

White, A.J.R. and Chappell, B.W., 1977. Ultrametamorphism and granitoid genesis. Tectonophysics, 43, 7-22.

White, A.J.R. and Chappell, B.W., 1983. Granitoid types and their distribution in the Lachlan Fold Belt, southeastern Australia in J.A. Roddick (Ed.), Circum-Pacific Plutonic Terranes. Geol. Soc. Am. Memoir 159, 21-34.

White, A.J.R. and Chappell, B.W., 1988. Some supracrustal (S- type) granites of the Lachlan Fold Belt. Trans. Roy. Soc. Edinburgh: Earth Sci., 79, 169-181.

White, A.J.R. and Chappell, B.W., 1991. Field and petrographic relationships of S- and I-type granites in the Lachlan Fold Belt in Second Hutton Symposium on Granites and Related Rocks, BMR Record 1991/25, 10.

White, A.J.R., Chappell, B.W. and Cleary, J.R., 1974. Geologic setting and emplacement of some Australian Paleozoic batholiths and implications of intrusive mechanisms. Pac. Geol., 8, 159- 171.

White, A.J.R., Clemens, J.D., Holloway, J.R., Silver, L.T., Chappell, B.W. and Wall, V.J., 1986. S-type granites and their probable absence in southwestern North America. Geology, 14, 115-118.

White, A.J.R., Wyborn, D. and Chappell, B.W., 1991. A granite classification for the economic geologist.

White, W.H., Bookstrom, A.A., Kamilli, R.J., Ganster, M.W., Smith, R.P., Ranta, D.E. and Steininger, R.C., 1981. Character and origin of Climax-type molybdenum deposits. Econ. Geol., 75th Anniversary Volume, 270-316.

Whiting, T.H., 1986. Aeromagnetics as an aid to geological mapping - a case history from the Arunta Inlier, Northern Territory. Austr J. Earth Sci., 33, 271-286.

Whiting, T.H., 1988. Magnetic mineral petrogenesis, rock magnetism and aeromagnetic response in the eastern Arunta Inlier, Northern Territory. Explor. Geophys., 19, 377-383.

Whitney, J.A., 1984. Fugacities of sulfurous gases in pyrrhotite-bearing silicic magmas. Am. Mineral., 69, 69-78.

Whitney, J.A. and Stormer, J.C., 1976. Geothermometry and geobarometry in epizonal granitic intrusions: a comparison of iron-titanium oxides and coexisting feldspars. Am. Mineral., 61, 751-761.

Whittaker, E.J.W. and Wicks, F.J., 1970. Chemical differences among the serpentine "polymorphs": a discussion. Am. Mineral., 55, 1025-25-25-25-1047.

Wicks, F.J. and O'Hanley, D.S., 1988. Serpentine minerals: structures and petrology. Rev. Mineral., 19, 91-167.

Williams, M.C., Shive, P.N., Fountain, D.M. and Frost, B.R., 1985. Magnetic properties of exposed deep crustal rocks from the Superior Province of Manitoba. Earth Planet. Sci. Lett., 76, 176-184.

Williams, R.J., 1971. Reaction constants in the system Fe-MgO- SiO2-O2: intensive parameters in the Skaergaard intrusion, east Greenland. Am. J. Sci., 271, 132-146.

Witt, W.K., 1991. Regional metamorphic controls on alteration associated with gold mineralization in the Eastern Goldfields province, Western Australia: implications for the timing and origin of Archean lode-gold deposits. Geology, 19, 982-985.

Witt, W.K. and Swager, 1989. Structural setting and geochemistry of Archaean I-type granites in the Bardoc-Coolgardie area of the Norseman-Wiluna belt, Western Australia. Precam. Res., 44, 323- 351.

Wones, D.R., 1980. Contributions of crystallography, mineralogy and petrology to the geology of the Lucerne pluton, Hancock County, Maine. Am. Mineral., 65, 411-437.

Wones, D.R., 1989. Significance of the assemblage titanite + magnetite + quartz in granitic rocks. Am. Mineral., 74, 744-749.

Wones, D.R. and Gilbert, M.C., 1982. Amphiboles in the igneous environment in D.R. Veblen and P.H. Hill (Eds), Amphiboles: petrology and experimental phase relations. Reviews of Mineralogy, ,355 -390.

Worden, R.H., Droop, G.T.R. and Champness, P.E., 1991. The reaction antigorite → olivine + talc + H2O in the Bergell aureole, N. Italy. Min. Mag., 55, 367-377.

Worm, H.U., 1989. Comment on "Can remanent magnetization in the deep crust contribute to long wavelength magnetic anomalies?" by Peter N. Shive. Geophys. Res. Lett., 16, 595-597.

Wyborn, D., Chappell, B.W. and Johnston, R.M., 1981. Three S- type volcanic suites from the Lachlan Fold Belt, southeast Australia. J. Geophys. Res., 86, 10,355-10,348.

Wyborn, D., Turner, B.S. and Chappell, B.W., 1987. The Boggy Plain Supersuite: a distinctive belt of I-type igneous rocks of potential economic significance in the Lachlan Fold Belt. Aust. J. Earth Sci., 34, 21-43.

Wyborn, L.A. and Drummond, B.J., 1991. Australian Proterozoic granites: important indicators of crustal evolution in Second Hutton Symposium on Granites and Related Rocks, BMR Record 1991/25, 10.

Wyllie, P.W., 1984. Sources of granitoid magmas at convergent plate boundaries. Phys. Earth Planet. Inter., 35, 12-18.

Wyllie, P.J., Huang, W.L., Stern, C.R. and Maalφe S., 1976. Granitic magmas: possible and impossible sources, water contents, and crystallization sequences. Can. J. Earth Sci., 13, 1007-1019.

Yeates, A.N., Wyatt, B.W. and Tucker, D.H., 1982. Application of gamma ray spectrometry to prospecting for tin and tungsten granites, particularly within the Lachlan Fold Belt, New South Wales. Econ. Geol., 77, 1725-1738.

Yudin, B.A. and Katseblin, P.I., 1978. Petrophysical characteristics of gabbro-labradorite complexes, Kola Peninsula. Int. Geol. Rev., 23, 517-523.

Zen, E-an, 1988. Phase relations of peraluminous granitic rocks and their petrogenetic implications. Ann. Rev. Earth Planet. Sci., 16, 21-51.

Zorpi, M.J., Coulon, C., Orsini, J.B. and Cocirta, C., 1989. Magma mingling, zoning and emplacement in calc-alkaline granitoid plutons. Tectonophysics, 157, 315-329.